VPI-SU-5648-5

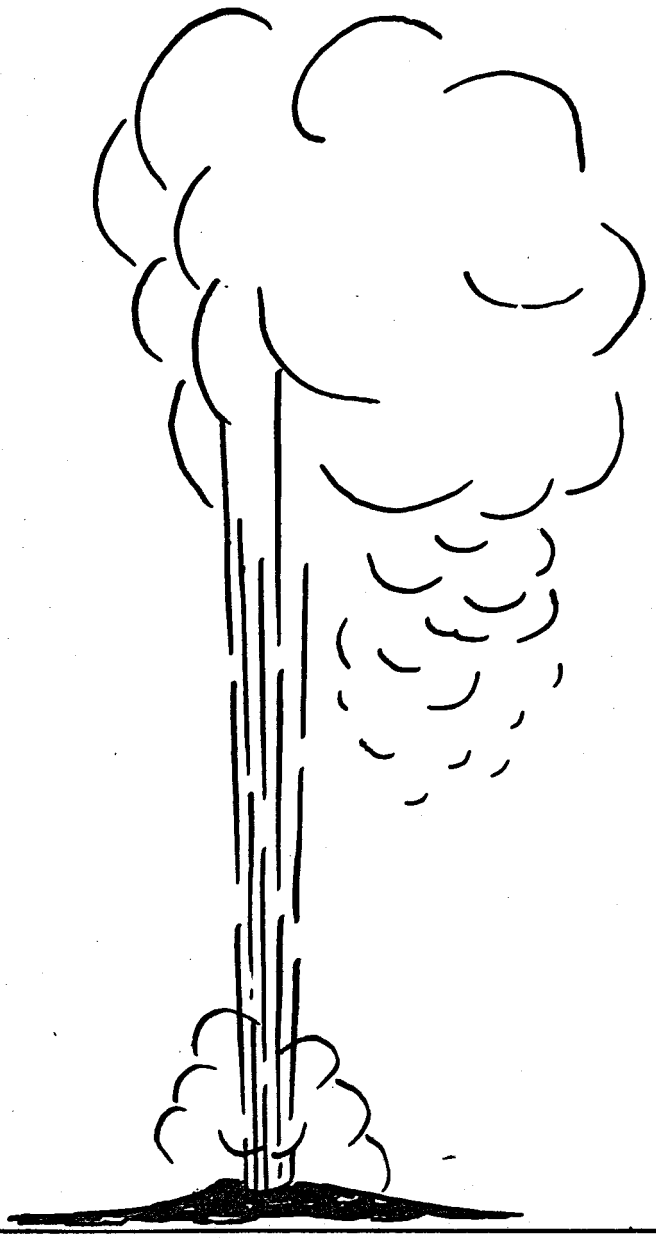

EVALUATION AND TARGETING OF GEOTHERMAL ENERGY RESOURCES IN THE SOUTHEASTERN UNITED STATES

Progress Report, October 1, 1978—March 30, 1979

By
John K. Costain
Lynn Glover III
A. Krishna Sinha

Work Performed Under Contract No. ET-78-C-05-5648

Virginia Polytechnic Institute and State University
Blacksburg, Virginia

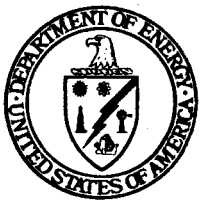

U. S. DEPARTMENT OF ENERGY
Geothermal Energy

DISCLAIMER

NOTICE

VPI-SU-5648-5
Distribution Category UC-66a

EVALUATION AND TARGETING OF GEOTHERMAL ENERGY RESOURCES IN THE SOUTHEASTERN UNITED STATES

Progress Report

John K. Costain, Lynn Glover III, and A. Krishna Sinha

Principal Investigators

Department of Geological Sciences

Virginia Polytechnic Institute and State University

Blacksburg, VA 24061

October 1, 1978 - March 30, 1979

PREPARED FOR THE U. S. DEPARTMENT OF ENERGY UNDER

CONTRACT NO. ET-78-C-05-5648

TABLE OF CONTENTS

ABSTRACT AND OVERVIEW

The Geothermal Program at V.P.I. & S.U. has two goals. The immediate goal is to locate sites favorable to the economic development of geothermal energy in the eastern U.S. A paper by Lambiase, Dashevsky, Costain, Gleason and McClung summarizes estimated and measured temperatures at the base of the Atlantic coastal plain in New Jersey, Delaware, Maryland, Virginia and North Carolina based on geothermal gradients measured in 66 holes. The gradients range from 16 to 50°C/km. Basement surface temperatures at several locations are estimated to be above an economically useful 40°C; the highest is 91°C. From this information, the most promising and best documented area for development of geothermal energy chosen by the authors is the Delmarva peninsula near Crisfield, MD. This is the location of the first deep geothermal test well on the East coast which is to be drilled within a month.

The second and long term goal of the Geothermal Program is to use the determined values of heat flow in conjunction with other geologic data in order to reach a better understanding of observed variations in heat flow. Knowledge of the relation between geology and heat flow will permit exploration for and evaluation of geothermal resources by indirect methods involving potential field data and geologic setting instead of by direct, expensive drilling methods. Costain, in "Geothermal Exploration Methods and Results, Altantic Coastal Plain," reviews this project's work on locating, evaluating and interpreting geothermal resources by geophysical techniques. He discusses the use of heat flow, gravity, magnetic and seismic data in the Atlantic coastal plain as well as in the Piedmont and Valley and Ridge provinces. The validity of this approach is demonstrated in a report by Perry on "Heat Flow in the Atlantic Coastal Plain." The heat flow values of 16 coastal plain holes are between 1.1 and 2.0 HFU (1HFU = 10^{-6} cal/cm^2-sec.). High heat flow values are usually associated with gravity lows, as predicted by interpretation of the lows as expressions of burried radiogenic, granitic heat sources. In the Portsmouth, VA, hole, the heat flow at the center of the gravity anomaly is 1.4 HFU, whereas the heat flow in a hole drilled on the flank of the anomaly is 1.1 HFU.

The direct information obtainable from drill holes in the coastal plain complements and constrains the geophysical exploration techniques. Gleason presents "Study of PreCretaceous Basement below the Atlantic Coastal Plain," which summarizes the results of his compilation of well data for New Jersey, Delaware, Maryland, Virginia, North Carolina and Georgia. The compilation consists of information from the literature and data obtained by this project. It includes 1) location of holes, 2) depths to basement and 3) nature of basement rocks. Structure contour maps of the basement surface are presented for North Carolina and Georgia.

Costain, Perry, Dashevsky and Higgins report four new heat flow values from the Piedmont in "Heat Flow and Heat Generation." The SM2 drill hole in the Siloam Pluton, GA has a heat flow of 1.58 HFU. The

EDI drill hole in the Cuffytown Creek Pluton, SC has a heat flow of 1.62 HFU. These two values are the highest reported to date for the Piedmont of the southeast U.S. The other two heat flow determinations are 0.94 HFU for the Palmetto 1, GA hole, and 1.05 HFU for the Rolesville 4, NC hole. Costain and Perry, in their discussion of the "Linear Relation between Heat Flow and Heat Generation," use these additional heat flow values in refining the linear relation for the small, post-metamorphic plutons and as a basis for discussing the probable causes some plutons fail to follow the same linear relation. They believe that the varying thicknesses of the plutons are primarily responsible. Points such as that from Rolesville 4, which fall above the line, are from large synmetamorphic plutons which are believed to be more deeply rooted than the small, post-metamorphic plutons. The point for Palmetto 1 is the only value that falls significantly below the line, which leads to the interpretation that the Palmetto pluton is a thin body of rock. Up to now it has not been a lack of hypotheses so much as lack of data which prevented an understanding of the deviations from the linear relationship between heat flow and heat generation. Costain and Perry suggest that determination of the thickness of the Rolesville and Palmetto plutons will provide a test of whether the thickness of the heat source is an essential component of the linear relationship, a test which is now feasible with the start-up of our VIBROSEIS reflection seismology system.

Discussion of the behavior of U in the radiogenic, granite heat sources continues with two papers. Speer presents a paper entitled "Prograde metamorphism of the pelitic rocks in the contact aureole and xenoliths of the Liberty Hill pluton, South Carolina." The paper is concerned with the detailed petrology and is written for submission to a professional journal, but the importance of the conclusions is summarized in an introduction. The behavior of U during the magmatic stage is strongly affected by the inward migration of fluid at the presently exposed level. Sinha, Hall and Sans report on the weathering history of the WIN 1 drill hole in "Correlation of Radioelement Content to Surficial Weathering Processes." During weathering, various elements have differing mobilities, from extremely mobile U to virtually immobile Al and Ti. Weathering indicies are found to be helpful, but the authors find the study of an intermediately mobile element more useful in understanding the processes of weathering. Sr is such an element. They find that Sr has been mobiized by weathering processes to a depth of 600 feet in the drill core and, by implication, U also.

RESEARCH OBJECTIVES

The objective of this research is to develop and apply targeting procedures for the evaluation of low-temperature radiogenically-derived geothermal resources in the eastern United States utilizing geological, geochemical, and geophysical data.

The optimum sites for geothermal development in the tectonically-stable Eastern United States will probably be associated with areas of relatively high heat flow derived from crustal igneous rocks containing relatively high concentrations of radiogenic heat-producing elements. The storage of commercially-exploitable geothermal heat at accessible depths (1-3 km) will also require favorable reservoir conditions in rocks overlying a radiogenic heat source. In order to systematically locate these sites, a methodology employing geological, geochemical, and geophysical prospecting techniques is being developed and applied. The distribution of radiogenic sources within the igneous rocks of various ages and magma types will be determined by a correlation between radioelement composition and the bulk chemistry of the rock. Surface sampling and measurement of the radiogenic heat-producing elements are known to be unreliable as they are preferentially removed by ground-water circulation and weathering. The correlation between the bulk chemistry of the rock (which can be measured reliably from surface samples) and radiogenic heat generation is being calibrated by detailed studies at a number of locations in the eastern United States.

Initial studies are developing a methodology for the location of radiogenic heat sources buried beneath the insulating sedimentary rocks of the Atlantic Coastal Plain. Choice of a drill site in the Atlantic Coastal Plain with a high geothermal resource potential depends on favorable:

(1) concentration of radiogenic elements in granitic rocks beneath a sedimentary insulator;
(2) thermal conductivity of the sedimentary insulator;
(3) thickness of the sedimentary insulator; and
(4) reservoir conditions in the permeable sedimentary rocks overlying the radiogenic heat source.

Because it is not economically feasible to select drilling sites on the Atlantic Coastal Plain without geophysical and geological models, it is advisable to base the development of these models on a substantial and accurate data base which can be partially derived from the exposed rocks of the Piedmont and enhanced by basement studies beneath the Atlantic Coastal Plain.

PERSONNEL OF PROGRAM

October 1, 1978 - March 30, 1979

GEOLOGY AND PETROLOGY, Lynn Glover III, Principal Investigator

J. A. Speer, Research Associate
S. S. Farrar, Research Associate
S. W. Becker, Research Associate
R. J. Gleason, Research Associate
G. Russell, Research Associate
W. Russell, Analytical Chemist
J. Reilly, Graduate Research Assistant
C. Newton, Graduate Research Assistant
P. Kaygi, Graduate Research Assistant

GEOCHEMISTRY, A. Krishna Sinha, Principal Investigator

J. R. Sans, Research Associate
S. T. Hall, Research Associate
D. McKay, Research Associate
B. Hanan, Graduate Research Assistant
S. Dickerson, Laboratory Aide
C. R. Miner, Laboratory Aide (part-time)
P. Stock, Laboratory Aide

GEOPHYSICS, John K. Costain, Principal Investigator

A. H. Cogbill, Research Associate
L. D. Perry, Research Associate
J. J. Lambiase, Research Associate
S. Dashevsky, Research Specialist
M. Svetlichny, Research Specialist
B. U. Sans, Research Specialist
W. McClung, Research Specialist
S. Higgins, Research Specialist
T. H. Arnold, Laboratory Aide (part-time)
M. McKinney, Laboratory Aide
G. Schafer, Laboratory Technician (part-time)
B. Thoreson, Computer Programmer (part-time)
R. Bard, Computer Programmer (part-time)
R. A. Davis, Co-op Student
R. Laczniak, Graduate Research Assistant

ADMINISTRATIVE ASSISTANT
Margaret Paterson

SECRETARIES

Sandra Long
Tish Glosh
Nhury Schurig
Marjorie Dellers

DRAFTSMAN-PHOTOGRAPHER

David Brown

SEISMIC AND DRILLING

W. G. Coulson, Supervisor and Core Driller
W. Shumate, Laboratory Instrument Maker
H. Neuburg, Research Associate
G. Dean, Core Driller Operator
D. Thomas, Core Driller Helper
R. Bowman, Core Driller Helper
C. Conway, Laboratory Technician
M. Friedly, Laboratory Technician
C. Greene, Laboratory Technician
J. Sheridan, Laboratory Technician

TALKS GIVEN TO DATE

Evaluation of the geothermal potential of hot springs in Northwestern Virginia, American Nuclear Society, Denver, Colorado, April, 1977 (Speaker: P.A. Geiser, University of Connecticut).

Structural controls of thermal springs in the Warm Springs Anticline, by P.A. Geiser and J.K. Costain, Southeastern Geological Society of America, Winston-Salem, North Carolina, April 1977 (Speaker: P.A. Geiser).

Low-temperature resources of the eastern United States, Second NATO-CCMS Meeting on Dry Hot Rock Geothermal Energy, Los Alamos Scientific Laboratory, Los Alamos, New Mexico, June 1977 (Speaker: J.K. Costain).

Low-temperature geothermal resources of the eastern United States, Geological Society of Washington, Washington, D.C., October 1977 (Speaker: J.K. Costain).

Low-temperature geothermal resources in the eastern United States, 1977 Annual Meeting of the Gological Society of America, November 1977 (Speaker: J.K. Costain).

Low-temperature geothermal resources in the eastern United States, Potomac Geophysical Society, November 1977 (Speaker: J.K. Costain).

Geothermal resource potential of the eastern United States, Geothermal Resource Council Special Short Course No. 7, "Geothermal Energy: A National Opportunity" (The Federal Impact), Washington D.C. May 1978 (Speaker: J.K. Costain).

Geothermal resource potential of the eastern United States, Nordic Symposium on Geothermal Energy, Gothenburg, Sweden, May 1978 (Speaker: J.K. Costain).

Geothermal resources of the Atlantic coastal plain, th Energy Technology Conference and Exposition, Washington D.C. February 1979 (Speaker: J.K. Costain).

Geothermal resource potential of the Atlantic Coastal Plain, North-South Carolina section of the American Institute of Mining Engineers, Raleigh, Noth Carolina, March 1979 (Speaker: J.J. Lambiase).

Geothermal resource potential of the Atlantic Coastal Plain, by J.J. Lambiase, S.S. Dashevsky, R.J. Gleason and J.K. Costain, 2nd Symposium on the Southeastern Coastal Plain, Americas, Georgia, March 1979 (Speaker: J.J. Lambiase).

Detailed temperature logging as a useful tool for lithologic interpretation, by J.J. Lambiase, M. Svetlichny, S.S. Dashevsky, B.U. Sans, and J.K. Costain, American Association of Petroleum Geologists Annual Meeting, Houston, Texas, March 1979 (Speaker: J.J. Lambiase).

ABSTRACTS PUBLISHED TO DATE

Geiser, P.A. and J.K. Costain. 1977. Evaluation of the geothermal potential of the hot springs of northwestern Virginia. Abstracts of ANS Topical Meeting on Energy and Mineral Resource Recovery. Golden, Colorado, April 12-14, p. 33.

Geiser, P.A. and J.K. Costain. 1977. Structural controls of thermal springs in the Warm Springs anticline, Virginia. Abstracts, Geol. Soc. America SE Section, Winston-Salem, North Carolina.

Costain, J.K., L. Glover III, A.K. Sinha. 1977. Low-temperature geothermal resources in the eastern United States. Program with Abstracts, Annual Meeting of Geological Society of America, Seattle, Washington.

Costain, J.K. and A.K. Sinha. 1978. Relationship between heat flow and heat generation in the southeastern United States. Program with Abstracts, Geological Society of America, SE Section Meeting, April.

Costain, J.K. A new model for the linear relationship between heat flow and heat generation. Transactions, American Geophysical Union. 59:p. 392.

Becker, S.W. 1978. Petrology of the Cuffytown Creek pluton. Geol. Soc. Amer. Abstracts with Programs, v. 10.

Farrar, S.S. 1979. Tectonics of the fault bounded Raleigh block, eastern Piedmont, North Carolina. Geol. Soc. Amer., Abstracts with Programs. v. 11.

Farrar, S.S. 1979. Lithology and metamophism of Raleigh block, eastern Piedmont, North Carolina. Geol. Soc. Amer. Abstracts with Programs. v. 11, p. 177-178.

PAPERS SUBMITTED FOR PUBLICATION

Low-temperature geothermal resource potential of the eastern United States. J. K. Costain, L. Glover, III, and A. K. Sinha. Submitted for publication in EOS, Transactions, American Geophysical Union.

Nature and distribution of geothermal energy. Proceedings: Klamath Falls Symposium on Geothermal Energy, in press. L.J.P. Muffler, J.K. Costain, D. Foley, E.A. Sammel and W. Youngquist.

Geothermal resource potential of the Northern Atlantic Coastal Plain. J.J. Lambiase, S.S.Dashevsky, J.K. Costain, R.J. Gleason and W.S. McClung. 1979. Submitted to Science.

Heat flow in western Virginia and a model for the origin of thermal springs in the folded Appalachians. L.D. Perry, J.K. Costain and P.A. Geiser. 1979, in press, Journal of Geophysical Research.

Prograde Metamorphism of the pelitic rocks in the contact aureole and xenoliths of the Liberty Hill pluton, South Carolina. J.A. Speer. 1979. Submitted to American Journal of Science.

Tectogenesis of the rocks surrounding the Winnsboro Intrusive Complex: W.C. Bourland and S. Farrar. 1979. Submitted to Geologic Notes, South Carolina Development Board, Division of Geology.

PAPERS PUBLISHED

Speer, J.A. 1978. Molybdenum mineralization in the Liberty Hill and Winnsboro plutons, South Carolina. Ec. Geol., v. 73, p.558-561.

Glover, L. III, 1979. General geology of the East Coast with emphasis on potential geothermal energy regions: a detailed summary. Proceedings: A Symposium of geothermal energy and its direct uses in the eastern United States - Geothermal Resources Council Special Report No. 5, p. 9-11.

Costain, J.K. 1979. Geothermal exploration methods and results: Atlantic Coastal Plain. Proceedings: A Symposium of geothermal energy and its direct uses in the eastern United States - Geothermal Resources Council Special Report No. 5, p.13-22.

PROGRESS

A. GEOLOGY AND PETROLOY

Lynn Glover, III, Principal Investigator

J. A. Speer, Research Associate

S. S. Farrar, Research Associate

S. W. Becker, Research Associate

R. J. Gleason, Research Associate

W. Russell, Geologist/Analytical Chemist

Operations Summary--January-March 1979

During the report period, J. A. Speer, S. S. Farrar, and S. W. Becker concentrated their efforts on several technical papers summarizing project-funded aspects of Piedmont geology. R. J. Gleason divided his time between office and laboratory work concerning Coastal Plain basement studies, and various activities requiring travel away from VPI & SU.

Speer completed a paper entitled "Prograde metamorphism of the pelitic rocks in the contact aureole and xenoliths of the Liberty Hill pluton, South Carolina" and has submitted it to the American Journal of Science for publication. Speer also spent four days in Wilmington, N.C., overseeing the drilling of Coastal Plain drill-hole #14 to basement. Approximately one week was devoted to preliminary petrographic and microprobe analyses of a short section of core from this hole. Speer, Farrar, and Becker collaborated on a paper, "Field relations and petrology of the post-metamorphic, coarse-grained granites and associated rocks in the southern Appalachian Piedmont," which was prepared for the upcoming I.U.G.S. Caledonide Project, convening in Blacksburg, Va. in September, 1979.

Farrar completed a paper, co-authored with W. C. Bourland, on "Tectogenesis of the rocks surrounding the Winnsboro intrusive complex," which will be published in Geologic Notes (South Carolina Development Board - Division of Geology). In addition, Farrar finished the text of "Correlation of aeromagnetic and geologic maps for the southern Raleigh belt and adjacent Carolina slate belt, N.C.", and he attended a related meeting with I. Zietz and R. Hatcher in Washington, D. C. Following the completion of the Butterwood Creek drill hole, Farrar prepared a lithologic log of the core from this location.

In addition to co-authoring the Caledonide Project paper with Speer and Farrar, Becker performed petrographic and microprobe analyses of sections of basement core from Dort, N.C. In addition, she has been preparing a paper for publication entitled "Petrology of the Cuffytown Creek pluton" and expects to complete this work by Summer, 1979.

Gleason spent approximately one quarter of the report period on work performed away from V.P.I.& S.U.. Ten days were spent monitoring the drilling of Coastal Plain drill-holes #15, #15-A, and #14-A, basement holes located respectively in Jacksonville, Folkstone, and Southport, N.C. Gleason and J. Lambiase prepared and presented data at a site selection meeting at Los Alamos Scientific Laboratory on potential hot dry rock sites at Wallops Island, Va. and Stumpy Point, N.C. Gleason also attended the annual meeting of the Northeast section of the Geological Society of America. At VPI & SU, Gleason prepared Coastal Plain basement depth and lithology data and presented it at the deep geothermal well site selection meeting held in Blacksburg in January. Georgia Coastal Plain basement data were used to prepare a generalized structure contour map of the basement surface. All existing basement data for the Atlantic Coastal Plain were prepared for

computerized filing. Gleason also logged the short basement core segments from Coastal Plain drill-holes #15 and #14 as well as initial core sections from drill-hole #25-A. Petrographic studies of basement from holes #15 and #25-A were initiated.

Lynn Glover, III and Richard J. Gleason attended the Deep Hole Selection Panel meeting at Blacksbury, VA on January 16-17 and presented a regional interpretation of basement heat sources. The Crisfield, MD deep test site was selected by the panel. Glover also attended a Department of Energy budget and planning meeting held in Washington, DC on January 30-February 1, 1979. An article, "General geology of the east coast with emphasis on potential geothermal energy regions: a detailed summary" by Lynn Glover, III appears in Special Report No. 5, A Symposium of Geothermal Energy and its Direct Uses in the Eastern United States.

In the following report, Speer presents his paper on "Prograde metamorphism of the pelitic rocks in the contact aureole and xenoliths of the Liberty Hill pluton, South Carolina." Gleason reports on the current status of the Atlantic Coastal Plain basement data compilation.

PROGRADE METAMORPHISM OF THE PELITIC ROCKS IN THE CONTACT AUREOLE AND XENOLITHS OF THE LIBERTY HILL PLUTON, SOUTH CAROLINA

J. Alexander Speer

The following section describes the contact metamorphism of the Liberty Hill pluton. This paper, written primarily for professional petrologists, has been submitted to the American Journal of Science. The work leads to several conclusions which increase the understanding of the variations in heat production and the behavior of U and Th in the Liberty Hill. These conclusions can be applied to other granites which the Liberty Hill closely resembles.

A fluid phase, dominantly water, flowed from the country rock into the granite. Because erosion has removed the top portion of the original pluton, the exposed granite is a section through the bottom of the pluton. The influx of water may thus represent the lower half of a convection cell of magmatic-"ground" water established by the cooling pluton. This movement of the fluid phase, with its attendant chemical gradients, provides a mechanism for changing mineral assemblages, isotopic compositons, and transporting trace elements.

Movement of the fluid phase in a convection cell has several implications for the Liberty Hill. In the magmatic stage, U and Th could not have been transported outward at the level currently exposed in the pluton because the dominant flow direction was inward. The chemical gradients did cause different U- and Th-bearing accessory minerals to form in the rim and core of the pluton. In the core, U and Th reside in allanite, zircon, titanite, and apatite. In the rim, in addition to the above minerals, uraninite, thorite, and xenotime provide sites for U and Th. The two assemblages may differ in their response to subsequent hydrothermal alteration and weathering.

If convection cells are a common feature of the coarse-grained granites, sytematic enrichment of U and Th may occur at certain levels under ideal conditions. Areal variations in U and Th have not been observed in the Liberty Hill, perhaps because of a low sample density. Extensive sampling, which may not be possible in the southeast, would be needed to detect small variations in U and Th. Enrichment of U and Th may also be limited because of the subdued nature of the convection cell around the Liberty Hill, compared to the more vigorous convection cells around plutons in the western U.S. The depth of emplacement of the Liberty Hill is greater than that of the shallower western plutons, which decreases the porosity of the rocks and inhibits circulation.

The upward concentration of U and Th in the continental crust is an attractive hypothesis to explain the linear relation between heat generation and heat flow. Whether the upward concentration is only generally true as a result of processes acting over geologic time or is true for all localities is a question of primary interest. Several methods have or can be used to investigate this question:

1. drill many, very deep holes in different lithologies in an area where the structure is well understood;

2. study a number of different lithologies in an area where significant topographic or structural relief is developed;

3. study a group of rocks of similar age, composition, and evolution whose depths of formation can be determined.

At present the third is the only method available in the southeast to study the possibility of decreasing U and Th with increasing depth. The following paper demonstrates the effort required to obtain one data point.

The work on the contact aureole of the Liberty Hill also produced an explanation of the magnetic anomaly encircling the pluton. Magnetic anomalies occur around several of the other plutons. These magnetic anomalies are a result of the contact metamorphism and can be used to identify the geologic features of similar plutons buried under the coastal plain.

ABSTRACT. The Liberty Hill pluton, South Carolina, one of the ca. 300 y. old, coarse-grained granites of the southeast U.S.A. Piedmont, is surrounded by a contact metamorphic aureole that ranges in width up to 4 km on the surface. The country rocks have an earlier, regional greenschist facies assemblage of chlorite + vermiculite + epidote + albite + quartz. The mineral isograds encountered toward the granite contact are: vermiculite-out, epidote-albite-out which coincides with cordierite-biotite-andesine-in, chlorite-out, K feldspar-in, and magnetite or muscovite-out. Andalusite, sillimanite, garnet and orthopyroxene appear in the xenoliths. The successive contact metamorphic facies are greenschist, amphibolite, and granulite. Electron microprobe analyses indicate that the Fe-Mg minerals vary systematically in composition with metamorphic grade. The most prominant change is the Fe enrichment of the silicate assemblage in the aureole, resulting from a succession of continuous reactions which consume the Fe-Ti oxides, muscovite, and chlorite to produce cordierite and biotite.

The estimated pressure for the contact metamorphism is 4.5 kb (4.5×10^8 Pa), which corresponds to a depth of emplacement of between 15 and 18 km for the Liberty Hill pluton. The temperatures estimated for the xenoliths are 670-740°C. Maximum estimates of temperature in the aureole are 680°C at the contact and less than 610°C in the outermost aureole. PH_2O is thought to be about half P_{total} in the xenoliths. PH_2O cannot be determined for the aureole. The Liberty Hill pluton has a core of biotite-amphibole granite with granulite facies xenoliths and a border comprised of biotite and muscovite-biotite granite with amphibolite facies xenoliths. This geometry suggests a radial variation in intensive parameters within the granite, most likely temperature, oxygen fugacity, and water fugacity.

Introduction

The granitic rocks of the southeastern Piedmont have been divided into several groups on the basis of age, composition, and field appearance (Butler and Ragland, 1969a; Fullagar, 1971; Wagener and Howell, 1973; Wright et al., 1975). The Liberty Hill is one of the ca. 300 m.y. post-metamorphic granitic plutons included in the eastern subgroup of coarse-grained granites (Butler and Ragland, 1969). Previous geologic mapping indicated that it has a cordierite-bearing, thermal metamorphic aureole (Bell et al., 1974), which is similar to the contact aureoles of several of the other plutons in the same group.

This paper is a result of a study of the magmatic and post-consolidation evolution of these granites. Examination of the contact metamorphism offers a better opportunity for estimating intensive parameters of pressure, temperature, oxygen fugacity, water fugacity, and their variation following emplacement than does study of the granite alone. The results also provide constraints on the regional conditions during intrusion, and, to a lesser extent, on the origin of the magma. In addition, the aureole of the Liberty Hill provides a clear picture of some mineral chemistries and metamorphic reactions that occur in the contact metamorphism of low grade slates which are often disregarded because of their fine-grain size.

Geologic Setting

The Liberty Hill pluton lies within the Carolina Slate belt of South Carolina, in Kershaw, Lancaster and Fairfield Counties (Figure A-1.1). It was first described as a discrete pluton by Overstreet and Bell (1965a,b), who determined an age for the pluton of 245 $\pm$ 30 m.y. by lead-alpha dating of zircons. Lead-alpha dating methods are commonly unreliable, however, and a whole-rock Rb/Sr age of 299 $\pm$ 8 m.y. (Fullagar, 1971) is probably a more accurate date. Reconnaissance mapping of the entire pluton was done by Wagener (1977). Geologic maps of sections of the pluton have been published by Bell et al. (1974) and by Shiver (1974). Petrographic descriptions of the granite are given by Sloan (1908), Watson (1910), Butler and Ragland (1969a), Wagener and Howell (1973) and Wagener (1977). A detailed study of the petrology of the Liberty Hill pluton has been completed (Speer, in preparation). Gravity data have been collected (Popenoe and Bell, 1975) and interpreted for the entire pluton by Bell and Popenoe (1976). Aeromagnetic measurements have been made in the eastern third of the pluton (U.S.G.S., 1970).

The Liberty Hill pluton comprises three major texturally and mineralogically distinct facies (Figure A-1.1). The predominant facies consists of a very coarse biotite-amphibole granite and quartz monzonite. The second facies, which occurs along the northern and eastern margin of the pluton, consists of a very coarse-grained biotite granite. This border facies on the northern margin of the pluton (Figure A-1.1) contains alkali feldspar phenocrysts up to 10 cm long and prominant muscovite. The border facies is locally separated from the main

Figure A-1.1. Geologic and sample location maps of the Liberty Hill pluton, South Carolina. The contact between the Carolina Slate belt metavolcanic rocks and phyllites is not sharply defined and only their general distribution is shown. The easily recognizable contact metamorphic aureole is best developed in the phyllites. The contact of the Dutchman's Creek gabbro is from McSween (1972). KR1, 2, and 3 are the locations of the bore holes encountering xenoliths. The sample numbers in the map at the lower left refer to the location of hornfels samples. The geology and samples of the area surrounding the Fort Hill and Dry Branch traverses are shown in Figure A-1.3.

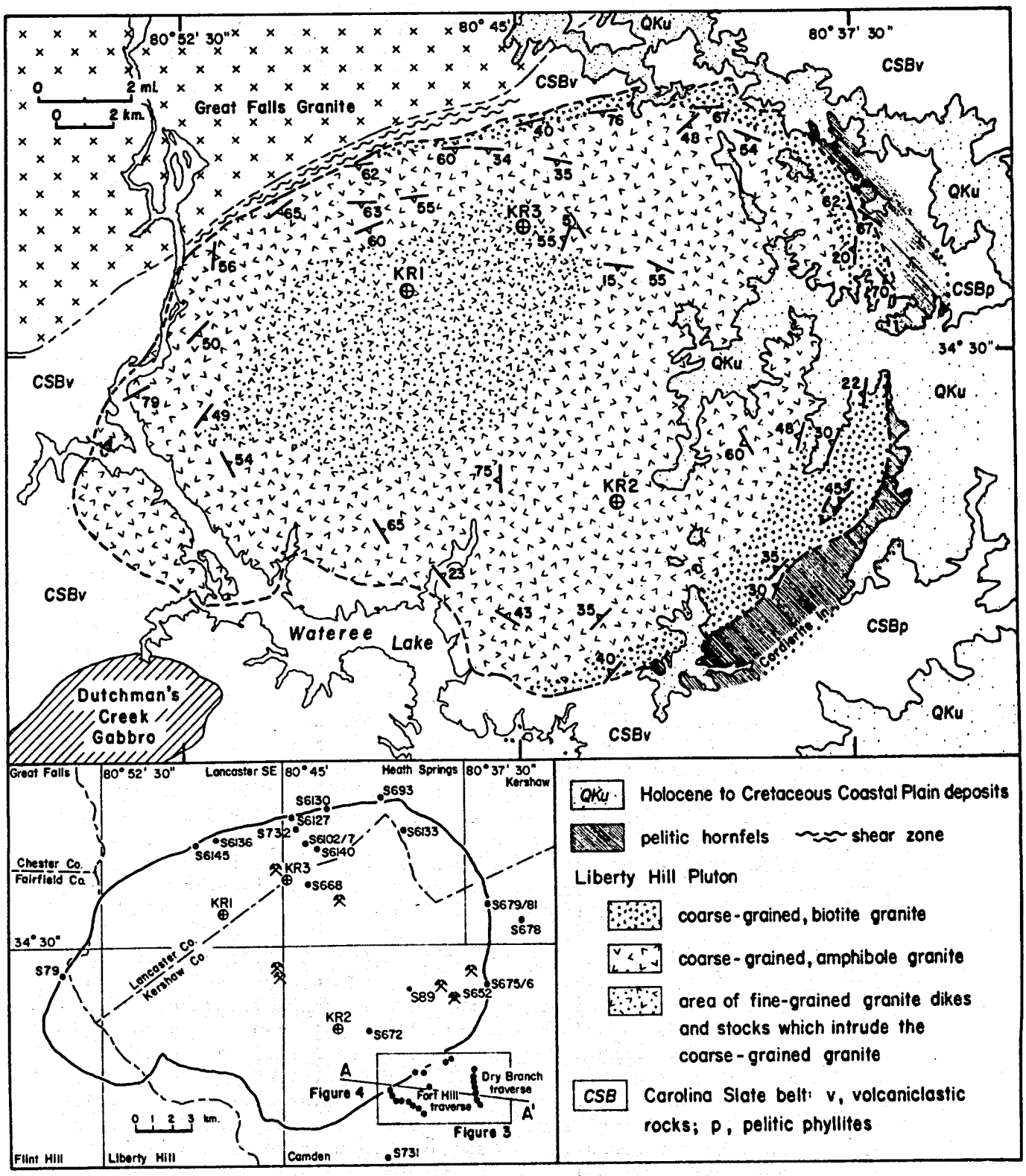
80° 52' 30"
80° 45'
80° 37' 30"
34° 30"
0 2 mi.
0 2 km.
Great Falls Granite
QKu
CSBv
CSBp
KR1
KR2
KR3
Wateree Lake
Dutchman's Creek Gabbro
Cordelia Inn.
Great Falls
Lancaster SE
Heath Springs
Kershaw
Chester Co.
Fairfield Co.
Lancaster Co.
Kershaw Co.
S693
S6130
S6127
S732
S6102/7
S6140
S6136
S6145
S6133
S668
S679/81
S678
S79
S89
S652
S675/6
S672
S731
A
A'
Figure 4
Figure 3
Dry Branch traverse
Fort Hill traverse
0 1 2 3 km.
Flint Hill
Liberty Hill
Camden
QKu Holocene to Cretaceous Coastal Plain deposits
pelitic hornfels
shear zone
Liberty Hill Pluton
coarse-grained, biotite granite
coarse-grained, amphibole granite
area of fine-grained granite dikes and stocks which intrude the coarse-grained granite
CSB Carolina Slate belt: v, volcaniclastic rocks; p, pelitic phyllites

pluton by a structurally conformable, discontinuous screen of hornfels which is best developed on the northern edge. The third and youngest facies is a fine- to medium-grained biotite granite that intruded the western part of the pluton in the form of large dikes and small stocks.

The boundary of the pluton is irregular on a scale of a kilometer and is believed to be a result of lit-par-lit intrusion. Country rocks mixed with a large volume of granite constitute the outer xenoliths. The scale of irregularity in the contact introduces uncertainty in the determination of the distance of hornfels samples from the granite contact.

The three-dimensional shape of the pluton is an asymmetric funnel as suggested by the igneous layering (Figure A-1.1). The igneous layering is defined by the alignment of tabular alkali feldspar crystals and the orientation of tabular xenoliths of country rock. The geometry agrees with the gravity model of Bell and Popenoe (1976).

The Liberty Hill pluton is emplaced mainly in the Carolina Slate belt which consists of weakly metamorphosed pyroclastic and epiclastic rocks. Many of the original textures are preserved. The regional metamorphism, considered to have been in the low-pressure, greenschist facies (McCauley, 1961; Wagener, 1968; Butler and Ragland, 1969b; Sundelius, 1970; Randazzo, 1969, 1972), probably occurred between 520 and 430 m.y. ago (Butler, 1972; Butler and Howell, 1976). The depositional age of the Carolina Slate belt rocks is most likely Cambrian, based on paleontological evidence (St. Jean, 1973), several Rb-Sr isotopic ages (Hills and Butler, 1968; Fullagar, 1971; Black and Fullagar, 1976; Black, 1978a,b) and U-Pb determinations on zircons (Wright and Seiders, 1977). Several suggestions have been made for formational names of lithostratigraphic units present in the Carolina Slate belt based on work in local areas (Conley and Bain, 1965; Stromquist and Sundelius, 1969; Secor and Wagener, 1968; Wagener, 1970). As the nature of any lateral facies changes between these type areas is unknown and interbedding or structural repetition of similar rock types is common, no attempt has been made to apply these designations in the vicinity of the Liberty Hill pluton.

The Carolina Slate belt enclosing the Liberty Hill pluton comprises mainly metamorphosed pyroclastic and hypabyssal rocks of intermediate to felsic compositions which are amphibolites and greenstones. Pelitic rocks are volumetrically significant only on the eastern margin of the Libery Hill pluton (Figure A-1.1), although they occur throughout the area. This work concentrates on these pelitic rocks, in which the contact aureole is best developed (Figure A-1.1). The pelitic rocks are phyllites with a grain size of generally less than 0.04 mm, bright green in color, and are massive to finely laminated. They were originally mudstones and siltstones. Calcareous rocks and fine-grained greywackes are locally interbedded with the metapelites. Sedimentary structures such as graded-bedding and cross-bedding, as well as structures resulting from penecontemporaneous deformation, are locally preserved. These regionally metamorp-

hosed pelitic rocks contain quartz, chlorite, white mica and plagioclase (albite) as well as lesser amounts of vermiculite, epidote, and opaques. Compositions were determined for metapelites representative of the different grades of contact metamorphism (Table A-1.1)*. The methods of analysis and calculation for AFM and AKF projections are given in Appendix A-1.1. Other analyses of Slate Belt phyllites have been presented by Laney (1910), Pogue (1910), Stuckey (1928), Conley (1962), McCauley (1961), Butler (1964), Sundelius (1970) and Seiders (1978). A comparison of all these rock analyses in AFM projection is shown in Figure A-1.2a. Rocks with extremely aluminous compositions reported in the literature have been omitted because they are from areas of intense hydrothermal alteration associated with base and precious metal deposits in the Carolina Slate belt. Average greywacke and shale compositions (Wedepohl, 1969) are also included for comparison. There is a wide range of compositions if all the available analyses are considered. For the phyllites in the area of the Liberty Hill pluton the analyses are fairly similar and the range smaller, except for the CaO, Na_2O, and K_2O contents. The variable content of these oxides results in the spread of A values among the samples in the AFM and AKF projections in Figure A-1.2. Fe/Fe+Mg for all samples lies between 0.56 and 0.72 and lies to the iron-rich side of the average greywacke and shale (Figure A-1.2a). With increasing metamorphic grade, water content decreases from 3.6-6 percent to 1 percent or less. No other systematic chemical changes with metamorphic grade are noted.

On the northwest, the Liberty Hill pluton is adjacent to the Great Falls metagranite (Figure A-1.1), which evidently includes the Pleasant Hill granite of Shiver (1974) and the "granite northwest of Heath Springs" of Wagener (1977). It is a monzogranite with variably developed gneissosity consisting of quartz, microcline, plagioclase (An_{28-10}), biotite, white mica, epidote, chlorite, garnet, zircon, and opaques. It has yielded a Rb/Sr isotopic age of 554 $\pm$ 63 m.y. (Fullagar, 1971) and appears to have been metamorphosed at a grade similar to that of the surrounding Carolina Slate belt. The contact between the Liberty Hill and Great Falls granites may be a fault contact. Outcrop and float along this zone consists of silicified rocks and quartz veins. Bell and Popenoe (1976) have interpreted this to be an extension of the boundary fault of the Triassic Crowburg basin.

Petrography

Pelitic hornfelses from the Liberty Hill contact aureole and xenoliths were collected from all areas of the pluton. Rocks outside the aureole were also sampled and examined (Figure A-1.1). Because rocks with pelitic compositions are most abundant on the southeastern margin of the pluton, this area was studied in detail to determine the prograde metamorphic sequence. Two traverses were sampled in the drainage basin of Quarter Creek, one along a stream south of Fort Hill and one along the west fork of Dry Branch Creek (Figure A-1.3). A

---

* Tables A-1.1 to A-1.9 are in Appendix A-1.3.

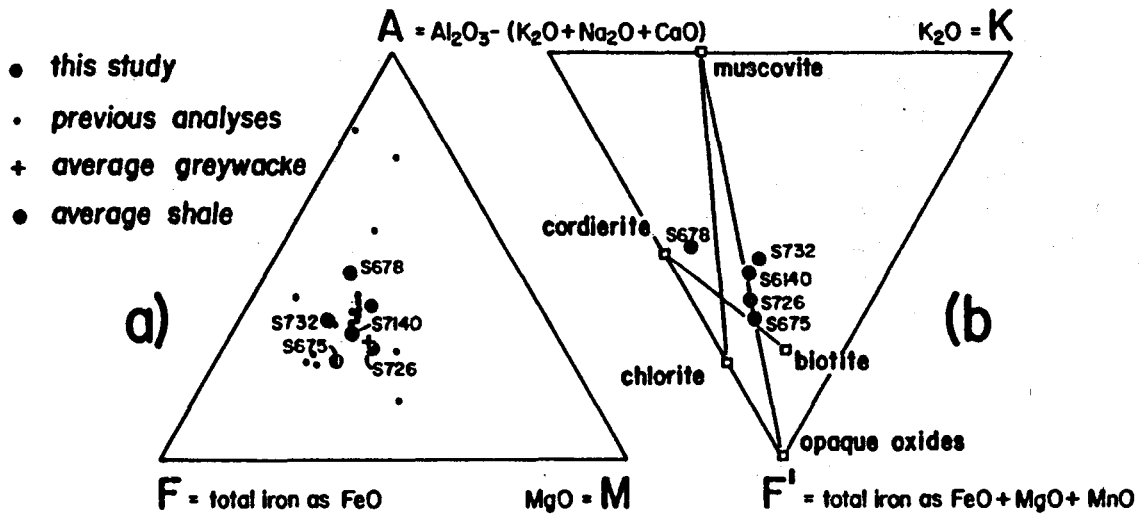

Figure A-1.2. (a) AFM projection through alkali feldspar showing compositions of the five Carolina Slate belt phyllites in the vicinity of the Liberty Hill pluton from Table A-1.1 (large, solid circles). For comparison, previously reported analyses of Carolina Slate belt phyllites are included (small circles), references for these are given in the text. The average greywacke and shale are from Wedepohl (1969). (b) AKF' diagram showing compositions of the Carolina Slate belt phyllites in the vicinity of the Liberty Hill pluton.

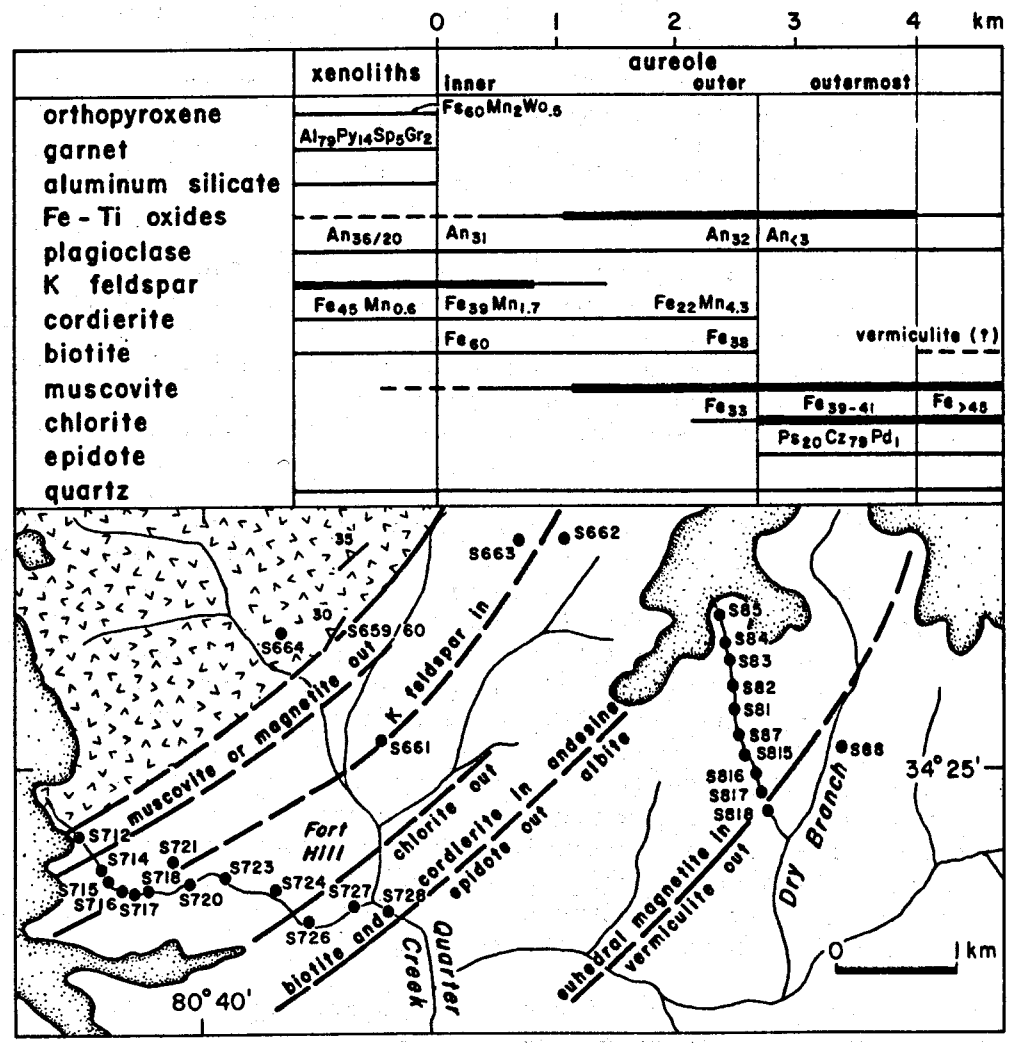

Figure A-1.3. Detailed geologic and location map in the vicinity of the Fort Hill and Dry Branch traverses. The chart above shows variation of mineralogy and mineral chemistry along an E-W profile. The isograds, defined by the first or last appearance of a given mineral in the pelitic rocks, are isoreaction-grads (Winkler, 1974). The granite in this section of the Liberty Hill pluton is a biotite granite, with an igneous lamination which dips to the northwest at about 30°. It is believed that the isograds parallel this attitude.

shallow granite contact dipping 30-40° in the area northwest of the traverses is indicated by the igneous foliation of the granite and substantiated by gravity and magnetic modeling (Bell and Popenoe, 1976; Dunbar and Speer, 1977). It is believed that the isogradic surfaces parallel this contact and dip at the same shallow angle. Additional samples were obtained from the xenoliths encountered in the three drill holes: KR1, KR2, and KR3 (Figure A-1.1) drilled to the depths of 129.5 m (425 ft), 128.0 m (420 ft), and 406.6 m (1334 ft), respectively.

The mineral sequence in the samples from the two traverses in the metamorphic aureole as well as the minerals present in the pelitic xenoliths and country rocks are shown in Figure A-1.3. Mineral assemblages for all samples are given in Appendix A-1.2. The isograds are defined by the first or last appearance of a given mineral in the pelitic rocks and as such are isoreaction-grads (Winkler, 1974).

Before the emplacement of the Liberty Hill pluton, the pelitic country rocks were subjected to, or were undergoing, a regional metamorphism in the greenschist facies. The regional metamorphic assemblage is vermiculite + white mica + chlorite + albite + epidote + quartz + opaques. What in thin section appears to be biotite occurs locally and is believed to be vermiculite as discussed in the section on mineralogy. Its sporadic occurrence is a result of either variable rock compositions or only local attainment of suitable metamorphic conditions. Vermiculite in the mineral assemblages of the Carolina Slate belt phyllites in the vicinity of the Liberty Hill pluton indicates conditions below biotite zone according to Velde's (1978) examination of similar assemblages in prograde metamorphic sequences. Velde's (1978) conclusion about the metamorphic stability is verified in the Liberty Hill aureole; the vermiculite disappears before the appearance of biotite in the aureole.

At the outermost edge of the contact aureole, only subtle changes in mineralogy, texture, and modes result from the thermal effects. Most noticeable is the disappearance of the biotite-like vermiculite and appearance of euhedral porphyroblasts of magnetite. That these crystals represent an increase in the modal amount of magnetite is indicated by the increase in the total magnetic field at the beginning of the metamorphic aureole (Figure A-1.4). Between the euhedral magnetite-in isograd and the cordierite-in isograd, the area is referred to as the outermost aureole (Figure A-1.3). Within the outermost aureole, the mineral assemblage is muscovite + chlorite + epidote + albite + magnetite + ilmenite + quartz. Megascopically the rocks are indistinguishable from the Carolina Slate belt phyllites outside the aureole.

The first new mineral phases to appear in the aureole are cordierite and biotite. Coincident with their appearance is the disappearance of epidote in the metapelites as well as the abrupt change in plagioclase composition from albite to andesine. These changes occur about 2.5 km from the contact and define the beginning of the outer aureole. The pelitic rocks of the outer aureole are distinctly dif-

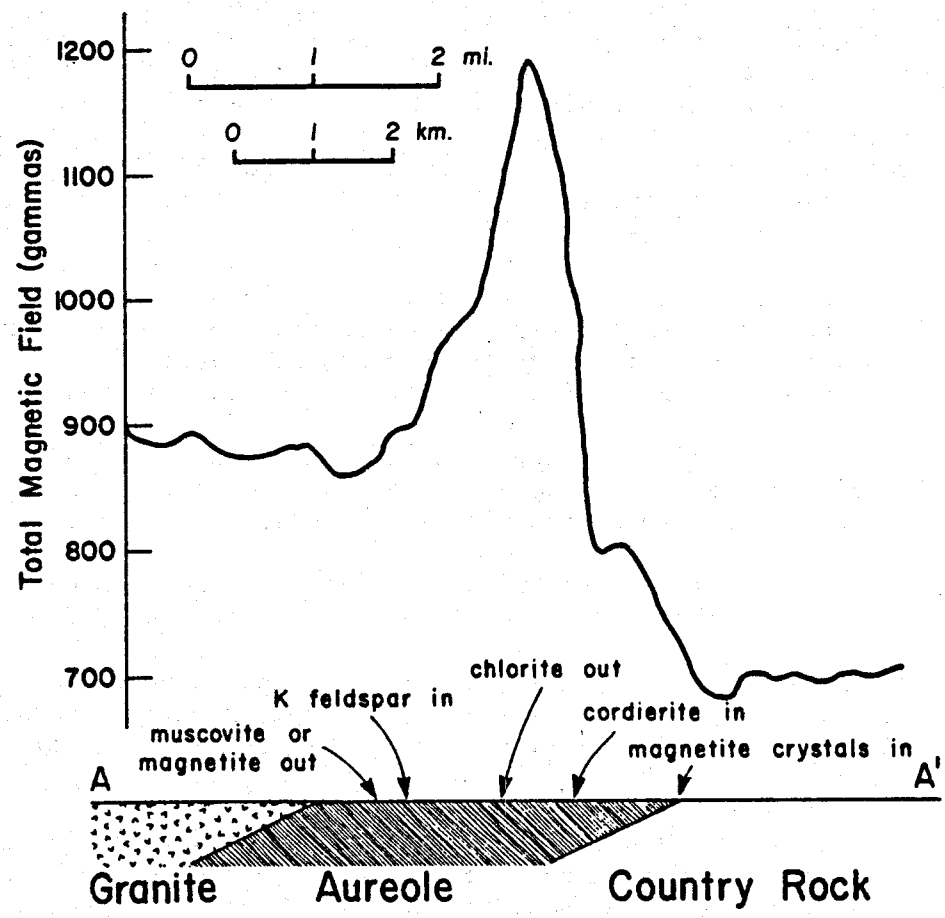

Figure A-1.4. Profile along the section A-A' (Figure A-1.1) of the magnetic anomaly near the Fort Hill traverse, taken from aeromagnetic data (USGS, 1970). At the edge of the outermost aureole, magnetite is produced from non-magnetic oxide minerals and chlorite. Significant amounts of magnetite are produced at the cordierite-in isograd by reaction (2). With the disappearance of chlorite, magnetite is consumed in several successive cordierite-producing reactions (10, 11, 12) until it disappears. The Liberty Hill has a uniformly higher magnetite content than the country rocks.

ferent from those farther from the granite and readily distinguishable as hornfelses. They are grey and have about the same grain size as the Carolina Slate belt phllites, which is too fine-grained to produce meaningful modal analyses. They are spotted with irregularly-shaped porphyroblasts of cordierite up to 2 mm in size. These porphyroblasts are most readily visible on weathered surfaces and are crowded with inclusions of quartz, plagioclase and opaques. At the lowest grades, cordierite appears to make up no more than 20% of the volume of the cordierite porphyroblasts. With increasing metamorphic grade, this percentage increases.

The decrease, by visual estimates, in modal amounts of chlorite and muscovite with the appearance of biotite and cordierite at the beginning of the outer aureole suggests the reaction

$$\text{chlorite} + \text{muscovite} + \text{quartz} - \text{cordierite} + \text{biotite} + H_2O \quad (1)$$

The jump in plagioclase composition from albite to sodic andesine and the disappearance of epidote at the same time as the formation of cordierite and biotite by reaction 1 may indicate a more complex reaction such as

$$\text{chlorite} + \text{muscovite} + \text{epidote} + An_0 + \text{quartz} \rightarrow \text{cordierite} + \text{biotite} + An_{30} + \text{magnetite} + H_2O \quad (2)$$

The appearance of significantly larger modal amounts of magnetite by reaction 2 is illustrated by the more rapid rise of the total magnetic field at the cordierite-in isograd than at the magnetite-in isograd (Figure A-1.4).

Even with the disappearance of chlorite by reaction 2 soon after the appearance of cordierite and biotite, cordierite apparently continues to increase in modal amount with a concurrent decrease of muscovite. The oxides, especially magnetite, which have previously been increasing in abundance from the outermost aureole, also begin to decrease in modal amount. This suggests a second cordierite-producing reaction, ideally summarized as

$$\text{muscovite} + \text{magnetite} + \text{quartz} \rightarrow \text{cordierite} + \text{biotite} + H_2O \quad (3)$$

The decrease in the modal amount of magnetite by reaction 3 following its increase by reaction 2 is illustrated by the peaking of the total magnetic field at the chlorite-out isograd (Figure A-1.4). The transition from the cordierite-producing reaction 2 to reaction 3 can be illustrated in the AKF diagram of Figure A-1.2b. The biotite-cordierite tie line crosses both the muscovite-chlorite and muscovite-magnetite tie lines. Because the muscovite + chlorite decomposition begins as a lower temperature reaction and the chlorite is consumed first, the only remaining crossing tie lines are biotite-cordierite and muscovite-magnetite.

The next new mineral phase to appear in the aureole is alkali feldspar, which marks the beginning of the inner aureole. Alkali feldspar does appear rarely outside the isograd of Figure A-1.3, but only as a relict, detrital mineral. The hornfelses of the inner

aureole are fairly dark, almost black, and have increased in grain size to 0.1 mm or less. Porphyroblasts are absent. Locally, the micas are aligned parallel to the granite contact, making the rocks semi-schists. Metamorphic recrystallization has destroyed most of the fine sedimentary textures in the inner aureole.

Above the alkali feldspar-in isograd, cordierite continues to increase in amount while muscovite and biotite decrease. Oxide minerals are fairly uncommon, as qualitatively indicated by the magnetitc field. No aluminum silicate mineral occurs in the aureole, as would be expected if alkali feldspar were produced from the decomposition of muscovite + quartz by the reaction

$$\text{muscovite} + \text{quartz} \rightarrow \text{aluminum silicate} + \text{K feldspar} + H_2O. \quad (4)$$

Therefore, the alkali feldspar probably forms as a result of an additional cordierite-producing reaction;

$$\text{muscovite} + \text{magnetite} + \text{quartz} \rightarrow \text{cordierite} + \text{K feldspar} + H_2O. \quad (5)$$

Immediately after the appearance of alkali feldspar, the last traces of magnetite disappear in most rocks. Locally, muscovite rather than magnetite may disappear. Whether there is disappearance of muscovite or magnetite by reaction 5 is controlled by the rock compositions. As shown in Figure A-1.2b, the rock analyses of Table A-1.1 fall on the muscovite side of the cordierite-biotite tie line and accounts for the more common disappearance of magnetite. As the granite contact is approached, the remaining muscovite does soon disappear in most rocks of the inner aureole. The disappearance of both muscovite and magnetite halts the cordierite-producing reactions 3 and 5. The rarity of aluminum silicates and the abundance of cordierite in the Liberty Hill hornfelses suggest that reaction 5 is responsible for the eventual disappearance of muscovite in most rocks. Muscovite + quartz persist locally in biotite-poor rocks and eventually may decompose by reaction 4 to form the scarce aluminum silicate minerals found in the outer xenoliths.

Muscovite that is texturally distinct occurs in some rocks of the inner aureole. Whereas the muscovite present in the lower prograde sequence conforms to the weak schistosity and occurs as discrete grains, this distinctive muscovite occurs as larger poikilitic grains oriented at all angles to the foliation or as intergrowths and overgrowths on biotite. Because of this textural evidence, it is believed that this muscovite is a result of retrograde reactions, largely the reversal of reactions 3 and 5.

The pelitic hornfelses of the xenoliths resemble the hornfelses of the inner aureole except for a coarser grain size of 0.2 mm or less, and garnet porphyroblasts, which, though small in number, are 3-5 mm across in rocks of appropriate composition. The garnets are commonly surrounded by a rim of felsic minerals devoid of biotite. Large pelitic xenoliths contain irregular 1-5 cm veins of felsic gran-

ite. Whether these veins are segregations of partial melt from the pelitic xenoliths or injection of molten material from the granite is unknown.

Several additional mineral phases appear in the xenoliths that are not present in the aureole. They are garnet, orthopyroxene, and the aluminum silicates: andalusite, sillimanite, and fibrolite. The metamorphic mineral assemblages observed in the pelitic xenoliths, which also contain quartz, plagioclase and alkali feldspar, are:

in the coarse, biotite granite
(1) cordierite + biotite ± muscovite
(2) sillimanite + muscovite
(3) andalusite + cordierite + biotite + muscovite
in the coarse, amphibole-biotite granite
(4) orthopyroxene + garnet + cordierite + biotite
(5) orthopyroxene + cordierite + biotite
(6) orthopyroxene + biotite
in both types of coarse granite
(7) biotite
(8) garnet + cordierite + biotite.

The first three assemblages have been found in xenoliths from the outer part of the Liberty Hill pluton, which is a biotite granite. Assemblages 4 to 6 are confined to the amphibole-biotite granite in the center of the Liberty Hill pluton. Assemblages 7 and 8 are ubiquitous. The differing assemblages found in the two granite types suggest that the inner xenoliths reached a higher grade of metamorphism, shown by the presence of orthopyroxene, and that there may be a continual spatial variation of intensive parameters such as temperature, water or oxygen fugacity in the pluton as well as the contact aureole.

There is no petrographic evidence indicating the reactions leading to the formation of the aluminum silicates, garnet or orthopyroxene. The aluminum silicates are thought to form by the decomposition of muscovite by reaction 5, perhaps, as well as by the reaction

$$\text{cordierite} + \text{muscovite} \rightarrow \text{aluminum silicate} + \text{biotite} + \text{quartz} + H_2O \quad (6)$$

On the basis of the mineral phases present, garnet is believed to result from the reaction

$$\text{biotite} + \text{cordierite} + \text{quartz} \rightarrow \text{garnet} + \text{K feldspar} + H_2O \quad (7)$$

and orthopyroxene by the decomposition of biotite + quartz according to the reaction

$$\text{biotite} + \text{quartz} - \text{orthopyroxene} + \text{K feldspar} + H_2O \quad (8)$$

Accessory minerals observed in the metapelites at all metamorphic grades in the aureole and xenoliths are apatite, zircon, tourmaline, and allanite. Iron sulfides are pyrrhotite in the xenoliths and inner aureole and pyrite in the outer and outermost aureole. Chalcopyrite

is scarce but widespread. Exsolved pentlandite in pyrrhotite was observed in several samples. Marcasite is a common alteration product of the pyrrhotite. The common oxide minerals are magnetite and a manganiferous ilmenite. In most cases they have well-developed exsolution features. Because the oxides participate in the metamorphic reactions, the phases present and their abundances change with metamorphic grade. The oxides of the outermost and outer aureole are abundant ilmenite and magnetite. As the inner aureole is approached, magnetite disappears and ilmenite becomes less abundant. Magnetite is usually absent in the xenoliths and ilmenite is scarce.

Mineral Chemistry

Compositions of coexisting mineral phases in polished thin sections were analyzed on a nine-spectrometer, automated ARL-EMX electron microprobe using well-characterized silicates and oxides as standards. The data were converted to oxide weight percentages by a computer program based on the alpha factor correction scheme of Ziebold and Ogilvie (1964) as extended by Bence and Albee (1968) using the correction factors of Albee and Ray (1970). Mineral formulas and components in Tables A-1.2 to A-1.9 were calculated using the computer program SUPERRECAL of Rucklidge (1971). The program also calculates a stoichiometric amount of water and adds it to the oxide weight percentages.

Biotite

Biotite analyses are listed in Table A-1.2. Their atomic ratios, Fe/(Fe+Mg), vary from 0.38 to 0.67 with a small and poorly defined sympathetic increase in tetrahedral aluminum content from 2.4 to 2.7 (Figure A-1.5a). Total interlayer and octahedral site occupancies are less than the ideal values. On the whole, the biotites lie to the aluminous side of an intermediate composition between the end members annite, siderophyllite, phlogopite and eastonite (Figure A-1.5a). The more magnesian and less aluminous biotites occur in the outer aureole. The biotites generally become more iron rich and aluminous with increasing metamorphic grade (Figure A-1.5a). The titanium content of the biotites is variable, showing an increase with both metamorphic grade and iron content of the biotite. Figure A-1.5b is a plot of the number of titanium atoms in the formula unit versus Fe/(Fe+Mg) of the biotite. All the biotites coexist with ilmenite, which is the only other significant titanium-bearing phase.

As discussed in more detail below, the Fe/(Fe+Mg) ratio of the biotite results from increasing metamorphic grade. The accompanying change in titanium and tetrahedral aluminum contents may be the result of either the variation in metamorphic conditions, independent of the Fe/(Fe+Mg) ratio of the biotite, or the Fe/(Fe+Mg) ratio which in turn is a result of the metamorphic grade and mineral assemblage. The weaker trend of increasing tetrahedral aluminum content with increasing titanium content could be explained as the result of the necessary substitution to retain charge balance of the type $2Si^{IV} + (Mg,Fe)^{VI} - 2Al^{IV} + Ti^{VI}$. But this does not explain the basic cause of the titanium or aluminum variation.

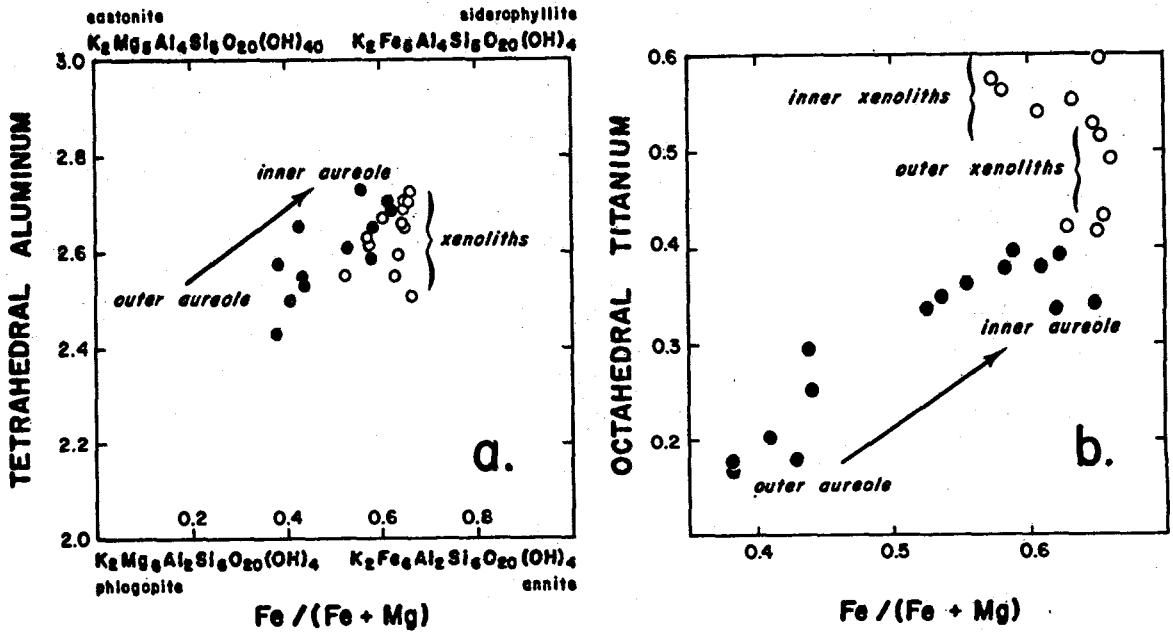

Figure A-1.5. (a) Biotite compositions of the Liberty Hill hornfelses of Table A-1.2 projected onto the phlogopite-annite-eastonite-siderophyllite field. Biotite of the xenoliths (open circles) are differentiated from the biotite of the aureole (filled circles). A weakly defined compositional trend progresses from outer aureole to inner aureole to xenoliths. (b) Octahedral titanium content of the Liberty Hill hornfelses biotite plotted against Fe/(Fe+Mg) contents. The symbols are the same as in Figure A-1.5a. The titanium contents clearly separate the biotites of the different metamorphic grades even when their Fe/(Fe+Mg) values overlap at the higher metamorphic grades.

Guidotti et al. (1977) demonstrated what they believed was a temperature dependent change in the titanium saturation limit of biotite in comparable mineral assemblages over a range of Fe/(Fe+Mg) values of biotites. The titanium content of the Liberty Hill contact aureole biotites also appears to be largely a function of increasing metamorphic grade, because titanium varies for biotites which have similar Fe/(Fe+Mg) values and that can be ordered into lower and higher metamorphic grade assemblages of the inner aureole and outer and inner xenoliths (Figure 5b). Guidotti et al. (1975a) have shown that the amount of tetrahedral aluminum is independent of Fe/(Fe+Mg) over most of the biotite compositional range. The work of Chinner(1960) and Mueller (1972) shows that the aluminum content in the biotites could reflect the continual change in the oxygen and water fugacities. Rutherford (1973) found that biotite becomes more aluminous with increasing temperature and/or oxygen fugacity in peraluminous systems. As discussed in the petrology section, there is a variation in oxygen fugacity with increasing metamorphism in the aureole. There is certainly an increase in temperature. Whether or not these are sufficient to cause the variations in tetrahedral aluminum is unknown. In summary, the Fe/(Fe+Mg) ratio, titanium content and perhaps to a lesser extent, tetrahedral aluminum content of the biotites vary with metamorphic conditions in the aureole. Variations of Ti, Si, and Al^{IV} associated with changes in Fe/(Fe+Mg) may not be independent of one another, both to retain charge balance and to obtain better dimensional fit of the tetrahedral and octahedral layers in the biotites.

The absolute titanium contents of the biotites are higher than those reported by Guidotti et al. (1977). The problem of systematic compositional errors of different workers involving small amounts of a component are no doubt as important here as in the case of muscovites (Guidotti and Sassi, 1976). However, an attractive alternative explanation is that the titanium solubility in biotite decreases with increasing pressure, a compositional relation similar to that found for synthetic phlogopites by Robert (1975), suggesting that the confining pressure of the Liberty Hill contact aureole may have been lower than in the area described by Guidotti et al. (1977).

Biotite only rarely occurs as inclusions in garnet. In the sample which was microprobed, K3-1068, the included biotite is more magnesian than the matrix biotite (Table A-1.2). This is the only place in the Libery Hill hornfelses where a mineral composition greatly differs on a thin section scale. It may be a result of either an earlier prograde biotite enclosed in a growing garnet or a reequilibration of the garnet-included biotite pair with decreasing temperature, the garnet-matrix biotite pair ceasing to reequilibrate at a higher temperature because of the greater distances involved. As will be seen in the section on physical conditions of metamorphism, the garnet-included biotite pairs yield much lower temperatures than do the garnet-matrix biotite pairs.

Chlorite

The chlorites outside the vermiculite-out isograd are ripidolites and brunsvigites according to the classification of Hey (1954). They have Fe/(Fe+Mg) values greater than 0.5 (Table A-1.3). The chlorites of the outermost aureole are more magnesian ripidolites with a range of Fe/(Fe+Mg) values of 0.43-0.37 (Figure A-1.6). The chlorites coexisting with cordierite in the outer aureole are ripidolites. They are the least iron-rich chlorites found and have a narrow Fe/(Fe+Mg) ratio of 0.32-0.34 (Figure A-1.6).

Cordierite

Cordierite is chemically homogeneous and the compositions from grain to grain in thin section are uniform. For the samples analyzed, Fe/(Fe+Mg) ranges from 0.51 to 0.25 (Table A-1.4). The least iron-rich cordierite occurs at the beginning of the outer aureole and iron content increases inward with metamorphic grade. The manganese content of the cordierite is small but exhibits a systematic decrease from 4.3 to 1.7 mol percent of the Mn-cordierite end member from the outer to inner aureole. Cordierites of the xenoliths have generally less than 1 mol percent of the manganese end member. This appears to be the only recorded instance of a systematic variation of manganese content of cordierite with metamorphic grade. Manganese may help to expand the stability field of cordierite to lower temperatures, a role similar to that of manganese in garnet (Dasgupta et al., 1974).

Epidote

Epidote + albite occur in the rocks of the outermost aureole and country rocks in place of a calcic plagioclase. The composition of the epidote varies a little about an average of clinozoisite$_{79}$ pistacite$_{20}$ piemontite$_{1}$ (Table A-1.5).

Feldspars

The plagioclase of the Carolina Slate belt phyllites and outermost aureole is An$_3$. The rapid change in plagioclase composition at the cordierite-in isograd coincides with the disappearance of epidote from the pelitic rocks. The calcium in the plagioclase is believed to come from the decomposition of epidote by reaction 2 as discussed earlier. The rapid plagioclase compositional change may be an effect of the peristerite solvus, but this cannot be determined from the available samples. No coexisting albite and andesine were found. The plagioclase remains an unzoned sodic andesine, within a narrow compositional range, in all pelitic rocks of the outer and inner aureoles.

Compositions of plagioclase from the xenoliths fall into one of two compositional groups: An$_{36}$ and An$_{12-22}$. The more sodic plagioclase coexists with garnet, suggesting equilibration of the anorthite content of the plagioclase and the grossular content of the garnet by a reaction similar to the following;

calcic plagioclase + biotite → garnet + K feldspar + sodic plagioclase + H_2O. (9)

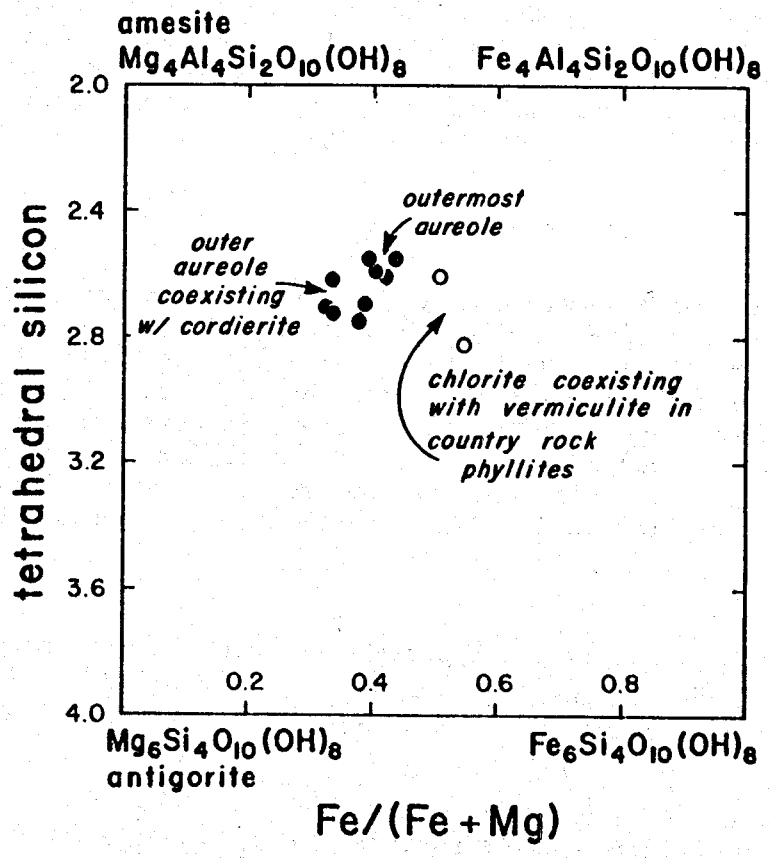

Figure A-1.6. Chlorite compositions of the Liberty Hill Hornfelses and Carolina Slate belt phyllites from Table A-1.3 showing the small compositional trend with increasing metamorphic grade.

The alkali feldspars are microcline microperthites with a fairly narrow compositional range around Or_{85}. Rare compositional extremes of Or_{58}-Or_{92} determined by microprobe analyses probably represent sampling of larger volumes of the exsolved phases.

Garnet

The Liberty Hill garnets are almandine-pyrope solid solutions with small amounts of grossularite and spessartine. They have a narrow compositional range about the average of Alm_{79} Py_{14} Sp_5 Gr_2 (Table A-1.6). Some garnet porphyroblasts are texturally zoned but no corresponding chemical zoning was detected. The textural zoning of the poikilitic garnets is defined by varying modal amounts and sizes of the biotite and quartz inclusions. Chemical inhomogeneity within a grain and from grain to grain in a thin section is less than 2 mol % almandine.

Muscovite

The white micas analyzed are muscovites with only minor paragonite and celadonite solid solution, Na/(Na+K) 0.09 and $(Fe+Mg)/(Fe+Mg+Al^{VI})$ 0.15 (Table A-1.7). The small paragonite and Mg-celadonite contents decrease from the outer to the inner aureoles as anticipated. The Fe-celadonite content is more erratic, making the total celadonite content variable. The sums for the interlayer sites for some of the muscovites in the outermost aureole and country rocks are particularly low in K + Na, suggesting they are in part illites.

Orthopyroxene

The orthopyroxenes are hypersthenes with a narrow range of compositions near $Wo_{0.3}$ $Fs_{60.4}$ $En_{37.4}$ $Mn_{1.9}$ (Table A-1.8). Aluminum content varies between 1.5 and 3.0 weight percent alumina.

Vermiculite

In thin section, the "biotites" in the Carolina Slate belt phyllites in the vicinity of the Liberty Hill pluton are small (<0.05 mm) flakes commonly intergrown with muscovite and chlorite and are fairly rare. They are readily distinguishable from the green chlorite by their tan to brown pleochroism and higher birefringence. This biotite-like mineral does not have the composition of biotite (Table A-1.9), rather, it has a composition similar to the chlorites but with slightly higher potassium and calcium contents. The occurrence of a similar mineral in metamorphic rocks below the biotite isograd has been recently discussed by Velde (1978). He interpreted the mineral as being vermiculite resulting from prograde, regional metamorphism. The vermiculite occurrence in the Carolina Slate belt is similar to the other occurrences summarized by Velde (1978).

Petrology of the ferromagnesian phases the AFM facies type

Understanding the progressive metamorphism of the pelitic rocks in the Liberty Hill pluton requires explanation of both the succession of mineral assemblages and the variation in mineral chemistries. These data for the ferromagnesian silicate phases described in the previous sections are summarized in the AFM projections of Figure A-1.7a-b. The most striking feature of the projections is that the mineral assemblages become more iron rich with increasing metamorphic grade. The greatest change takes place from the outer to the inner aureole (Figure A-1.7a). The xenolith assemblages (7b) lie to the iron-rich side of the aureole assemblages. The orthopyroxene-bearing assemblages reverse this iron enrichment trend (7b). There are too few aluminum silicate-bearing rocks to determine their compositional behavior with changing metamorphic grade.

The chemical analyses of Carolina Slate belt phyllites in the vicinity of the Liberty Hill (Table A-1.1) demonstrate that the iron enrichment of the silicate assemblages does not result from a systematic change in rock chemistry. Rather, the participation in the reactions of iron-bearing oxide minerals and iron-bearing silicate minerals not included in the AFM projection results in an increasingly iron-rich silicate assemblage. The presence of iron in non-silicate phases also causes many of the silicate assemblage compositions to fall on the magnesian side of the range of phyllite compositions (Table A-1.1) in Figure A-1.7 as well as Figures A-1.8 and A-1.9 presented below. No doubt a larger range of Fe/(Fe+Mg) rock values is present than those analyzed. But in most cases, the silicate and rock compositions can be made to coincide by including the coexisting oxide minerals or epidote which would plot on the iron end. At the higher metamorphic grades, where almost all the oxides have reacted to form silicates, the bulk silicate chemistry approaches that of the rock chemistry.

The position of the tie lines and compatibility triangles for the Liberty Hill hornfelses is affected by the intensive parameters of temperature, pressure, water fugacity and oxygen fugacity. The contact metamorphism caused by the Liberty Hill pluton was probably largely isobaric, and constant pressure is a good assumption for the small area covered by the two traverses of the contact aureole shown in Figure A-1.3. This means temperature and water and oxygen fugacities are the only significantly varying intensive parameters in the metamorphism.

Figure A-1.8 illustrates the location of the mineral isograds and the compositional change of the coexisting Fe-Mg phases with distance from the granite contact along the two aureole traverses. The systematic and progressive changes in mineral chemistry with increasing metamorphic grade demonstrate the importance of compositional control by continuous metamorphic reactions. This is further substantiated by the widespread occurrence in the aureole of what should otherwise be univariant assemblages. The other significant feature of Figure A-1.8

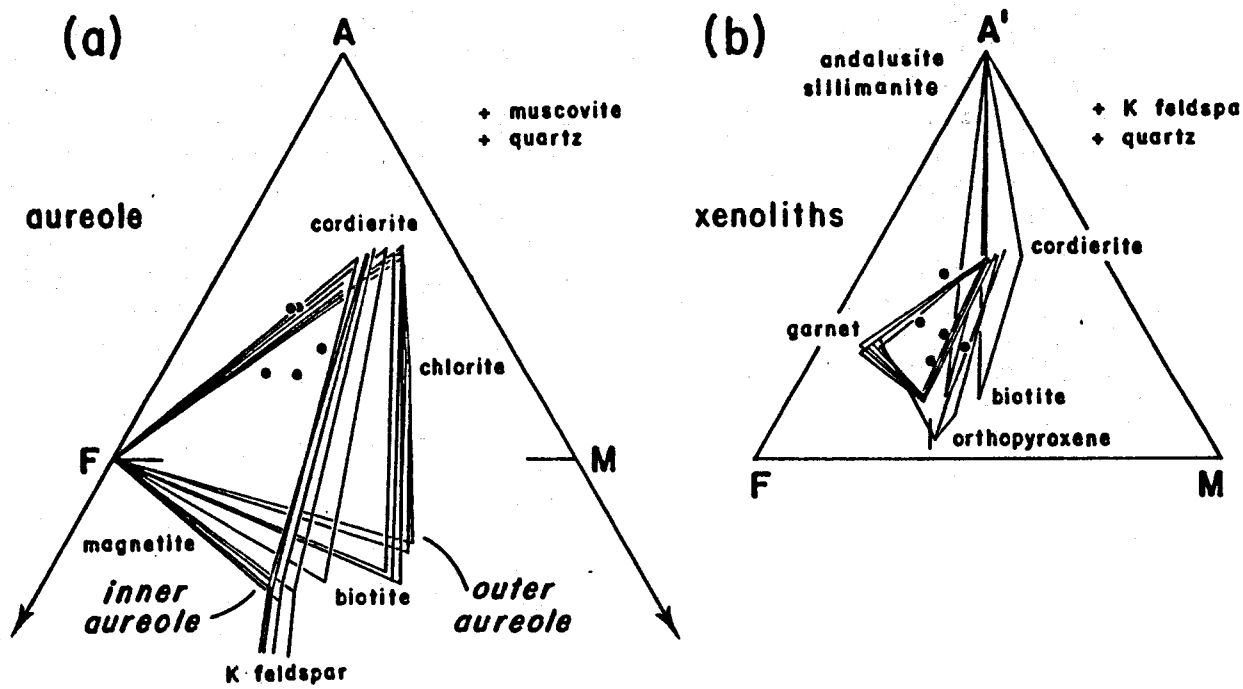

Figure A-1.7. AFM projection showing mineral compositions and their tie lines for hornfelses of the Liberty Hill contact aureole. Rock compositions from Table A-1.1 are included and shown as dots. (a) Mineral compositions, projected from muscovite, of the aureole mineral assemblages showing iron enrichment of the silicate minerals going from the outer to inner aureole. (b) Mineral compositions, projected from K feldspar, of the xenolith mineral assemblages.

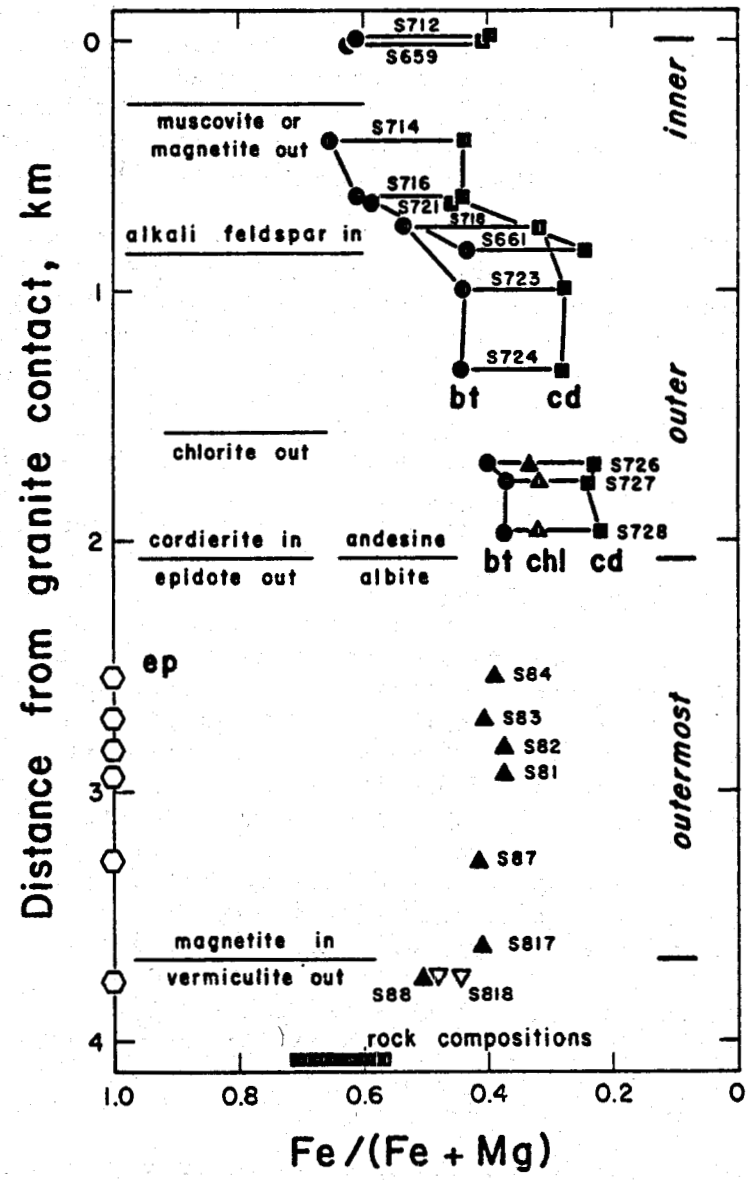

Figure A-1.8. Variation in composition of the Fe-Mg silicate mineral phases with distance from the Liberty Hill Contact along the Fort Hill and Dry Branch traverses (Figure A-1.3). Isograd locations are indicated at the left. Because heat transfer by conduction is an exponential function, temperatures in the aureole would decrease exponentially away from the granite. The symbols are: circles--biotite; triangles--chlorite; squares--cordierite; hexagons--epidote; inverted open triangles---vermiculite. Magnetite is a part of all mineral assemblages beyond the magnetite-out isograd. The heavy lines connect the phases of the rocks believed to be participating in the same continuous reactions.

is the fairly abrupt changes in position slope or direction of the compositional variation at the appearance or disappearance of a mineral phase. As demonstrated below, these changes are a result of a different continuous metamorphic reaction characterizing or predominating in the mineral assemblage between each isograd.

Thompson (1976a,b) has shown that continuous and discontinuous reactions in the system K_2O-FeO-MgO-Al_2O_3-SiO_2-H_2O can be effectively presented in isobaric T-X(Fe-Mg) sections. Combination and super-position of the divariant loops and discontinuous reactions located by experimental work on end member compositions should predict the probable progressive metamorphic mineral assemblages and compositional changes. A sequence of possible continuous and discontinuous reactions for the Liberty Hill hornfelses have been located on a T-X(Fe-Mg) section (Figure A-1.9). The diagram is drawn for $P_T = PH_2O = 4.5$ kb, which is the estimated total pressure as discussed in the following section. The configuration is similar to Thompson's (1976a,b) Figures 1C and 5. Figure A-1.9 is meant to be largely schematic with respect to temperature because the experimental data for many of the reactions are insufficient to permit construction of an accurate T-X(Fe-Mg) section. Additional components or conditions of PH_2O less than P_{total} will also change the temperatures of reactions. However, a relative framework of compositions and temperature was obtained using, in addition to Thompson's work, the experimental work of Seifert (1970,1976), Hensen and Green (1973), Chatterjee and Johannes (1974), and Holdaway and Lee (1977). The additional reactions 11, 12, and 16 that occur in the Liberty Hill aureole, for which there is no experimental data, are located according to the sequence and compositions which are observed. The aluminum silicate phase transition, andalusite to sillimanite, is not included. The compositions of the coexisting mineral phases from Tables A-1.2 to A-1.9 are plotted so that for each coexisting Fe-Mg mineral assemblage the points for biotite coincide with the lines drawn for the biotite compositional variation. Biotite was chosen because it is ubiquitous.

The reactions involving the ferric minerals do not strictly belong in the T-X(Fe-Mg) section, which is defined only for ferrous iron. However, the decrease and eventual disappearance of ferric iron-bearing mineral phases in the contact aureole necessitates the incorporation of the iron as ferrous iron in the product mineral phases. To show the complete reactions, the loops which denote the compositions of the coexisting reactants and products should touch on the iron side to include the ferric oxide phases, as well as epidote at lower metamorphic grades. In Figure A-1.9, the representation of the continuous reactions as loops assumes that the iron oxides are excess phases similar to quartz.

At the lowest metamorphic grades in the country rocks and outermost aureole, the reactions responsible for the compositional variation of the mineral phases are only partly known. With the disappearance of vermiculite at the beginning of the outermost aureole, chlorite becomes much more magnesian (Figures A-1.6, A-1.8, A-1.9). The balance of the iron is probably incorporated in the euhedral mag-

Figure A-1.9. T-X(Fe-Mg) section at PH_2O - 4.5 kb for the continuous and discontinuous reactions for the Liberty Hill contact metamorphic aureole. Bracketed numbers refer to numbered reactions in the text. Loops are for continuous reactions, horizontal lines are for discontinuous reactions. Experimental data for the location of reactions are from Seifert (1970, 1976), Hensen and Green (1973), Chatterjee and Johannes (1974), and Holdaway and Lee (1977). Additional reactions 11, 12, and 16 are located according to the sequence and compositions which are observed in the hornfelses of Liberty Hill pluton. The effects of the aluminum silicate boundaries are not shown. Mineral compositions: solid circles--biotite; solid squares--cordierite; solid triangles--chlorite; open circles-- garnet; open triangles--orthopyroxene; and inverted open triangles--vermiculite.

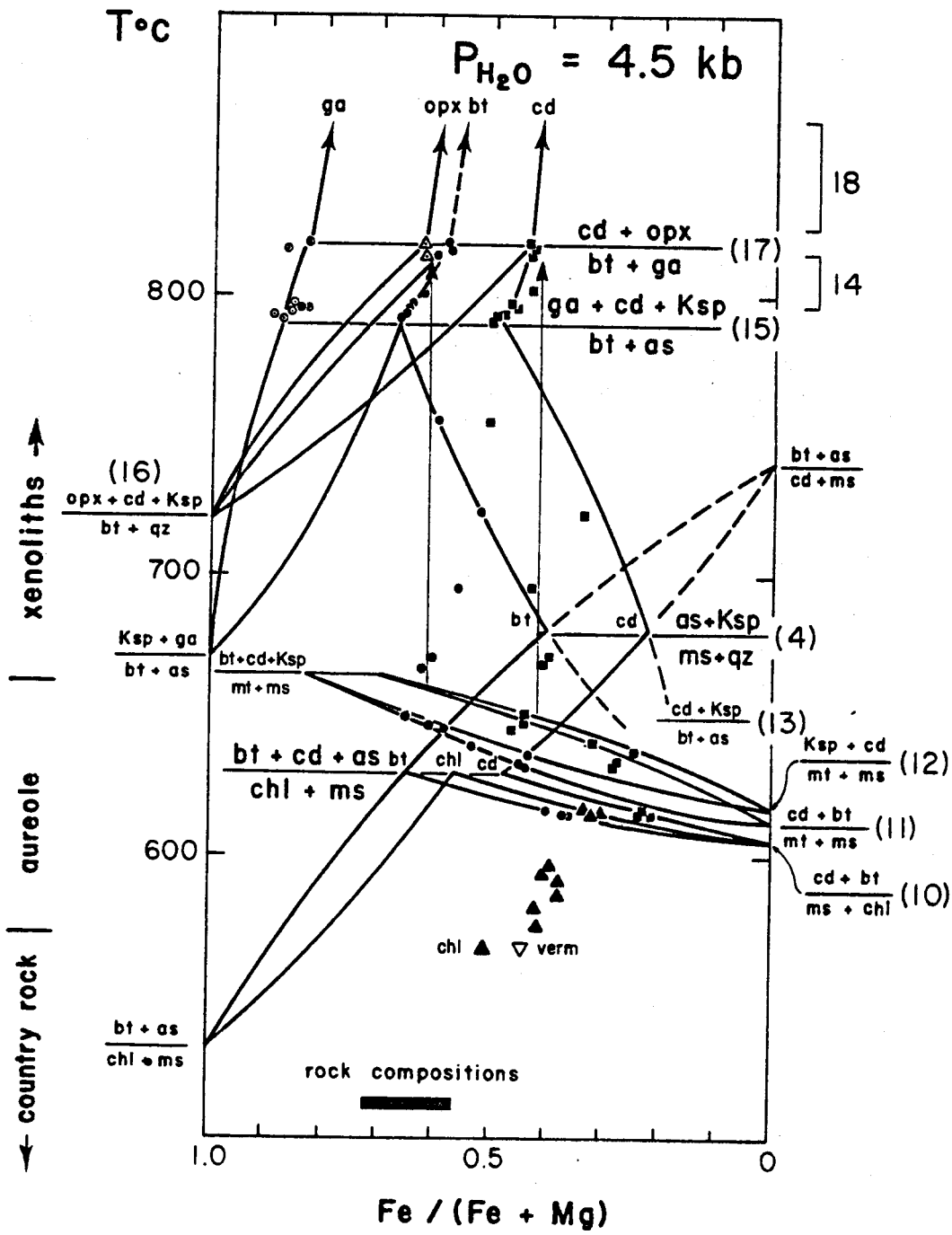
T°C
P_{H_2O} = 4.5 kb
ga
opx bt
cd
18
14
cd + opx
bt + ga
(17)
ga + cd + Ksp
bt + as
(15)
800
(16)
opx + cd + Ksp
bt + qz
700
Ksp + ga
bt + as
bt+cd+Ksp
mt+ms
bt + as
cd + ms
bt
cd
as+Ksp
ms+qz
(4)
cd + Ksp
bt + as
(13)
bt + cd + as
chl + ms
bt
chl
cd
Ksp + cd
mt + ms
(12)
cd + bt
mt + ms
(11)
cd + bt
ms + chl
(10)
600
chl ▲ ▽ verm
bt + as
chl + ms
rock compositions
xenoliths
aureole
country rock
1.0
0.5
0
Fe / (Fe + Mg)

netite crystals which appear at the same time. No detectable compositional change occurs in the outermost aureole until the cordierite-in isograd, suggesting that no continuous reactions occur in the outermost aureole.

Several mineralogic changes which take place at the cordierite-in isograd are summarized by reaction 2. Epidote and albite disappear abruptly while chlorite lingers until its disappearance at the chlorite-out isograd. This indicates that between the cordierite-in and chlorite-out isograds the continuous reaction 1, chlorite + muscovite - cordierite + biotite + H_2O, occurs. Mineral compositions vary along the loop for this reaction in Figure A-1.9, suggesting that reaction 1 should be written

$$\text{chlorite(1)} + \text{biotite(1)} + \text{cordierite(1)} + \text{muscovite} \rightarrow \text{chlorite(2)} + \text{biotite(2)} + \text{cordierite(2)} + H_2O \quad (10)$$

where the products, chlorite(2) + biotite(2) + cordierite(2), are more iron rich than the reactants. This reaction ceases when the chlorite is consumed. If the coexisting iron oxide is ignored, the cordierite-biotite side of the three-phase triangle cordierite + biotite + chlorite lies on the iron side of the chlorite compositions in Figure A-1.7a. This topology agrees with that suggested by Albee (1972) but differs from that observed by Tewhey and Hess (1974) and Guidotti et al. (1975b) for these coexisting minerals in rocks from Maine. Thompson (1976a) would predict both situations, where the difference is a result of differing bulk chemistries. The Liberty Hill hornfelses are evidently more iron rich than the Maine rocks.

The rapid decrease of modal magnetite and the continual increase of cordierite after the chlorite-out isograd can be explained by reaction 3, muscovite + magnetite - cordierite + biotite. This reaction is shown as a continuous reaction in Figure A-1.9 with an iron-enrichment trend with increasing metamorphic grade. This is based on the observed assemblages and suggests that reaction 3 should be more properly written as

$$\text{cordierite(1)} + \text{biotite(1)} + \text{magnetite} + \text{muscovite} + \text{quartz} \rightarrow \text{cordierite(2)} + \text{biotite(2)} + H_2O \quad (11)$$

where cordierite(2) and biotite(2) are more iron rich than cordierite(1) and biotite(1). That these compositional changes do not begin until some distance from the chlorite-out (Figure A-1.8) suggests that reaction 11 does not begin immediately at the chlorite-out isograd.

The appearance of alkali feldspar is believed to be a result of reaction 5, muscovite + magnetite + quartz - cordierite + K feldspar + H_2O. Because of the iron-enrichment of the silicate assemblage between the alkali feldspar-in and muscovite- or magnetite-out isograds (Figure A-1.8), reaction 5 is better written as:

$$\text{cordierite(1)} + \text{biotite(1)} + \text{magnetite} + \text{muscovite} + \text{quartz} \rightarrow \text{cordierite(2)} + \text{biotite(2)} + \text{K feldspar} + H_2O \quad (12)$$

where the products cordierite(2) and biotite(2) are more iron rich than the reactants cordierite(1) and biotite(1). Except for the pro-

duction of alkali feldspar in reaction 12, reactions 11 and 12 are identical. They result in overlapping Fe-Mg compositions of the coexisting cordierite and biotite (Figure A-1.8) and occur under very similar conditions. For these reasons, these two continuous reactions are drawn with their loops nearly coinciding in Figure A-1.9. They are also shown as terminating at the discontinuous reaction magnetite + muscovite + quartz → biotite + cordierite + K feldspar + H_2O.

The T-X (Fe-Mg) section of Figure A-1.9 is an intricate interrelationship of discontinuous and continuous reactions. As demonstrated thus far, the rocks between the isograds record that they were undergoing continuous reactions and this would explain the widespread occurrence of univariant assemblages. The significance of the isograds with respect to the T-X (Fe-Mg) section is not as simple. The epidote- and albite-out and cordierite-, biotite-, and oligoclase-in isograd, summarized by reaction 2, is a terminal, discontinuous reaction, but hardly one effectively represented in an AFM projection. The "monomineralic" isograds, magnetite-in, chlorite-out, K feldspar-in, muscovite- or magnetite-out, and possibly vermiculite-out, represent change from one continuous reaction to another. They do result in a change of the topology of the AFM projection, but only for the rock and fluid compositions of the Liberty Hill hornfelses. As evidenced by the experimental work and petrography of other localities used to construct Figure A-1.9, these continuous reactions occur over a much wider Fe-Mg compositional range. Because of the limited compositions of the Carolina slate belt phyllites in the Liberty Hill contact aureole and metamorphic conditions bringing the occurrence of the continuous reactions close together, the monomineralic isograds mark the end of one and beginning of another continuous reaction.

As suggested in the case of the outermost aureole and reaction 11, a continuous reaction need not begin immediately after the stopping of the previous reaction. A certain temperature or fluid composition change may need to occur for the rock compositions present. A similar situation is believed to take place above the muscovite- or magnetite-out isograd until the occurrence of the various reactions giving rise to the mineral assemblages of the pelitic xenoliths. The compositions of cordierite and biotite above the muscovite- or magnetite-out isograd, S659 and S712, have nearly the same compositions as the cordierite and biotite assemblage of a xenolith, K3-306, associated with orthopyroxene-bearing assemblages. In another cordierite-biotite pair from a xenolith, S89, the biotite is more magnesian. The biotite is also more aluminous, suggesting that some of the iron in the other biotites may be ferric iron. The variation may also be a result of differing bulk compositions or distribution coefficients. In Figure A-1.9, these cordierite-biotite pairs have been plotted schematically as vertical lines drawn to show their trend. These lines differ from the other lines in the figure because they do not represent a reaction. The mineral compositions move off these lines when the minerals are involved in additional reactions. The remaining reactions and mineral assemblages at higher metamorphic grade occur in the xenoliths.

The appearance of the aluminum silicate minerals by reactions 4 or 6 causes those assemblages to be controlled by the continuous reaction

$$\text{aluminum silicate} + \text{biotite(1)} + \text{cordierite(1)} + \text{quartz} \rightarrow \text{biotite(2)} + \text{cordierite(2)} + \text{K feldspar} + H_2O \quad (13)$$

where the reactants are more magnesian than the products (Figure A-1.9). It produces cordierite at the expense of aluminum silicates and with only the small amounts of muscovite remaining from reaction 11 and, in addition to the rock compositions, accounts for the rarity of aluminum silicates in the Liberty Hill hornfelses.

At higher metamorphic conditions in the xenoliths, the biotite-cordierite assemblages participate in the continuous reaction 7 to produce garnet. The mineral compositions suggest the reaction should be written

$$\text{cordierite(1)} + \text{biotite(1)} + \text{quartz} \rightarrow \text{cordierite(2)} + \text{biotite(2)} + \text{garnet} + \text{K feldspar} + H_2O \quad (14)$$

where the products are more magnesian than the reactants (Figure A-1.9). Garnet could have also been produced by the discontinuous reaction

$$\text{aluminum silicate} + \text{biotite} \rightarrow \text{garnet} + \text{cordierite} + \text{K feldspar} + H_2O \quad (15)$$

which is located at the intersection of continuous reactions 13 and 14. Because of the rarity of aluminum silicate minerals in the hornfelses, reaction 15 was probably unimportant.

At the high grade end of the T-X(Fe-Mg) diagram, a continuous orthopyroxene-producing reaction has been added. The biotites and cordierites of the orthopyroxene-bearing assemblages are more magnesian than those without orthopyroxene (Figure A-1.5b). In addition, the biotite coexisting with orthopyroxene is less aluminous. For these reasons, the ideal reaction for the appearance of orthopyroxene by the decomposition of biotite + quartz by reaction 8 has been expanded to

$$\text{biotite(1)} + \text{cordierite(1)} + \text{quartz} \rightarrow \text{orthopyroxene} + \text{cordierite(2)} + \text{biotite(2)} + \text{K feldspar} + H_2O \quad (16)$$

The products biotite(2) and cordierite(2) are more magnesian, and biotite(2) is less aluminous than the reactants biotite(1) and cordierite(1). Because no data are available for the reaction, its location is schematic and governed only by the limited Liberty Hill data.

The intersection of the continuous reactions 14 and 16 occurs at the discontinuous reaction

$$\text{biotite} + \text{garnet} + \text{quartz} \rightarrow \text{cordierite} + \text{orthopyroxene} + \text{K feldspar} + H_2O \quad (17)$$

Because most orthopyroxene in the Liberty Hill xenoliths occurs in garnet-bearing assemblages, this discontinuous reaction 17 is probably the important orthopyroxene-producing reaction in the Liberty Hill hornfelses.

The high-temperature continuous reaction above the discontinuous reaction 16 is

cordierite + orthopyroxene → garnet + quartz (18)

where, with increasing temperature, the garnet becomes more magnesian and the cordierite more iron rich according to the work of Hensen and Green (1972, 1973). The four-phase assemblage garnet-orthopyroxene-cordierite-biotite observed in the xenoliths represents either conditions at the discontinuous reaction 17 or at conditions above it with biotite persisting as a result of the additional component, titanium. For this reason the line representing the biotite compositions for reaction 18 is dashed.

Physical Conditions of Metamorphism

Pressure

An estimate of the pressure during granite emplacement can be made from the assemblage cordierite + garnet + orthopyroxene + quartz, which was calibrated by Hensen and Green (1973) and reviewed by Hensen (1977). For the xenoliths in drill hole KR3, the indicated pressure is 4.5 kb (4.5×10^8 Pa). The aluminum silicate minerals in the xenoliths are andalusite and sillimanite as well as fibrolite. Some of the sillimanite coexists with muscovite, alkali feldspar and quartz. Thus the thermal metamorphism of the Liberty Hill contact aureole occurred at pressures below the aluminum silicate triple point and above the intersection of the andalusite-sillimanite transition and decomposition of muscovite + quartz. Using the muscovite stability data of Chatterjee and Johannes (1974) and the aluminum silicate stability data of Richardson et al. (1969), pressure brackets of 5.5 and 4 kb are obtained. These pressure brackets agree with the estimated pressure of 4.5 kb better than the aluminum silicate stability data of Holdaway (1971) which would yield brackets of 3.5 and 2 kb. In addition, the higher pressure bracket is consistent with the intersection of the granite melting and muscovite + quartz decomposition curves at about 3.8 kb, which is a minimum pressure estimate if the muscovite-bearing xenoliths were enclosed in a granitic magma. This pressure estimate increases if PH_2O is less than P_{total}, if the granite departs from the haplogranite system, or if the muscovite is not the end-member composition.

Temperature

Temperature estimates can be made from the partitioning coefficients of Fe and Mg among coexisting phases and from a petrogenetic grid using experimentally determined reactions. Figure A-1.9 incorporates the applicable experimental results of metamorphic reactions for a petrogenetic grid at the estimated pressure. Because the compositional relations in Figure A-1.9 are drawn for $PH_2O = P_{total}$, all temperatures are maximum estimates. The assemblages of the inner xenoliths with garnet and orthopyroxene result from temperatures above discontinuous reaction 15, biotite + aluminum silicate - garnet + cordierite + K feldspar at 790°C. Inner aureole temperatures lie between

680° and 630°C. Temperatures in the outermost aureole and country rocks lie below 610°C.

Assuming the xenoliths reached the temperature of the enclosing magma, a minimum temperature estimate for the xenoliths can be made from the solidus reaction in the water-saturated haplogranite system. At 4.5 kb this would lie between 640° and 650°C (Luth et al., 1964).

Most metamorphic geothermometers based on Fe-Mg partitioning involve garnet and can be applied only to the garnet-bearing assemblages in the xenoliths. There are several garnet-cordierite and garnet-biotite geothermometer calibrations which offer an opportunity for comparison. Perchuk's (1977) empirical geothermometers, based on natural assemblages calibrated with an amphibole-garnet geothermometer, yield median temperature estimates of 702 ± 67°C for garnet-biotite and 666 ± 60°C for garnet-cordierite pairs. The number following the plus-minus is the temperature spread on either side of the median. Thompson's (1976b) geothermometers, similarly based on natural assemblages, give slightly greater temperature estimates of 740 ± 90°C for garnet-biotite and 707 ± 87°C for garnet-cordierite pairs. In this same range is the 730°C temperature estimate for the orthopyroxene-garnet-cordierite geothermometer-geobarometer of Hensen and Green (1973). The highest temperature estimates are 830 ± 49°C for the garnet-biotite geothermometer calibrated with oxygen isotopes by Goldman and Albee (1977) and 841 ± 148°C for the garnet-biotite geothermometer experimentally calibrated by Ferry and Spear (1978).

The various geothermometric techniques applied to the garnet-bearing xenoliths give a large estimated temperature range of 606°-989°C. The variation in temperatures obtained for the same garnet-biotite or garnet-cordierite pairs using the different authors' geothermometers indicates that most of the temperature range results from the different calibrations. Several other, more geologic reasons may further explain the variation in temperature estimates from any particular geothermometer. The temperature may vary from xenolith to xenolith. Sample S79, which occurs at the margins of the pluton, gives a consistently lower temperature estimate which may reflect a lower marginal temperature. The mineral pairs from drill hole KR3 give a smaller but still wide range of temperature estimates. Holdaway and Lee (1977) found that variations in XH_2O will change the compositions of coexisting phases at a fixed total pressure and temperature. The water pressure may not be the same within all Liberty Hill xenoliths, or similar to the water pressures of rocks used to calibrate the geothermometers. Without specification of the other coexisting phases, the compositions of an individual mineral pair may be insufficient for temperature determination. The mineral assemblages of the Liberty Hill hornfelses are fairly similar to one another but differ substantially from the assemblages in the rocks used to calibrate the geothermometers. Finally, the varying temperature estimates derived from different mineral pairs may also reflect the varying extent of each mineral's participation in retrograde reequilibration of Fe and Mg. The occurrence of compositional zoning in garnet in contact with other ferromagnesian minerals has been the widely used

way to document a retrograde process (Tracy et al., 1976). No zoning was detected in the Liberty Hill hornfels garnets. However, two populations of biotite compositions, one group as inclusions in garnet, the other group as the matrix biotite, were found in one sample, K3-1068 (Table A-1.2). The included biotites yield temperatures 50° to 100°C lower than the garnet-matrix biotite pairs. The included biotites are believed to be an earlier, prograde biotite enclosed in a growing garnet because of the absence of zoning in the garnet as would be anticipated by the reequilibration of the garnet-included biotite pair with decreasing temperature.

For the Liberty Hill xenoliths, the high temperature estimates of 830 ± 49°C by the Goldman and Albee (1977) garnet-biotite geothermometer and 841 ± 148°C by the Ferry and Spear (1978) garnet-biotite geothermometer are probably too high. At such temperatures orthopyroxene-bearing assemblages would be expected to be more abundant. The remaining estimated temperature range of 670°-740°C is relatively small and there is no basis on which to narrow it further. The estimated temperatures of the xenoliths lie above the granite solvus of 645°C and at the high end of the estimated aureole temperatures.

Water Pressure

There is no evidence to suggest that water pressure was less than total pressure in the aureole. If it were, the activity of water would have been successively buffered by the dehydration reactions (10, 11, and 12) with increasing metamorphic grade. That PH_2O was less than P_{total} in the xenoliths is suggested by the contrasting temperature estimates. The maximum temperature estimate for PH_2O = 4.5 kb from Figure A-1.9 places the xenoliths above 790°C. The geothermometers yield lower temperatures at about 700°C. A 100°C drop in the discontinuous reaction 15 biotite + sillimanite + quartz - cordierite + garnet + alkali feldspar + H_2O has been shown by Holdaway and Lee (1977) to be feasible if the water pressure is about half the total pressure of 4.5 kb, $PH_2O = 0.5\ P_{total}$ = 2.3 kb.

Similarly, Holdaway and Lee (1977) state that formation of the assemblage almandine + biotite + cordierite + alkali feldspar + quartz requires that PH_2O is less than P_{total}, or a granite melt would be generated. In comparing their data with Kerrick's (1972) diagram for granite melting at differing partial water pressures, Lee and Holdaway (1977) show that the cordierite + garnet + alkali feldspar-bearing assemblage would melt at 4.5 kb total pressure at conditions of XH_2O greater than 0.5. Textural evidence is not sufficient to argue for the presence or absence of a melt generated from the pelitic xenoliths because the xenoliths were enclosed in a granitic magma. The compositions of the pelitic xenoliths, however, do not differ systematically in the components which would be lost in the generation of a granitic liquid, which argues against melting of the xenoliths and suggests that the water pressure must have been low.

Oxygen Fugacity

The buffering assemblage for oxygen in the Liberty Hill granite probably involves iron-titanium minerals in a reaction suggested by Carmichael et al. (1974) for hornblende-bearing granites as

$$\text{titanite} + \text{magnetite} + \text{phlogopite} + \text{quartz} \rightarrow \text{annite} + \text{K feldspar} + \text{ilmenite} + \text{tremolite} + O_2. \quad (19)$$

This buffer of the Liberty Hill granite differs from the ilmenite-magnetite buffer of the Carolina Slate belt phyllites. In the outermost aureole, the oxygen buffer includes ilmenite-magnetite until the consumption of magnetite in most rocks by reactions 10 and 11 in the inner aureole. Ilmenite remains as the only oxide, and with increasing metamorphic grade, it also disappears, and titanium apparently is incorporated into biotite. Continuing in toward the center of the pluton, a border phase of biotite granite separates the country rock from the amphibole-biotite granite. The absence of hornblende suggests that the buffer of the border phase is

$$\text{annite} + O_2 \rightarrow \text{magnetite} + \text{K feldspar} + H_2O \quad (20)$$

which eventually gives way to the buffer of reaction 19 in the central, amphibolite-biotite granite.

In the sequence of metapelites from the country rock beyond the outermost aureole to the xenoliths in the Liberty Hill granite the oxygen fugacity would have been buffered during metamorphism by a succession of assemblages: magnetite-ilmenite in the country rock up to the inner aureole; ilmenite + Fe-Ti silicates or biotite + cordierite + magnetite + K feldspar in the inner aureole; then biotite + magnetite + K feldspar in the xenoliths of biotite granite border phase; and the buffer of the amphibole-biotite granite represented by reaction 19 for the inner xenoliths. These successive reactions are indicative of the difference in the oxygen fugacity between the granite magma and the pelitic country rocks. The oxygen fugacity of the granite was probably lower than that of the country rock and decreased along the intermediate buffers toward the granite.

Differences in water and oxygen fugacity on a small scale can be seen in a xenolith encountered between the depths of 316 and 360 m (1038-1083 ft) in the KR3 drill hole; the assemblages garnet-cordierite-biotite and orthopyroxene-garnet-cordierite-biotite occur interlayered on a centimeter scale. According to Figure A-1.9, this indicates variable temperature; more likely it is caused by the variability on a small scale of oxygen fugacity, partial water pressure, or both.

Variations in oxygen fugacity and water pressure may also account for the high and low grade metamorphic assemblages of the inner and outer xenoliths, although temperature variation cannot be discounted. The high grade xenolith assemblages occur in the amphibole-biotite granite whereas the lower grade xenolith assemblages occur in the biotite and muscovite-biotite granites of the borders of the eastern half of the Libery Hill pluton. The granites are otherwise identical

and may differ in mineralogy largely as a result of the influx of water from the enclosing country rocks. In the least, the oxygen fugacity buffers, reactions 19 and 20, differ between the two granites.

Conclusions

The Liberty Hill contact aureole is a good illustration of contact metamorphism of low-grade, argillaceous rocks. Examination of the variations in mineral chemistry and the changes in mineral assemblages establishes the relationship of the continuous and discontinuous metamorphic reactions which occur in such situations and the dominance of the continuous reactions. It can be seen that the isograds in this case do not correspond with the discontinuous reactions. Rather, the isograds represent the change from one continuous reaction to another in the rocks with increasing metamorphic grade. This change, in large measure, depends on the bulk chemistry. The participation of nearly all mineral phases in the continual metamorphic reequilibration is well demonstrated and shows the disparity between ideal and real mineral reactions. Reactions in the aureole illustrate the importance of the oxide minerals, which are often ignored in discussions of silicate assemblages, metamorphic reactions and mineral chemistries. The behavior of the oxides also accounts for the changes in size of the magnetic anomaly encircling the pluton.

It is tempting to regard the metamorphism of the Liberty Hill aureole in terms of a progressive increase in temperature. A relatively rapid emplacement of the Liberty Hill magma may have allowed the rate of heating to equal or exceed that of reaction. Rather than a progressive metamorphism, the hornfelses may represent the direct crystallization of the original rock to the final assemblage. This may help to explain the lack of chemical zoning in the minerals, and textures resulting from incomplete reactions near isograds. Temperature is probably the most important variable, but the mineral reactions should be considered a result of increasing metamorphic grade, which includes changes in partial fluid pressures and oxygen fugacity as well.

The metamorphic rocks clearly represent a contact metamorphism, but the mineral assemblages are equally representative of a low pressure regional metamorphic facies series. Using a mineralogic rather than genetic definition of the metamorphic facies, the common low-pressure facies series of metamorphism, both regional and contact, is greenschist, amphibolite, and granulite. The traditional facies of the Liberty Hill contact aureole would be muscovite-, amphibole-, and pyroxene hornfels facies.

The estimated conditions of metamorphism of the contact aureole reveal several features about the Liberty Hill pluton and the rock which it intruded. The estimated pressure of 4.5 kb (4.5×10^8 Pa) corresponds to a depth of 15-18 km during emplacement. The estimated temperatures of 670°-740°C and water pressure of about half the total pressure in the xenoliths probably reflect the conditions of the gran-

ite melt, which at 4.5 kb indicates the granite was just above or at the solidus (Kerrick, 1972). Temperatures in the aureole were lower, with a maximum temperature estimate of about 680°C in the inner aureole, with temperature decreasing away from the contact. Thermal effects are evident up to 4 km from the contact on the present erosional surface, although this is not perpendicular to the thermal gradient. That distance is about 2 km. Country rock temperatures were less than 600°C; and below conditions of the biotite zone. There is no indication of the water pressure in the aureole and it may have been equal to the total pressure, or at the very least buffered by the dehydration reactions occurring in the aureole.

The Liberty Hill granite, which is largely a hornblende-biotite granite has a rim of biotite and muscovite-biotite granite on its northern and eastern border. The amphibole-bearing granite of the interior contains pelitic xenoliths in the granulite facies. The biotite and biotite-muscovite granite on the rim contains pelitic xenoliths in the amphibolite facies. These phenomena are believed to result in part from the spatial variation in temperature, as indicated by the geothermometers, oxygen fugacity, as indicated by the contrasting oxygen buffers of the magnetite-ilmenite the country rock and reaction 19 for the interior of the granite, and water content, with water migrating in from rock, and lowering the water pressure of the inner aureole.

Acknowledgements

This paper is part of an investigation of low-temperature, geothermal resources supported by U. S. Department of Energy Contract No. ET-78-C-05-5648 awarded to J. K. Costain, Lynn Glover III, and A. Krishna Sinha. The paper benefited from reviews by S. W. Becker and D. A. Hewitt.

References

Albee, A. L., 1972, Metamorphism of pelitic schist: reaction relations of chloritoid and staurolite: Geol. Soc. America Bull., v. 83, p. 3249-3268.

Albee, A. L. and Ray, L., 1970, Correction factors for electron-probe microanalysis of silicates, oxides, carbonates, phosphates, and sulfates: Anal. Chem., v. 42, p. 1408-1414.

Bell, H., Butler, J. R., Howell, D. E., and Wheeler, W. H., 1974, Geology of the Piedmont and Coastal Plain near Pageland, South Carolina and Wadesboro, North Carolina. Carolina Geol. Soc. Fieldtrip Guidebook, Div. of Geol., S. C. State Devel. Board.

Bell, H., III, and Popenoe, P., 1976, Gravity studies in the Carolina Slate Belt near the Haile and Brewer mines, northcentral South Carolina: Jour. Reseach, U. S. Geol. Survey, v. 4, p. 667-682.

Bence, A. E. and Albee, A. L., 1968, Empirical correction factors for the electron microanalysis of silicates and oxides: Jour. Geology, v. 76, p. 382-403.

Black, W. W., 1978a, Chemical characteristics and Rb/Sr ages of metavolcanics from the Carolina Slate belt of North Carolina: Geol. Soc. America Abstracts with Programs, v. 10, p. 162-163.

Black, W. W., 1978b, Considerations in obtaining Rb/Sr dates for low rank metavolcanic rocks, Carolina Slate belt: Geol. Soc. America Abstracts with Programs, v. 10, p. 163.

Black, W. W. and Fullagar, P. D., 1976, Avalonian ages of metavolanics and plutons of the Carolina slate belt near Chapel Hill, N. C.: Geol. Soc. America Abstracts with Programs, v. 8, p. 136.

Butler, J. R., 1964, Chemical analyses of rocks of the Carolina Slate Belt: Southeastern Geology, v. 5, p. 101-112.

Butler, J. R., 1972, Age of Paleozoic regional metamorphism in the Carolinas, Georgia, and Tennessee Southern Appalachians: Am. Jour. Sci., v. 272, p. 319-333.

Butler, J. R. and Ragland, P. C., 1969a, A petrochemical survey of plutonic intrusions in the Piedmont, southeastern Appalachians, U. S. A.: Contrib. Mineral. Petrol., v. 24, p. 164-190.

Butler, J. R. and Ragland, P., 1969b, Petrology and chemistry of metaigneous rocks in the Albemarle area, North Carolina slate belt: Am. Jour. Sci., v. 267, p. 700-726.

Butler, J. R. and Howell, D. E., 1976, Geology of the Taxahaw quadrangle, Lancaster County, South Carolina: Div. of Geology, S. C. State Devel. Board, Geologic Notes 20, p. 133-149.

Carmichael, I. S. E., Turner, F. J., and Verhoogen, J., 1974, Igneous Petrology: New York, McGraw-Hill, Inc., 739 p.

Chatterjee, N. D. and W. Johannes, 1974, Thermal stability and standard thermodynamic properties of synthetic 2M1-muscovite $KAl_2[AlSi_3O_{10}(OH)_2]$: Contrib. Mineral. Petrol., v. 48, p. 89-114.

Chinner, G. A., 1960, Pelitic gneisses with varying ferrous/ferric ratios from Glen Clova, Angus, Scotland: J. Petrology, v. 1, p. 178-217.

Conley, J. F., 1962, Geology and mineral resources of Moore County, North Carolina: N. C. Div. of Mineral Resources Bulletin 76, 40 p.

Conley, J. F., and Bain, G. L., 1965, Geology of the Carolina Slate Belt west of the Deep River-Wadesboro Triassic Basin, North Carolina: Southeastern Geology, v. 6, p. 117-138.

Dasgupta, H. C., Seifert, F., and Schreyer, W., 1974, Stability of manganocordierite and related phase equilibria in part of the system $MnO-Al_2O_3-SiO_2-H_2O$: Contrib. Mineral. Petrol., v. 43, p. 275-294.

Dunbar, J., and Speer, J. A., 1977, Magnetic modeling of the Liberty Hill pluton and its contact aureole with comments on the mineralogy of magnetic phases: U.S. Natl. Tech. Inf. Serv. VPI-SU-5103-3, p. A32 - A48.

Ferry, J. M., and Spear, F. S., 1978, Experimental calibration of the partitioning of Fe and Mg between biotite and garnet: Contrib. Mineral. Petrol., v. 66, p. 113-117.

Fullagar, P. D., 1971, Age and origin of plutonic intrusions in the Piedmont of the southeastern Appalachians: Geol. Soc. America Bull., v. 82, p. 2845-2862.

Goldman, D. S. and Albee, A. L., 1977, Correlation of Mg/Fe partitioning between garnet and biotite with $^{18}O/^{16}O$ partitioning between quartz and magnetite: Am. Jour. Sci., v. 277, p. 750-767.

Guidotti, C. V., Cheney, J. T., and Conatore, P., 1975a, Interrelationship between Mg/Fe ratio and octahedral Al content in biotite: Am. Mineralogist, v. 60, p. 849-853.

Guidotti, C. V., Cheney, J. T., and Conatore, P., 1975b, Coexisting cordierite + biotite + chlorite from the Rumford Quadrangle, Maine: Geology, v. 3, p. 147-148.

Guidotti, C. F. and Sassi, F. P., 1976, Muscovite as a petrogenetic indicator mineral in pelitic schists: Neues Jahrb. Mineralogie Abh., v. 127, p. 97-142.

Guidotti, C. V., Cheney, J. T., and Guggenheim, S., 1977, Distribution of titanium between coexisting muscovite and biotite in pelitic schists from northwestern Maine: Am. Mineralogist, v. 62, p. 438-448.

Hensen, B. J., 1977, Cordierite-garnet bearing assemblages as geothermometers and barometers in granulite facies terranes: Tectonophysics, v. 43, p. 73-88.

Hensen, B. J. and Green, D. H., 1972, Experimental study of the stability of cordierite and garnet in pelitic compositions at high pressures and temperatures. II. Compositions without excess alumino-silicate: Contrib. Mineral. Petrol., v. 35, p. 331-354.

Hensen, B. J. and Green, D. H., 1973, Experimental study of the stability of cordierite and garnet in pelitic compositions at high pressures and temperatures. III. Synthesis of experimental data and geological implications: Contrib. Mineral. Petrol. v. 38, p. 151-166.

Hey, M. H., 1954, A new review of the chlorites: Mineralogical Mag., v. 30, p. 277-292.

Hills, F. A. and Butler, J. R., 1968, Rubidium-strontium dates for some rhyolites from the Carolina slate belt of the North Carolina Piedmont (abstr.): Geol. Soc. America Spec. Pap. 121, p. 445.

Holdaway, M. J., 1971, Stability of andalusite and the aluminum silicate phase diagram: Am. Jour. Sci., v. 271, p. 97-131.

Holdaway, M. J. and Lee, S. M., 1977, Fe-Mg cordierite stability in high-grade pelitic rocks based on experimental, theoretical, and natural observations: Contrib. Mineral. Petrol., v. 63, p. 175-198.

Kerrick, D. M., 1972, Experimental determination of muscovite + quartz stability with PH_2O P_{total}: Am. Jour. Sci., v. 272, p. 946-958.

Laney, F. B., 1910, The Gold Hill mining district of North Carolina: N. C. Geological and Economic Survey Bulletin 21, 137 p.

Lee, S. M., and Holdaway, M. J., 1977, Significance of Fe-Mg cordierite stability relations on temperature, pressure, and water pressure in cordierite granulites: Am. Geophys. Union Monograph 20, p. 79-94.

Luth, W. C., Jahns, R. H., and Tuttle, O. F., 1964, The granite system at pressures of 4 to 10 kilobars: J. Geophys. Res., v. 69, p. 759-771.

McCauley, J. F., 1961, Rock analyses in the Carolina Slate belt and the Charlotte belt of Newberry County, South Carolina: Southeastern Geology, v. 3, p. 1-20.

McSween, H. Y., Jr., 1972, An investigation of the Dutchmans Creek Gabbro, Fairfield County, South Carolina: Div. of Geology, S. C. State Devel. Board, Geologic Notes, v. 16, p. 19-42.

Mueller, R. F., 1972, Stability of biotite: A Discussion: Am. Mineralogist, v. 57, p. 300-316.

Overstreet, W. C. and Bell, H., III, 1965a, The crystalline rocks of South Carolina: U. S. Geol. Survey Bull. 1183, 136 p.

Overstreet, W. C. and Bell, H., III, 1965b, Geologic map of the crystalline rocks of South Carolina: U. S. Geol. Survey, Misc. Geol. Inv. Map I-413, 1:250,000.

Perchuk, L. L., 1977, Thermodynamic control of metamorphic processes, in Saxena, S. K. and Bhattacharjii, S., eds., Energetics of Geological Processes: New York, Springer-Verlag, p. 285-352.

Pogue, J. E., Jr., 1910, Cid mining district of Davidson County, North Carolina: N. C. Geologic and Economic Survey Bull. 22, 144 p.

Popenoe, P. and Bell, H., III, 1975, Simple Bouguer gravity map of part of the Carolina slate belt including the Haile and Brewer Mine areas, north- central South Carolina: U. S. Geol. Survey Map GP-904.

Randazzo, A. F., 1969, X-ray analyses of rocks of the Carolina Slate Belt, Union County, North Carolina: Southeastern Geology, v. 10, p. 77-86.

Randazzo, A. F., 1972, Petrography and stratigraphy of the Carolina Slate Belt, Union County, North Carolina: N. C. Dept. of Natural and Economic Resources, Spec. Pub. 4, 38 p.

Richardson, S. W., Gilbert, M. C., and Bell, D. M., 1969, Experimental determination of kyanite-andalusite and andalusite-sillimanite equilibria; the aluminum silicate triple point: Am. Jour. Sci., v. 267, p. 259-272.

Robert, J. L., 1975, An experimental study of phlogopite solid solutions in the system K_2O-MgO-Al_2O_3-SiO_2-H_2O. Solubility of titanium in phlogopite solid solutions: Geol. Soc. America Abstracts with Programs, v. 7, p. 844-845.

Rucklidge, J. C., 1971, Specifications of Fortran program SUPERRECAL: Dept. of Geology, Univ. of Toronto.

Rutherford, M. J., 1973, The phase relations of aluminous iron biotites in the system $KAlSi_3O_8$-$KAlSiO_4$- Al_2O_3-Fe-O-H: J. Petrology, v. 14, p. 159-180.

Secor, D. T., Jr. and Wagener, 1968, Stratigraphy and petrology of the Piedmont in Central South Carolina: Div. of Geology, S. C. State Devel. Board, Geologic Notes, v. 12, p. 67-84.

Seiders, V. M., 1978, A chemically bimodal, calc-alkalic suite of volcanic rocks, Carolina volcanic slate belt, central North Carolina: Southeastern Geology, v. 19, p. 241 - 265.

Seifert, F., 1970, Low-temperature compatibility relations of cordierite in haplopelites of the system K_2O-MgO-Al_2O_3-SiO_2-H_2O: Jour. Petrology, v. 11, p. 73-99.

Seifert, F., 1976, Stability of the assemblage cordierite + K feldspar + quartz: Contrib. Mineral. Petrol. v, 57, p. 179-185.

Shiver, R. S., 1974, The geology of the Heath Springs quadrangle, Heath Springs, South Carolina: M. S. thesis, North Carolina State University of Raleigh, 39 p.

Sloan, E., 1908, Catalogue of the mineral localities of South Carolina: S. C. Geol. Survey Bull. 2, 505 p., reprinted 1958 by Div. of Geology, S. C. State Devel. Board.

St. Jean, J., 1973, A new Cambrian trilobite from the Piedmont of North Carolina: Am. Jour. Sci., v. 273-A, p. 196-216.

Stromquist, A. A. and Sundelius, H. W., 1969, Stratigraphy of the Albemarle Group of the Carolina Slate belt in Central North Carolina: USGS Bull. 1274-B, 22 p. Stuckey, J. L., 1928, The pyrophyllite deposits of North Carolina: N. C. Dept. of Conservation and Development Bull. 37, 62 p.

Sundelius, H. W., 1970, The Carolina slate belt; in G. W. Fisher et al., eds., Studies of Appalachian Geology: Central and Southern: New York, John Wiley and Sons, Inc., 351-367.

Tewhey, J. D., and Hess, P. C., 1974, Continuous metamorphic facies changes as related to chlorite-disappearance in a contact metamorphic aureole: Geol. Soc. America Abstracts with Programs, v. 6, p. 80.

Thompson, A. B., 1976a, Mineral reactions in the pelitic rocks: I. Predication of P-T-X (Fe,Mg) phase relations: Am. Jour. Sci., v. 276, p. 401-424.

Thompson, A. B., 1976b, Mineral reactions in pelitic rocks: II. Calculations of some P-T-X (Fe,Mg) phase relations: Am. Jour. Sci., v. 276, p. 425-454.

Tracy, R. J., Robinson, P., and Thompson, A. B., 1976, Garnet composition and zoning in the determination of temperature and pressure of metamorphism, central Massachusetts: Am. Mineralogist, v. 61, p. 762-775.

U. S. Geol. Survey open-file report, 1970, Aeromagnetic map of the Camden-Kershaw area, northcentral South Carolina.

Velde, B., 1978, High temperature or metamorphic vermiculites: Contrib. Mineral. Petrol., v. 66, p. 319-323.

Wagener, H. D., 1968, Notes on metamorphic rocks of the eastern Piedmont of South Carolina: Winnsboro area: Div. of Geology, S. C. State Devel. Board, Geologic Notes, v. 12, p. 25-29.

Wagener, H. D., 1970, Geology of the southern two-thirds of the Winnsboro 15-minute quadrangle, South Carolina: Div. of Geology, S. C. State Devel. Board, MS-17, 34 p.

Wagener, H. D., 1977, The granitic stone resources of South Carolina: S. C. Geol. Survey Mineral Resources Series 5.

Wagener, H. D., and Howell, D. E., 1973, Granitic plutons of the central and eastern Piedmont of South Carolina: Guidebook, 34th Ann. Mtg. Carolina Geol. Soc.: Div. of Geology, S. C. State Devel. Board, 25 p.

Watson, T. L., 1910, Granites of the Southeastern Atlantic States: U. S. Geol. Survey Bull. 426, p. 3-282.

Wedepohl, K. H., 1969, Composition and abundance of common sedimentary rocks; in K. H. Wedepohl, ed., Handbook of Geochemistry, 1, New York, Springer-Verlag, p.

Winkler, H. G., F., 1974, Petrogenesis of Metamorphic Rocks: New York, Springer-Verlag, 320 p.

Wright, J. E., Sinha, A. K., and Glover, L., III, 1975, Age of zircons from the Petersburg granite, Virginia; with comments on belts of plutons in the Piedmont: Am. Jour. Sci., v. 275, p. 848-856.

Wright, J. E. and Seiders, V. M., 1977, U-Pb dating of zircons from the Carolina volanic slate belt, central North Carolina: Geol. Soc. America Abstracts with Programs, v. 9, p. 197-198.

Ziebold, T. O. and Ogilvie, R. E., 1964, An empirical method for electron microanalysis: Anal. Chemistry, v. 36, p. 322-327.

Appendix A-1.1. Methods of Rock Analyses

Compositions of the first three rocks of Table A-1.1 were obtained by wet chemical analysis of powder splits dried at 105°C. SiO_2 was determined gravimetrically following a sodium carbonate fusion and double dehydration with perchloric acid. Al_2O_3 was determined by difference from the R_2O_3 separation corrected for TiO_2, Fe_2O_3 and P_2O_5. TiO_2 was by a colorimetric determination with sodium peroxide from the R_2O_3 separation. FeO was solutioned with sulfuric acid/hydrofluoric acid in the presence of a known quantity of cerric ion, with titration of the excess cerric ion with a standard ferrous ammonium sulfate solution. Total iron was determined by titration with a standard potassium dichromate solution and Fe_2O_3 obtained by correcting for ferrous iron. MnO, MgO and CaO were determined by atomic absorption on a hydrofluoric/hydrochloric/perchloric acid solution. Na_2O and K_2O were otained by flame emission analysis on the same solution. P_2O_5 was determined by an alkalimetric method. Samples were heated to 900°C and the evolved water absorbed in magnesium perchlorate and weighed for combined water. All elements in analyses 4 and 5, except ferric and ferrous iron and water, were determined by atomic absorption using a hydrofluoric/nitric/hydrochloric acid and diluted to 5%. FeO was determined on a 0.5 gram sample using a hydrofluoric/sulfuric acid digestion, followed by a dichromate titration. Fe_2O_3 was calculated from the total iron corrected for FeO. H_2O^- was determined at 105°C and loss on ignition at 1000°C by difference.

Rock compositions in the AFM and A'KF' projections (Figures A-1.2a and A-1.2b) are uncorrected for the oxide minerals. All iron is treated as FeO, and CaO is corrected for apatite and calcite from the rock analyses. AFM and A'KF' values for the rock and mineral compositions are calculated according to:

$$A = Al_2O_3 - 3(K_2O)$$
$$A' = Al_2O_3 - K_2O - Na_2O - CaO$$
$$F = FeO$$
$$M = MgO$$
$$F' = FeO + MgO + MnO$$
$$K = K_2O$$

where the elemental values are molecular proportions.

Appendix A-1.2. Observed Mineral Assemblages in the Liberty Hill Contact Aureole and Xenoliths

The underlined minerals indicate those for which microprobe compositions were obtained. The mineral abbreviations are:

and	andalusite	An	plagioclase An-content
sil	sillimanite	opx	orthopyroxene
fib	fibrolite	qz	quartz
as	aluminum silicate	ms	muscovite
bt	biotite	mt	magnetite
cd	cordierite	il	ilmenite
chl	chlorite	py	pyrite
ga	garnet	po	pyrrhotite
ksp	K feldspar	pn	pentlandite
pc	plagioclase	cp	chalcopyrite
ep	epidote		
verm	vermiculite		

accessory minerals include: zircon, apatite, tourmaline, allanite

Underlined mineral abbreviations indicate the phase has a microprobe composition.

Xenoliths

S652	bt-Ksp-pc-qz-mt-po
S664	and-fib-cd-bt-ms-Ksp-An_{30-43}-qz-cp-pn-il-po
S668	opx-cd-bt-Ksp-An_{20}-qz-po-pn-cp-py
S672	cd-bt-Ksp-pc-qz
S6102/107	ga-cd-bt-Ksp-An_{23}-qz-il-po
S6127	sil-fib-ms-qz-il
S6130	cd-bt-ms-Ksp-pc-qz
S6133	cd-bt-Ksp-pc-qz
S6136	cd-bt-Ksp-pc-qz-py
S6140	ga-cd-bt-Ksp-An_{22}-qz
S6145	ga-cd-bt-Ks p-pc-qz
S732	fib-cd-bt-ms-Ksp-An_{30}-qz
S89	cd-bt-ms-Ksp-An_{38}-qz
K2-3-3	bt-Ksp-pc-qz
K2-304	cd-bt-Ksp-pc-qz
K2-308	opx-cd-bt-Ksp-An_{10}-qz
K2-309	cd-bt-Ksp-pc-qz
K2-310	cd-bt-Ksp-pc-qz
K3-3-6	cd-bt-An_{24}-qz-mt-il
K3-438	gar-cd-bt-Ksp-An_{12}-qz
K3-439	opx-bt-An_{38}-qz
K3-444	ga-cd-bt-Ksp-An_{24}-qz
K3-465	ga-cd-bt-Ksp-An_{22}-qz
K3-472	opx-bt-An_{37}-qz
K3-1068	ga-cd-bt-Ksp-An_{21}-qz
K3-1074	opx-ga-cd-bt-Ksp-An_{24}-qz-po-pn-py

Aureole

S659	cd-bt-Ksp-An_{28}-qz-mt-il-cp
S660	cd-bt-Ksp-pc-qz-il
S661	cd-bt-ms-An_{32}-Ksp(?)-qz-mt-il
S662	cd-bt-ms-Ksp-pc-qz-mt-py
S663	cd-bt-Ksp-pc-qz-il-mt
S675/76	cd-bt-ms(?)-Ksp-pc-qz-il-mt
S678	chl-ms-bt-An_{0}-qz
S679	bt-ms-Ksp-An_{42}-qz-mt-il
S680	cd-bt-ms-Ksp-An_{38}-qz
S681	cd-bt-ms-Ksp-An_{36}-qz-mt-il
S693	cd-bt-Ksp-pc-qz-il-mt
S79	ga-cd-bt-Ksp-An_{18}-qz-il
S712	cd-bt-ms-Ksp-An_{31}-qz
S714	cd-bt-ms-Ksp-An_{35}-qz-mt-il
S715	cd-bt-ms-Ksp-pc-qz
S716	cd-bt-ms-Ksp-pc-qz-il-mt
S717	cd-bt-ms-Ksp-pc-qz-il-mt
S718	cd-bt-ms-pc-qz
S720	cd-bt-ms-pc-qz
S721	cd-bt-ms-pc-Ksp-qz-mt
S723	cd-bt-ms-pc-qz-mt-il
S724	cd-bt-ms-An_{29-36}-qz-mt-il
S726	cd-bt-chl-ms-An_{35}-qz
S727	cd-bt-chl-ms-An_{38}-qz-mt-il
S728	cd-bt-chl-ms-An_{32}-qz-mt-il

S731	ep-ms-An_1-qz
S81	ep-chl-ms-pc-qz
S82	ep-chl-ms-pc-qz
S83	ep-chl-ms-An_1-qz
S84	ep-chl-ms-An_1-qz
S85	ep-chl-ms-pc-qz
S87	ep-chl-ms-An_0-qz
S88A	ep-chl-ms-An_1-qz
S815	ep-chl-ms-An_2-qz
S816	ep-chl-ms-pc-qz
S817	ep-chl-ms-An_{2-3}-qz
S818	ep-chl-ms-verm-An_1-qz

APPENDIX A-1.3

Table A-1.1
Compositions of metapelite rocks from the xenoliths and contact aureole of the Liberty Hill pluton, S.C.

	1	2	3	4	5
SiO_2	61.82	62.76	63.36	64.6	62.0
Al_2O_3	17.65	16.74	16.83	17.0	16.2
TiO_2	1.13	1.10	0.88	1.1	1.1
FeO	3.57	3.86	4.73	2.9	2.6
Fe_2O_3	4.91	3.99	3.56	3.8	4.7
MnO	0.10	0.11	0.10	0.9	0.17
MgO	2.62	2.19	2.17	1.4	3.0
CaO	0.84	2.80	0.09	1.2	2.0
K_2O	3.92	2.17	1.93	4.2	3.0
Na_2O	2.43	2.78	0.43	2.3	1.9
P_2O_5	0.12	0.16	0.06	<0.02	0.08
H_2O^+	1.07	1.16	6.01	0.3*	1.6*
H_2O^-	-	-	-	<0.1	<0.1
	100.18	99.82	100.15	99.82	98.45

1. AS6-140, garnet-cordierite-biotite-K feldspar-plagioclase-quartz xenolith hornfels.
2. AS6-75, cordierite-biotite-muscovite-K feldspar-plagioclase-quartz aureole hornfels.
3. AS6-78, chlorite-muscovite-biotite-plagioclase-quartz country rock phyllite.
4. AS7-32, fibrolite-cordierite-biotite-muscovite-plagioclase-K feldspar-quartz xenolith hornfels.
5. AS7-26, cordierite-chlorite-biotite-muscovite-plagioclase-quartz aureole hornfels.

1-3. Analysis by Andrew S. McCreath & Son, Inc., Harrisburg, PA.
4-5. Analysis by Skyline Labs, Inc., Wheat Ridge, CO.

* Loss on Ignition at 1000°C

Table A-1.2

Microprobe analyses of biotite

	S659	S661	S664	S668	S681	S6107	S6140	S79	S712	S714	S716	S718	S721	S723
SiO_2	35.49	36.05	34.46	33.47	35.79	34.96	34.34	33.69	35.30	34.74	34.12	36.12	35.46	35.57
Al_2O_3	19.75	19.84	19.98	16.13	19.37	19.35	19.49	18.75	19.71	20.45	19.39	19.44	19.10	18.58
FeO*	21.82	15.97	19.56	21.88	19.71	22.39	22.71	21.69	20.71	21.81	21.07	18.82	19.41	16.21
TiO_2	3.49	2.66	2.15	4.51	3.24	3.80	3.53	4.18	3.36	2.94	2.88	3.11	3.33	2.18
MnO	0.16	0.24	0.14	0.13	0.17	0.08	0.13	0.07	0.17	0.20	0.15	0.30	0.30	0.26
CaO	0.02	0.03	0.0	0.02	0.01	0.01	0.02	0.03	0.0	0.06	0.01	0.04	0.02	0.02
MgO	7.47	11.66	7.39	8.00	7.97	6.64	6.36	6.26	7.52	6.62	7.26	9.30	7.82	11.66
Na_2O	0.11	0.09	0.14	0.04	0.11	0.07	0.09	0.07	0.08	0.11	0.10	0.10	0.09	0.25
K_2O	9.52	9.73	8.77	8.44	9.64	9.60	9.04	9.65	9.88	8.91	9.58	9.54	9.56	8.94
H_2O**	4.00	4.04	3.83	3.76	3.96	3.94	3.89	3.83	3.96	3.93	3.86	4.01	3.92	3.93
Sum	101.84	100.33	96.42	96.38	100.00	100.86	99.60	98.24	100.71	99.77	98.44	100.78	99.01	97.60
Formulas based on 24 (O,OH)														
Si	5.316	5.342	5.388	5.335	5.412	5.313	5.286	5.271	5.334	5.301	5.299	5.392	5.416	5.419
Al	2.684	2.658	2.612	2.665	2.588	2.687	2.714	2.729	2.666	2.699	2.701	2.608	2.584	2.581
	8.000	8.000	8.000	8.000	8.000	8.000	8.000	8.000	8.000	8.000	8.000	8.000	8.000	8.000
Al	0.810	0.807	1.068	0.365	0.863	0.778	0.822	0.727	0.844	0.977	0.847	0.812	0.853	0.755
Ti	0.393	0.296	0.253	0.541	0.369	0.434	0.409	0.492	0.382	0.337	0.337	0.349	0.382	0.250
Fe	2.734	1.979	2.558	2.917	2.493	2.846	2.924	2.838	2.618	2.782	2.736	2.350	2.479	2.065
Mn	0.020	0.031	0.019	0.018	0.022	0.011	0.017	0.009	0.022	0.025	0.020	0.038	0.039	0.034
Mg	1.668	2.576	1.723	1.900	1.796	1.505	1.459	1.460	1.695	1.505	1.681	2.069	1.780	2.648
	5.616	5.689	5.621	5.740	5.543	5.575	5.631	5.527	5.561	5.627	5.621	5.618	5.533	5.752
Ca	0.004	0.005	0.0	0.004	0.002	0.002	0.003	0.005	0.0	0.010	0.002	0.006	0.003	0.003
Na	0.033	0.027	0.041	0.011	0.032	0.021	0.027	0.023	0.025	0.034	0.030	0.029	0.027	0.074
K	1.819	1.839	1.750	1.715	1.859	1.861	1.775	1.926	1.904	1.735	1.897	1.816	1.862	1.737
	1.856	1.871	1.791	1.730	1.894	1.884	1.805	1.954	1.929	1.778	1.930	1.852	1.892	1.814

	S724	S726	S727	S728	S732	S89	K3306	K3438	K3444	K3465	K3472	K31068[1]	K31068[2]	K31074
SiO	36.80	36.87	37.74	36.61	38.16	36.29	35.64	34.60	34.80	35.09	34.86	35.41	35.43	35.33
Al_2O_3	20.23	19.11	19.15	19.55	22.18	21.03	18.05	17.91	17.55	18.51	14.98	17.59	17.13	16.42
FeO*	16.18	14.80	14.38	14.60	15.51	18.12	22.38	22.14	23.09	21.73	23.22	21.90	20.19	21.39
TiO_2	1.62	1.81	1.57	1.53	2.51	3.18	3.56	4.43	5.22	4.62	4.70	4.47	4.53	4.92
MnO	0.22	0.32	0.21	0.27	0.17	0.16	0.24	0.08	0.11	0.09	0.14	0.11	0.03	0.09
CaO	0.01	0.0	0.0	0.03	0.0	0.0	0.02	0.01	0.02	0.0	0.04	0.11	0.14	0.01
MgO	11.96	12.25	12.95	13.43	7.93	8.28	7.45	6.61	6.93	6.66	7.63	7.66	9.03	8.74
Na_2O	0.24	0.26	0.29	0.16	0.16	0.15	0.19	0.10	0.11	0.04	0.01	0.26	0.23	0.08
K_2O	8.77	9.50	9.36	8.90	9.25	9.79	9.53	9.55	9.54	9.92	9.81	8.81	8.90	9.63
H_2O**	4.06	4.02	4.07	4.04	4.09	4.05	3.95	3.87	3.93	3.93	3.83	3.93	3.93	3.93
Sum	100.09	98.93	99.72	99.11	99.99	101.05	101.04	99.33	101.34	100.61	99.26	100.25	99.56	100.56
Formulas based on 24 (O,OH)														
Si	5.427	5.500	5.555	5.427	5.584	5.374	5.411	5.353	5.300	5.346	5.457	5.393	5.398	5.385
Al	2.573	2.500	2.445	2.573	2.416	2.626	2.589	2.647	2.700	2.654	2.543	2.607	2.602	2.615
	8.000	8.000	8.000	8.000	8.000	8.000	8.000	8.000	8.000	8.000	8.000	8.000	8.000	8.000
Al	0.942	0.860	0.877	0.842	1.409	1.043	0.642	0.619	0.450	0.669	0.221	0.550	0.474	0.335
Ti	0.180	0.203	0.174	0.170	0.277	0.354	0.407	0.516	0.598	0.529	0.553	0.512	0.519	0.564
Fe	1.995	1.846	1.770	1.810	1.899	2.244	2.842	2.865	2.941	2.769	3.040	2.789	2.572	2.726
Mn	0.027	0.041	0.026	0.034	0.022	0.020	0.031	0.011	0.015	0.012	0.019	0.014	0.005	0.012
Mg	2.629	2.723	2.841	2.968	1.730	1.827	1.687	1.524	1.574	1.512	1.781	1.739	2.052	1.986
	5.773	5.673	5.688	5.825	5.336	5.489	5.609	5.535	5.578	5.491	5.616	5.603	5.621	5.624
Ca	0.002	0.0	0.0	0.004	0.001	0.0	0.003	0.002	0.004	0.001	0.008	0.018	0.023	0.002
Na	0.069	0.076	0.083	0.046	0.047	0.043	0.057	0.031	0.032	0.012	0.005	0.077	0.069	0.023
K	1.650	1.807	1.757	1.683	1.727	1.849	1.847	1.885	1.854	1.927	9.960	1.711	1.729	1.873
	1.720	1.883	1.840	1.733	1.774	1.892	1.907	1.919	1.890	1.940	1.972	1.805	1.822	1.898

*total iron as FeO
**calculated to give 24 (O,OH)

[1]matrix biotite
[2]biotite included in garnet

Table A-1.3

Microprobe analyses of chlorites

	S726	S727	S728	S81	S82	S83	S84B	S88A	S88B	S817
SiO_2	28.24	26.20	26.07	26.49	26.70	25.60	24.45	24.79	27.16	24.85
Al_2O_3	21.31	21.97	24.80	22.85	21.82	25.07	24.10	23.35	23.84	25.36
FeO*	17.62	16.59	16.84	19.64	19.23	20.12	18.65	25.15	24.46	20.77
TiO_2	0.29	0.29	0.10	0.08	0.08	0.0	0.0	0.12	0.11	0.0
MnO	0.50	0.49	0.50	0.66	0.63	0.69	0.63	0.52	0.44	0.65
CaO	0.0	0.0	0.0	0.05	0.02	0.0	0.0	0.04	0.07	0.0
MgO	19.17	19.77	19.74	18.47	18.43	17.04	16.94	13.84	11.72	16.12
Na_2O	0.0	0.03	0.0	0.03	0.04	0.0	0.0	0.02	0.07	0.0
K_2O	0.01	0.02	0.0	0.02	0.0	0.0	0.0	0.02	0.40	0.0
H_2O**	11.84	11.60	11.99	11.82	11.66	11.84	11.37	11.40	11.58	11.68
Sum	98.98	96.96	100.04	100.11	98.61	100.37	96.14	99.25	99.87	99.43
Formulas based on 18 (O,OH)										
Si	2.858	2.707	2.606	2.685	2.744	2.591	2.576	2.605	2.809	2.549
Al	1.142	1.293	1.394	1.315	1.256	1.409	1.424	1.395	1.191	1.451
	4.000	4.000	4.000	4.000	4.000	4.000	4.000	4.000	4.000	4.000
Al	1.399	1.383	1.527	1.415	1.386	1.581	1.568	1.497	1.716	1.614
Ti	0.022	0.023	0.008	0.006	0.006	0.0	0.0	0.009	0.008	0.0
Fe	1.491	1.434	1.408	1.665	1.652	1.703	1.643	2.210	2.116	1.782
Mn	0.043	0.043	0.042	0.057	0.055	0.059	0.056	0.046	0.039	0.056
Mg	2.892	3.045	2.941	2.791	2.823	2.570	2.660	2.168	1.808	2.465
Ca	0.0	0.0	0.0	0.0	0.0	0.0	0.0	0.0	0.0	0.0
Na	0.0	0.006	0.0	0.006	0.008	0.001	0.0	0.004	0.014	0.0
K	0.001	0.003	0.0	0.003	0.0	0.0	0.0	0.003	0.053	0.0
	5.849	5.935	5.925	5.947	5.932	5.913	5.927	5.942	5.761	5.917

*total iron as FeO
**calculated to give 18 (O,OH)

Table A-1.4

Microprobe analyses of cordierite

	S659	S661	S664	S668	S681	S6107	S6140	S79	S712	S714	S716	S718	S721
SiO_2	49.26	50.00	47.33	48.04	49.23	48.43	46.99	47.94	48.45	48.34	47.23	48.09	48.18
Al_2O_3	33.98	34.11	31.49	32.00	33.35	33.03	31.83	32.49	33.29	33.78	32.00	33.66	33.26
FeO*	9.39	5.74	10.99	9.73	8.18	10.92	11.11	10.75	8.62	9.27	9.46	6.82	7.82
TiO_2	0.03	0.06	0.0	0.0	0.02	0.03	0.0	0.01	0.0	0.0	0.53	0.20	0.21
MnO	0.36	0.54	0.27	0.28	0.41	0.24	0.26	0.15	0.38	0.47	0.40	0.64	0.57
CaO	0.0	0.0	0.0	0.0	0.0	0.0	0.0	0.0	0.0	0.0	0.39	0.01	0.0
MgO	7.80	10.16	5.97	7.46	7.80	6.73	6.40	6.27	7.52	7.16	6.82	8.47	7.67
Na_2O	0.13	0.15	0.17	0.09	0.12	0.10	0.12	0.12	0.14	0.14	0.19	0.13	0.13
K_2O	0.0	0.0	0.0	0.0	0.0	0.0	0.0	0.0	0.0	0.0	0.01	0.01	0.0
Sum	100.95	100.76	96.21	97.59	99.12	99.49	96.72	97.74	98.42	99.16	97.02	98.03	97.86
Formulas based on 18 oxygens													
Si	4.965	4.974	5.046	5.020	5.024	4.987	4.992	5.019	4.993	4.962	4.976	4.946	4.982
Ti	0.002	0.004	0.0	0.0	0.002	0.003	0.0	0.001	0.0	0.0	0.042	0.015	0.017
Al	1.032	1.022	0.954	0.980	0.974	1.010	1.008	0.980	1.007	1.038	0.982	1.038	1.002
	6.000	6.000	6.000	6.000	6.000	6.000	6.000	6.000	6.000	6.000	6.000	6.000	6.000
Al	3.005	2.977	3.003	2.961	3.035	2.998	2.977	3.028	3.036	3.047	2.990	3.041	3.051
Fe	0.792	0.478	0.980	0.850	0.698	0.941	0.987	0.941	0.743	0.796	0.834	0.587	0.677
Mg	1.171	1.506	0.948	1.162	1.186	1.034	1.014	0.979	1.156	1.095	1.070	1.298	1.182
Mn	0.031	0.045	0.024	0.025	0.036	0.021	0.023	0.014	0.034	0.041	0.035	0.056	0.050
	1.994	2.029	1.952	2.037	1.920	1.995	2.024	1.934	1.933	1.932	1.940	1.941	1.909
Ca	0.0	0.0	0.0	0.0	0.0	0.0	0.0	0.0	0.0	0.0	0.044	0.001	0.0
Na	0.025	0.029	0.035	0.018	0.024	0.020	0.024	0.024	0.028	0.028	0.039	0.026	0.027
K	0.0	0.0	0.0	0.0	0.0	0.0	0.0	0.0	0.0	0.0	0.001	0.001	0.0
	0.025	0.029	0.035	0.018	0.024	0.021	0.024	0.024	0.028	0.028	0.084	0.028	0.027

	S723	S724	S726	S727	S728	S732	S89	K3 306	K3 438	K3 444	K3 465	K3 1068	K3 1074
SiO_2	56.52	48.33	48.36	49.43	51.05	47.23	49.28	48.50	47.56	48.39	48.20	48.36	48.85
Al_2O_3	28.27	34.45	33.58	32.55	31.97	33.33	34.14	31.90	32.36	33.08	33.60	32.78	33.20
FeO*	5.02	5.67	5.07	5.03	4.43	7.43	9.32	9.15	9.79	10.86	10.20	9.37	9.70
TiO_2	0.20	0.0	0.21	0.02	0.0	0.20	0.0	0.0	0.03	0.02	0.02	0.03	0.01
MnO	0.57	0.51	0.77	0.72	0.87	0.36	0.29	0.41	0.13	0.20	0.14	0.14	0.28
CaO	0.06	0.02	0.07	0.08	0.11	0.0	0.0	0.0	0.10	0.0	0.0	0.0	0.0
MgO	7.37	8.88	9.13	8.95	8.57	8.10	7.18	7.02	6.59	6.94	6.65	7.18	7.12
Na_2O	0.36	0.26	0.50	0.53	0.46	0.09	0.21	0.17	0.24	0.07	0.06	0.10	0.04
K_2O	0.0	0.0	0.0	0.07	0.0	0.0	0.0	0.0	0.03	0.01	0.0	0.0	0.01
Sum	98.39	98.12	97.70	97.41	97.46	96.76	100.42	97.17	96.83	99.58	98.88	97.97	99.21
Formulas based on 18 oxygens													
Si	5.670	4.936	4.961	5.076	5.209	4.931	4.987	5.074	5.010	4.978	4.973	5.017	5.012
Ti	0.015	0.0	0.016	0.002	0.0	0.016	0.0	0.0	0.002	0.002	0.002	0.003	0.001
Al	0.315	1.064	1.023	0.922	0.791	1.053	1.013	0.926	0.987	1.020	1.026	0.980	0.987
	6.000	6.000	6.000	6.000	6.000	6.000	6.000	6.000	6.000	6.000	6.000	6.000	6.000
Al	3.027	3.081	3.036	3.017	3.053	3.048	3.058	3.007	3.030	2.990	3.059	3.028	3.027
Fe	0.422	0.484	0.435	0.432	0.378	0.649	0.789	0.800	0.863	0.934	0.880	0.813	0.833
Mg	1.103	1.352	1.396	1.371	1.303	1.261	1.083	1.095	1.035	1.064	1.023	1.110	1.088
Mn	0.049	0.044	0.067	0.063	0.075	0.032	0.025	0.037	0.012	0.017	0.012	0.013	0.024
	1.573	1.880	1.897	1.865	1.757	1.942	1.897	1.932	1.909	2.016	1.916	1.936	1.945
Ca	0.006	0.002	0.008	0.009	0.012	0.0	0.0	0.0	0.001	0.0	0.0	0.0	0.0
Na	0.070	0.051	0.099	0.107	0.091	0.019	0.041	0.035	0.049	0.014	0.013	0.020	0.009
K	0.0	0.0	0.001	0.010	0.0	0.0	0.0	0.0	0.004	0.001	0.0	0.0	0.001
	0.076	0.054	0.108	0.126	0.103	0.019	0.041	0.035	0.064	0.015	0.013	0.020	0.010

*total iron as FeO

Table A-1.5

Microprobe analyses of epidote

	S83	S84B	S88A	S817	S818
SiO_2	36.72	36.66	36.04	38.26	37.44
Al_2O_3	27.93	27.56	27.46	23.63	28.40
Fe_2O_3*	11.01	13.13	11.30	13.19	9.67
TiO_2	0.0	0.0	0.0	0.0	0.0
MnO	0.47	0.26	0.75	0.32	1.68
CaO	22.48	23.47	22.30	23.49	21.51
MgO	0.05	0.05	0.07	0.01	0.04
Na_2O	0.0	0.0	0.01	0.0	0.01
K_2O	0.0	0.0	0.0	0.0	0.0
H_2O**	1.91	1.94	1.89	1.90	1.92
Sum	100.57	103.07	99.82	100.80	100.67
Formulas based on 13 (O,OH)					
Si	2.872	2.823	2.851	3.015	2.915
Al	0.128	0.177	0.149	0.0	0.085
	3.000	3.000	3.000	3.015	3.000
Al	2.446	2.324	2.410	2.194	2.521
Ti	0.0	0.0	0.0	0.0	0.0
Mg	0.006	0.006	0.008	0.001	0.005
Fe^{3+}	0.648	0.761	0.673	0.782	0.567
Mn	0.031	0.017	0.050	0.021	0.111
	3.131	3.108	3.141	2.999	3.203
Ca	1.884	1.937	1.890	1.983	1.794
K	0.0	0.0	0.0	0.0	0.0
Na	0.0	0.0	0.002	0.0	0.002
	1.884	1.937	1.891	1.983	1.796
Mol % Ps	19.9	23.2	20.5	26.1	17.3
Mol % Cz	79.1	76.3	77.9	73.2	79.4
Mol % Pt	0.9	0.5	1.5	0.7	3.3

*total iron as Fe_2O_3
**calculated to give 13 (O,OH)

Table A-1.6

Microprobe analyses of garnets

	S6107	S6140	S79	K3 438	K3 444	K3 465	K3 1068	K3 1074
SiO_2	37.12	35.91	35.85	36.99	37.31	38.10	38.00	38.27
Al_2O_3	22.42	22.16	23.10	23.06	22.58	20.55	20.13	20.00
FeO*	35.43	36.24	36.27	35.65	35.06	35.33	35.48	34.70
TiO_2	0.15	0.07	0.21	0.16	0.11	0.14	0.10	0.08
MnO	2.37	2.57	1.92	1.27	1.72	1.59	2.28	1.95
CaO	0.88	0.78	0.67	0.56	0.81	0.83	0.81	0.86
MgO	3.43	3.03	2.58	3.87	4.33	3.43	3.18	4.10
Na_2O	0.0	0.0	0.0	0.0	0.0	0.0	0.0	0.0
K_2O	0.02	0.01	0.02	0.01	0.01	0.02	0.01	0.02
Sum	101.82	100.78	100.62	101.57	101.96	99.99	99.99	99.98
Formulas based on 12 oxygens								
Si	2.934	2.893	2.880	2.915	2.929	3.055	3.061	3.067
Ti	0.009	0.004	0.013	0.009	0.007	0.008	0.006	0.005
Al	0.057	0.103	0.108	0.075	0.064	0.0	0.0	0.0
	3.000	3.000	3.000	3.000	3.000	3.063	3.067	3.072
Al	2.031	2.001	2.079	2.066	2.025	1.942	1.911	1.889
Fe	2.343	2.442	2.436	2.350	2.302	2.369	2.390	2.326
Mg	0.404	0.363	0.309	0.455	0.507	0.410	0.382	0.490
Mn	0.159	0.175	0.131	0.085	0.115	0.108	0.156	0.132
Ca	0.075	0.067	0.058	0.047	0.069	0.071	0.070	0.074
Na	0.0	0.0	0.0	0.0	0.0	0.0	0.0	0.0
K	0.002	0.001	0.002	0.001	0.002	0.002	0.001	0.002
	2.981	3.049	2.936	2.937	2.994	2.960	2.999	3.024
Mol % Alm	78.6	80.1	83.0	80.0	76.9	80.1	79.7	76.9
Mol % Pyr	13.6	11.9	10.5	15.5	16.9	13.8	12.7	16.2
Mol % Sp	5.3	5.8	4.5	2.9	3.8	3.6	5.2	4.4
Mol % Gr	2.5	2.2	1.9	1.6	2.3	2.4	2.3	2.4

*total iron as FeO

Table A-1.7

Microprobe analyses of muscovite

	S661	S681	S712	S714	S716	S724	S726	S727	S83	S84B	S815	S817	S818
SiO_2	45.52	47.16	45.57	45.44	44.20	45.19	47.10	47.35	47.07	48.05	45.85	47.53	46.30
Al_2O_3	34.11	35.75	36.01	36.68	34.81	33.69	29.72	35.87	36.59	35.84	35.44	36.07	34.46
FeO*	3.79	3.42	3.34	3.07	3.38	3.40	2.52	1.94	3.62	2.46	3.36	2.73	4.04
TiO_2	0.80	1.35	0.82	0.35	0.69	0.33	1.08	0.71	0.0	0.08	0.0	0.02	0.09
MnO	0.01	0.01	0.0	0.07	0.01	0.09	0.07	0.01	0.05	0.07	0.02	0.06	0.06
CaO	0.0	0.0	0.0	0.0	0.0	0.0	0.0	0.0	0.0	0.10	0.04	0.05	0.05
MgO	0.86	0.39	0.36	0.37	0.53	0.71	1.19	0.74	0.96	1.02	1.02	0.86	0.76
Na_2O	0.31	0.27	0.36	0.33	0.44	0.48	0.51	0.48	0.42	0.21	0.38	0.36	0.45
K_2O	10.32	8.32	10.34	10.45	10.70	8.24	9.76	9.57	9.86	5.73	8.93	8.07	9.03
H_2O*	4.46	4.59	4.53	4.53	4.41	4.36	4.33	4.59	4.63	4.55	4.49	4.58	4.48
Sum	100.19	101.28	101.37	101.29	99.18	96.49	96.30	101.27	103.20	98.11	99.53	100.32	99.73
Formulas based on 24 oxygens (O,OH)													
Si	6.110	6.154	6.027	6.007	6.007	6.208	6.515	6.182	6.090	6.323	6.120	6.223	6.193
Al	1.890	1.846	1.973	1.993	1.993	1.792	9.485	1.818	1.910	1.677	1.880	1.777	1.807
	8.000	8.000	8.000	8.000	8.000	8.000	8.000	8.000	8.000	8.000	8.000	8.000	8.000
Al	3.505	3.650	3.639	3.720	3.583	3.661	3.359	3.700	3.669	3.880	3.694	3.788	3.623
Ti	0.081	0.133	0.082	0.035	0.071	0.034	0.112	0.070	0.0	0.008	0.0	0.002	0.010
Fe	0.426	0.373	0.370	0.399	0.384	0.391	0.292	0.212	0.392	0.271	0.375	0.299	0.452
Mn	0.001	0.002	0.001	0.008	0.001	0.010	0.009	0.001	0.005	0.008	0.002	0.007	0.007
Mg	0.173	0.077	0.072	0.073	0.107	0.145	0.246	0.144	0.185	0.200	0.203	0.168	0.152
	4.185	4.235	4.163	4.175	4.146	4.242	4.018	4.128	4.251	4.366	4.274	4.264	4.243
Ca	0.0	0.0	0.0	0.0	0.0	0.0	0.0	0.0	0.0	0.014	0.006	0.007	0.008
Na	0.080	0.068	0.092	0.085	0.116	0.128	0.137	0.121	0.105	0.054	0.098	0.091	0.117
K	1.767	1.385	1.745	1.762	1.855	1.444	1.723	1.594	1.627	0.962	1.520	1.348	1.540
	1.847	1.453	1.837	1.836	1.971	1.572	1.859	1.715	1.733	1.029	1.624	1.446	1.664

*total iron as FeO
**calculated go give 24 (O,OH)

Table A-1.8

Microprobe analyses of orthopyroxenes

	S668	K3 472	K3 1074.2
SiO_2	46.39	49.08	48.71
Al_2O_3	3.05	1.51	2.81
FeO*	35.85	34.77	34.72
TiO_2	0.12	0.15	0.15
MnO	1.02	1.17	1.09
CaO	0.06	0.23	0.10
MgO	12.53	11.77	12.28
Na_2O	0.01	0.0	0.0
K_2O	0.01	0.01	0.03
Sum	99.03	98.71	99.90
Formulas based on 6 oxygens			
Si	1.881	1.977	1.935
Al	0.119	0.023	0.065
	2.000	2.000	2.000
Al	0.027	0.049	0.067
Ca	0.0	0.0	0.0
Mg	0.758	0.707	0.727
Fe	1.216	1.171	1.154
Mn	0.035	0.040	0.037
Ti	0.004	0.005	0.004
K	0.001	0.001	0.002
Na	0.0	0.0	0.0
	2.043	1.982	1.995
Mol % Wo	0.12	0.53	0.23
Mol % Fs	60.46	60.75	60.03
Mol % En	37.67	36.65	37.83
Mol % Mn	1.75	2.07	1.91

*total iron as FeO

Table A-1.9

Microprobe analyses of vermiculites

	S88A	S818
SiO_2	28.93	32.09
Al_2O_3	21.88	21.53
FeO*	20.30	18.50
TiO_2	0.01	0.05
MnO	0.38	0.44
CaO	0.13	0.29
MgO	12.05	13.10
Na_2O	0.01	0.07
K_2O	0.15	0.32
Sum	83.84	86.39
A	0.266	0.257
F	0.486	0.442

*total iron as FeO

STUDY OF THE PRE-CRETACEOUS BASEMENT BELOW THE ATLANTIC COASTAL PLAIN

R. J. Gleason

INTRODUCTION

An investigation of the potential for low-temperature geothermal energy resources in the Atlantic Coastal Plain requires detailed knowledge of two aspects of the geology along the eastern seaboard: (1) the lithology and structure of rocks below the Coastal Plain sediments (henceforth referred to as "basement"), and (2) the thickness and lithology of the overlying sediments. It is necessary to know the basement lithology because some crystalline rocks are highly radiogenic and produce relatively high quantities of heat, whereas other types of crystalline rock are relatively "cold". Knowledge of the sediment thickness and lithology is required because thicker sections provide more insulation for the underlying radiogenic heat producers, and some lithologies have lower thermal conductivities and are therefore better insulators.

Basement depth and lithologic information may be obtained from a variety of sources, including regional gravity and magnetic studies, seismic investigations, and subsurface well data. The following discussion focuses on the ongoing compilation of all basement well data from the entire Coastal Plain, application of the data to the present Department of Energy-VPI & SU heatflow determination drilling program, and petrographic/petrologic studies of basement drill cores collected during the course of the project.

BASEMENT WELL DATA COMPILATION

A systematic state-by-state compilation of all existing data for wells drilled to basement beneath the Atlantic Coastal Plain has been underway since 1977. This compilation has involved an exhaustive literature search for each state, including review of professional journals, oil and gas reports, and U.S. as well as state geological survey publications. In several cases, geologists at various state surveys have been able to provide additional data regarding basement wells in their states. While continuing drilling and discovery of new data sources require periodic updating of the compilation, data files are at present complete for New Jersey, Maryland, Delaware, Virginia, North Carolina, and Georgia. The compilation of South Carolina data is not yet finished.

Figures A-2.1 to A-2.5 show the distribution and nature of basement well data for the states completed to date. Symbols for each well designate the type of data presently recorded, i.e., basement lithology, depth to basement, lithology and depth, or location of a basement well with no supplementay data. At locations near the western edge of the Coastal Plain, several wells have often been drilled at approximately the same location; one symbol represents all wells in

Figure A-2.1: Map showing locations of wells drilled to basement in New Jersey and nature of data included in VPI & SU compilation.

WELLS TO BASEMENT IN
NEW JERSEY COASTAL PLAIN

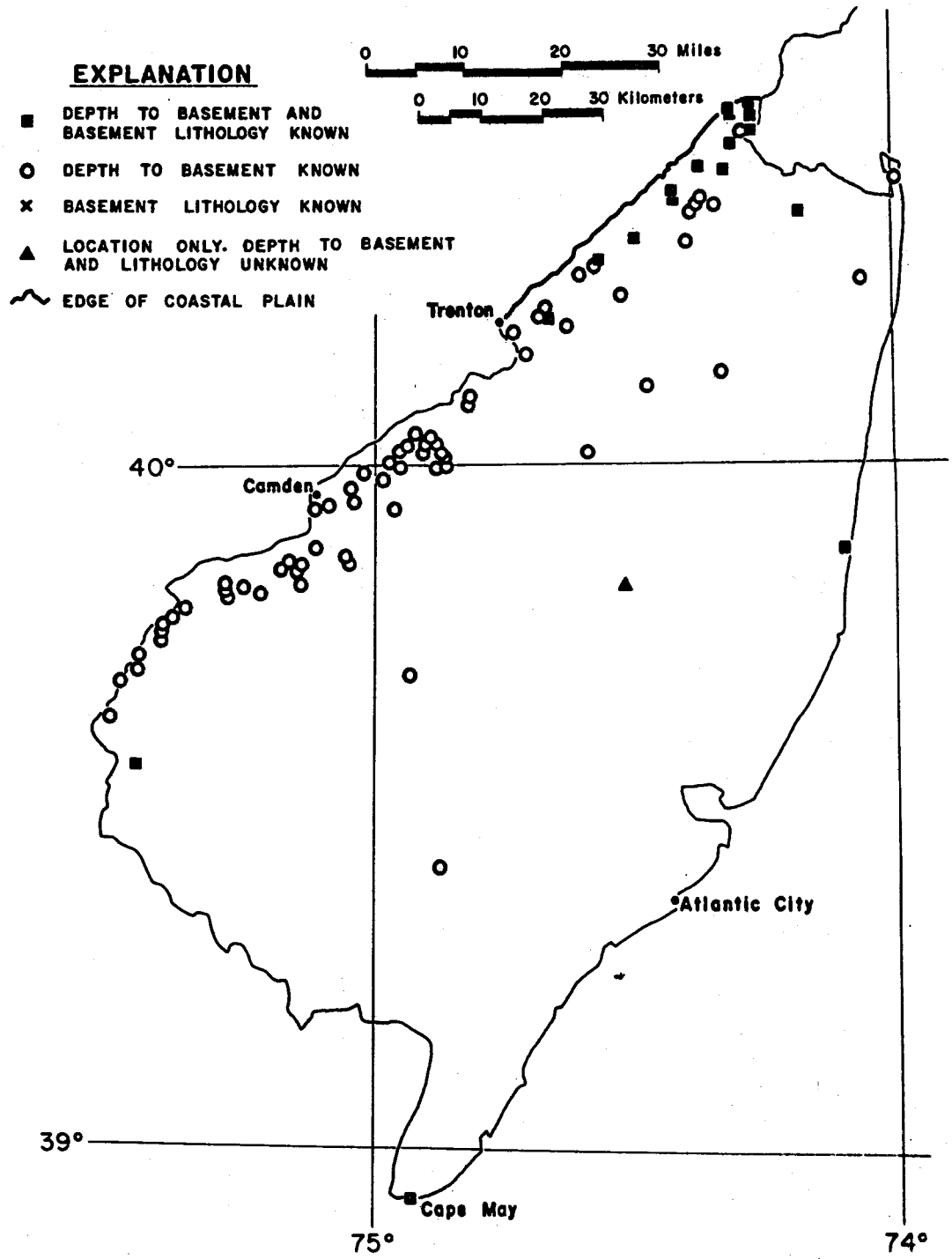

such cases. A brief summary of each state compilation is presented below.

New Jersey

Eighty-nine basement wells have been included in the compilation for New Jersey (Figure A-2.1). Of these wells, only twenty were drilled to depths of greater than 500' (152 m), indicating the overwhelming concentration of data at shallow depths close to the edge of the Coastal Plain. For seventy-two of the eighty-nine wells, no lithologic description of basement rock has been found, while for the remaining seventeen wells, general descriptions are available. Depth to the top of pre-Cretaceous rock has been recorded for every New Jersey well.

Delaware

At present, forty-nine wells drilled to basement have been identified in Delaware (Figure A-2.2). All of these wells are located in Newcastle County. Fourteen of these wells have been drilled to depths exceeding 500' (152 m); only one of them exceeds 1500' (457 m): a Shell Oil test well in Deakyneville drilled in 1961, to a depth of 2312' (704.7 m). Basement data south of this well is non-existent. No basement lithologic descriptions have been found for any of the Delaware wells; basement depths have been recorded for all but four of the wells.

Maryland

Eighty-six basement wells are presently included in the compilation of Maryland data (Figure A-2.2). There is a paucity of data in the eastern part of the state, with only two deep test wells, the Ohio Oil Hammond well, and the Socony-Vacuum Bethards well located on the Maryland portion of the Delmarva peninsula. The remainder of the basement wells are located within approximately 50 kilometers of the edge of the Coastal Plain. A majority of the wells included in the compilation were drilled to depths exceeding 500' (152 m), but only nineteen, including the two wells on the peninsula, were drilled to depths greater than 1500' (457 m). Basement lithology is known for thirty of the eighty-six wells; depth to basement is recorded for seventy-six of the Maryland wells.

Virginia

One hundred and eighty-one basement wells have been identified in Virginia to date (Figure A-2.3). This large number of wells, compared to the number in the preceding states, is due to inclusion of many more shallow water wells near the edge of the Coastal Plain. All but ten of the Virginia wells are located within 50 kilometers of the western boundary of the Coastal Plain. Fifty-one of the Virginia wells were drilled to depths exceeding 500' (152 m), but only eleven were drilled deeper than 1500' (457 m). In the deepest section of the Virginia Coastal Plain, the Delmarva peninsula, only one deep oil

Figure A-2.2: Map showing locations of wells drilled to basement in Delaware and Maryland and nature of data included in VPI & SU compilation.

WELLS TO BASEMENT IN MARYLAND-DELAWARE COASTAL PLAIN

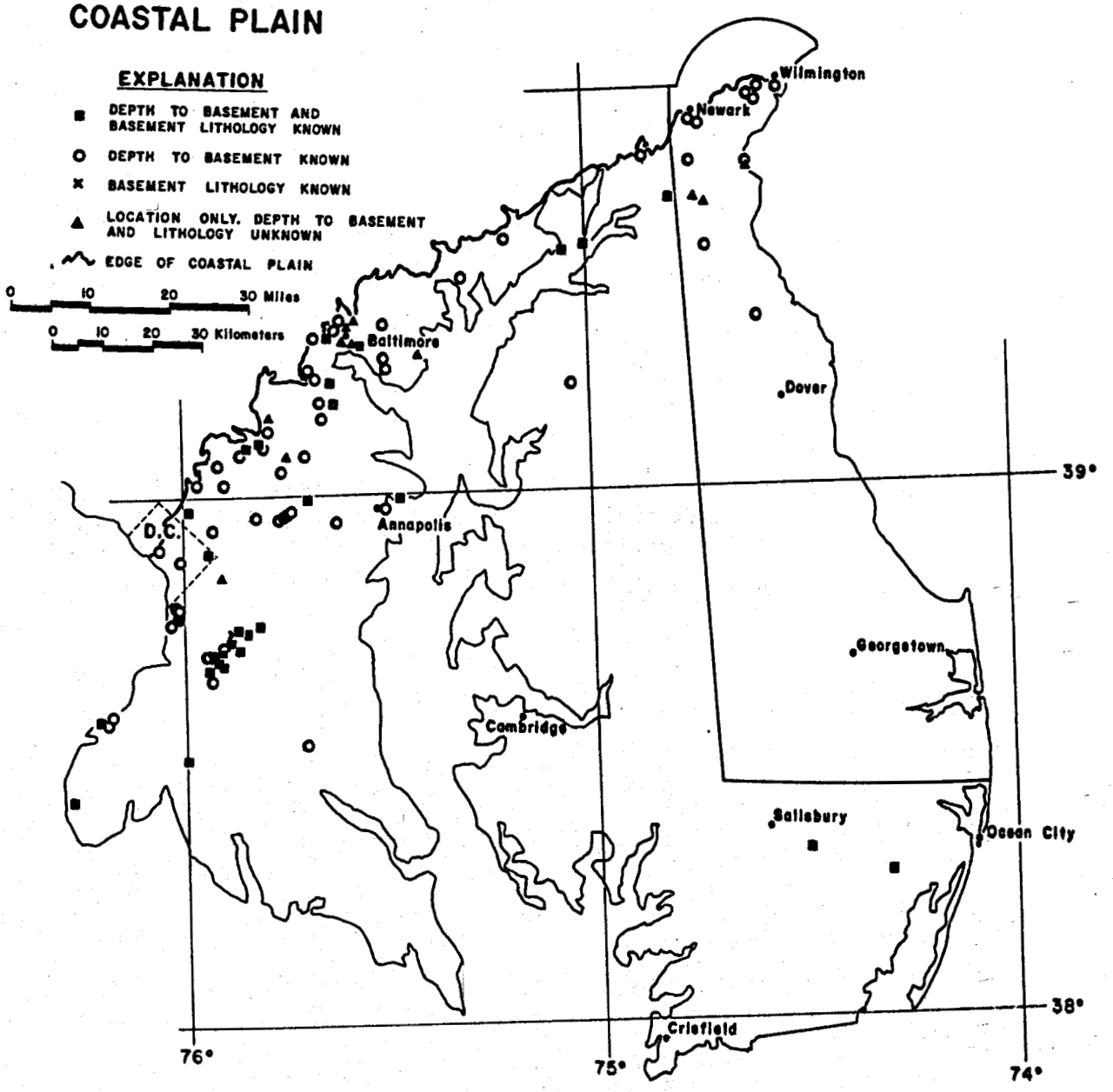

Figure A-2.3: Map showing locations of wells drilled to basement in Virginia and nature of data included in VPI & SU compilation.

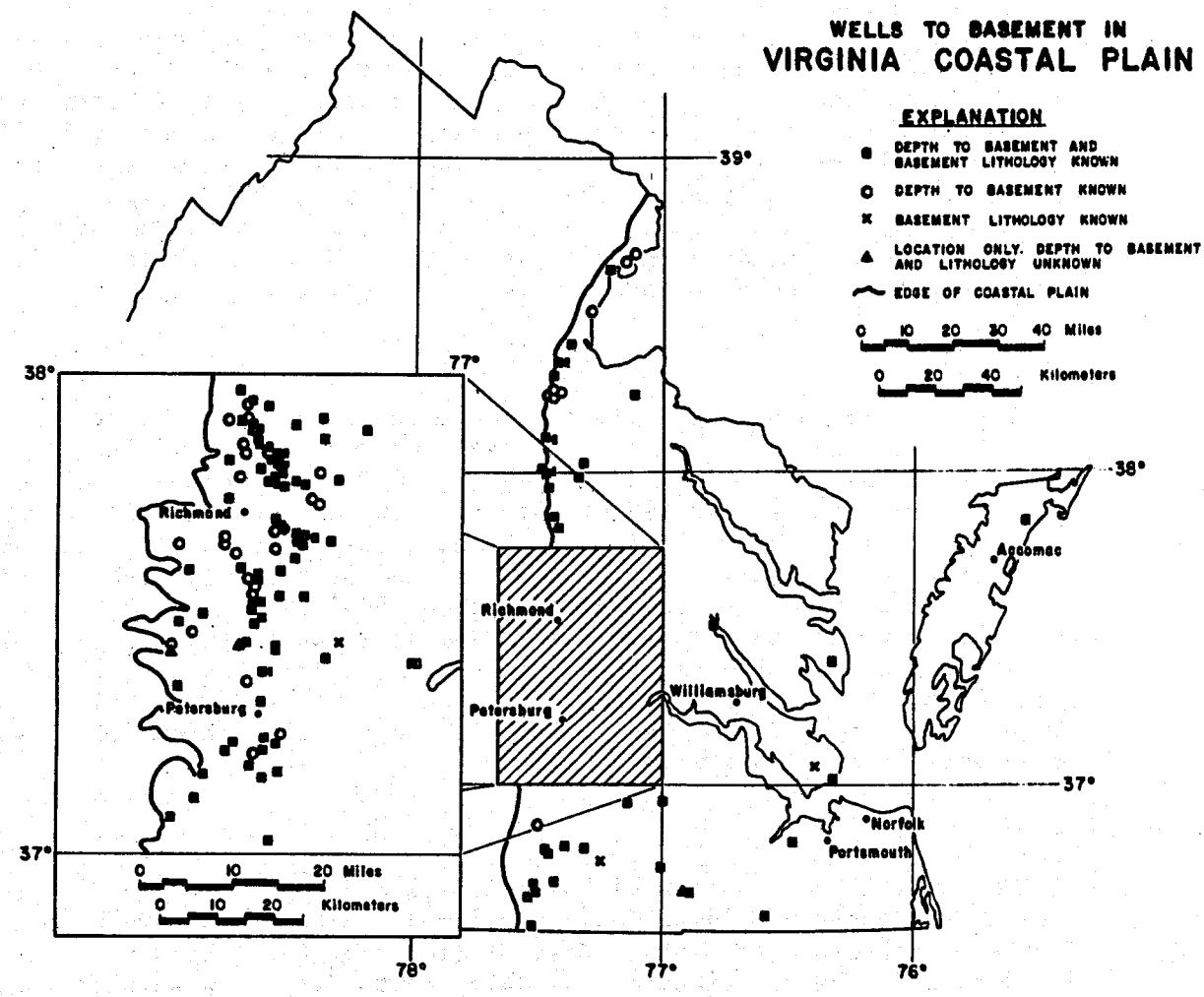
WELLS TO BASEMENT IN
VIRGINIA COASTAL PLAIN
EXPLANATION
DEPTH TO BASEMENT AND BASEMENT LITHOLOGY KNOWN
DEPTH TO BASEMENT KNOWN
BASEMENT LITHOLOGY KNOWN
LOCATION ONLY. DEPTH TO BASEMENT AND LITHOLOGY UNKNOWN
EDGE OF COASTAL PLAIN
0 10 20 30 40 Miles
0 20 40 Kilometers
39°
38°
37°
77°
78°
76°
Richmond
Petersburg
Williamsburg
Norfolk
Portsmouth
Accomac
0 10 20 Miles
0 10 20 Kilometers

test, the J. and J. Enterprises Taylor well, provides any information about the basement below the Coastal Plain. Of the one hundred and eighty-one basement wells in Virginia, basement lithology descriptions have been compiled for one hundred and thirty-one. Depths to basement have been recorded for one hundred and seventy-four wells.

North Carolina

The compilation of basement wells in North Carolina includes four hundred and forty-five well locations (Figure A-2.4). This extremely large number relative to other states results primarily from a large number of shallow water wells listed in various state survey literature, but there are also a considerable number of deep oil and gas tests. In fact, seventy four of the basement wells are located more than 50 kilometers from the edge of the Coastal Plain. Fifty-one wells encountered pre-Cretaceous basement at depths exceeding 1500' (457 m); thirty-four of these reached basement at depths exceeding 3000' (915 m). The deepest of these, the Esso #1 Hatteras Light well, penetrated basement at 9878' (3010.8 m). Basement lithology is recorded for three hundred and fifty-nine North Carolina wells, while basement depth is known for one hundred and forty-five.

Georgia

Ninety-three basement wells have been catalogued for the state of Georgia (Figure A-2.5). Although this number seems low relative to the number of wells compiled for Virginia and North Carolina, considerable information is available concerning the myriad of oil and gas exploration wells that were drilled because of the proximity to the petroleum-producing Gulf Coast province to the west. Only nineteen of the listed Georgia wells are shallower than 500' (152 m), and sixty-five of the wells reached basement at depths greater than 1500' (457 m). The ninety-three Georgia basement wells are fairly evenly distributed across the Coastal Plain of the state. Basement lithology is known for seventy-seven of the wells, and depth to basement is known for seventy-nine of the wells.

The overall compilation of basement well data from New Jersey to Georgia (presently excluding South Carolina) exhibits a severe paucity of data in deeper parts of the Coastal Plain north of North Carolina. In addition, the distribution of data north of North Carolina is strongly skewed toward the western edge of the Coastal Plain, where buried basement rocks are encountered at shallow depths. Because of the poor distribution and lack of deep well data in the northern part of the Coastal Plain, only a few generalizations can be proffered concerning basement lithologies and depths to basement in this area. The better distribution and greater number of deep wells in North Carolina and Georgia are sufficient for constructing general basement lithology and structure contour maps.

Figure A-2.4: Map showing locations of wells drilled to basement in North Carolina and nature of data included in VPI & SU compilation.

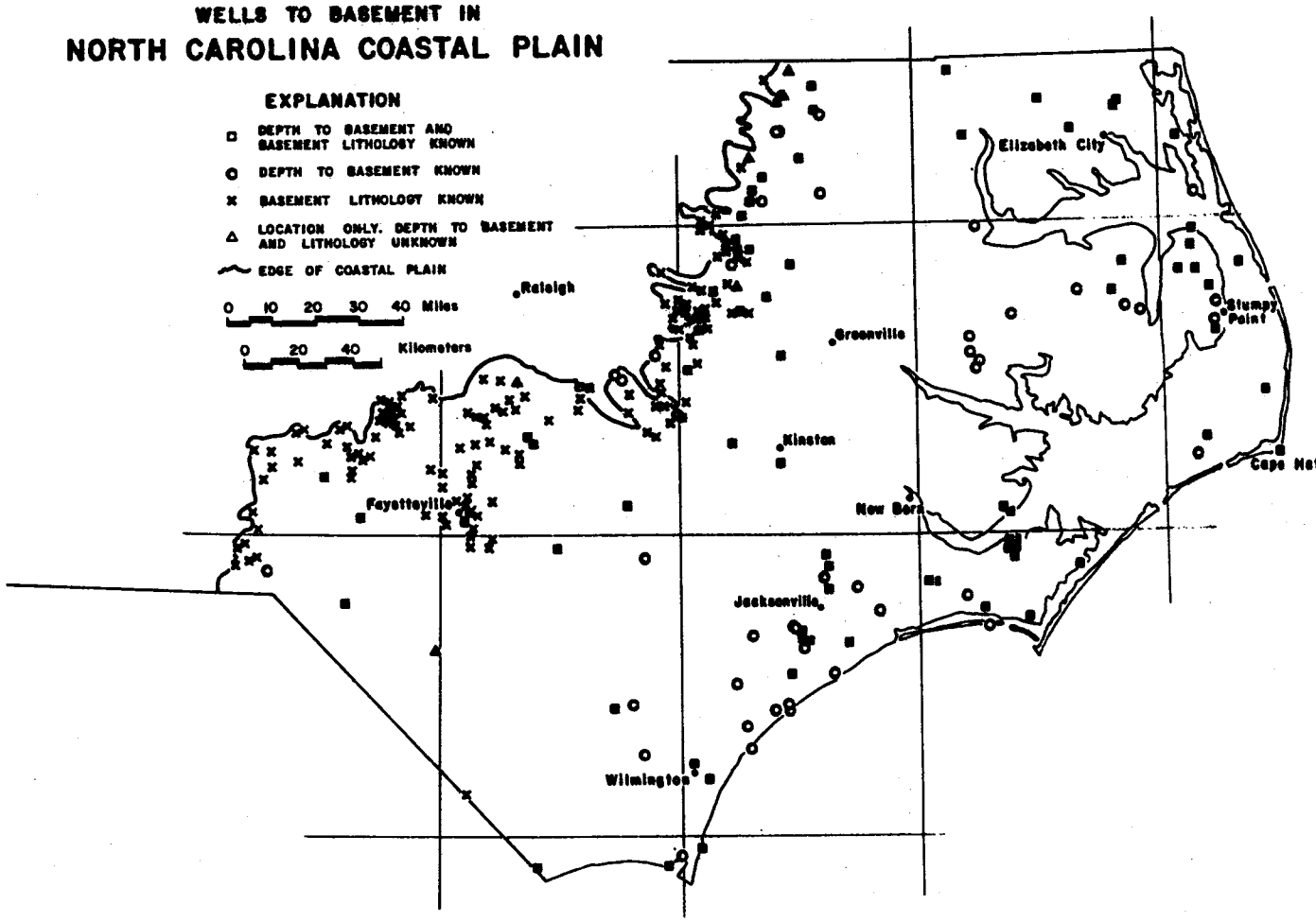
WELLS TO BASEMENT IN
NORTH CAROLINA COASTAL PLAIN
EXPLANATION
DEPTH TO BASEMENT AND BASEMENT LITHOLOGY KNOWN
DEPTH TO BASEMENT KNOWN
BASEMENT LITHOLOGY KNOWN
LOCATION ONLY. DEPTH TO BASEMENT AND LITHOLOGY UNKNOWN
EDGE OF COASTAL PLAIN
0 10 20 30 40 Miles
0 20 40 Kilometers
Raleigh
Elizabeth City
Greenville
Kinston
Fayetteville
New Bern
Jacksonville
Wilmington
Stumpy Point
Cape Hat

Figure A-2.5: Map showing locations of wells drilled to basement in Georgia and nature of data included in VPI & SU compilation.

WELLS TO BASEMENT IN GEORGIA COASTAL PLAIN

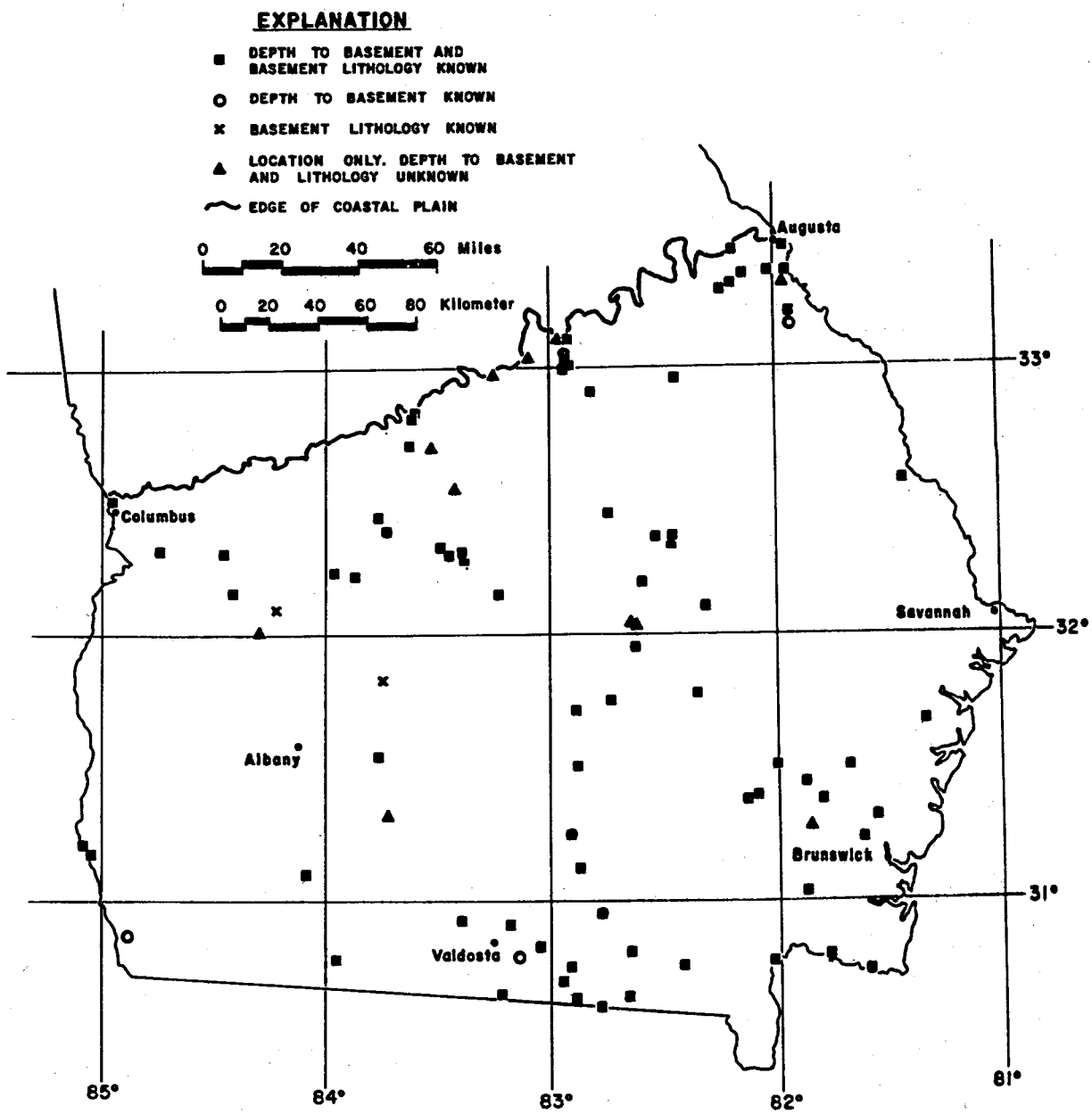

Correlations of basement geologic trends will not be discussed in the present report. Few samples of basement material have been studied by VPI & SU personnel; after the compilation of South Carolina data has been completed, efforts will be devoted to obtaining and analysing chip or core samples from selected wells.

DEPTH TO BASEMENT

The distribution of Coastal Plain wells for which depths to the pre-Cretaceous rocks are available is too heavily concentrated near the edge of the Coastal Plain to allow construction of an accurate structure contour map of the basement surface between New Jersey and Virginia. In North Carolina, however, basement wells in the deeper section of the Coastal Plain are far more numerous, and when combined with existing seismic data (Skeels, 1950; Bonini and Woollard, 1960), may be used to prepare a structure contour map of the North Carolina basement. This map is presented as Figure A-2.6, and represents a more complete and refined version than previously published maps (Spangler, 1950; Bonini and Woollard, 1960; Dennison et al., 1967; Flawn, 1967; Maher, 1971; Brown et al., 1972). Because this map has been constructed to aid in estimation of basement depths at several of the Department of Energy funded Coastal Plain drill holes in North Carolina, contours are drawn in English measures. Estimates of depths to basement derived from this map proved fairly accurate for five holes drilled for the project - actual depths to basement in these wells were all within 1-2% of predictions. These drill-holes were all less than 2000 feet deep; somewhat less accuracy might be expected in areas where the Coastal Plain sediments are thicker and the basement dip is correspondingly steeper.

Deep well data (deeper than 1500' or 457 m) are actually more numerous in Georgia than in North Carolina (sixty-five in GA vs. fifty-one in NC), but the far greater area of deep basement and the smaller total number of wells with reported basement depths in Georgia preclude a structure contour map for Georgia as refined as that presented for North Carolina. Figure A-2.7 is a generalized map of the Georgia basement surface, and while it is somewhat speculative in certain areas, it should be a more accurate portrayal of the configuration of the pre-Cretaceous surface than those presented in other accounts based on fewer data (Applin, 1951; Herrick and Vorhis, 1963; Flawn, 1967; Maher, 1971; Brown et al., 1972; Cramer, 1974).

A prerequisite to the evaluation of low-temperature geothermal resources along the Atlantic Coastal Plain is the accurate prediction of sediment thickness overlying a basement heat source. Sediment thickness is important in the determination of the insulating capability of the Coastal Plain sediments and in the extrapolation of measured temperature gradients to the base of the Coastal Plain sequence. The thickness of Coastal Plain sediments is also an important consideration in the calculation of the cost of drilling to basement at any particular location. The present data compilation enables predictions of the depth to basement to be made with reasonable accuracy in North Carolina, and with a lesser degree of accuracy in Georgia. Depth

Figure A-2.6: Structure contour map of pre-Cretaceous basement beneath North Carolina Coastal Plain.

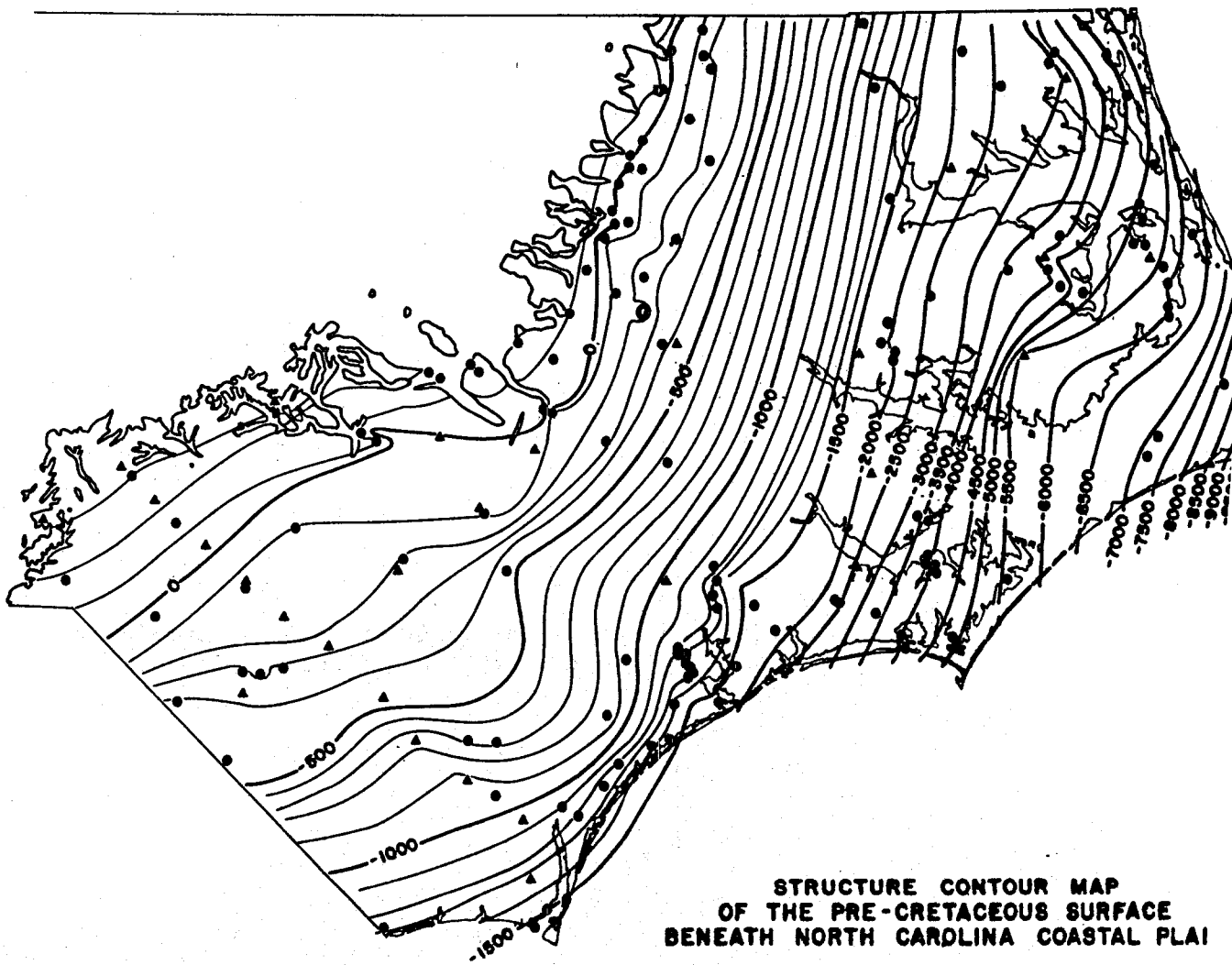

STRUCTURE CONTOUR MAP
OF THE PRE-CRETACEOUS SURFACE
BENEATH NORTH CAROLINA COASTAL PLAI

0 10 20 30 40 50 Miles

0 20 40 60 Kilometers

CONTOUR INTERVAL: 100' ABOVE -1500'
500' BELOW -1500'
MEAN SEA LEVEL DATUM

▲ SEISMIC DATA
● WELL DATA

Figure A-2.7: Generalized structure contour map of pre-Cretaceous basement beneath Georgia Coastal Plain.

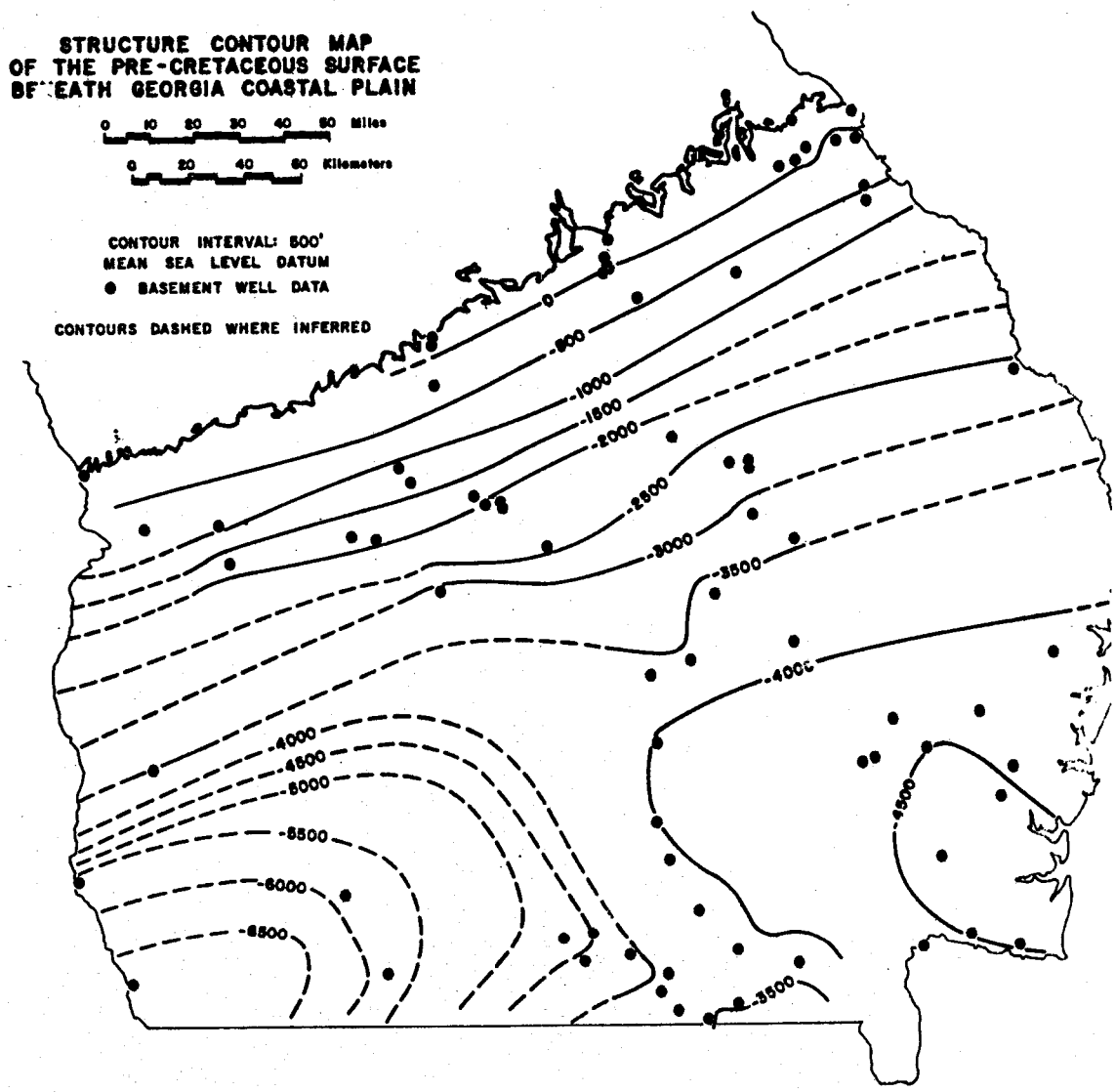
STRUCTURE CONTOUR MAP
OF THE PRE-CRETACEOUS SURFACE
BENEATH GEORGIA COASTAL PLAIN
0 10 20 30 40 50 Miles
0 20 40 60 Kilometers
CONTOUR INTERVAL: 500'
MEAN SEA LEVEL DATUM
● BASEMENT WELL DATA
CONTOURS DASHED WHERE INFERRED
0
-500
-1000
-1500
-2000
-2500
-3000
-3500
-4000
-4500
-5000
-5500
-6000
-6500

estimates between New Jersey and Virginia must be computed by interpolation and extrapolation between known basement well (and locally, seismic) data points. Depths to pre-Cretaceous basement have been estimated for each of the heat flow test holes which have been drilled to date. These data are presented in Table A-2.1.

Table A-2.1: Estimated depths to basement in Coastal Plain drill-holes.

Coastal Plain Drill-hole #	Location	Estimated depth to basement
60	Hampton, VA	2175'-2250' (665-685 m)
59	Near Sunnybank, VA	2900'-3500' (884 - 1067 m)
57	Near Atlantic, VA	∿6300' (∿1920 m)
56	Near Eastville, VA	3025' - 3150' (920-960 m)
55	Tasley, VA	∿5300' (∿1615m)
54	Nr. Greenwood, DE	∿4100' (∿1250 m)
53	Snow Hill, MD	∿6500' (∿1980 m)
52	Nr. Whiteburg, MD	∿5450' (∿1660 m)
51	Kingston, MD	∿4600' (∿1400 m)
50	Rehoboth, MD	∿5500' (∿1675 m)
49	Nr. Oak Hall, VA	∿5600' (∿1700 m)
48	Nr. Atlantic, VA	∿6350' (∿1935 m)
47	Salisbury	∿5300' (∿1615 m)
46	No. Salisbury, MD	∿4650' (∿1415 m)
45	Nr. Hebron, MD	∿4400' (∿1340 m)
43B	North of Ocean City, MD	∿8500' (∿2590 m)
41	Sea Girt, NJ	∿2075' (∿633 m)
40	Fort Monmouth, NJ	∿1100' (∿335 m)
39A	Forked River, NJ	∿3275' (∿1000 m)
38	Atlantic City, NJ	∿5300' (∿1615 m)
36	Cape May, NJ	6250' (1905 m)
35	SE of Dover, DE	3200'-4000' (975-1220 m)
34E	Assawoman Bay, DE	6300'-7600' (1920-2320 m)
34C	Nr. Ellendale, DE	∿4500' (∿1370 m)
34	Lewes, DE	550'-6500' (1675-1980m)
33	Nr. Blackwater. MD	∿3350' (∿1020 m)
32A	Crisfield, MD	∿4250' (∿1300 m)
31C	Salisbury, MD	∿4625' (∿1410 m)
30A	Ocean City, MD	∿8500' (∿2590 m)
29	Wallops Island, VA	∿7500' (∿2285 m)
28A	Nr. Cheriton, VA	3025'-3150' (920-960 m)
27	Hampton, VA	2050'-2150' (625-655 m)
26	Isle of Wright, VA	1350'-1420' (410-435 m)
25A*	Portsmouth, VA	1828' (557 m)
24	Norfolk, VA	2250'-2350' (685-715 m)
23	Virginia Beach, VA	∿3100' (∿945 m)
22	So. of Virginia Beach, VA	3400'-3700' (1035-1125 m)
21	Nr. Barco, NC	3850'-4150' (1175-1265 m)
20	Elizabeth City, NC	2900'-3350' (885-1020 m)
19	Nr. Stumpy Point, NC	5750'-5940' (1755-1810 m)
18	Engelhard, NC	5850'-6200' (1785-1890 m)
17	Nr. Morehead City, NC	4365'-4565' (1330-1390 m)
16A*	Kinston, NC	680' (207 m)
16	Nr. Havelock, NC	2725'-2775' (830-845 m)
15A	Nr. Folkstone, NC	1615'-1640' (490-500 m)
15*	Camp LeJeune, NC	1648' (502 m)
14A*	Nr. Southport, NC	1525' (465 m)
14*	East Wilmington, NC	1263' (385 m)

*Basement encountered in drill-hole

DEPARTMENT OF ENERGY FUNDED BASEMENT DRILL-HOLES

To date, basement samples have been obtained from seven drill-holes which were funded as part of the VPI & SU Geothermal Project or Targets of Opportunity, Project of The Department of Energy, (Figure A-2.8). These drill-holes were the C. D. Hopkins et al. well (JE-1) in Jesup, GA, holes drilled by VPI & SU in Sussex Co., VA (PT-1), and Dort, NC (DO-1), three heat flow test holes drilled by Gruy Federal, Inc. in Kinston, NC (#16-A), Camp LeJeune, NC (#15),and Wilmington, NC (#14), and a hole drilled to basement in Portsmouth, VA (#25-A) by Gruy Federal, Inc. This last hole is presently being extended into the basement by the VPI & SU drill.

The Hopkins well was discussed in a previous report (VPI & SU-5648-3), and heat flow/gradient data were presented for PT-1 in the same report. Sixty-four feet of core were obtained from DO-1 in late 1978, with more coring scheduled for completion by Summer, 1979. Coastal Plain drill holes #16-A, #15, and #14 were all completed between December, 1978 and January, 1979. Chip samples of basement rock were obtained from hole #16A, and short cores of basement rock were obtained from holes #15 and #14. Basement is currently being cored in hole #25-A.

Petrologic studies of basement samples from DO-1, C.P. #'s 14, 15, 16A, and 25A are all in initial stages. In the course of this work, studies will include petrography, chemistry, age-dating, and microprobe analyses of the cores from DO-1, C.P. #'s 14, 15, and 25-A, and petrographic and microprobe analyses of the chip samples from C.P. #16-A.

Figure A-2.8: Map showing location of holes drilled to basement for which basement samples have been collected as part of the DOE-VPI & SU Geothermal Project.

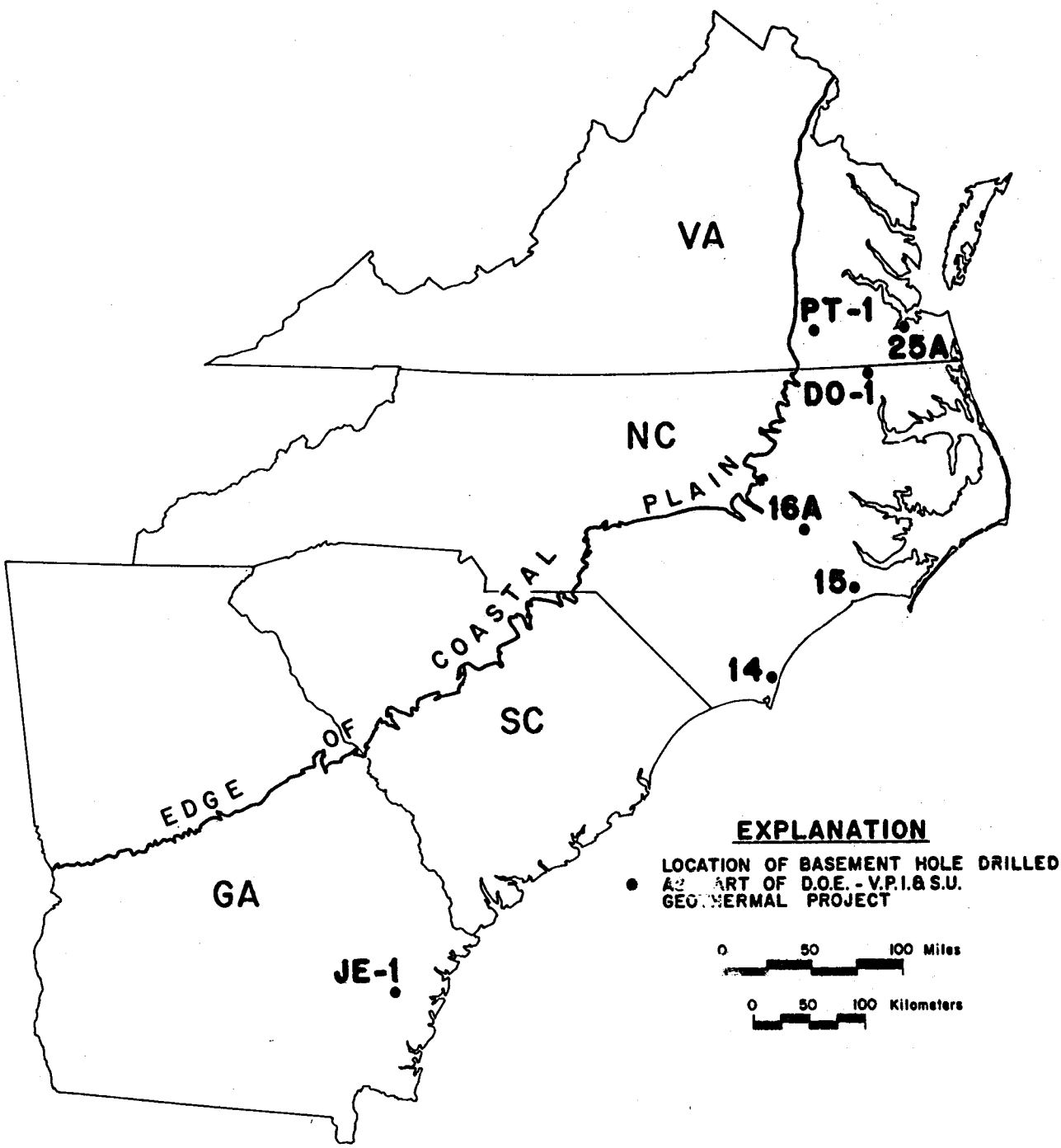
VA
NC
SC
GA
PT-1
25A
DO-1
16A
15.
14.
JE-1
PLAIN
COASTAL
EDGE OF
EXPLANATION
LOCATION OF BASEMENT HOLE DRILLED AS PART OF D.O.E. - V.P.I.& S.U. GEOTHERMAL PROJECT
0 50 100 Miles
0 50 100 Kilometers

References

Applin, P. L., 1951. Preliminary report on buried pre-Mesozoic rocks in Florida and adjacent states; U.S. Geol. Survey Circular #91, 28p.

Bonini, W. E. and Woollard, G. P., 1960. Subsurface geology of North Carolina - South Carolina Coastal Plain from seismic data; Bull. Amer. Assoc. Petrol. Geol., vol. 44, p. 298-315.

Brown, P. M. , Miller, J. A. and Swain, F. M., 1972. Structural and stratigraphic framework and spatial distribution of permeability of the Atlantic Coastal Plain, North Carolina to New Jersey; U.S. Geol. Survey Prof. Paper 796, 79p.

Cramer, H. R., 1974. Isopach and lithofacies analyses of the Cretaceous and Cenozoic rocks of the Coastal Plain of Georgia, in Symposium on the petroleum geology of the Georgia Coastal Plain; GA Geol. Survey Bull. 87, p. 21-43.

Dennison, R. E., Raveling, H. P., and Rouse, J. T., 1967. Age and description of subsurface basement rocks, Pamlico and Albemarle Sound areas, North Carolina; Bull. Amer. Assoc. Petrol. Geol., vol. 51, p. 268-272.

Flawn, P. T., 1967. Basement map of North America, Basement Rock Project Committee; Amer. Assoc. Petrol. Geol. and U.S. Geol. Survey.

Herrick, S. M. and Vorhis, R. C., 1963. Subsurface geology of the Georgia Coastal Plain; GA Geol. Survey Info. Circ. 25, 78p.

Maher, J. C., 1971. Geologic framework and petroleum potential of the Atlantic Coastal Plain and Continental Shelf; U.S. Geol. Survey Prof. Paper 659, 98p.

Skeels, D. C., 1950. Geophysical data on the North Carolina Coastal Plain; Geophysics, vol. 15, p. 409-425.

Spangler, W. B., 1950. Subsurface geology of the Atlantic Coastal Plain of North Carolina; Bull. Amer. Assoc. Petrol. Geol., vol. 34, p 100-132.

B. GEOCHEMISTRY

A. K. Sinha, Principal Investigator

J. R. Sans, Research Associate

S. T. Hall, Research Associate

D. M. McKay, Research Associate

B. B. Hanan, Grad. Research Associate

CORRELATION OF RADIOELEMENT CONTENT TO SURFICIAL WEATHERING PROCESSES

A. K. Sinha, S. T. Hall and J. R. Sans

The evaluation of any geochemical correlations to predict the extent of radioelement redistribution has to be based on the recognition of the original (magmatic) sites in the granitoid rocks. Information on site locations provided by fission track maps only permit documentation of uranium (and thorium) as observed today, not of the initial (magmatic) distribution.

The mobility of uranium has been documented in great detail by mumerous researchers. The question that still remains unresolved is the distinction between losses generated by low temperature meteoric water or post-crystallization and significantly later hydrothermal fluids.

Most of the plutons, if not all, in the southeastern U.S. being studied have undergone both types of fluid interaction. Therefore the problem of separating the meteoric water related losses is made more acute.

Our preliminary data on U-Pb disequilibrium studies (VPI & SU report 5648-3) strongly suggests redistribution of uranium about 200 m.y. ago and in this report we report on methods that can be used to understand recent losses of uranium.

1. The differential mobilities of uranium and thorium

Although uranium has been demonstrated to be extremely mobile in any oxidizing environment, thorium appears to be more resisant to solution transport at non-magmatic (lower) temperatures. In a study of the radioelement distribution in the Woodstock granite in Maryland, the variations in uranium content can be demonstrated to be related to surficial weathering processes. On the other hand, the thorium abundances were clearly related to magmatic distribution and even showed zoning in the pluton. The changes in U/Th ratios could be accounted for by uranium depletion, and for the Woodstock pluton, we can suggest an empirical relationship:

Th= (-.0.731) (DI) + 74.8, where Th is the thorium concentration in ppm, and DI is Differentiation Index (normative Q + Or +Ab) expressed in percent.

A similar exercise has been attempted on the Rion pluton, where the WIN-1 hole is located. In correlation diagrams of U vs. U/Th the best fit line has a steeper slope than simple U loss lines suggesting depletion of uranium in both core and surface samples during weathering processes. As such, we have attempted to show by the use of trace elements that the weathering process may have affected samples to depths of nearly 500'.

2. Use of differential mobilities of elements

The abundance of the element strontium is primarily controlled by the volume of feldspars present in a rock, because the partitioning coefficient of Sr between melt and feldspars is significantly greater than 1 (KD of Sr for K-feldspar is 3.9 and plagioclase is between 1.5 to 4.4; Hanson, 1978). As feldspars are the first minerals to alter to clay, loss of Sr (which does not partition into clay minerals) by solution transport is likely to change in the bulk rock.

Figure 1 suggests that Sr loss has occurred to depths of nearly 500 feet and perhaps as deep as 600 feet. The element titanium (shown as TiO2) is extremely immobile in most metamorphic processes, of which weathering can be considered to be a low temperature-pressure type. As such, samples which have not suffered any type of alteration would show a positive correlation between Ti and Sr. It can be seen from Fig. 1 that such a correlation exists for most the core samples. However, three samples from depths of 80', 290' and 500' fall off the trend and apparently appear to have lost strontium suggesting that weathering may have caused this depletion.

When surface samples are plotted on the same diagram, they generally show strontium contents similar to the unaffected core samples. This is in contradiction to the apparent strontium loss to nearly 500' as seen in the core. A possible mechanism to explain this discordancy would be if the strontium removed from feldspars by weathering were to be tied up in calcite which is present in most surface samples.

To check the validity of this interpretation, four samples (three from the surface and 80' core sample) were acid washed in cold dilute HCl acid. The analyses of the acid washed samples are given in Table 1.

Surface sample		1	2	3	Core 80'
Before leaching	Ti%	.37	.16	.39	.27
	Sr (ppm)	382	310	360	142
After leaching	Ti%	.38	.16	.39	.27
	Sr (ppm)	108	90	384	152

It can be seen that for samples 1 and 2, although the Ti content did not change, there was a substantial loss of strontium. Sample 3 from the surface showed essentially no change and appears to be as fresh as the deeper parts of the core. The core sample gave similar values between the leached and unleached fractions. The preliminary data from only four samples suggests that calcite bound strontium is easily removed and in those samples where strontium loss has occurred with no carbonate precipitation, i.e. feldspar alteration to clay, the lattice bound strontium in feldspars cannot be removed by dilute acid solutions.

This process needs to be more rigorously tested by using more samples for acid leaching and a more detailed analyses of suboptical presence of clay in feldspars. Additional problems that need to be addressed include: i) identification and separation of clay fractions related to higher temperature hydrothermal alteration versus lower temperature clay produced by weathering. ii) identification of the nature of the chemical gradient induced in the rock by the two types of alterations.

3. Parker Weathering Index

Uranium is thought to be redistributed by weathering processes. Hence, we have calculated several weathering indices based on major element chemistry and compared them with uranium abundance down the length of a core. We have calculated the indices described by Ruxton (1968) and Parker (1970). The weathering index suggested by Parker seems to be the most useful, because it is universally applicable and involves the fewest assumptions.

About twenty or twenty-five chemical analyses have been done for each core depending on the length of the core. Some of the cores contain abundant pegmatites, aplites, altered zones, fractures and slickensides. For such cores, the Parker Weathering Index does not exhibit an obvious pattern.

For the remaining cores, which are relatively free of disturbing influences, the pattern is relatively consistent. The Parker Index is fairly low at the surface indicating a weathered rock. For example, the WIN-1 core has a Parker Index of about 81 near the surface. Down to a depth of about 200 meters the Parker Index either remains about the same or increases slightly. Below 200 meters, the Parker Index increases systematically. For example, in the WIN-1 core the Parker Index increases from about 82 at 200 meters to 86 at 400 meters. At deeper depths the Parker Index does not fluctuate much except when pegmatites, etc., are encountered. The variations in uranium concentration seem to be sympathetic with the variations in the Parker Weathering Index, but there appears to be no correlation with thorium concentrations.

Summary

Preliminary geochemical analysis of WIN-1 core by using various techniques suggests some measurable degree of weathering to depths of nearly 500'. The leaching experiments need to be more rigorously pursued and the two generations of calcite need to be analyzed for delta O18 and Sr87/Sr86 ratios. It will permit an understanding of the nature of the fluid so we can discriminate between fresh versus marine water interactions. Preliminary samples are being processed for such studies and results should be available for the next report.

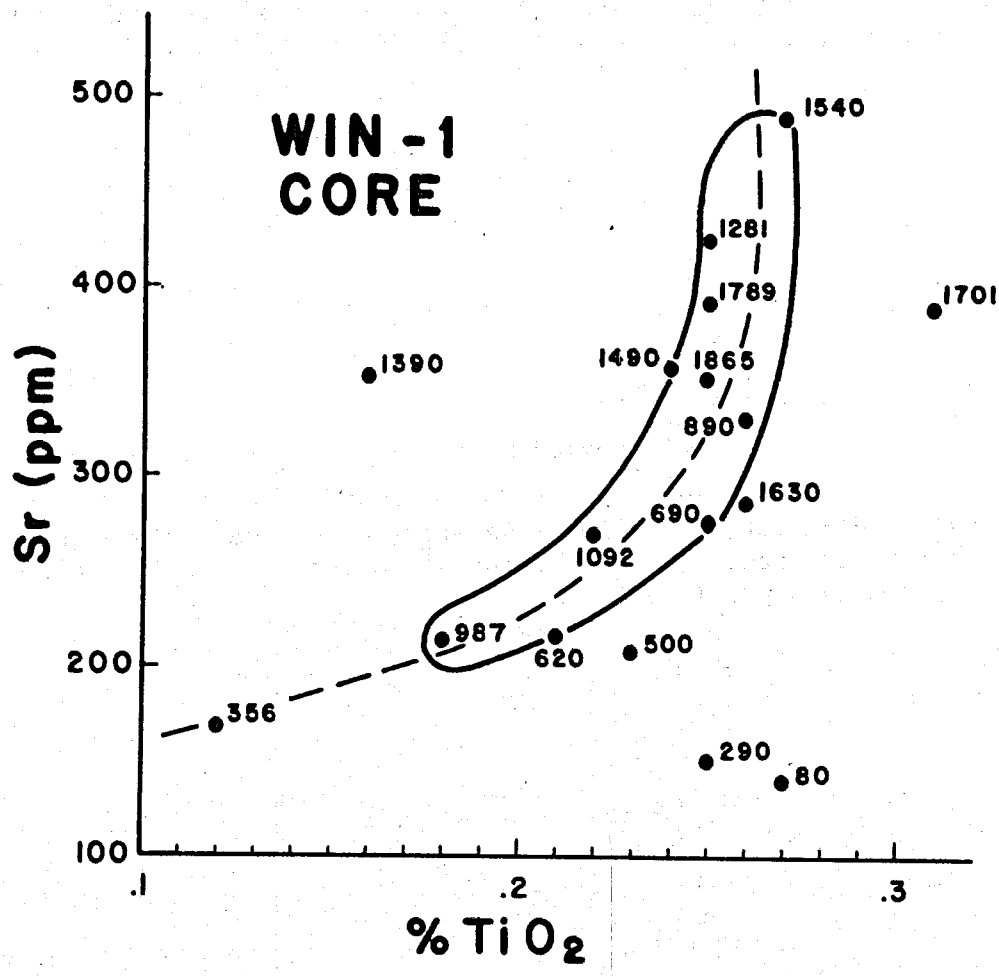

Figure 1. Correlation diagram between mobile strontium and immobile titanium. Numbers by dots indicate depth in feet. See text for discussion of results.

References

Hanson, G. W. (1978). The application of trace elements to the petrogenesis of igneous rocks of granitic composition. EPSL 38, 26-43.

Parker, Andrew (1970) An index of weathering for silicate rocks, Geological Magazine, Vol. 107, p. 501-504.

Ruxton, Bryan P. (1968) Measures of the degree of chemical weathering of rocks, Journal of Geology, Vol. 76, p. 518-527.

Acknowledgments

Partial funding for this effort was provided by the National Uranium Resource Evaluation, U.S. Department of Energy. Their interest in our program is appreciated.

C. GEOPHYSICS

John K. Costain, Principal Investigator

S. S. Dashevsky, Research Specialist

S. P. Higgins, Research Specialist

J. J. Lambiase, Research Associate

W. S. McClung, Research Specialist

L. D. Perry, Research Associate

M. Svetlichny, Research Specialist

Geothermal Exploration Methods and Results
Atlantic Coastal Plain

John K. Costain

Introduction

The first systematic effort to estimate the geothermal resources of the entire United States was made by the U. S. Geological Survey in 1975 and published as USGS Circular 726 (White and Williams, 1975). This study has been updated by a second assessment and published as USGS Circular 790 (Muffler, 1979). Muffler and Cataldi (1979) proposed the use of a consistent terminology for geothermal resource assessment. The 'geothermal resource base' is defined as all of the thermal energy in the earth's crust under a given area, measured from the mean annual temperature. The 'accessible resource base' is that part of the resource base which is shallow enough to be tapped by production drilling, and is divided into 'useful' and 'residual' components. The 'useful' component is defined as thermal energy that could be extracted at costs competitive with other forms of energy at some specified future time. This useful component is defined as the 'geothermal resource'. Much exploration remains to be done before the nature and extent of the geothermal resource in the eastern United States can be adequately defined.

Exploration for geothermal resources in the eastern United States takes place in a geologic environment quite unlike that of the west where generation of electric power from geothermal energy is well documented. Use of geothermal energy in the east will probably first be oriented toward non-electric applications using relatively low-temperature fluids as a source of energy for space heating and industrial processes and systems.

This paper briefly discusses the geophysical techniques we have used to investigate the geologic framework of potential geothermal resources of parts of the eastern United States. Geothermal resources in the Appalachian Mountain system and the Atlantic Coastal Plain can be grouped into four types:

I) Radiogenic heat-producing granite buried beneath a thick blanket of sediments of low thermal conductivity,
II) Normal geothermal gradient resources,
III) Warm water emanating from fault zones,
IV) Hot-dry-rock in regions of abnormal geothermal gradient.

Resource I is the principal subject of this paper. Resource II is widely available throughout much of the United States and is discussed by Sammel (1979). Resource III has been recognized in the eastern United States since before 1884 (Rogers, 1884). Resource IV is described by Pettitt (Symposium on Geothermal Energy and its Direct Uses in the Eastern U.S., held in Roanoke, VA, April 5-7, 1979. Sponsored by Geothermal Resources Council (GRC)).

Optimum sites for the development of geothermal energy in the eastern United States will probably be associated with the flat-lying, relatively unconsolidated sediments that underlie the Atlantic Coastal Plain (Figure C-1.1). In many locations, these sediments are known to yield large quantities of water. The water in these sediments at any given depth is hotter in some locations than in others and depends on the local value of the geothermal gradient. The gradient depends on the heat flow through the rocks and on the thermal conductivity of the rocks. In a series of extremely important papers Birch et al. (1968), Lachenbruch (1968), and Roy et al.(1968) showed that the local heat flow has a well-defined relationship to the concentration of uranium (U) and thorium (Th) in fresh, unweathered samples of granite collected from the surface of the earth. The immediate implication of their observation is that the distribution of U and Th in the upper 10 to 20 km (33,000 to 66,000 ft) of the earth's crust is primarily responsible for the observed lateral variations in surface heat flow in the eastern United States.

One of the principal objectives of the geothermal program at Virginia Polytechnic Institute and State University is to locate relatively young (330 million years old and younger) U- and Th-bearing granite in the basement rocks beneath the sediments of the Atlantic Coastal Plain. The targeting procedure integrates the disciplines of geology, geochemistry, and geophysics. Geologic and geochemical techniques are being applied to the rocks in the Piedmont in an effort to understand the ages, chemistry, and areal distribution of exposed granite plutons (see paper by Glover, GRC Symposium). Geophysical techniques include the interpretation of gravity and magnetic potential field data, as well as seismic data, and are being applied to both the Piedmont and the Coastal Plain.

Warm water emanating from fracture zones (resource III) is not the principal focus of this paper. Nevertheless, it is appropriate to mention this known resource. The origin of the hot springs in the eastern United States has been discussed by several authors (Rogers,1884; Reeves, 1932; Hewett and Crickmay, 1937; Stose and Stose, 1947; Dennison and Johnson, 1971; Lowell, 1975; Costain et al., 1976; Geiser, 1976; Hobba et al, 1977; Hobba et al., 1978). Perry et al. (1979) proposed a model for the hot springs in Virginia that we believe applies to most of the hot springs in the eastern United States. Before discussing the geologic framework for the hot springs in Virginia it will be useful to review selected geophysical methods we have used to date in the eastern United States for the exploration of geothermal resources.

Geophysical Exploration of Geothermal Resources in the Eastern United States

It is beyond the scope of this paper to discuss in detail the various geophysical, geochemical, and geological techniques that are commonly used to evaluate geothermal resources. The exploration methods used are dependent upon the nature of the geothermal resource. Many of the conventional geophysical methods of exploration are discussed by Dobrin (1977) and are, of course, not restricted to geothermal applications. We have used several kinds of geophysical data during the course of our geothermal program. They are discussed briefly below before summarizing the results of our studies on the Atlantic Coastal Plain.

Heat flow. The most important geophysical data for the exploration of geothermal resources in the east consist of values of regional and local heat flow flowing towards the surface of the earth. Heat flow, q, is described by the conduction equation

$$q = K\,G$$

where the units of q are calories per square cm per sec, K is thermal conductivity (millicalories per cm-sec-°C), and G is the geothermal gradient in °C/Km (1 °F/100 ft = 18.23 °C/Km). This equation applies only to the transport of heat by conduction. Heat transport by fluid convection (hot water) is much more efficient. Any successful geothermal system must incorporate both conduction and convection. A hole drilled to a depth of, say, 300 m (1000 ft) will usually encounter different rock types, each with a different thermal conductivity, K. Because q is constant at any depth in the hole , then as K decreases the geothermal gradient, G, will increase to keep the product KG constant. Simply stated, this means that for any given heat flow, the highest temperature gradients occur in rocks with the lowest thermal conductivities. Shales in the Valley and Ridge province of the Appalacian Mountain System will have temperature gradients that are much higher than those found in holes drilled into dolomite $CaMg(CO_3)_2$. For the same value of the heat flow, q, higher temperatures will be reached at shallower depths if holes are drilled into thick sequences of shale rather than into dolomite. Shale is a better insulator. The unconsolidated sediments of the Atlantic Coastal Plain have an even lower thermal conductivity.

A major unresolved problem in geology and geophysics is the reason for regional and local variations in surface heat flow. For the development of a geothermal resource, it is apparent that the combination of high heat flow and low thermal conductivity will result in the highest subsurface temperatures at the shallowest depths. It is beyond the scope of this paper to speculate on the many hypotheses advanced to explain lateral variations in surface heat flow. One undisputed explanation, however, is that variations in lateral and vertical concentrations of U and Th in basement rocks will result in substantial variations in heat flow (Birch et al., 1968).

The generation of heat by the process of radioactive decay is one of conversion of mass to energy according to Einstein's equation, $E=mc^2$. Only three elements have isotopes with long enough halflives to be important for radioactive heat generation in rocks. These are isotopes of U, Th, and potassium (K). Radioactive isotopes of these elements have halflives of the order of 1 billion years or more. The heat contribution, H, in calories/gram per year from the radioactive decay of these isotopes is given by the equation

$$H = 0.72U + 0.20Th + 0.27K$$

where U is in parts per million (ppm) uranium, Th is in ppm thorium, and K is in per cent potassium (Birch, 1954). The constants in this equation have been revised slightly by Rybach (1976). Thorium is usually more abundant than uranium in granite, the Th/U ratio falling between 3 and 4. Most of the heat produced comes from U and Th; only about 10 - 15% comes from K. The U, Th, and K concentrations of the Cuffytown Creek pluton in South Carolina are about 10 ppm U, 33 ppm Th, and 3.7% K. Thus this granite generates about 15 calories per gram per year. The density of the granite is about 2.67 grams per cubic centimeter. The granite therefore generates about 12×10^{-13} calories per cubic cm per sec, or about 20,000 watts per cubic mile. In fact, most of the heat flowing towards the surface in the Cuffytown Creek granite comes from the heat generated by the radioactive decay of isotopes of U, Th, and K.

Granitic rocks relatively enriched in U and Th (concentrations as high or higher(?) than the Cuffytown Creek) occur locally in the basement rocks beneath the sediments of the Atlantic Coastal Plain. The concentrations of U and Th in the granites are low, a few parts per million, but these concentrations are higher than those in adjacent rocks in the basement. In spite of these low concentrations, large volumes of granite with U and Th will increase substantially the subsurface temperature. Thus, higher temperatures will be found at shallower depths within the overlying sediments. Radiogenic heat is in addition to the normal heat flow around and beneath the granite plutons and can be greater by more than a factor of 2 than the background heat flow that constitutes the normal heat leaving the earth. In some parts of New England, for example, radiogenic heat from granite constitutes two-thirds of the total heat flow leaving the earth in that area (Birch et al., 1968). An understanding of the distribution of granites and of U and Th in the basement rocks is therefore important to define locations where the highest temperatures will occur at the shallowest depths.

Granite plutons are exposed in the Piedmont Province northwest of the Atlantic Coastal Plain (Figure C-1.1). These exposed basement rocks are concealed to the southeast by a seward-thickening wedge of sediments beneath the Atlantic Coastal Plain. Few holes have been drilled through the sediments to basement, but the sediment thickness is known to be about 3 km (9900 ft) at Cape Hatteras, N.C.

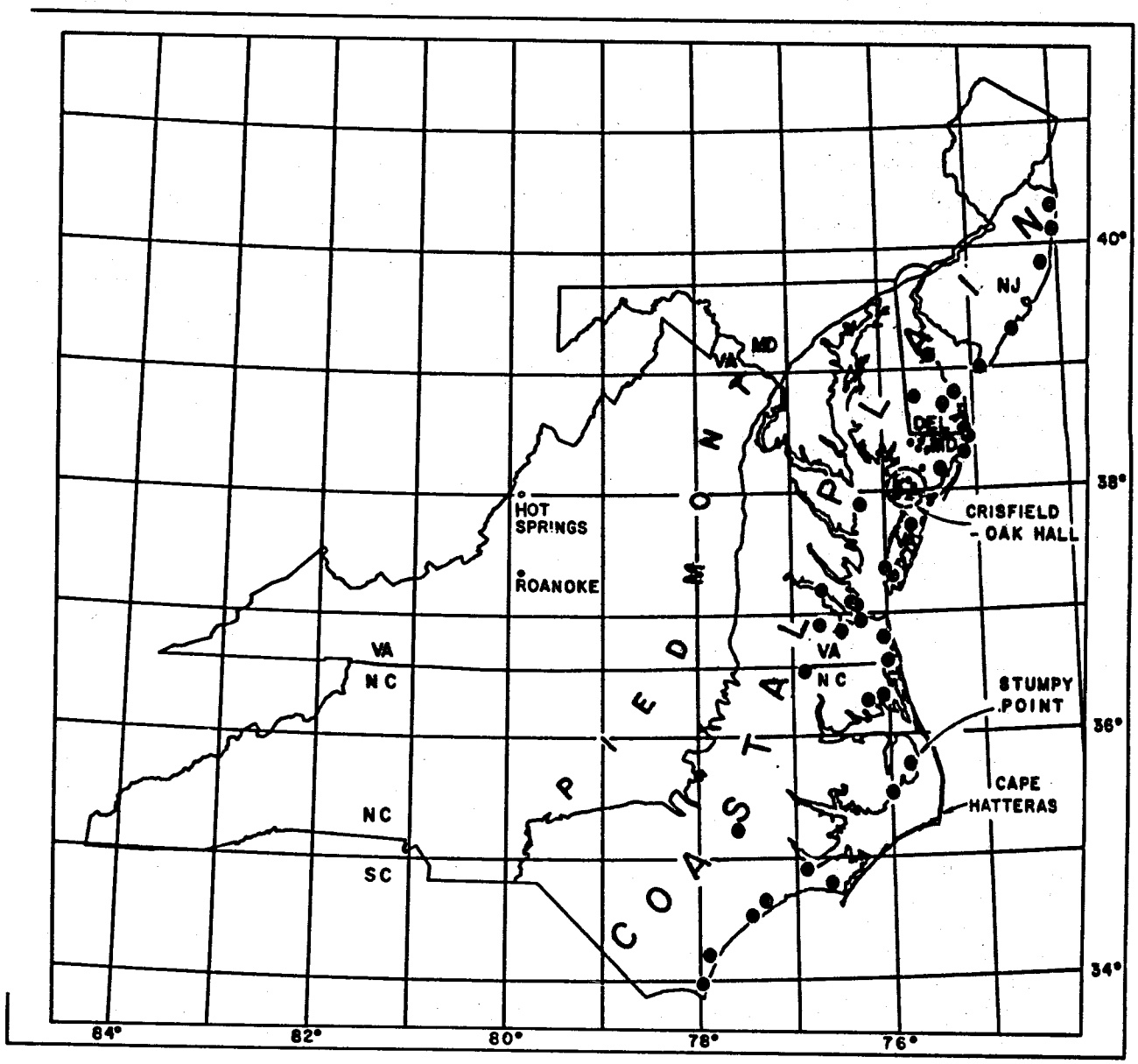

Figure C-1.1. Locations of shallow (300 m) heat flow holes drilled on Atlantic Coastal Plain are shown as small dots.

Figure C-1.2 illustrates the effect on subsurface temperature where basement rocks are covered with a thick sequence of sediments of relatively low thermal conductivity. Moderate amounts of heat-producing elements occur in the basement rocks, concentrated primarily in granite. The concentrations assumed are not unreasonable. Heat generations of 15 HGU (1 HGU = 10^{-13} cal/cm^3 per sec) have been determined by us in granite plutons exposed in the Piedmont. In New England, exposed granite plutons locally have heat productions of 24 HGU (Birch et al., 1968). The leftmost curve in Figure C-1.2 is the temperature-depth profile in basement crystalline rocks that contain no heat-producing elements, and are not overlain by sediments. As U and Th are added to produce first 10 HGU and then 20 HGU, the subsurface temperature (and therefore the geothermal gradient) increases. Finally, if U- and Th-bearing granite is blanketed by sediments that have a relatively low thermal conductivity, the subsurface temperature is increased further. The relatively unconsolidated sediments of the Atlantic Coastal Plain that overlie granite plutons in the basement is the geologic environment of high geothermal resource potential in the east. Heat flow and the geothermal gradient should be higher over these granites if the granites contain modest concentrations of U and Th. Locations of shallow (300 m) holes drilled by the Department of Energy on the Atlantic Coastal Plain during 1978-79 to determine the geothermal gradient and heat flow were based primarily on the interpretation of gravity and magnetic potential field data.

Gravity data. The magnitude of the gravitational field at any location on the surface of the earth depends locally on the different rock types at depth. Different rock types have different densities. Some rocks weigh more than others. Granite is the least dense of the igneous intrusive rocks that occur in large volumes. Since granite is less dense than the country rocks into which it has been emplaced, a negative gravity anomaly results (Figure C-1.3). If, however, granite was emplaced in country rock that was <u>also</u> granitic in chemical composition, then the gravity field will <u>not</u> be well-defined over the granite and additional geophysical and/or geological techniques must be used.

An important consideration in the targeting of concealed radiogenic granites beneath the sediments of the Atlantic Coastal Plain is an understanding of the regional geologic framework (see paper by Glover, this volume). In the absence of a gravity or magnetic anomaly an understanding of the regional geology and the possible nature of concealed basement trends is important. Relatively few holes have sampled the basement to date.

Magnetic data. The normal (approximately symmetrical) magnetic dipole field of the earth is distorted by the presence of magnetic minerals in rocks, the most important of which is magnetite. Granite plutons usually contain a small percentage of magnetite. The first step in the interpretation of aeromagnetic data is to subtract the earth's dipole field and examine the 'magnetic anomalies' that remain (see Costain, 1979 for a general summary of the description and interpretation of magnetic anomalies). An excellent magnetic anomaly

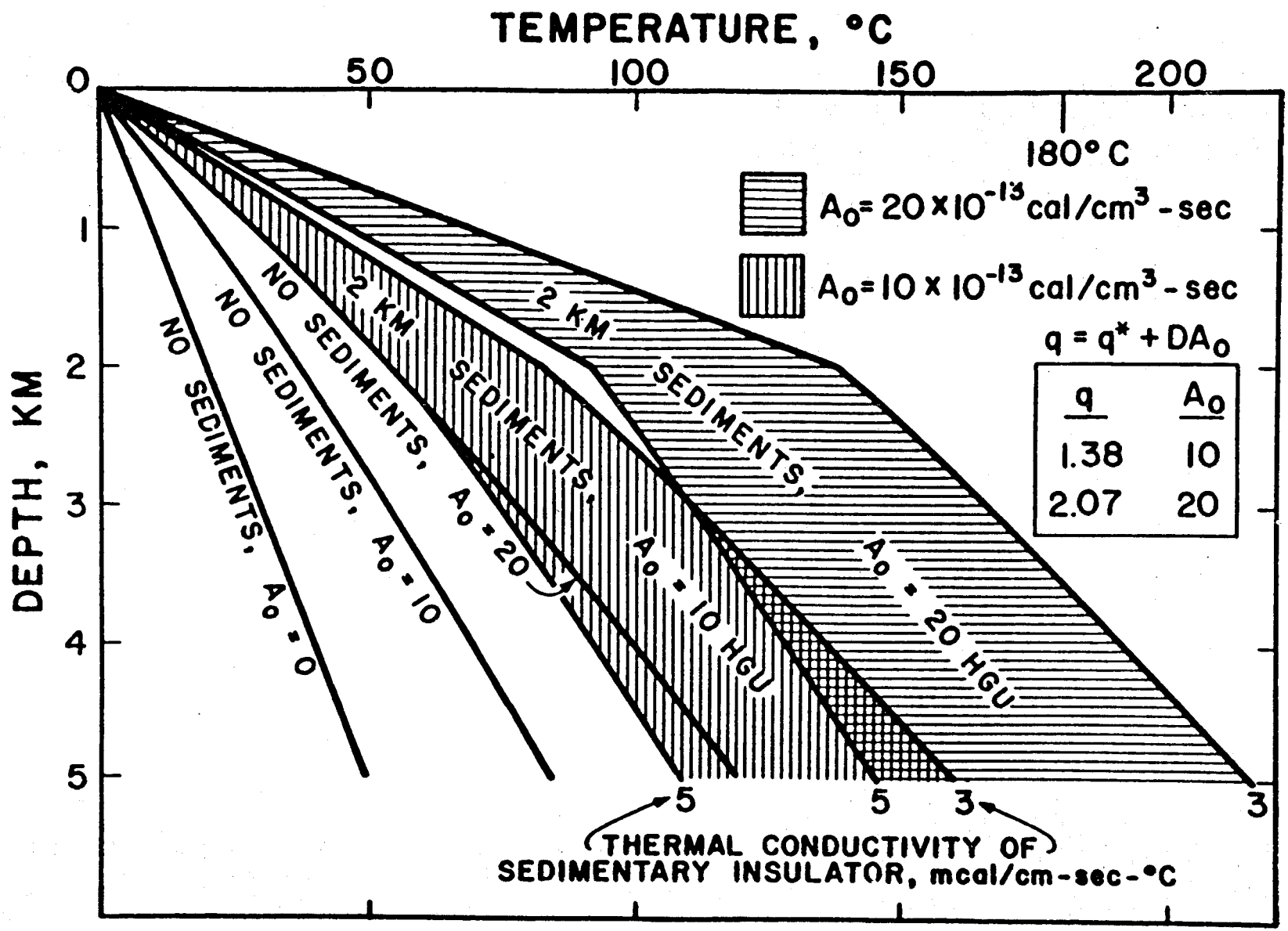

Figure C-1.2. Effect on subsurface temperatures of insulating blanket of sediments of low thermal conductivity.

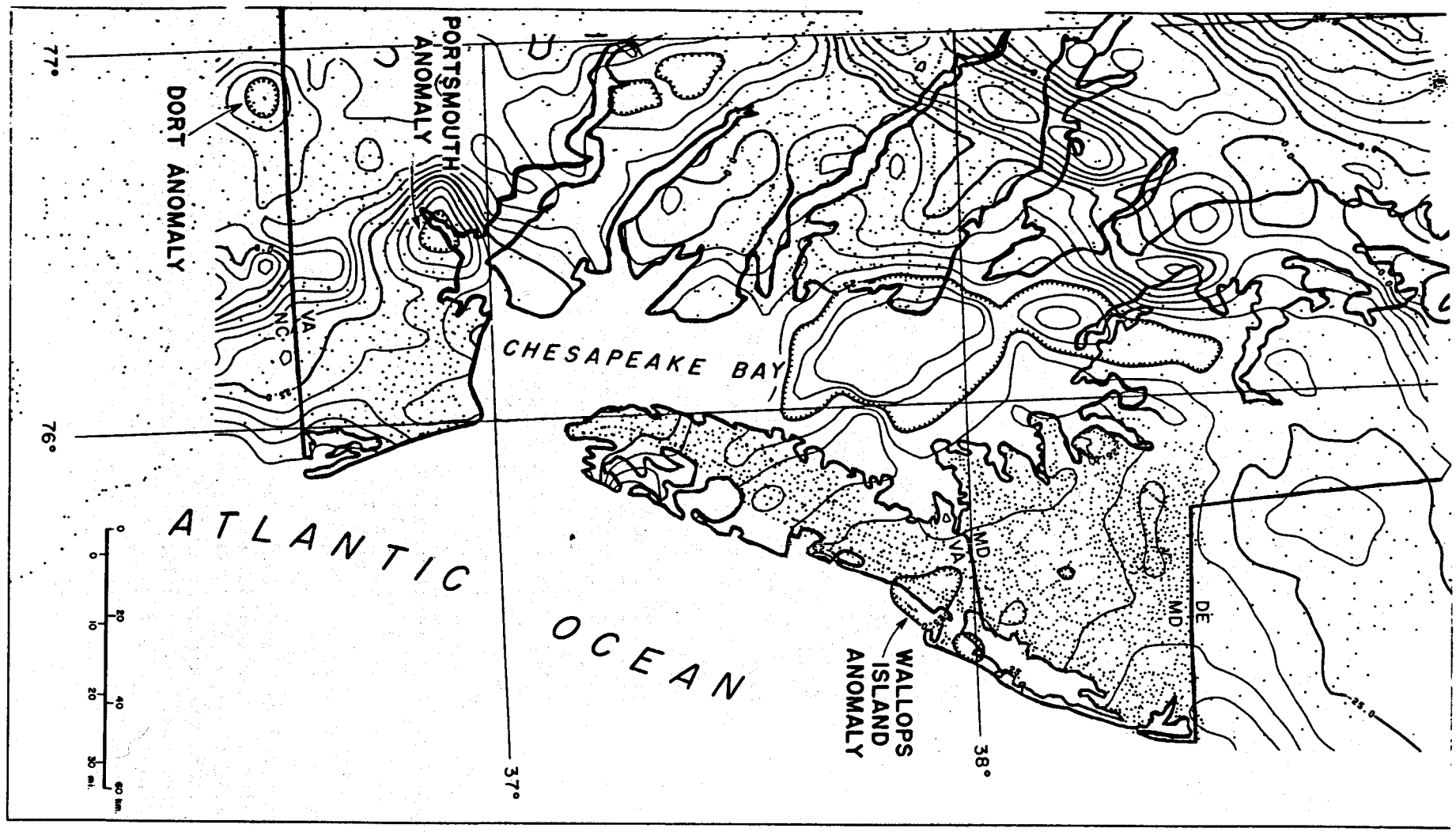

Figure C-1.3 Gravity map of parts of Delaware, Maryland, and North Carolina. Contour interval is 5 milligals. Gravity stations indicated by small dots.

associated with a granite exposed in the Piedmont is shown in Figure C-1.4. Similar granite bodies concealed beneath the sediments of the Atlantic Coastal Plain might be detected by their magnetic signatures if the depth of burial is not too great and if metamorphism has not destroyed the magnetic properties of the mineral assemblages. Examination of existing magnetic data obtained over the Coastal Plain suggests that granitic plutons occur in the basement.

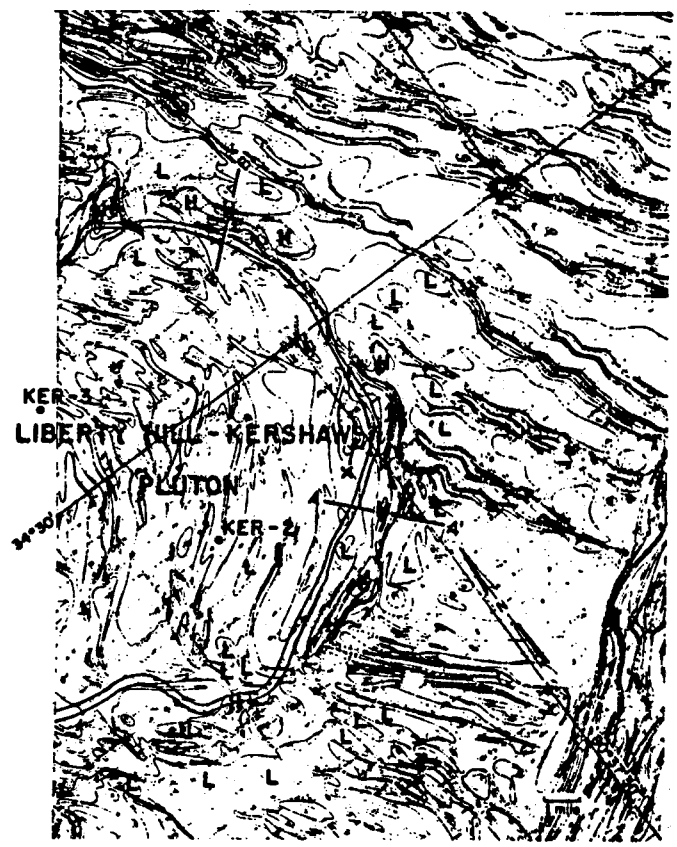

Figure C-1.4. Circular magnetic anomaly associated with the Liberty Hill-Kershaw granite pluton. Northwest-trending linear anomalies are Triassic dikes.

Seismic data. Standard techniques of reflection seismology are essential to define the subsurface geometry of a potential geothermal resource in the eastern United States. In general, reflection seismology offers the highest resolution of any geophysical method used to investigate subsurface geology. In particular, reflection seismology is appropriate to

1) determine depth to crystalline basement,
2) define faults in the basement and/or overlying sediments

3) examine lateral and vertical changes in velocity in the sedimentary section which can then be correlated with lateral changes in thermal conductivity or changes in thickness of potential deep aquifers.

Figure C-1.5 shows a reflection seismic section recently obtained (February, 1979) near Salisbury, Md. The reflection that originates from the basement is well-defined as are several other reflections from within the overlying sedimentary section.

Excellent reflection seismic data can be obtained on the Atlantic Coastal Plain. Proper recording procedures are essential in order to assure that the desired reflections are not obscured by multiple (Dobrin, 1976, p. 89) reflections.

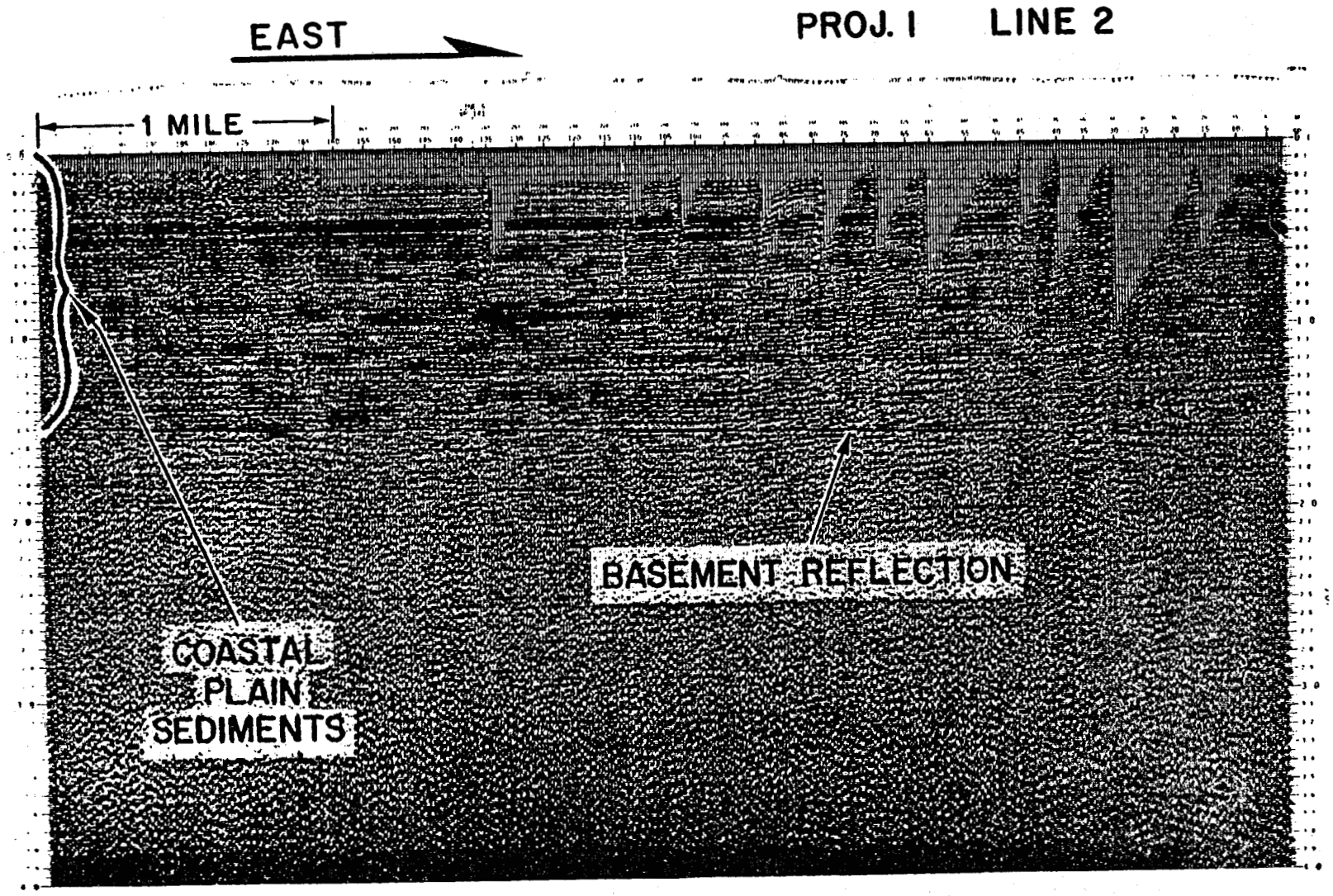

Figure C-1.5. Reflection seismic section (24-fold) obtained near Salisbury, Maryland.

Origin of the Hot Springs of Virginia

In the northwestern part of Virginia and adjacent parts of West Virginia there are approximately 100 springs that have temperatures ranging from slightly above the mean annual air temperature (9 - 12 °C; 48 - 54 °F) to about 41 °C (106 °F). In Virginia, nearly all of the warm springs appear to issue from limestone formations of Middle Ordovician age where these formations are brought to the surface by anticlinal folding. The geographic distribution of the springs has been described by Reeves (1932) and summarized by Sammel (1979).

The hottest springs are located in the Warm Springs anticline in Bath and Alleghany Counties in Virginia where four groups of springs known as the Warm Springs, Hot Springs, Healing Springs, and Falling Springs occur. Each group of springs consists of at least three separate springs in close proximity. The group at Warm Springs is made up of three springs within about 30 m (100 ft) of each other and a forth about 250 m (820 ft) to the southwest. At Hot Springs, eight warm springs occur over an area of about 4000 square m (6 square miles). Healing springs consists of three separate springs less than 3 m apart. Falling Springs are made up of a number of flows and seepages at a generally lower temperature (25 °C; 77 °F max) than the other warm springs in the Warm Springs Anticline, and with a much greater discharge (250 L/sec= 3960 gpm = 5,700,000 gpd) than any other warm springs in the region. The flow rate of Hot Springs is 63 L/sec (= 998 gpm = 1,438,000 gpd) at a maximum temperature of 41 °C (106 °F). At Bolar Spring, the flow rate is 130 L/sec (=2060 gpm =2,900,000 gpd) at a maximum temperature of 22 °C (72 °F). Flow rates are taken from Sammel (1979).

Rogers (1884) and Reeves(1932) both concluded that the warm and moderately warm springs issue from rocks of Cambrian and Ordovician age where these formations rise from considerable depth as the result of anticlinal folding of sedimentary rocks. Rogers proposed that surface water entering the rocks at their outcrop in high ridges sinks to considerable depths along joints and fissures until it reaches a permeable bed, and then rises along the dip of this bed to its outcrop in an adjacent valley. According to Reeves (1932, p. 26), however, some of the anticlines are broken by thrust faults, but he states that there is no positive evidence that any of the warm springs are along faults. Reeves further concluded that most of the springs of the region undoubtedly are not so located, and that few of the springs are probably fed by water rising along fault planes or through fissures bordering fault planes. Reeves (1932, p. 28) concluded that the springs are produced by meteoric (rain) water entering a permeable bed along its outcrop at a relatively high altitude on the crest or limb of one anticline and rising to the surface where the same bed crops out at a lower altidude in another anticline, the temperature of the waters being an expression of the normal earth temperature in the deep synclinal basins through which the water circulates. Reeves' hypothesis is similar to Rogers' in that it attributes the temperature of the springs to normal earth temperatures. It differs from Rogers' hypothesis in that it predicts movement through permeable beds from one

anticline to another rather than movement through joints and fissures from an anticlinal ridge to adjacent valleys.

Rogers (1884), Watson (1924), Reeves(1932) and Hobba et al. (1977) all concluded that the spring waters are of meteoric origin. The occurrence of igneous sills and dikes in Highland County, Va. suggested to Dennison and Johnson (1971) an alternative heat source other than deep circulation of meteoric water. Igneous intrusions are exposed just 30 km (20 miles) north of Hot Springs, Va. They suggested that a deep still-cooling pluton provides heat to the thermal springs centered in Bath County, and that the pluton is either the source of the dikes in Highland County, or possibly represents a later thermal pulse related to the 38th parallel fracture zone, which has been an east-west zone of sporadic igneous activity from late Precambrian to Eocene time.

A hole approximately 305 m (1000 ft) in depth was drilled into the Beekmantown dolomite in the Warm Springs anticline about 8 km southwest of Hot Springs, Va. specifically for the purpose of obtaining a reliable heat flow determination (Costain et al., 1976). The geothermal gradient in the hole was 9.3 °C/Km (0.5 °F/100 ft). The thermal conductivity of the Beekmantown dolomite was 12.4 mcal/cm-sec-°C. The heat flow is therefore about 1.2 HFU (1 HFU = 10^{-6} cal/cm^2-sec). This is a representative heat flow value for the region and does not support the hypothesis of a still-cooling pluton at depth.

The gradient within the core of the Warm Springs Anticline is about 10 °C/Km in the Beekmantown Dolomite. If this low gradient is maintained to greater depths, water would have to circulate to a depth of only approximately 3 km (10,000 ft) to be heated to the temperatures observed at the surface. Since the thickness of sediments in the area is greater than 4 km (13000 ft), deep circulation of meteoric water completely within the sedimentary section is possible. It then remains to identify the ground water recharge area for the springs and the factors that control locations where the springs discharge. Perry et al., 1979) proposed the following model.

All of the warm springs in the valley are grouped near topographic gaps associated with vertical transverse fracture zones (linears). The limited data available suggest that faults and/or joints play an important role in the location of the springs, since gaps have developed only along these zones. The Warm Springs anticline is a doubly-plunging anticline with a near-vertical to overturned northwestern limb. The resistant Silurian quartzites are responsible for the high relief in the area. It is postulated that meteoric water enters the fractured Silurian quartzites and possibly adjacent carbonate units along steep to vertical bedding planes on the northwest limb of the anticline, extends to depths sufficient to heat the water, and then rises rapidly along the essentially east-west transverse fracture zones which intersect the bedding-plane permeability at depth. A cross section of this model oriented approximately at right angles to the transverse fracture zones is shown in Figure

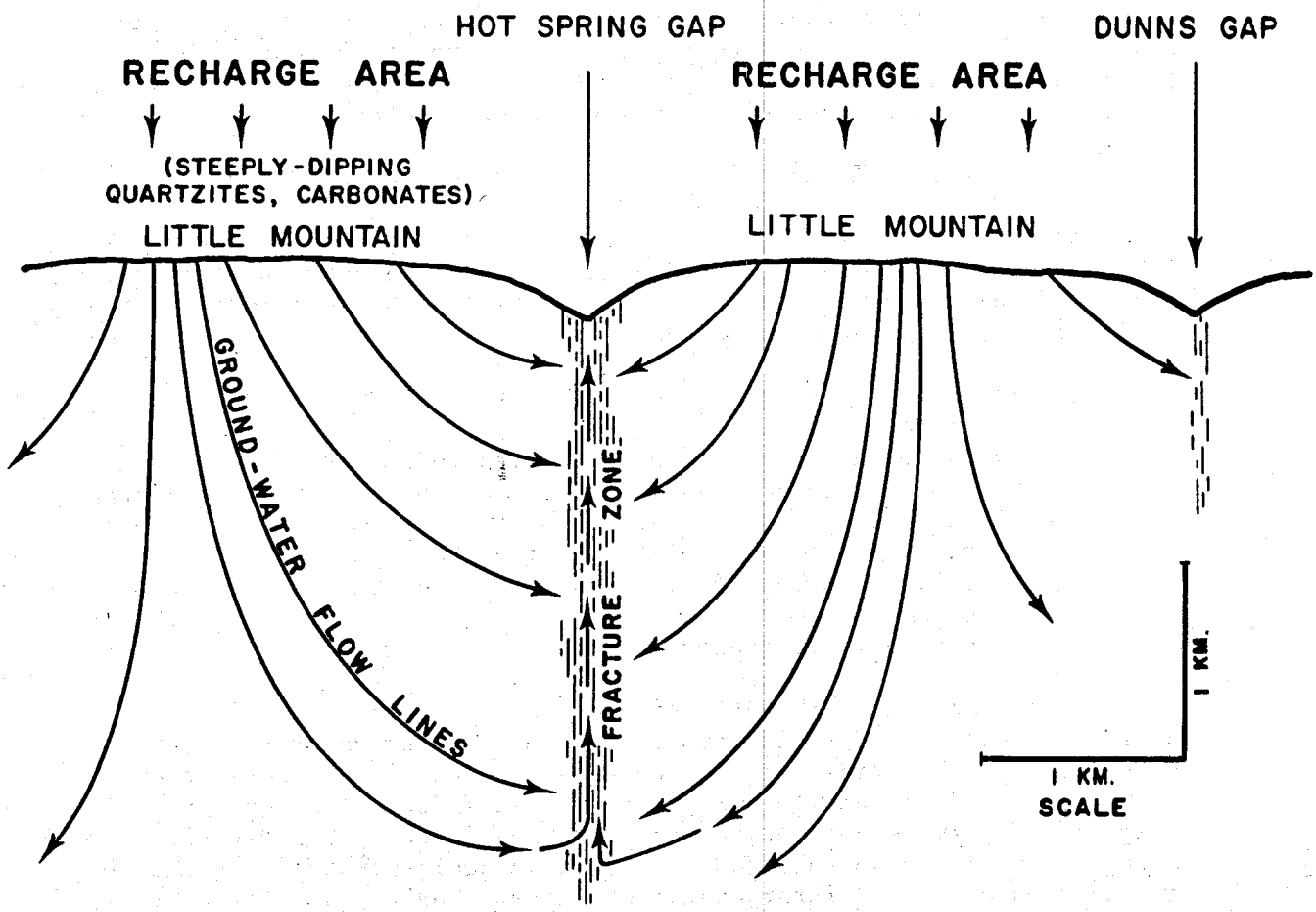

Figure C-1.6. Hypothetical vertical cross section at Hot Springs, Virginia. Section is oriented at approximately right angles to transverse fracture zones.

C-1.6. In this model, ground-water flow lines are shown with an essentially vertical orientation beneath the recharge areas. They diverge at depth and intersect the transverse fracture zones. The temperature of the water issuing from springs located along the transverse fracture zones depends to a large extent on the degree of mixing that has taken place as the meteoric water rises rapidly to the surface along the relatively permeable fracture zone.

In support of this model, there appears to be a correlation between the coincidence of water gaps, the occurrence of warm springs, and the presence of nearby steeply-dipping to vertical quartzite units in areas other than the Warm Springs Anticline. The warm spring (22 °C; 72 °F) at Bolar occurs in the same geologic setting.

Geothermal Exploration of the Atlantic Coastal Plain

During 1978-79, 49 holes were drilled to a depth of approximately 300 m (1000 ft) on the Atlantic Coastal Plain. The geographic distribution of the holes is shown in Figure C-1.1. The locations of the drill sites were chosen on the basis of:

1) gravity data,
2) magnetic data,
3) known thickness of Coastal Plain sediments,
4) apparent thermal anomalies based on geothermal gradients determined in existing holes,
5) much of the available basement core data,
6) suitable sites for the evaluation of the radiogenic pluton model,
7) proximity to energy markets.

The sediments of the Atlantic Coastal Plain include a number of semi-confined 'leaky' aquifers. These aquifers are separated by relatively impermeable sediments. The water present in the pore space of each semi-confined aquifer may have a different 'energy per unit weight', otherwise defined as 'hyraulic head', h. Three quantities determine the value of h at any point in an aquifer: the elevation of the point above an arbitrary reference level (basement), the pressure energy (the higher the fluid pressure the greater the pressure energy), and the kinetic energy (speed at which water moves through the pore space of the aquifer). If there were no confining beds, the value of the hydraulic head ,h, would be approximately the same anywhere in the sediments above basement (except for small differences associated with variations in ground-water velocity).

The fundamental equation of groundwater flow is governed by Darcy's Law,

$$V = P(dh/dl)$$

where V is the 'Darcy velocity' of ground water flow. The actual velocity of water through the pore space is given by V/n where n is the porosity of the aquifer. P is the permeability of the aquifer; the

'hydraulic gradient' is dh/dl. The equation simply states that water flows from a higher energy state (hydraulic head, h) to a lower energy state, always. The difference in energy states is accounted for by energy lost due to friction as the water moves through the pore space of the aquifer. The presence of confining beds causes different values of h to occur in different aquifers. A hole drilled into the sediments of the Coastal Plain will encounter different values of h, which would result in upward (or downward) flow in the hole and prevent the determination of an accurate geothermal gradient. For this reason, each hole was cased to its total depth and cemented to prevent circulation between aquifers. Convection in or near a hole can result in an unreliable geothermal gradient determined in a shallow (300 m) hole.

Temperatures were measured at intervals of 2.5 m (8 ft) in each hole. Average gradients, G, were determined in each hole by the least-squares fit of a straight line over the entire interval of the hole below a depth of about 50 m (160 ft). An attempt was made to recover two sediment core samples, each 8 m (25 ft) in length from each hole. Core recovery was variable because of the unconsolidated nature of the sediments. Thermal conductivity, K, was determined in the laboratory using needle probe techniques.

Temperature profiles, geothermal gradients, and thermal conductivities are reported in a series of progress reports (Costain et. al., 1977, 1978, 1979).

Because the difference in concentrations of U and Th in basement rocks affects the geothermal gradient in the overlying sediments, it was important to site several holes both on and off potential field anomalies. The Portsmouth gravity anomaly (Figure C-1.3) is an excellent example of a negative gravity anomaly over a presumed buried granite pluton. A magnetic anomaly is also present. The sediments here are about 600 m (1900 ft) in thickness. A hole was drilled that encountered granite at a depth of about 600 m, and 90 m (300 ft) of continuous granite core (BQ) are now being recovered. Determinations of heat generation, age, and chemistry will be made on the core. A heat flow value will also be determined over the 90-m interval in the granite to confirm the value of heat flow determined in the overlying sediments. The geothermal gradient in the hole over the gravity anomaly is about 42 °C/Km; the gradient in a hole drill nearby (12 km) but off the anomaly in the same lithologic sequence of sediments is 27 °C/Km. We regard this as excellent confirmation of the radiogenic pluton model.

Lambiase et al. (1979) discuss in detail the distribution and values of the geothermal gradients obtained in the holes drilled on the Atlantic Coastal Plain. The most promising area to date appears to be between Crisfield, Md., and Oak Hall, Va. in southern Maryland and northern Virginia on the Eastern Shore (Figure C-1.1). Higher gradients (50 °C/Km) were found elsewhere, for example within the large negative gravity anomaly in the vicinity of Chesapeake Bay, but the depth to basement there is less.

References

Bell, H., III, and P. Popenoe, 1976, Gravity studies in the Carolina slate belt near the Haile and Brewer Mines, north-central South Carolina. Journ. Res. U.S. Geol. Survey, v. 4, 667-682.

Birch, F., 1954, Heat from radioactivity, In Nuclear Geology, H. Faul, editor, John Wiley and Sons, New York, p. 148-174.

Birch, F., R. F. Roy, and E. R. Decker, 1968, Heat flow and thermal history in New England and New York. In Studies of Appalachian Geology, E-an Zen, W. S. White, J. B. Hadley, and J. B. Thompson, Jr., editors, Interscience, New York, p. 437-451.

Costain, J. K., G. V. Keller, and R. A. Crewdson, 1976, Geological and geophysical study of the origin of the warm springs in Bath County, Virginia. Report prepared for the Department of Energy under Contract E-(40-1)-4920. Available from National Technical Information Service, Springfield, VA, 22161.

Costain, J. K., L. Glover, III, and A. K. Sinha, 1977, -78, -79, Evaluation and targeting of geothermal energy resources in the southeastern United States. Series of Progress Reports VPI&SU-5103, and VPI&SU-5648, prepared for the Department of Energy. Available from National Technical Information Service, Springfield, VA, 22161, 184 p.

Costain, J. K., 1979, Computation of anomalous magnetic fields from point-pole source distributions, in press, J. Mathematical Geology.

Dennison, J. J. and R. W. Johnson, Jr., 1971, Tertiary intrusions and associated phenomena near the thirty-eighth parallel fracture zone in Virginia and West Virginia, Geol. Soc. Amer. Bull., v. 82, 501.

Dobrin, M. B., 1976, Introduction to Geophysical Prospecting, McGraw-Hill, Inc., 630 p.

Geiser, P. A., 1976, Structural mapping in the Warm Springs Anticline, northwestern Virginia. In Evaluation and Targeting of Geothermal Energy Resources in the Southeastern United States, Progress Report VPI&SU-2, prepared for the Department of Energy under Contract E-(40-1)-5103, p. 116-164.

Hewett, D. F., and Crickmay, G. W., 1937, The warm springs of Georgia, their geologic relations and origin: U.S. Geological Survey Water-Supply Paper 819, 40 p.

Hobba, W. A., Jr., Chemerys, J. C., Fisher, D. W., and Pearson, F. J., Jr., 1977, Geochemical and hydrologic data for wells and springs in thermal-spring areas of the Appalachians: U.S. Geological Survey Water-Resources Investigations Report 77-25, 36 p.

Hobba, W. A., Jr., Fisher, D. W., Pearson, F. J., Jr., and Chemerys, J. C., 1978, Hydrology and geochemsitry of thermal springs of the Appalachians: U.S. Geological Survey Professional Paper 1044 (in press).

Lachenbruch, A. H., 1968, Preliminary geothermal model for the Sierra Nevada, Journ. Geophys. Res., v. 73, 6977-6989.

Lambiase, J. J., Dashevsky, S. S., Costain, J. K., R. J. Gleason, and W. McClung, 1979, Geothermal resources potential of the northern Atlantic Coastal Plain, submitted for publication.

Lowell, R. P., 1975, Circulation in fractures, hot springs, and convective heat transport on mid-ocean ridge crests, Geophys. J. Roy. Astr. Soc., v. 40, 351-365.

Muffler, L. J. P., ed., 1979, Assessment of geothermal resources of the United States--1978, U.S. Geological Survey Circular 790, 163 p.

Muffler, L. J. P., and Cataldi, R., 1979, Methods for regional assessment of geothermal resources: Geothermics, v. 7, no. 2-4 (in press).

Nettleton, L. L., 1971, Elementary gravity and magnetics for geologists and seismologists, Society of Exploration Geophysicists, P. O. Box 3098, Tulsa, Oklahoma 74101, 121 p.

Perry, L. D., J. K. Costain, and P. A. Geiser, 1979, Heat flow in western Virginia and a model for the origin of thermal springs in the folded Appalachians, in press, J. Geophys. Res.

Reeves, F., 1932, Thermal springs of Virginia: Virginia Geological Survey Bulletin 36, 56 p.

Rogers, W. B., 1884, On the connection of thermal springs in Virginia with anticlinal axes and faults, Assoc. Am. Geologists and Naturalists, Report of 1st, 2nd, and 3rd meetings, p. 328-330, 1840-1842. A reprint: Geology of the Virginias, p. 577-597, New York.

Roy, R. F., D. D. Blackwell, and F. Birch, 1968, Heat generation of plutonic rocks and continental heat flow provinces, Earth Planet, Sci. Letters, v. 5, 1-12.

Rybach, L., 1976, Radioactive heat production in rocks and its relation to other petrophysical parameters, Pageoph., v. 114, Birkhauser Verlag, Basel.

Sammel, E. A., 1979, Occurrence of low temperature geothermal waters in the United States, In Assessment of Geothermal Resources of the United States--1978, L. J. P. Muffler, ed., U.S. Geological Survey Circular 790.

Stose, G. W., and Stose, A. J., 1947, Origin of the hot springs at Hot Springs, North Carolina: American Journal of Science, v. 245, no. 10, p. 624-644.

U.S. Geological Survey Open-file Report, 1970, Aeromagnetic map of the Camden-Kershaw area, north-central South Carolina.

Watson, T. L., 1924, Thermal springs of the south-east Atlantic States, Journ. Geology, v. 32, no. 5.

White, D. E., and Williams, D. L., eds., 1975, Assessment of geothermal resources of the United States--1975, U.S. Geological Survey Circular 726, 155 p.

Geothermal Resource Potential of the Northern Atlantic Coastal Plain

J. J. Lambiase, S. S. Dashevsky, J. K. Costain,
R. J. Gleason, and W. S. McClung

Abstract

Geothermal gradients determined in 66 exploratory holes in the Atlantic Coastal Plain suggest that, in many areas, temperatures will be in excess of 60° at the basement surface. The transmissibility of the deep aquifers beneath the Coastal Plain must be determined before the feasibility of a geothermal resource can be evaluated.

Geological and geophysical investigations of the sedimentary wedge and basement beneath the Atlantic Coastal Plain are in progress as part of a program sponsored by the Department of Energy to explore the low-temperature geothermal resource potential in the eastern United States. Exploration is based on a proposed model (Costain, et al, 1979) that predicts optimum sites for the development of geothermal resources in the Atlantic Coastal Plain. Granite plutons with moderate concentrations of U and Th occur in the crystalline basement underlying the Coastal Plain. These granites are sources of heat that is produced by the natural radioactive decay of uranium and thorium isotopes (Birch, F., 1954). Because thermal conductivity of the Coastal Plain sediments is low, the sediments will act as a thermal insulator, and elevate temperatures at the base of and within the wedge of sediments. If a thick sedimentary section occurs above a radiogenic granite, isotherms will be warped upward and higher temperatures will occur at shallower depths.

Two important aspects of the resource potential of the Atlantic Coastal Plain are the temperature gradient and the basement surface temperature, that is, the maximum temperature at the base of the Coastal Plain sediments. The latter is a function of both the temperature gradient and the local thickness of the Coastal Plain sediments.

During 1978, 49 exploratory holes, each approximately 300 m in depth, were drilled in New Jersey, Delaware, Maryland, Virginia and North Carolina (Figure C-2.1). The locations were chosen to test the proposed radiogenic pluton model (Costain, et al, 1979), and to locate areas with a high potential for geothermal development. The holes were cased to their total depth and cemented to prevent ground-water flow in the hole between aquifers with different hydraulic heads.

Prior to the 1978 drilling program, existing holes in the Atlantic Coastal Plain were logged for temperature. Thermal gradients in sixteen of these holes are shown in Figure C-2.1. Geothermal gradients in these holes were determined from discrete temperature measurements made at intervals of 2.5 m.

Gradients in the 49 new holes drilled specifically for the geothermal program were determined from temperature measurements made at 0.5 m intervals by a rapid response thermistor probe (time constant = 1 s) that was moved down the hole continuously at 5 m per minute. Comparative temperature logs made with the two systems in a hole in thermal equilibrium showed agreement between geothermal gradients to within 0.1 °C/km over the entire hole.

Geothermal gradients were calculated by fitting a least squares straight line to measurements of temperature and depth. The gradients given are within 2% of thermal equilibrium, and are calculated over a depth interval that starts below the obvious influence of ground water circulation and extends to the bottom of the hole.

Figure C-2.1 shows the distribution of hole locations and geothermal gradients in the northern Atlantic Coastal Plain. With the

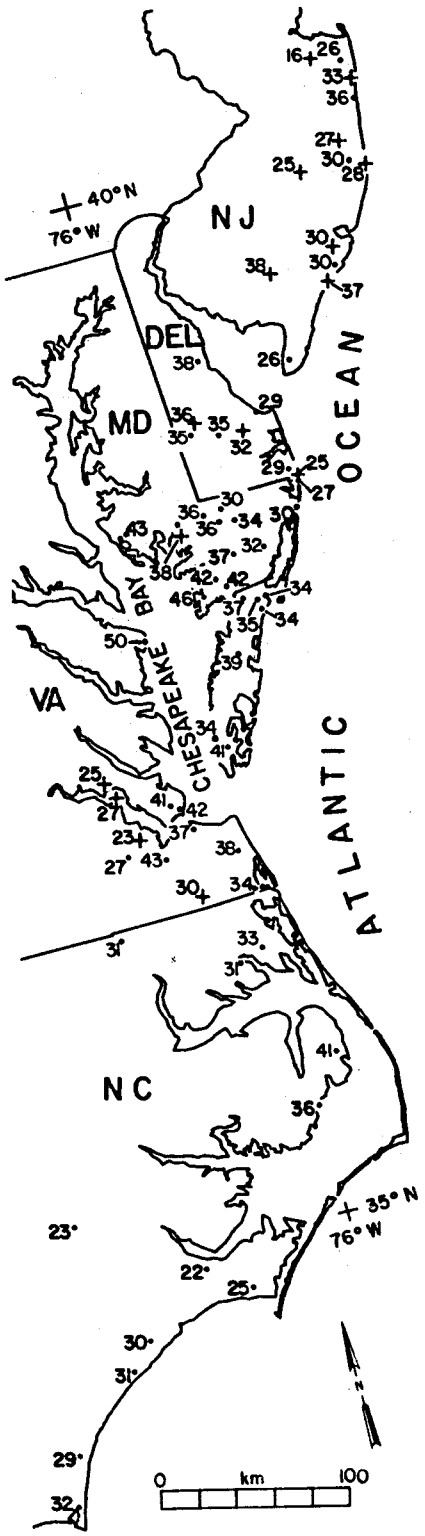

Figure C-2.1. Geothermal gradients in the 40 exploratory holes drilled during 1978 (marked as circles) and the 16 older holes (marked with crosses). All values are °C/km, and are within 2% of equilibrium except for those in North Carolina, which are within 4% of equilibrium.

exception of two holes in New Jersey, gradients along the coastline of New Jersey, Delaware, and Maryland are low with values that are between 16 °C/km and 30 °C/km. Higher gradients occur throughout most of the Delmarva Peninsula where values are between 30 °C/km and 46 °C/km (Figure C-2.1). Near Chesapeake Bay, temperature gradients are the highest of any in the five state area with values that vary between 39 °C/km and 50 °C/km. A gradient of 40 °C/km was determined in one hole in northeastern North Carolina. Other new exploratory holes in this area have thermal gradients between 31 °C/km and 35 °C/km. In southeastern North Carolina, gradients are lower, and vary from 22 °C/km to 32 °C/km.

Basement surface temperatures were extrapolated by extending the overall geothermal gradients from the temperatures measured at the bottom of the exploratory holes to the estimated depth of the basement surface. Basement surface depths were estimated by interpolating between known basement well control with adjustments for regional trends in basement topography.

Estimated basement surface temperatures are displayed on Figure C-2.2. Values vary from 21 °C to 91 °C. In southern Virginia, estimated temperatures are relatively low despite high geothermal gradients. This is primarily because basement occurs at a shallow depth. In New Jersey, estimated temperatures are low because low geothermal gradients coincide with areas where the basement surface is shallow.

Generally, basement surface temperatures on the Delmarva Peninsula are expected to be high (Figure C-2.2). Along the Atlantic Coast, geothermal gradients are relatively low, but the thick sequence of Coastal Plain sediments (up to 2.34 km) results in high basement surface temperatures. On the western margin of the Peninsula, gradients are higher, but the Coastal Plain is thinner (average thickness is approximately 1.52 km). The estimated basement surface temperatures are slightly lower than those along the Atlantic Coast (Figure C-2.2).

The temperature predicted by extending the near-surface geothermal gradient to basement has been found to be accurate for several locations in the Coastal Plain. Near Jesup, Georgia, basement was encountered at a depth of 1.33 km. At this depth, the temperature estimated from the average gradient over the upper 296 m is 60 °C. This is identical to the 60 °C basement surface temperature that we measured.

Basement was reached in four exploratory holes drilled during 1978. These holes were drilled to depths up to 500 m to identify the basement rock type. Basement surface temperatures predicted by the gradients in the upper 300 m are within 3% of the measured values.

Basement surface temperature will be less than predicted if the geothermal gradient decreases with depth due to an increase in thermal conductivity of the Coastal Plain sediments. Thermal conductivity varies with sediment type, and there are rapid lateral and vertical

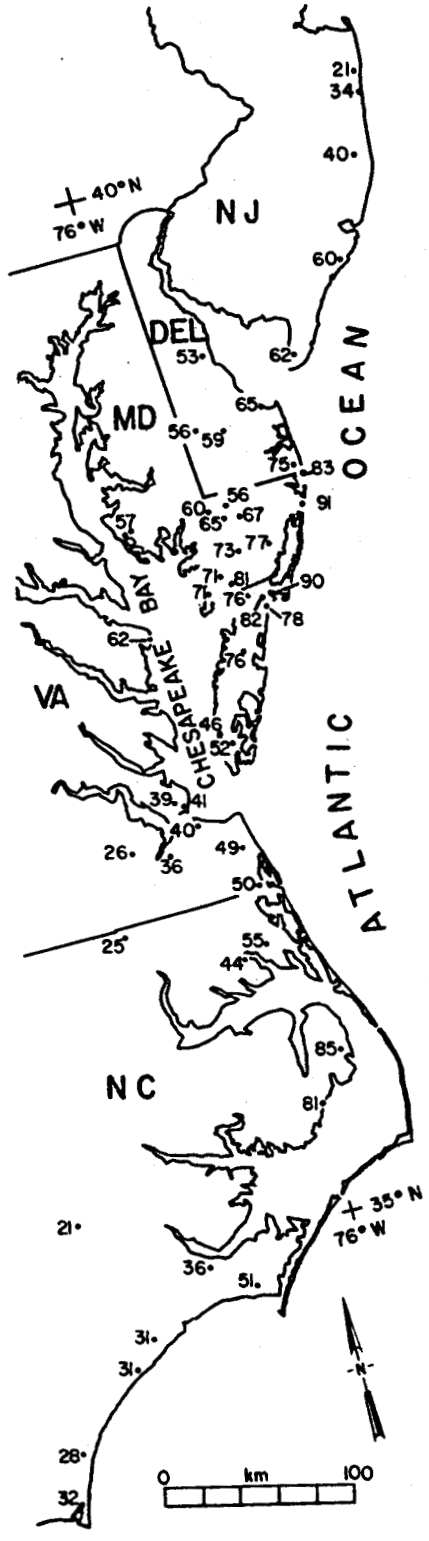

Figure C-2.2. Estimated basement surface temperatures in the 40 holes drilled during the 1978 program. Temperatures are in °C.

facies changes within the Coastal Plain (Brown, P. M., et al, 1972) that make lithologic prediction difficult. Generally, the deeper section of the northern Coastal Plain is more sandy than the top 300 m; this tends to increase thermal conductivity in the deeper part of the section relative to the upper part.

Thermal conductivity will increase if compaction occurs. Compaction increases grain-to-grain contact by decreasing porosity and, therefore, water content. Introduction of cement into a sedimentary unit also will increase thermal conductivity by decreasing porosity and replacing water with material of higher conductivity.

Recent results from a hole that we drilled to basement (540 m) near Portsmouth, Virginia suggest that in some locations the thermal conductivity of Atlantic Coastal Plain sediment does increase with depth. This causes a decrease in the geothermal gradient with depth, and consequently, a basement surface temperature that is lower than expected. In the Portsmouth hole, if the average geothermal gradient in the upper 300 m remained constant to the basement surface, the predicted temperature would be 39 °C. However, the measured temperature at that depth is 36 °C.

The uncertainty of actual depth to basement can introduce an uncertainty into the prediction of basement surface temperatures. In many areas control is poor, and a difference of 100 m between the actual depth to basement and the estimated depth could cause an error in temperature estimation of up to 5 °C.

Several other factors are involved in the evaluation of the geothermal resource potential of the Atlantic Coastal Plain. Available markets and costs obviously are essential to evaluate the resource, but it is beyond the scope of this report to discuss economic factors. Energy market considerations for this area have been discussed elsewhere (Toth, W. J. and Paddison, F. C., 1979).

The geothermal resource is expected to be a hydrothermal resource. The yield of water from the deep aquifers is an essential factor because water is the medium by which the heat at depth is transferred to the surface. The yield must be sufficient to meet energy demands. This is partially an economic problem, but it also involves the intrinsic porosity and transmissivity of the aquifer. Unfortunately, there is a paucity of data concerning the hydrology of deep aquifers in the northern Atlantic Coastal Plain. A test hole near Norfolk, Virginia (Brown, D. L., 1968) penetrated the thick Cretaceous sand unit that is the basal unit throughout much of the northern Coastal Plain. Reasonably good porosities were reported from the lower part of the section to the total depth of 786 m. Also, electric logs from older wells on the Delmarva Peninsula in Virginia suggest that the basal sands of the Coastal Plain are potential aquifers (VA Water Control Board, 1974).

The geothermal gradients and their areal trends are valid, but speculation between or below drill holes must be done with caution.

The unknown distribution of radiogenic heat sources in the basement makes geothermal gradients strictly site specific so that continuity between test holes is uncertain.

The basement temperatures displayed in Figure C-2.2 indicate that there are several areas beneath the northern Atlantic Coastal Plain that are expected to have temperatures above 60 °C. Temperatures in the 59 °C to 70 °C range are being used successfully for district heating of 7,000 apartments in the Paris Basin, France (Bur. Recherches Geol. Mminieres, 1978), and it is anticipated that 800,000 apartments will be geothermally heated by 1990.

At present, the areal distribution of isotherms beneath the Atlantic Coastal Plain, and the ground-water hydrology at depth, is poorly defined. Therefore, it is impossible to estimate the rate at which heat could be extracted at any location or to predict the lifetime of the resource. However, the available data suggest that a substantial geothermal resource does exist beneath the Atlantic Coastal Plain.

References and Notes

Birch, F., 1954, Heat from radioactivity, In Nuclear Geology, H. Faul, editor, John Wiley and Sones, New York, p. 148-174.

Brown, D. L., 1968, Memorandum report on test drilling at Norfolk, Virginia, U.S.G.S. Open-file Report, 28 p.

Brown, P. M., J. A. Miller, and F. M. Swain, 1972, Structural and stratigraphic framework and spatial distribution of permeability of the Atlantic Coastal Plain, North Carolina to New York, U.S.G.S. OProf. Paper 796, 79 p.

Costain, J. K., Lynn Glover, III, and A. K. Sinha, 1979, Low-temperature geothermal resources in the Eastern United States, in press, EOS, Amer. Geophys. Union, 26 p.

La Geothermie en France, 1975, Bulletin Bureau le Recherches Geologiques et Minieres, Paris, 72 p.

Toth, W. J. and F. C. Paddison, 1979, Geothermal Energy Markets on the Atlantic Coastal Plain, presented at the Sixth Energy Technology Conference, Washington, DC, February.

VA State Water Control Board Planning Bulletin 45, 1975, Groundwater conditions in the eastern shore of Virginia, 59 p.

Heat Flow in the Atlantic Coastal Plain

L. D. Perry

Heat flow values are now complete for sixteen holes in the Atlantic Coastal Plain. Figure C-3.1 shows the locations of the values. Table C-3.1 lists the values along with locations, intervals, gradients, and conductivity values. Tables C-3.2 through C-3.19 list individual thermal conductivity values from each hole.

Core recovery has been variable because some of the sediments are unconsolidated. Recovery ranges from zero in some sandy formations to twenty-five feet in muds and clays. Where recovery was sufficient, the heat flow was determined from the mean thermal conductivity and the least squares gradient from the same depth as the core. For example, in Hole C19, a heat flow value of 2.0 $\pm$ 0.3 HFU was obtained from the gradient over the interval 196.7-205.8 m and the thermal conductivity values of the core from the interval 198.3 - 202.4 m. In holes where the gradient was nearly constant above and/or below the cored section, that gradient was also calculated and used to determine the heat flow. In C19 a gradient of 57.05 $\pm$ 0.77 °C/Km was determined from the interval 187.1-221.7 m and when appplied to the same mean thermal conductivity value gave a heat flow of 1.9 $\pm$ 0.1 HFU. The rationale for extending the observed thermal conductivity values to the gradient of a larger interval is that if the gradient remains constant the conductivity must also. A third situation arises in C19 and several other holes. In some holes, after recovering core from an interval at the bottom of the hole, no temperature log could be obtained from the same interval because of a faulty cementing job which plugged the bottom several meters of the hole. In this case, the last observed gradient is assumed to extend to the depth of the thermal conductivity values.

The values completed to date confirm the model that gravity lows are associated with basement radiogenic heat sources. Heat flow values of 1.6 HFU, 1.8 HFU, and 1.85 HFU are significantly higher than normal and are associated with a gravity low on the Virginia Peninsula. The gravity low at Stumpy Point, NC, is coincident with a heat flow of 1.9 HFU. Hole C25 at Portsmouth, VA was drilled in the center of a gravity low and has a heat flow of 1.4 HFU. Hole C26 on the flank of the same low is more nearly normal at 1.1 HFU. The difference in magnitude of the anomalies at Portsmouth and Wallop's Island probably suggests a higher heat production in the crust at Wallop's Island. Core samples from basement at Portsmouth are being prepared for analysis of U and Th content now and will be reported next quarter.

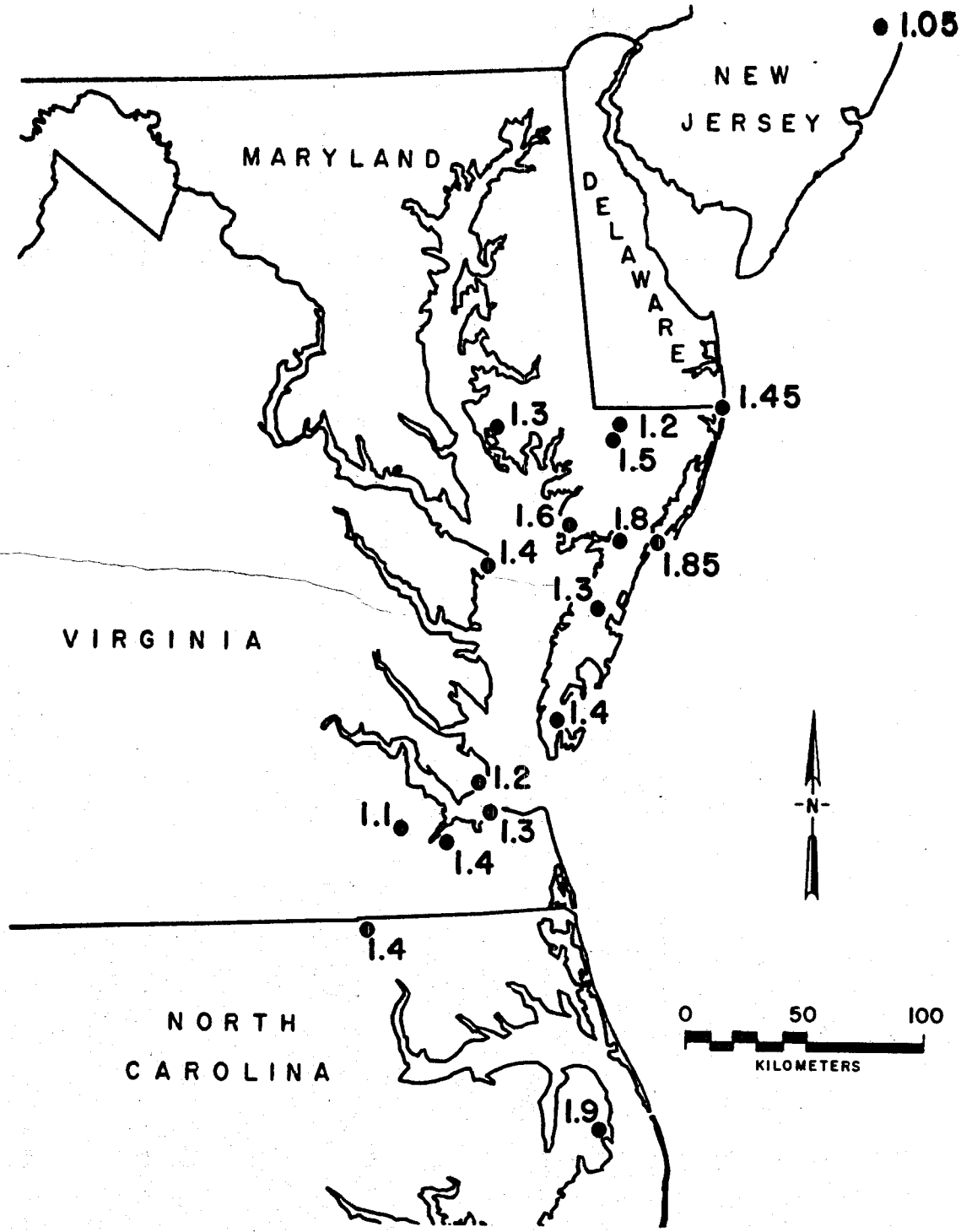

Figure C-3.1. Location of heat flow values in the Atlantic Coastal Plain (unites are 10^{-6} cal/cm^2-sec).

TABLE C-3.1

HOLE	LATITUDE LONGITUDE	INTERVAL(M)	GRADIENT SIGMA(REGR, N) (°C/KM)	COND SIGMA(N)	HEAT FLOW	ESTIMATED BASEMENT SURFACE DEPTH (KM)	TEMPERATURE (°C)
SOUTHPORT, N.C.							
C14A	33 58.00 77 58.20	60-463	32 *			465	32
WILMINGTON, N.C.							
C14	34 12.00 77 53.40	45-380	29 *			.385	28
SNEADS FERRY, N.C.							
C15A	34 31.60 77 27.30	30-475	31 *			.495	31
JACKSONVILLE, N.C.							
C15	34 39.00 77 19.00	50-500	30 *			.505	31
KINSTON, N.C.							
C16A	35 15.70 77 35.30	69-217	23 *			.210	21
CHERRY POINT, N.C.							
C16	34 54.70 76 53.30	80-308	22 *			.84	36
BEAUFORT, N.C.							
C17	34 46.30 76 38.70	45-302	25 *			1.36	51
ENGLEHARD, N.C.							
C18	35 31.20 75 59.26	49-304	36 *			1.84	81
STUMPY POINT, N.C.							
C19	35 45.12 75 47.65	53-269	40 *		1.94	1.78	85
		187.1-221.7	57.05±0.77(0.988, 68)1	3.3±0.18(14)	1.9±0.1		
		196.7-205.8	60.01±6.71(0.842, 17)2	3.3±0.18(14)	2.0±0.3		
		248.1-296.3	54.14±1.38(0.966, 56)3	3.9±0.91(15)	2.1±0.6		
ELIZABETH CITY, N.C.							
C20	36 16.81 76 12.58	50-313	31 *			.95	44
BELLCROSS, N.C.							
C21	36 19.59 76 03.54	23-308	33 *			1.22	55
CREEDS, VA.							
C22	36 36.38 76 00.43	89-307	34 *			1.08	50
OCEANA, VA.							
C23	36 48.09 76 02.62	75-296	38 *			.94	49
NORFOLK, VA.							
C24	36 57.40 76 16.20	17-316	37 *		1.34		
		152.4-173.3	44.14±0.57(0.994, 41)2	3.4±0.45(25)	1.5±0.2		
		161.7-174.3	49.00±1.64(0.975, 25)2	3.4±0.45(25)	1.7±0.3		
		252.8-316.7	24.75±0.04(1.000,124)1	3.7±0.96(12)	0.9±0.2		
		303.2-308.5	29.13±2.17(0.957, 10)2	3.7±0.96(12)	1.1±0.4		
SUFFOLK, VA.							
C25	36 51.01 76 28.83	21-307	43 *		1.44	.557	39
		295.8-309.9	26.85±0.39(0.996, 23)1	5.0±1.04(24)	1.4±0.3		

TABLE C-3.1

HOLE	LATITUDE LONGITUDE	INTERVAL(M)	GRADIENT SIGMA(REGR, N) (°C/KM)	COND SIGMA(N)	HEAT FLOW	ESTIMATED BASEMENT SURFACE DEPTH (KM)	TEMPERATURE (°C)
SUFFOLK, VA.							
C25A	36 51.01 76 28.83	25-554	39 *			.557	36
ISLE OF WIGHT, VA.							
C26	36 54.51 76 42.13	35-303	27 *		1.14	.42	26
		268.9-303.4	21.37±0.12(0.998, 67)1	5.3±0.92(29)	1.1±0.2		
		294.1-304.3	21.61±0.85(0.976, 18)2	5.3±0.92(29)	1.1±0.3		
HAMPTON, VA							
C27	37 05.53 76 22.21	75-307	40 *				
CHERITON, VA							
C28	37 17.79 75 55.86	30-314	41 *		1.44		
		188.6-242.2	46.53±0.10(0.999,108)1	3.3±0.30(30)	1.5±0.1		
		211.3-225.8	44.59±0.62(0.995, 29)2	3.3±0.30(30)	1.5±0.2		
		292.9-309.3	64.10±2.09(0.968, 33)1	2.1±0.14(29)	1.4±0.1		
		296.3-308.3	53.56±1.46(0.984, 24)2	2.1±0.14(29)	1.1±0.1		
WALLOPS ISLAND, VA							
C29	37 56.60 75 27.27	75-295	36 *		1.854		
		163.2-185.2	37.34±0.41(0.995, 43)1	4.5±1.00(47)	1.7±0.4		
		272.8-305.1	55.42±0.51(0.997, 40)1	3.7±0.73(47)	2.0±0.4		
OCEAN CITY, MD							
C30	38 18.61 75 07.07	67-303	30 *			2.59	91
SALISBURY, MD							
C31	38 20.55 75 36.43	77-303	36 *		1.54	1.46	65
		222.7-229.7	34.20±1.47(0.978, 14)2	4.0±0.86(16)	1.4±0.4		
		223.2-238.1	39.84±0.73(0.991, 29)1	4.0±0.86(16)	1.6±0.4		
CRISFIELD, MD							
C32	38 00.97 75 49.57	60-294	46 *		1.64	1.28	71
		156.8-172.3	57.39±0.41(0.999, 31)1	2.8±0.26(49)	1.6±0.2		
		164.6-172.8	60.37±0.75(0.998, 17)2	2.8±0.26(49)	1.7±0.2		
		286.7-311.9	29.30±0.62(0.994, 16)1	3.7±1.63(3)	1.1±0.5		
GOLDEN HILL, MD							
C33	38 24.13 76 11.19	40-301	43 *			1.12	61
		252.0-312.9	29.59±0.48(0.994, 26)3	4.5±0.78(3)	1.3±0.3		
ASSAWOMAN BAY, DE							
C34E	38 29.90 75 05.82	47-294	29 *			2.12	75
ELLENDALE, DE							
C34C	38 44.58 75 27.71	75-293	35 *			1.36	59
LEWES, DE							
C34	38 48.18 75 11.67	75-284	29 *			1.83	65
DOVER, DE							
C35	39 06.70 75 27.69		38 *				

TABLE C-3.1

HOLE	LATITUDE LONGITUDE	INTERVAL(M)	GRADIENT SIGMA(REGR, N) ('C/KM)	COND SIGMA(N)	HEAT FLOW	ESTIMATED BASEMENT SURFACE DEPTH (KM)	TEMPERATURE ('C)
CAPE MAY, NJ							
C36	39 00.03 74 54.16	40-294	26 *			1.91	62
ATLANTIC CITY, NJ							
C38	39 22.76 74 27.24	75-294	30 *			1.62	60
FORKED RIVER, NJ							
C39	39 50.44 74 10.87	75-279	30 *		1.054	1.00	40
		220.5-228.6	33.97±1.00(0.988, 16)2	3.3±0.33(16)	1.1±0.1		
		219.2-252.7	31.53±0.13(0.999, 66)1	3.3±0.33(16)	1.0±0.1		
EATONTOWN, NJ							
C40	40 18.81 74 03.02	75-307	26 *			.335	20
SEA GIRT, NJ							
C41	40 7.26 74 2.25	50-296	36 *			.633	34
OCEAN CITY, MD							
C43	38 26.04 75 03.57	43-376	27 *		1.454	2.60	83
		150.2-181.2	41.50±0.17(0.999, 62)1	3.4±0.42(25)	1.4±0.2		
		166.9-177.8	42.82±0.80(0.993, 22)2	3.4±0.42(25)	1.5±0.2		
SALISBURY, MD							
C45	38 23.43 75 41.40	50-318	36 *				
SALISBURY, MD							
C465	38 23.96 75 34.49	34-318	30 *		1.24	1.46	57
		204.3-228.2	25.91±0.19(0.997, 47)1	3.5±0.30(10)	0.9±0.1		
		224.3-232.6	41.35±0.99(0.992, 16)2	3.8±0.42(18)	1.6±0.2		
		295.6-301.9	57.62±3.87(0.953, 13)2	3.0±0.46(5)	1.7±0.4		
SALISBURY, MD							
C47	38 19.91 75 30.66	38-311	34 *			1.59	64
WATTSVILLE, VA							
C48	37 56.06 75 30.60	50-302	35 *				
WITHAMS, VA							
C49	37 57.52 75 35.64	50-314	41 *		1.84		
		207.0-243.0	63.35±0.41(0.997, 72)1	3.0±0.43(30)	1.9±0.3		
		209.9-221.6	59.25±1.92(0.978, 23)2	3.0±0.43(30)	1.8±0.3		
		292.3-317.6	64.48±1.04(0.989, 44)1	2.3±0.42(29)	1.5±0.3		
		308.3-317.6	81.26±8.25(0.907, 12)2	2.3±0.42(29)	1.9±0.6		
REHOBETH, MD							
C50	38 02.12 75 40.28	80-316	42 *			1.67	8
KINGSTON, MD							
C51	38 04.89 75 43.53	65-311	42 *			1.40	7
PRINCESS ANNE, MD							
C52	38 10.50 75 34.49	38-311	37 *			1.54	6

TABLE C-3.1

HOLE	LATITUDE LONGITUDE	INTERVAL(M)	GRADIENT SIGMA(REGR, N) ('C/KM)	COND SIGMA(N)	HEAT FLOW	ESTIMATED BASEMENT SURFACE DEPTH (KM)	TEMPERATURE ('C)
SNOW HILL, MD							
C53	38 10.30 75 22.84	75-308	33 *				
BRIDGEVILLE, DE							
C54	38 46.71 75 37.81	25-302	35 *				
TASLEY, VA							
C55	37 42.53 75 42.85	25-282	40 *		1.34		
		161.9-176.9	31.34±0.39(0.996, 30)1	4.2±0.46(27)	1.3±0.2		
		165.1-173.7	29.42±0.40(0.997, 17)2	4.2±0.46(27)	1.2±0.2		
		268.3-297.5	49.10±0.88(0.992, 28)3	3.0±0.39(10)	1.5±0.2		
EASTVILLE, VA							
C56	37 21.26 75 59.56	40-290	34 *				
ATLANTIC, VA							
C57	37 53.24 75 30.03	50-307	34 *				
SMITH POINT, VA							
C59	37 53.02 76 15.09	50-293	48 *		1.44		
		135.8-162.5	49.84±0.74(0.989, 53)1	2.8±0.23(25)	1.4±0.1		
		268.9-300.7	34.35±0.44(0.993, 48)3	4.0±0.75(5)	1.4±0.3		
HAMPTON, VA							
C60	37 03.98 76 19.28	35-305	42 *		1.24		
		239.3-304.0	27.78±0.07(0.999,128)1	4.2±0.67(10)	1.2±0.2		
		278.2-284.8	26.50±3.61(0.830, 13)2	4.2±0.67(10)	1.1±0.4		
D01	36 31.71 76 52.53	45-316	33 *				

1. Gradient from the longest linear interval which includes the cored section
2. Gradient from the cored section
3. Gradient extrapolated to the cored section
4. Best heat flow value (the weighted mean using the inverse of the error as the weighting factor)
5. Gradient still shows disturbance due to drilling and cementing the hole

* Average gradient from most recent temperature log

TABLE C-3.2 C-3.2

THERMAL CONDUCTIVITY VALUES FROM CORE OF DRILL HOLE C19
(SAMPLES ARE 2.680 CM IN DIAMETER BY 1.270 CM THICK)

SAMPLE NAME	DEPTH (METERS)	K*	SAMPLE NAME	DEPTH (METERS)	K*
C19- 650.5	198.3	3.2	C19- 954.5	290.9	3.1
C19- 651.5	198.6	3.1	C19- 955.5	291.2	3.9
C19- 652.5	198.9	3.3	C19- 956.5	291.5	3.9
C19- 653.5	199.2	3.3	C19- 957.5	291.8	3.6
C19- 654.5	199.5	3.2	C19- 958.5	292.2	4.2
C19- 655.5	199.8	3.6	C19- 959.5	292.5	4.6
C19- 656.5	200.1	3.1	C19- 960.5	292.8	3.6
C19- 657.5	200.4	3.7	C19- 961.5	293.1	3.6
C19- 658.5	200.7	3.3	C19- 964.5	294.0	2.4
C19- 659.5	201.0	3.2	C19- 966.5	294.6	6.5
C19- 661.0	201.5	3.1	C19- 967.5	294.9	3.5
C19- 662.0	201.8	3.4	C19- 968.5	295.2	3.3
C19- 663.0	202.1	3.2	C19- 969.5	295.5	4.1
C19- 664.0	202.4	3.4	C19- 970.5	295.8	3.3

MEAN 3.56
STANDARD DEVIATION 0.72

*...UNITS OF K = MCAL/CM-SEC-'C

TABLE C-3.3

THERMAL CONDUCTIVITY VALUES FROM CORE OF DRILL HOLE C24
(SAMPLES ARE 2.680 CM IN DIAMETER BY 1.270 CM THICK)

SAMPLE NAME	DEPTH (METERS)	K*	SAMPLE NAME	DEPTH (METERS)	K*
C24- 535.5	163.2	3.1	C24- 553.5	168.7	3.4
C24- 536.5	163.5	3.1	C24- 555.5	169.3	4.4
C24- 537.5	163.8	3.1	C24- 556.5	169.6	4.4
C24- 538.5	164.1	3.1	C24- 557.5	169.9	4.3
C24- 539.5	164.4	3.2	C24- 558.5	170.2	4.3
C24- 540.5	164.7	3.1	C24- 559.5	170.5	3.6
C24- 541.5	165.0	3.2	C24- 1000.0	304.8	3.3
C24- 542.5	165.4	3.3	C24- 1000.0	304.8	3.0
C24- 543.5	165.7	3.1	C24- 1000.0	304.8	5.5
C24- 544.5	166.0	3.1	C24- 1000.0	304.8	5.7
C24- 545.5	166.3	3.4	C24- 1005.0	306.3	4.4
C24- 546.5	166.6	3.2	C24- 1005.0	306.3	3.7
C24- 547.5	166.9	3.2	C24- 1005.0	306.3	3.2
C24- 548.5	167.2	3.2	C24- 1005.0	306.3	3.3
C24- 549.5	167.5	3.1	C24- 1005.0	306.3	3.1
C24- 550.5	167.8	3.3	C24- 1005.0	306.3	3.1
C24- 551.5	168.1	3.0	C24- 1005.0	306.3	3.1
C24- 552.5	168.4	3.3			

MEAN 3.51
STANDARD DEVIATION 0.68

*...UNITS OF K = MCAL/CM-SEC-'C

TABLE C-3.- C-3.4

THERMAL CONDUCTIVITY VALUES FROM CORE OF DRILL HOLE C25
(SAMPLES ARE 2.680 CM IN DIAMETER BY 1.270 CM THICK)

SAMPLE NAME	DEPTH (METERS)	K*	SAMPLE NAME	DEPTH (METERS)	K*
C25- 975.0	297.2	4.9	C25- 987.5	301.0	5.4
C25- 976.0	297.5	5.7	C25- 988.5	301.3	4.9
C25- 977.0	297.8	6.4	C25- 989.5	301.6	4.7
C25- 983.0	299.6	7.3	C25- 990.0	301.8	4.4
C25- 984.5	300.1	4.5	C25- 991.0	302.1	4.7
C25- 985.5	300.4	5.3	C25- 992.0	302.4	4.3
C25- 986.5	300.7	5.1			

MEAN 5.20
STANDARD DEVIATION 0.86

*...UNITS OF K = MCAL/CM-SEC-'C

TABLE C-3.5

THERMAL CONDUCTIVITY VALUES FROM CORE OF DRILL HOLE C26
(SAMPLES ARE 2.680 CM IN DIAMETER BY 1.270 CM THICK)

SAMPLE NAME	DEPTH (METERS)	K*	SAMPLE NAME	DEPTH (METERS)	K*
C26- 971.5	296.1	5.7	C26- 984.5	300.1	6.3
C26- 972.5	296.4	5.7	C26- 985.5	300.4	5.6
C26- 979.5	298.6	5.5	C26- 986.5	300.7	5.9
C26- 980.5	298.9	5.2	C26- 987.0	300.8	4.9
C26- 981.5	299.2	5.9	C26- 988.0	301.1	5.8
C26- 982.5	299.5	6.0	C26- 989.0	301.4	4.3
C26- 983.5	299.8	6.0	C26- 990.0	301.8	3.9

MEAN	5.49
STANDARD DEVIATION	0.68

*...UNITS OF K = MCAL/CM-SEC-'C

TABLE C-3.6 C-3.6

THERMAL CONDUCTIVITY VALUES FROM CORE OF DRILL HOLE C28
(SAMPLES ARE 2.680 CM IN DIAMETER BY 1.270 CM THICK)

SAMPLE NAME	DEPTH (METERS)	K*	SAMPLE NAME	DEPTH (METERS)	K*
C28- 696.5	212.3	3.2	C28- 975.5	297.3	2.2
C28- 697.5	212.6	3.4	C28- 976.5	297.6	2.2
C28- 698.5	212.9	3.4	C28- 977.5	297.9	2.2
C28- 699.5	213.2	3.4	C28- 978.5	298.2	2.3
C28- 700.5	213.5	3.6	C28- 979.5	298.6	1.8
C28- 701.5	213.8	3.9	C28- 980.5	298.9	2.1
C28- 702.5	214.1	3.3	C28- 981.5	299.2	2.1
C28- 703.5	214.4	3.2	C28- 982.5	299.5	2.2
C28- 704.5	214.7	3.2	C28- 983.5	299.8	2.2
C28- 705.5	215.0	3.0	C28- 984.5	300.1	2.1
C28- 706.5	215.3	2.9	C28- 985.5	300.4	2.1
C28- 707.5	215.6	2.8	C28- 986.5	300.7	2.1
C28- 708.5	216.0	2.8	C28- 987.5	301.0	2.0
C28- 709.5	216.3	2.9	C28- 988.5	301.3	1.9
C28- 710.5	216.6	3.0	C28- 989.5	301.6	2.0
C28- 711.5	216.9	2.8	C28- 990.5	301.9	2.0
C28- 712.5	217.2	3.1	C28- 991.5	302.2	2.0
C28- 713.5	217.5	3.0	C28- 992.5	302.5	1.9
C28- 714.5	217.8	3.7	C28- 993.5	302.8	2.0
C28- 715.5	218.1	3.7	C28- 994.5	303.1	2.0
C28- 716.5	218.4	3.4	C28- 995.5	303.4	2.1
C28- 717.5	218.7	3.7	C28- 996.5	303.7	2.3
C28- 718.5	219.0	3.0	C28- 997.0	303.9	2.3
C28- 719.5	219.3	3.2	C28- 998.5	304.3	2.3
C28- 720.5	219.6	3.7	C28- 999.5	304.6	2.3
C28- 721.5	219.9	3.4	C28- 1001.0	305.1	2.3
C28- 722.5	220.2	3.4	C28- 1002.0	305.4	2.3
C28- 723.5	220.5	3.1	C28- 1003.0	305.7	2.2
C28- 724.5	220.8	3.3	C28- 1004.0	306.0	2.1
C28- 725.5	221.1	3.1			

MEAN 2.70
STANDARD DEVIATION 0.62

*...UNITS OF K = MCAL/CM-SEC-'C

TABLE C-3.7 C-3.7

THERMAL CONDUCTIVITY VALUES FROM CORE OF DRILL HOLE C29
(SAMPLES ARE 2.680 CM IN DIAMETER BY 1.270 CM THICK)

SAMPLE NAME	DEPTH (METERS)	K*	SAMPLE NAME	DEPTH (METERS)	K*
C29- 584.5	178.2	2.8	C29- 598.5	182.4	4.2
C29- 585.5	178.5	3.4	C29- 599.5	182.7	3.7
C29- 586.5	178.8	3.6	C29- 990.5	301.9	4.1
C29- 587.5	179.1	5.1	C29- 991.5	302.2	4.2
C29- 588.5	179.4	4.8	C29- 992.5	302.5	4.1
C29- 589.5	179.7	5.2	C29- 993.5	302.8	3.7
C29- 590.5	180.0	4.9	C29- 994.5	303.1	3.9
C29- 591.5	180.3	4.6	C29- 995.5	303.4	3.0
C29- 592.5	180.6	5.1	C29- 996.5	303.7	3.0
C29- 593.5	180.9	6.2	C29- 997.5	304.0	3.4
C29- 594.5	181.2	4.9	C29- 998.5	304.3	3.4
C29- 595.5	181.5	4.1	C29- 999.5	304.6	3.5
C29- 596.5	181.8	5.1			

MEAN 4.15
STANDARD DEVIATION 0.85

*...UNITS OF K = MCAL/CM-SEC-°C

TABLE C-3.8 C-3.8

THERMAL CONDUCTIVITY VALUES FROM CORE OF DRILL HOLE C30A
(SAMPLES ARE 2.680 CM IN DIAMETER BY 1.270 CM THICK)

SAMPLE NAME	DEPTH (METERS)	K*	SAMPLE NAME	DEPTH (METERS)	K*
C30- 241.5	73.6	3.5	C30- 1016.0	309.7	2.7
C30- 242.5	73.9	3.2	C30- 1017.0	310.0	2.5
C30- 243.5	74.2	3.0	C30- 1018.0	310.3	2.5
C30- 244.5	74.5	4.0	C30- 1019.0	310.6	2.4
C30- 245.5	74.8	3.6	C30- 1020.0	310.9	2.5
C30- 246.5	75.1	3.2	C30- 1021.0	311.2	2.4
C30- 247.5	75.4	4.1	C30- 1022.0	311.5	2.3
C30- 535.5	163.2	4.3	C30- 1023.5	312.0	2.3
C30- 536.5	163.5	3.5	C30- 1024.5	312.3	2.4
C30- 537.5	163.8	3.7	C30- 1025.5	312.6	2.5
C30- 538.5	164.1	3.8	C30- 1026.5	312.9	2.5
C30- 539.5	164.4	3.4	C30- 1027.5	313.2	2.5
C30- 540.5	164.7	3.4	C30- 1029.0	313.6	2.6
C30- 1009.0	307.5	2.6	C30- 1030.0	313.9	2.6
C30- 1010.0	307.8	2.5	C30- 1031.0	314.2	2.7
C30- 1011.0	308.2	2.8	C30- 1032.0	314.6	2.7
C30- 1012.0	308.5	2.8	C30- 1203.5	366.8	2.4
C30- 1013.0	308.8	3.0	C30- 1204.5	367.1	2.2
C30- 1014.0	309.1	2.9	C30- 1207.5	368.0	2.0
C30- 1015.0	309.4	2.6			

MEAN 2.89
STANDARD DEVIATION 0.57

*...UNITS OF K = MCAL/CM-SEC-'C

TABLE C-3.9 C-3.9

THERMAL CONDUCTIVITY VALUES FROM CORE OF DRILL HOLE C31
(SAMPLES ARE 2.680 CM IN DIAMETER BY 1.270 CM THICK)

SAMPLE NAME	DEPTH (METERS)	K*	SAMPLE NAME	DEPTH (METERS)	K*
C31- 732.5	223.3	3.1	C31- 982.5	299.5	3.7
C31- 733.5	223.6	2.5	C31- 983.5	299.8	3.7
C31- 734.5	223.9	3.1	C31- 984.5	300.1	3.7
C31- 735.5	224.2	4.2	C31- 986.5	300.7	3.4
C31- 736.5	224.5	3.8	C31- 987.5	301.0	3.1
C31- 737.5	224.8	4.5	C31- 988.5	301.3	3.0
C31- 738.5	225.1	6.6	C31- 989.5	301.6	2.5
C31- 739.5	225.4	4.1	C31- 990.5	301.9	2.8
C31- 740.5	225.7	3.9	C31- 991.5	302.2	2.8
C31- 741.5	226.0	4.0	C31- 992.5	302.5	2.7
C31- 742.5	226.3	4.2	C31- 992.5	302.5	2.5
C31- 743.5	226.6	4.1	C31- 993.5	302.8	2.8
C31- 744.5	226.9	3.9	C31- 994.5	303.1	2.8
C31- 745.5	227.2	4.1	C31- 995.5	303.4	2.5
C31- 746.5	227.5	4.0	C31- 996.5	303.7	2.7
C31- 747.5	227.8	4.0	C31- 997.5	304.0	2.7
C31- 980.5	298.9	3.4	C31- 998.5	304.3	2.8
C31- 981.5	299.2	3.5	C31- 999.5	304.6	3.0

MEAN 3.45
STANDARD DEVIATION 0.81

*...UNITS OF K = MCAL/CM-SEC-'C

TABLE C-3.10 C-3.10

THERMAL CONDUCTIVITY VALUES FROM CORE OF DRILL HOLE C32
(SAMPLES ARE 2.680 CM IN DIAMETER BY 1.270 CM THICK)

SAMPLE NAME	DEPTH (METERS)	K*	SAMPLE NAME	DEPTH (METERS)	K*
C32- 541.5	165.0	3.1	C32- 553.5	168.7	2.9
C32- 542.5	165.4	3.1	C32- 554.5	169.0	2.9
C32- 543.5	165.7	3.0	C32- 555.5	169.3	2.9
C32- 544.5	166.0	2.7	C32- 556.5	169.6	2.7
C32- 545.5	166.3	2.8	C32- 557.5	169.9	2.8
C32- 546.5	166.6	2.9	C32- 558.5	170.2	2.7
C32- 547.5	166.9	3.0	C32- 559.5	170.5	2.9
C32- 548.5	167.2	2.6	C32- 560.5	170.8	2.5
C32- 549.5	167.5	2.7	C32- 1019.0	310.6	3.0
C32- 550.5	167.8	3.2	C32- 1020.5	311.0	4.1
C32- 551.5	168.1	2.7	C32- 1034.5	315.3	4.8
C32- 552.5	168.4	3.1			

MEAN 3.00
STANDARD DEVIATION 0.50

*...UNITS OF K = MCAL/CM-SEC-'C

TABLE C-3.11

THERMAL CONDUCTIVITY VALUES FROM CORE OF DRILL HOLE C33
(SAMPLES ARE 2.680 CM IN DIAMETER BY 1.270 CM THICK)

SAMPLE NAME	DEPTH (METERS)	K*	SAMPLE NAME	DEPTH (METERS)	K*
C33-1013.5	308.9	5.4	C33- 1015.5	309.5	4.0
C33-1014.5	309.2	4.1			

MEAN	4.50
STANDARD DEVIATION	0.78

*...UNITS OF K = MCAL/CM-SEC-'C

TABLE C-3.12

THERMAL CONDUCTIVITY VALUES FROM CORE OF DRILL HOLE C39A
(SAMPLES ARE 2.680 CM IN DIAMETER BY 1.270 CM THICK)

SAMPLE NAME	DEPTH (METERS)	K*	SAMPLE NAME	DEPTH (METERS)	K*
C39- 723.5	220.5	3.2	C39- 739.5	225.4	3.2
C39- 724.5	220.8	2.8	C39- 740.5	225.7	3.1
C39- 732.5	223.3	2.9	C39- 741.5	226.0	3.6
C39- 733.5	223.6	3.3	C39- 742.5	226.3	3.4
C39- 734.5	223.9	3.1	C39- 744.5	226.9	3.7
C39- 735.5	224.2	3.6	C39- 745.5	227.2	3.2
C39- 736.5	224.5	3.4	C39- 746.5	227.5	3.1
C39- 737.5	224.8	4.1			

MEAN 3.31
STANDARD DEVIATION 0.33

*...UNITS OF K = MCAL/CM-SEC-'C

TABLE C-3.13

THERMAL CONDUCTIVITY VALUES FROM CORE OF DRILL HOLE C40
(SAMPLES ARE 2.680 CM IN DIAMETER BY 1.270 CM THICK)

SAMPLE NAME	DEPTH (METERS)	K*	SAMPLE NAME	DEPTH (METERS)	K*
C40- 764A	232.9	3.2	C40- 967	294.7	5.5
C40- 746B	227.4	4.5	C40- 967	294.7	6.4
C40- 765A	233.2	2.9	C40- 971A	296.0	4.2
C40- 765B	233.2	3.2	C40- 971B	296.0	4.3
C40- 767A	233.8	5.5	C40- 973A	296.6	6.0
C40- 767B	233.8	4.9	C40- 973B	296.6	6.9
C40- 768	234.1	1.6	C40- 973C	296.6	6.7
C40- 769A	234.4	4.0	C40- 973D	296.6	6.5
C40- 769B	234.4	4.3	C40- 985A	300.2	4.6
C40- 770	234.6	3.9	C40- 985B	300.2	4.3
C40- 966A	294.4	7.0	C40- 987A	300.8	5.6
C40- 966B	294.4	4.9	C40- 987B	300.8	4.1

MEAN 4.79
STANDARD DEVIATION 1.38

*...UNITS OF K = MCAL/CM-SEC-'C

TABLE C-3.14

THERMAL CONDUCTIVITY VALUES FROM CORE OF DRILL HOLE C41
(SAMPLES ARE 2.680 CM IN DIAMETER BY 1.270 CM THICK)

SAMPLE NAME	DEPTH (METERS)	K*	SAMPLE NAME	DEPTH (METERS)	K*
C41- 813	247.7	2.6	C41- 979	298.3	4.3
C41- 814	248.0	2.9	C41- 980	298.6	4.5
C41- 815	248.3	3.0	C41- 981	298.9	3.9
C41- 816	248.6	2.9	C41- 982	299.2	4.8
C41- 964	293.8	3.2	C41- 983	299.3	5.2
C41- 965	294.1	3.1	C41- 984	299.6	3.3
C41- 975	297.2	4.6	C41- 986	300.4	5.9
C41- 976	297.4	4.7	C41- 987	300.5	3.9
C41- 977	297.8	4.8	C41- 988A	301.1	3.6
C41- 978	298.0	2.4	C41- 988B	301.1	3.8

MEAN 3.87
STANDARD DEVIATION 0.95

*...UNITS OF K = MCAL/CM-SEC-'C

TABLE C-3.15

THERMAL CONDUCTIVITY VALUES FROM CORE OF DRILL HOLE C43
(SAMPLES ARE 2.680 CM IN DIAMETER BY 1.270 CM THICK)

SAMPLE NAME	DEPTH (METERS)	K*	SAMPLE NAME	DEPTH (METERS)	K*
C43- 550.5	167.8	3.3	C43- 562.5	171.4	3.5
C43- 551.5	168.1	2.9	C43- 563.5	171.8	3.7
C43- 552.5	168.4	3.0	C43- 564.5	172.1	3.5
C43- 554.5	169.0	2.9	C43- 566.5	172.7	3.3
C43- 555.5	169.3	3.2	C43- 567.5	173.0	3.0
C43- 556.5	169.6	3.1	C43- 568.5	173.3	3.1
C43- 557.5	169.9	3.4	C43- 569.5	173.6	2.9
C43- 558.5	170.2	3.2	C43- 571.2	174.1	4.3
C43- 559.5	170.5	3.7	C43- 572.3	174.4	3.7
C43- 560.5	170.8	3.7	C43- 573.2	174.7	3.9
C43- 561.5	171.1	3.6	C43- 1039.5	316.8	2.9

MEAN 3.35
STANDARD DEVIATION 0.38

*...UNITS OF K = MCAL/CM-SEC-°C

TABLE C-3.16

THERMAL CONDUCTIVITY VALUES FROM CORE OF DRILL HOLE C46
(SAMPLES ARE 2.680 CM IN DIAMETER BY 1.270 CM THICK)

SAMPLE NAME	DEPTH (METERS)	K*	SAMPLE NAME	DEPTH (METERS)	K*
C46- 739.5	225.4	3.3	C46- 752.7	229.4	4.2
C46- 740.5	225.7	3.3	C46- 753.5	229.7	4.3
C46- 741.5	226.0	3.3	C46- 754.0	229.8	4.2
C46- 742.5	226.3	3.6	C46- 966.5	294.6	2.3
C46- 743.5	226.6	3.1	C46- 967.5	294.9	2.4
C46- 745.5	227.2	3.5	C46- 968.5	295.2	3.1
C46- 746.5	227.5	3.8	C46- 969.0	295.4	3.7
C46- 747.5	227.8	3.7	C46- 970.3	295.7	2.6
C46- 748.5	228.1	3.9	C46- 971.3	296.1	2.6
C46- 749.5	228.4	3.7	C46- 973.3	296.7	3.2
C46- 750.5	228.8	4.3	C46- 974.3	297.0	3.7
C46- 751.5	229.1	4.4	C46- 975.3	297.3	2.9

MEAN 3.46
STANDARD DEVIATION 0.61

*...UNITS OF K = MCAL/CM-SEC-'C

TABLE C-3.17

THERMAL CONDUCTIVITY VALUES FROM CORE OF DRILL HOLE C55
(SAMPLES ARE 2.680 CM IN DIAMETER BY 1.270 CM THICK)

SAMPLE NAME	DEPTH (METERS)	K*	SAMPLE NAME	DEPTH (METERS)	K*
C55- 545.5	166.3	4.7	C55- 562.5	171.4	4.8
C55- 546.5	166.6	4.0	C55- 563.5	171.8	4.0
C55- 547.5	166.9	3.9	C55- 564.5	172.1	4.4
C55- 548.5	167.2	4.0	C55- 565.5	172.4	4.3
C55- 549.5	167.5	4.0	C55- 566.5	172.7	3.8
C55- 550.5	167.8	4.3	C55- 944.5	287.9	3.6
C55- 552.5	168.4	4.2	C55- 945.5	288.2	3.1
C55- 553.5	168.7	3.7	C55- 946.5	288.5	3.6
C55- 554.5	169.0	3.9	C55- 949.5	289.4	2.8
C55- 555.5	169.3	3.8	C55- 950.5	289.7	2.7
C55- 556.5	169.6	3.7	C55- 969.5	295.5	2.5
C55- 557.5	169.9	3.7	C55- 970.5	295.8	3.1
C55- 558.5	170.2	4.3	C55- 972.5	296.4	3.0
C55- 559.5	170.5	4.2	C55- 973.5	296.7	2.9
C55- 560.5	170.8	4.8	C55- 974.5	297.0	2.5
C55- 561.5	171.1	5.8			

MEAN 3.81
STANDARD DEVIATION 0.74

*...UNITS OF K = MCAL/CM-SEC-°C

TABLE C-3.18

THERMAL CONDUCTIVITY VALUES FROM CORE OF DRILL HOLE C59
(SAMPLES ARE 2.680 CM IN DIAMETER BY 1.270 CM THICK)

SAMPLE NAME	DEPTH (METERS)	K*	SAMPLE NAME	DEPTH (METERS)	K*
C59- 477.5	145.5	3.1	C59- 493.5	150.4	2.7
C59- 478.5	145.8	3.0	C59- 494.5	150.7	2.9
C59- 479.5	146.2	2.9	C59- 495.5	151.0	2.8
C59- 481.5	146.8	2.9	C59- 496.5	151.3	2.9
C59- 482.5	147.1	3.3	C59- 497.5	151.6	3.1
C59- 483.5	147.4	2.6	C59- 498.9	152.1	2.5
C59- 484.5	147.7	2.6	C59- 499.9	152.4	3.1
C59- 485.5	148.0	2.5	C59- 500.9	152.7	2.6
C59- 486.5	148.3	2.5	C59- 501.9	153.0	2.7
C59- 487.5	148.6	2.6	C59- 502.9	153.3	3.1
C59- 488.5	148.9	2.7	C59- 979.5	298.6	3.0
C59- 489.5	149.2	2.7	C59- 980.5	298.9	3.7
C59- 490.5	149.5	2.5	C59- 981.5	299.2	4.7
C59- 491.5	149.8	2.7	C59- 982.5	299.5	4.8
C59- 492.5	150.1	2.7	C59- 983.5	299.8	3.9

MEAN 2.99
STANDARD DEVIATION 0.58

*...UNITS OF K = MCAL/CM-SEC-'C

TABLE C-3.19

THERMAL CONDUCTIVITY VALUES FROM CORE OF DRILL HOLE C60
(SAMPLES ARE 2.680 CM IN DIAMETER BY 1.270 CM THICK)

SAMPLE NAME	DEPTH (METERS)	K*	SAMPLE NAME	DEPTH (METERS)	K*
C60- 918.5	280.0	4.8	C60- 924.7	281.8	4.0
C60- 919.5	280.3	5.5	C60- 925.9	282.2	4.5
C60- 920.5	280.6	3.6	C60- 926.9	282.5	4.2
C60- 921.7	280.8	4.3	C60- 927.9	282.8	4.5
C60- 922.7	281.2	4.3	C60- 928.9	283.1	3.7
C60- 923.7	281.5	3.1			

MEAN 4.23
STANDARD DEVIATION 0.64

*...UNITS OF K = MCAL/CM-SEC-'C

Lithologic Analysis of Sediment Samples from the Intermediate Drilling Program

Michael Svetlichny

During the period October 1, 1978 - March 15, 1979, 32 holes were completed as part of the Atlantic Coastal Plain drilling program. In each of the 300 m deep holes, drill cuttings were collected at 3.0 m intervals and sealed in airtight plastic bags to prevent sediments from drying out.

At least two attempts were made to recover core in each hole. A minimum of 15 m was cored. Recovery of unconsolidated, clean sand frequently was poor because material tends to be washed away by the coring process, and sediments were not always retained in the core barrel by the core catcher. In an effort to maximize core recovery and minimize drilling costs, one coring interval was selected to be within a thick (†15 m) sequence of clayey, silty, or consolidated sediments, and the other coring attempt was made near the maximum depth of 300 m. Detailed analyses of the cores has begun, but there are no results to report as yet.

Lithologic descriptions of the drill cuttings have been completed for each hole; the results are presented as a table following this text. The descriptions are based on Folk's (1974) classification. Each category reflects the proportion of gravel, sand, and silt plus clay in that sample. In cases where well-sorted gravel was present, a distinction was made between granules, pebbles, and cobbles. Similarly, the sand fraction was subdivided into very fine, fine, medium, coarse, and very coarse sand. If silt and clay occurred in equal proportion, they were collectively referred to as mud. Whole and fragmented macrofossils were reported as shells.

Selected samples from each hole are being wet sieved with a number 230 U.S. standard sieve to determine the proportion of sediment that is finer than 4.0 phi. This work began recently so that the data set is incomplete. The results to date are included in the table that follows this text.

ACKNOWLEDGEMENT

The following Gruy Federal Personnel assisted in sample descriptions and sieving: Kenneth Hurst, Ronald Herzick, Paul Caprio, Michael Hoffman, and Donald Hostvedt.

NEW JERSEY

NO. 41 Gea Girt, NJ

INTERVAL (METERS)	FORMATION-AGE	DESCRIPTION	COMMENTS	SAMPLES SIEVED	RATIO COARSE/FINE	PERCENT FINES
0-21.3	Kirkwood		No samples			
21.3-24.4	Kirkwood	Slightly silty medium-coarse sand with granules				
24.4-27.4	Kirkwood	Slightly silty medium-coarse sand with granules				
27.4-30.5	Kirkwood	Slightly silty medium-coarse sand with granules				
30.5-33.5	Kirkwood	Silty coarse sand, slightly granular		30.5-33.5	6.82	12.7
33.5-39.6	Kirkwood		No samples			
39.6-42.7	Kirkwood	Coarse sand				
42.7-45.7	Kirkwood		No samples			
45.7-48.8	Shark River Manasquan	Coarse sandy and granular mud, slightly micaceous				
48.8-51.8	Shark River-Manasquan	Slightly granular and coarse sandy mud				
51.8-54.9	Shark River-Manasquan	Clayey coarse sand				
54.9-57.9	Shark River-Manasquan	Slightly silty coarse sand with some granules and indurated sand fragments				
57.9-61.0	Shark River-Manasquan	Slightly granular clay		57.9-61.0	0.45	69.1
61.0-64.0	Shark River-Manasquan	Slightly granular clay				
64.0-67.1	Shark River-Manasquan	Slightly coarse sandy clay				

67.1-70.1	Shark River-Manasquan	Slightly granular clay		67.1-70.1	0.88	53.1
70.1-73.2	Shark River-Manasquan	Slightly fine sandy mud				
73.2-76.2	Vincentown		No samples			
76.2-82.3	Vincentown	Limy silty clay		76.2-79.2	0.55	64.4
82.3-85.3	Vincentown	Limy silty clay with minor granules				
85.3-103.6	Vincentown	Slightly glauconitic fine sandy limy mud		85.3-88.4 91.4-94.5	0.55 0.59	64.4 62.9
103.6-106.7	Vincentown		No samples			
106.7-109.7	Hornerstown	Slightly coarse sandy limy mud with glauconite				
109.7-112.8	Hornerstown	Slightly sandy micaceous limy mud		109.7-112.8	0.52	65.8
112.8-115.8	Tinton	Glauconitic sandy clay		112.8-115.8	0.86	53.7
115.8-118.9	Tinton	Glauconitic clay				
118.9-121.9	Sandy Hook Member	Slightly fine sandy clay		118.9-121.9	1.30	43.5
121.9-128.0	Sandy Hook Member	Micaceous silty clay		121.9-125.0	0.43	69.8
128.0-131.1	Sandy Hook Member	Slightly fine sandy clay		128.0-131.1	0.19	84.4
131.1-134.1	Sandy Hook	Slightly fine sandy limy micaceous clay				
134.1-137.2			No samples			
137.2-140.2	Sandy Hook Member	Slightly limy glauconitic clay				
140.2-143.3	Sandy Hook Member	Glauconitic micaceous clay				
143.3-146.3	Sandy Hook Member	Glauconitic micaceous clay	Minor shell			
146.3-149.4	Sandy Hook	Clayey, glaucon-	Shells	146.3-149.4	1.79	35.8

	Member	itic fine sand				
149.4-152.4	Sandy Hook Member	Clayey, glaucon-itic fine sand	Shells			
152.4-164.6	Shrewsbury Member 161.5	Muddy fine-medium sand	Shells from 161.5-164.6	152.4-155.4 158.5-161.5	1.90 1.63	34.5 38.0
164.6-167.6	Navesink	Silty glauconitic limy sand				
167.6-176.8	Navesink 173.7	Muddy glauconitic sand		167.6-170.7	2.27	30.6
176.8-179.8	Mt. Laurel	Limy fine-coarse micaceous sand with glauconite		176.8-179.8	2.64	27.5
179.8-185.9	Mt. Laurel 182.9	Same as 176.8-179.8 but no coarse sand		182.9-185.9	1.00	50.0
185.9-189.0	Wenonah	Muddy fine-coarse sand		185.9-189.0	2.87	25.9
189.0-201.2	Wenonah 198.1	Muddy fine-medium micaceous sand, slightly limy	Shells from 192.0-198.1	189.0-192.0	2.25	30.7
201.2-204.2	Marshalltown	Granular medium sandy mud		201.2-204.2	.64	61.1
204.2-207.3	Englishtown	Slightly sandy mud				
207.3-210.3	Englishtown	Muddy medium sand		207.3-210.3	1.20	45.5
210.3-216.4	Englishtown	Slightly sandy micaceous clay				
216.4-219.5	Englishtown	Granular pebbly fine sand with minor silt.				
219.5-222.5	Englishtown	Granular fine sand with minor silt		219.5-222.5	12.6	07.3
222.5-225.6	Englishtown	Silty medium-coarse sand with granules				
225.6-228.6	Englishtown	Slightly silty coarse limy sand with granules and pebbles		225.6-228.6	3.67	21.4

228.6-231.6	Englishtown	Slightly silty coarse limy sand with granules and claystone fragments				
231.6-234.7			No samples			
234.7-237.7	Englishtown	Muddy medium-coarse sand with granules and pebbles		234.7-237.7	3.81	20.8
237.7-240.8	Englishtown	Muddy medium-coarse sand with granules and lignite		237.7-240.8	3.83	20.7
240.8-243.8	Englishtown	Muddy medium-coarse sand, slightly granular.				
243.8-253.0	Woodbury		No samples			
253.0-259.1	Woodbury	Coarse sandy micaceous mud		256.0-259.1	0.59	63.0
259.1-262.1	Woodbury	Slightly fine sandy mud				
262.1-265.2	Woodbury	Slightly fine sandy mud				
265.2-268.2	Merchantville	Fine sandy limy mud		265.2-268.2	1.08	48.1
268.2-274.3	Merchantville	Slightly granular fine sandy clay		268.2-271.3	0.78	56.3
274.3-277.4	Merchantville	Slightly sandy clay		274.3-277.4	0.46	68.4
277.4-289.6	Merchantville		No samples			
289.6-292.6	Magothy	Clay	Minor shell			
292.6-295.7	Magothy	Slightly fine sandy clay		292.6-295.7	0.23	81.1

NO. 40 Ft. Monmouth, NJ

INTERVAL (METERS)	FORMATION-AGE	DESCRIPTION	COMMENTS	SAMPLES SIEVED	RATIO COARSE/FINE	PERCENT FINES
0-15.2		Glauconitic fine-medium sand				
15.2-18.3		Glauconitic muddy fine - medium sand				
18.3-42.7		Limy silty fine glauconitic sand				
42.7-48.8		Limy clay				
48.8-51.8		Micaceous clay with some gravel				
51.8-61.0		Micaceous clay				
61.0-64.0		Micaceous silty clay				
64.0-73.2		Micaceous limy clay with some gravel	Shells			
73.2-91.4		Silty micaceous clay with some gravel				
91.4-94.5		Silty clay				
94.5-182.9		Limy clay	Shells 152.4-170.7 Missing			
182.9-185.9		Clay	Shells			
185.9-189.9		Limy clay	Shells			
189.9-195.1		Abundance of mica, lignite, and gravel	Abundant shells			
195.1-198.1		Limy silty micaceous clay with lignite				
198.1-201.2		Micaceous clay				
201.2-210.3		Limy micaceous clay with some gravel	Shells			
210.3-213.4		Limy micaceous clay	Minor shells			
213.4-234.7		Silty micaceous clay				
234.7-240.8		Fine sand				

240.8-268.2	Fine coarse sand with micaceous clay	Minor shells

NO. 39A Forked River, NJ

INTERVAL (METERS)	FORMATION-AGE	DESCRIPTION	COMMENTS	SAMPLES SIEVED	RATIO COARSE/FINE	PERCENT FINES
0-9.1			No samples			
9.1-24.4		Fine-medium yellow sand				
24.4-27.4			No samples			
27.4-67.1		Fine-medium yellow sand	Becomes mostly medium sand toward end of interval			
67.1-85.3		Granular medium-coarse yellow and grey sand	Some small pebbles at beginning of interval			
85.3-109.7		Silt with minor amounts of medium coarse sand				
109.7-125.0		Fine-medium sand with some silt	Granules and pebbles in upper part of interval			
125.0-140.2		Silty fine-medium black sand with granules.	Silt increases over interval. Chalk from 137.2-140.2			
140.2-149.4		Fine-medium yellow sand with fine black grains	Some silt at end of interval			
149.4-161.5		Silty sand	Grains increase from fine to fine-coarse over the interval. Silt greatest at mid-interval. Granules from middle to end of interval. Chalk from 158.5-161.5			
161.5-210.3		Granular fine-coarse light grey sand with fine black grains. Slightly pebbly.				
210.3-213.4			No samples			
213.4-219.5		Same as 161.5-210.3				

219.5-243.8		No samples
243.8-256.0	Granules with coarse sand	
256.0-262.1	Light grey clayey gravel with minor amount of fine black sand	
262.1-271.3	Slightly gravelly light grey sand	
271.3-286.5	Sandy light grey clay with minor amounts of granules and pebbles	
286.5-298.7	Silty grey clay with minor amounts of fine black sand and granules	

NO. 38 Atlantic City, NJ

INTERVAL (METERS)	FORMATION-AGE	DESCRIPTION	COMMENTS	SAMPLES SIEVED	RATIO COARSE/FINE	PERCENT FINES
0-21.3		Granular fine-coarse sand	Grain size decreases over interval			
21.3-36.6		Fine-medium sand. Minor amount of silt at mid-interval				
36.6-70.1		Granular fine-coarse sand				
70.1-73.2		Fine-medium sand with granules				
73.2-76.2			No samples			
76.2-82.3		Silty fine-coarse sand	Silt decreases over interval			
82.3-91.4		Fine-medium sand with some silt and granules toward end of interval				
91.4-94.5		Granular medium-coarse sand with some silt				
94.5-103.6		Fine-medium sand with some silt	Shells. Granules increase toward end of interval			
103.6-106.7		Silty fine-coarse sand	Shells			
106.7-109.7		Silty granular shell hash				
109.7-115.8		Silt with shell hash and some granules				
115.8-121.9		Silty medium-coarse sand				
121.9-134.1		Silt with medium sand in center of interval	Shells			
134.1-140.2		Fine-coarse sand				

	with some silt	
140.2-143.3	Silt with minor amounts of coarse sand	
143.3-146.3	Fine-medium sand with minor amounts of silt	
146.3-149.4	Silt	
149.4-161.5	Medium-coarse sand with minor amounts of silt	
161.5-179.8	Silt with medium-coarse sand	Sand content decreases throughout interval
179.8-189.0		No samples
189.0-198.1	Fine sand with minor amounts of silt	
198.1-210.3	Medium-coarse sand with increasing silt	
210.3-213.4	Silty medium sand with shell hash	
213.4-249.9	Medium sand	Shells at beginning of interval
249.9-253.0	Fine sandy silt	
253.0-256.0	Silt and granules	Minor shells
256.0-277.4	Fine-coarse sand with minor amounts of silt, pebbles and granules	

NO. 36 Cape May, NJ

INTERVAL (METERS)	FORMATION-AGE	DESCRIPTION	COMMENTS	SAMPLES SIEVED	RATIO COARSE/FINE	PERCENT FINES
0-45.7			No samples			
45.7-61.0		Silty coarse sand with some granules and pebbles				
61.0-64.0			No samples			
64.0-73.2		Silty coarse sand with some granules and pebbles				
73.2-82.3		Granules - pebbles				
82.3-97.5			No samples			
97.5-106.7		Granules - pebbles				
106.7-112.8		Granular-pebbly medium-coarse sand				
112.8-125.0			No samples			
125.0-131.1		Granular grey silty sand with some pebbles				
131.1-149.4		Grey silty fine-medium sand with some pebbles and shell hash	Core recovery from 139.3-144.8			
149.4-158.5		Fine-medium sand, slightly silty	Shells			
158.5-304.8			No samples. Core recovery from 303.0-306.6			

DELAWARE

NO. 54 Bridgeville, DE

INTERVAL (METERS)	FORMATION-AGE	DESCRIPTION	COMMENTS	SAMPLES SIEVED	RATIO COARSE/FINES	PERCENT FINES
0-3.0		Fine to very coarse clean sand				
3.0-24.4		Coarse sandy clay	Becomes more sandy toward end of interval			

24.4-27.4	Grey silty fine - coarse sand	
27.4-36.6	Very fine-coarse clean sand	
36.6-57.9	Muddy fine sand	Becomes less sandy toward end of interval
57.9-70.1	Fine sandy clay	Shells
70.1-73.2	Muddy sand	Abundant shells
73.2-106.7	Grey limy clay with gravel	Abundant shells
106.7-109.7		No samples
109.7-125.0	Limy clay with gravel	Abundant shells
125.0-164.6	Limy clay with gravel	Abundant shells
164.6-179.8	Cored	Recoveries from 164.6-167.0 and 172.2-179.5
179.8-185.9	Muddy sand with minor gravel	Shells
185.9-295.7	Fine sand and limy clay with minor gravel	Minor shells. Highly calcareous below 277.6 m
295.7-298.4	Cored	Recovery from 295.7-298.4

NO. 34 Lewes, DE

INTERVAL (METERS)	FORMATION-AGE	DESCRIPTION	COMMENTS	SAMPLES SIEVED	RATIO COARSE/FINES	PERCENT FINES
0-39.6			No samples			
39.6-45.7		Fine-medium sand with some white clay	Lignite			
45.7-57.9		Very fine sandy clay				
57.9-118.9		Very fine- fine sand	Below 100.6- highly calcareous			
118.9-160.9			No samples			
160.9-170.7		Cored	Recovery from 160.9-170.1			
170.7-210.3		Silty fine limy sand	Shells, lignite			
210.3-222.5		Limy clayey sand and gravel	Shells			
222.5-228.6		Silty fine-very coarse sand	Abundant shells			
228.6-256.0		Limy clay	Indurated fragments of silty sand. Shells shell fragments			
256.0-298.7		Very fine-fine sand with limy clay				
298.7-309.3		Cored	Recovery from 307.8-309.3			

NO. 34C Ellendale State Tree Forest, DE

INTERVAL (METERS)	FORMATION-AGE	DESCRIPTION	COMMENTS	SAMPLES SIEVED	RATIO COARSE/FINES	PERCENT FINES
0-33.5			No samples			
33.5-45.7		Very clean coarse sand and gravel				
45.7-61.0		Silty very coarse sand and gravel				
61.0-76.2		Clay and gravel	Gravel is in alternating increasing and decreasing amounts			
76.2-82.3		Clay and gravel				
82.3-88.4		Silt and gravel				
88.4-97.5		Clay and gravel				
97.5-100.6		Silty clay with gravel	Shells			
100.6-149.4		Clay and gravel	Shells			
149.4-179.8		Alternating silty and fine sandy clay with minor gravel	Shells			
179.8-182.9		Silty cobbles				
182.9-185.9			No samples			
185.9-213.4		Cored	Recovery from 192.3-196.1			
213.4-240.8		Silty fine to very coarse sand with gravel				
240.8-249.9		Fine glauconitic sand with some medium sand and granules				
249.9-310.9		Fine glauconitic sand				
310.9-318.1		Cored	Recovery from 310.9-318.1			

NO. 34E Assawoman Bay, DE

INTERVAL (METERS)	FORMATION-AGE	DESCRIPTION	COMMENTS	SAMPLES SIEVED	RATIO COARSE/FINES	PERCENT FINES
0-42.7			No samples			
42.7-67.1		Fine sand				
67.1-73.2		Fine-medium well rounded sand.Some very coarse sand and gravel	Shells			
73.2-137.2		Very fine-fine sand	Minor shells			
137.2-140.2		Fine-medium sand with organic mud	Shells			
140.2-143.3		Fine-medium sand	Shells			
143.3-158.5		Fine-medium sand with organic mud	Shells			
158.5-164.6		Medium-coarse sand	Shells			
164.6-183.0		Cored	Recovery from 178.9-182.0			
183.0-189.0		Clay				
189.0-192.0		Muddy fine-medium sand				
192.0-213.4		Clay	Shells			
213.4-268.2		Silty clay with some sand and gravel	Shells			
268.2-289.6		Clay and silt	Shells			
289.6-295.7		Sandy clay	Shells			
295.7-301.1		Cored	Recovery from 299.3-301.1			

NO. 53 Snow hill, MD MARYLAND

INTERVAL (METERS)	FORMATION-AGE	DESCRIPTION	COMMENTS	SAMPLES SIEVED	RATIO COARSE/FINE	PERCENT FINES
0-6.1		Very fine sand				
6.1-9.1		Fine-medium clean				

	sand	
9.1-15.2	Silty fine sand	
15.2-27.	Fine-medium sand	
27.4-36.6	Silty very fine sandy clay	
36.6-45.7	Silty fine sand	Abundant shells
45.7-54.9	Medium-coarse clean sand	Shells
54.9-97.5	Silty fine sandy clay. Glauconitic	Shells are abundant to 76.2, then decrease
97.5-185.9	Mostly clay with silt and sand	Grades downward into clay. Shells
185.9-219.5	Mostly clay with fine sand and silt	Shells
219.5-265.2	Limy clay with fine sand	Shells. Core recovery from 239.6-247.5
265.2-295.7	Clay. Some fine sand	Shells
295.7-304.8	SECOND CORE DRILLED -	Recovery from 296.5-304.5

NO. 52 Princess Anne, MD

INTERVAL (METERS)	FORMATION-AGE	DESCRIPTION	COMMENTS	SAMPLES SIEVED	RATIO COARSE/FINE	PERCENT FINES
0-18.3		Fine clean sand.				
18.3-146.3			Missing			
146.3-176.8		Clay and gravel	(167.6-176.8 - limy clay) Minor shells			
176.8-204.2		Clay and gravel	Minor shells			
204.2-213.4		Limy clay with gravel	Shells			
213.4-222.5		Cored	Recovery from 215.5-221.0			
222.5-240.8		Green limy clay with gravel	Shells			
240.8-262.1		Sandy limy clay with gravel	Shells. Gravel increases throughout interval			
262.1-295.7		Slightly granular limy clay	Shells			
295.7-308.8		Cored	Recovery from 299.6-308.8			

NO. 51 Kingston, MD

INTERVAL (METERS)	FORMATION-AGE	DESCRIPTION	COMMENTS	SAMPLES SIEVED	RATIO COARSE/FINE	PERCENT FINES
0-24.4		Silty clay				
24.4-121.9		Clay with very coarse sand and gravel	Minor shells. Sand and gravel fraction decreases toward end of interval			
121.9-213.4		Slightly gravelly clay	Minor shells			
213.4-274.3		Fine to coarse sandy clay	Core recovery from 212.8-221.3 clay			
274.3-289.6		Silty clay				
289.6-297.8		Clay				
297.8-300.8		Cored	Recovery from 297.8-300.8			

NO. 50 Rehobeth, MD

INTERVAL (METERS)	FORMATION-AGE	DESCRIPTION	COMMENTS	SAMPLES SIEVED	RATIO COARSE/FINE	PERCENT FINES
0-21.3		Clean fine- medium sand with gravel	Shells			
21.3-27.4		Fine - medium sand with gravel and clay lenses	Shells			
27.4-51.8		Very fine - medium sand	Shells			
51.8-57.9		Fine - medium sand with clay lenses	Shells			
57.9-61.0		Fine - medium sand with gravel	Shells			
61.0-131.1		Fine to medium sandy clay with some gravel	Gravel fraction increases with depth up to 100 m			
131.1-137.2		Silty fine - medium sand	Shells			
137.2-146.3		Fine sandy limy clay	Shells			
146.3-161.5		Muddy medium - coarse limy sand	Shells			
161.5-176.8		Fine - coarse sandy limy clay with some gravel	Shells			
176.8-210.3		Muddy fine - medium sand with gravel	Shells			
210.3-213.4		Limy clay				
213.4-228.6		Fine sandy clay, slightly granular	Shells			
228.6-237.7		Cored	Recovery from 229.8-237.4			
237.7-298.4		Fine sandy limy clay	Shells. Slightly 237.7-253.0			
298.4-306.0		Cored	Recovery from 298.4-299.3			

NO. 47 Salisbury Airport, MD

INTERVAL (METERS)	FORMATION-AGE	DESCRIPTION	COMMENTS	SAMPLES SIEVED	RATIO COARSE/FINE	PERCENT FINES
0-185.9		Fine sand	Shells			
185.9-262.1		Glauconitic fine sand	Core recovery from 233.2-240.3			
262.1-295.7		Slightly glauconitic fine sand	Shells			
			Throughout the samples are limestone fragments and asphalt believed to have been washed from the surface and into the well as drilling occurred. No recovery from second core.			

NO. 46 Salisbury, off Zion Road, MD

INTERVAL (METERS)	FORMATION-AGE	DESCRIPTION	COMMENTS	SAMPLES SIEVED	RATIO COARSE/FINE	PERCENT FINES
0-39.6		Very fine-fine clean sand with quartz gravel				
39.6-45.7		Silty fine sand with gravel, slightly glauconitic				
45.7-57.9		Fine sand				
57.9-67.1		Very fine-medium sand with gravel	Some coarse sand and silt near end of interval			
67.1-76.2		Fine sand				
76.2-100.6		Fine-medium sand, slightly glauconitic				
100.6-103.6		Silty medium-coarse sand				
103.6-112.8		Very fine-medium sand, slightly glauconitic	Some clay near bottom of interval			
112.8-115.8		Very fine-coarse sand with gravel	Shells			
115.8-125.0		Silty fine sand with some gravel and coarse sand. Glauconitic				
125.0-131.1		Silty clay with some sand and gravel. Glauconitic				
131.1-152.4		Silty fine sand with coarse sand and gravel	Shells			
152.4-155.4		Silty clay with sand and gravel				
155.4-171.0		Fine-coarse sand with gravel	Minor shells			
171.0-176.8		Silty fine grey	Shells			

	sand with some coarse sand. Glauconitic	
176.8-132.9	Granular muddy sand	
182.9-189.0	Very fine-fine sand with some coarse sand	
189.0-222.5	Fine sandy limy clay, slightly glauconitic	Becoming more gravelly and shelly toward end of interval
222.5-231.6	Cored	Recovery from 224.9-230.1
231.6-240.8	Very fine-fine limy sand. Glauconitic	Minor shells
240.8-243.8	Sandy clay, slightly glauconitic	Shells
243.8-246.9	Slightly granular fine-very fine limy sand. Glauconitic	Shells
246.9-259.1	Silty fine sand with gravel	Shells
259.1-271.3	Fine sandy clay grading into silty fine sand	
271.3-289.6	Silty fine sand with gravel	
289.6-294.4	Silty fine sand	
294.4-305.0	Cored	Recovery from 294.4-298.6

NO. 45 Hebron (off Fire Tower Road), MD

INTERVAL (METERS)	FORMATION-AGE	DESCRIPTION	COMMENTS	SAMPLES SIEVED	RATIO COARSE/FINE	PERCENT FINES
0-27.4		Fine clean sand, slightly glauconitic				
27.4-36.6		Silty fine sand				
36.6-67.1		Very fine-fine clean sand				
67.1-73.2		Very fine-medium clean sand				
73.2-103.6		Silty fine sand	Alternating silty and sandy clay			
103.6-106.7		Fine sandy clay	Alternating silty and sandy clay			
106.7-109.7		Silty fine sand	Alternating silty and sandy clay			
109.7-112.8		Fine sandy clay	Alternating silty and sandy clay			
112.8-125.0		Silty fine sand	Alternating silty and sandy clay			
125.0-189.0		Fine sandy clay	Alternating silty and sandy clay			
189.0-192.0		Silty clay with gravel	Abundant shells			
192.0-201.2		Fine sandy clay with gravel	Shells			
201.2-214.9		Silty clay with gravel	Shells			
214.9-222.5		Cored	Recovery from 214.9-220.5			
222.5-283.5		Fine silty clay	Minor shells			
283.5-295.7		Fine sandy clay	Shells			
295.7-304.8		Cored	Recovery from 297.2-304.8			

NO. 43 Ocean City, MD

INTERVAL (METERS)	FORMATION-AGE	DESCRIPTION	COMMENTS	SAMPLES SIEVED	RATIO COARSE/FINE	PERCENT FINES
0-3.0		Fine to medium sand				
3.0-9.1		Clay and silty fine sand	Shells			
9.1-12.2		Silty clay				
12.2-15.2		Silty fine sand	Shells			
15.2-24.4		Silty fine-medium sand with gravel	Minor shells			
24.4-30.5		Fine-very coarse sand with silt				
30.5-36.6		Silty medium very coarse sand	Shells			
36.6-39.6		Gravel, sand and silt				
39.6-45.7		Silty coarse sand and gravel				
45.7-61.0		Silty clay	Minor shells			
61.0-73.2		Sandy clay, slightly glauconitic				
73.2-103.6		Silty clay	Shells			
103.6-112.6		Clay	Shells			
112.8-121.9		Silty fine-coarse sand with gravel				
121.9-125.0		Silty fine-medium sand with gravel	Minor shells			
125.0-149.4		Very fine-very coarse sand and gravel				
149.4-152.4		Fine-medium sand with some quartz gravel				
152.4-155.4		Silty fine-medium sand with gravel				

	and siltstone	
155.4-167.6	Clay	Minor shells
167.6-175.3	Cored	Recovery from 167.6-175.3

NO. 43A Ocean City, MD

INTERVAL (METERS)	FORMATION-AGE	DESCRIPTION	COMMENTS	SAMPLES SIEVED	RATIO COARSE/FINE	PERCENT FINES
0-61		Very fine to medium sand		30.5-33.5 51.8-54.9	6.09 7.36	14.10 11.96
61.0-70.1		Fine to coarse sand	Abundant shells			
70.1-88.4		Fine to coarse sand		73.2-76.2 82.3-85.3	6.33 15.80	13.65 5.95
88.4-121.9		Medium to coarse sand	Minor shells	91.4-94.5 100.6-103.6 112.8-115.8	10.70 12.30 8.54	8.55 7.52 10.48
121.9-125.0		Medium to very coarse sand	Abundant shells	131.1-134.1	14.95	6.27
125.0-137.2		Fine to medium sand	Shells	131.1-134.1	14.95	6.27
137.2-140.2		Medium to very coarse sand	Minor shells			
140.2-167.6		Fine to medium micaceous sand.	Shells	143.3-146.3 161.5-164.6	12.16 15.44	7.60 6.08
167.6-189.0		Silty medium to coarse sand	Shells	182.9-185.9	9.12	9.88
189.0-204.2		Fine to medium sand	Shells	19 8.1-201.2	11.35	8.10
204.2-210.3		Medium to coarse sand	Shells			
210.3-231.6		Fine to very coarse sand	Minor shells	210.3-213.4 228.6-231.6	20.35 29.53	4.68 3.28
231.6-240.8		Fine to medium sand with some very coarse sand	Minor shells	234.7-237.7	26.91	3.58
240.8-259.1		Medium to very coarse sand	Shells	240.8-243.8	38.77	2.51
259.1-268.2		Medium to coarse sand	Minor shells	259.1-262.1	20.96	4.55
268.2-280.4		Fine to very coarse sand	Shells	268.2-271.3	6.61	13.14

280.4–283.5	Fine to very coarse sand	Shells			
283.5–289.9	Silty medium to very coarse sand	Shells	283.5–286.5	10.52	8.86
289.9–297.8	Cored	Recovery from 289.9–297.8			
297.8–313.9	Silty medium to coarse sand	Shells	298.7–301.8 307.8–310.9	16.86 18.60	5.60 5.10
313.9–320.0	Silty fine sand with some very coarse grains	Minor shells			
320.0–338.3	Silty medium-coarse sand with some very coarse grains	Minor shells	329.2–332.2	11.48	8.01
338.3–341.1	Fine to medium sandy mud. Some gravel.	Minor shells			
341.1–344.4	Silty fine sand with some coarse grains.	Minor shells			
344.4–347.5	Muddy fine to medium sand with some gravel	Minor shells			
347.5–353.6	Fine sand with coarse grains.	Minor shells	347.5–350.5	26.16	3.68
353.6–364.0	Silty medium to coarse sand.	Minor shells			
364.0–373.1	Cored	Recovery from 364.8–373.1			

NO. 33 Cambridge, MD

INTERVAL (METERS)	FORMATION-AGE	DESCRIPTION	COMMENTS	SAMPLES SIEVED	RATIO COARSE/FINE	PERCENT FINES
0-15			No samples			
15.2-21.3		Silty grey clay				
21.3-33.5		Silty grey clay	Shells toward end of interval			
33.5-48.8		Fine sandy silt with pebbles	Decreasing sand over interval. Shells.			
48.8-115.8		Grey clayey silt	Shells			
115.8-121.9		Sandy grey silt				
121.9-137.2		Light grey fine-medium sand	Shells at beginning of interval. Some dark grey silt at center of interval			
137.2-158.5		Slightly granular grey silty fine sand	Silt increases over interval			
158.5-164.5		Fine sandy grey silt				
164.5-178.3		Cored	Recoveries from 170.7-172.5 and 176.1-178.3			
178.3-192.0		Fine black sandy grey silt with some medium-coarse sand	Clay at center of interval			
192.0-201.2		Granular light clayey grey silt with pebbles	Fine black sand. Shells			
201.2-207.3		Silty light grey clay				
207.3-216.4		Fine-coarse sandy dark grey silt	Shells			
216.4-222.5		Fine-coarse sandy grey silt with some clay				

222.5-237.7	Slightly pebbly coarse sandy red and grey clay	Sand decreasing over interval
237.7-253.0	Red clay	Some dark grey silt at center of interval. Coarse sand near end of interval
253.0-256.0	Slightly coarse sandy dark grey silty red clay	
256.0-298.7	Red clay	Increasing fine-medium sand up to 286.5. Some grey silt at end of interval
298.7-312.4	Cored	Recovery from 309.7-312.4

NO. 32A Crisfield, MD

INTERVAL (METERS)	FORMATION-AGE	DESCRIPTION	COMMENTS	SAMPLES SIEVED	RATIO COARSE/FINE	PERCENT FINES
0-12		Limy clay				
12.2-36.6		Clay, slightly silty				
36.6-61.0		Limy silty clay with gravel				
61.0-64.0		Slightly limy clay with minor gravel	Shells			
64.0-85.3		Clay with small amount of fine sand and gravel	Shells			
85.3-94.5		Fine sandy clay with gravel	Shells			
94.5-106.7		Silty fine sandy limy clay with gravel	Shells			
106.7-112.8		Silty fine sandy clay with gravel	Shells increasing in abundance throughout interval			
112.8-152.3		Muddy shell hash				
152.3-161.5		Limy clay	Abundant shell			
161.5-164.6		Limy clay	Shells			
164.6-173.7		Cored	Recovery from 164.9-172.5			
173.7-192.0		Silty fine sandy limy clay	Shells			
192.0-231.6		Limy muddy fine sand with minor gravel	Shells			
231.6-237.7		Limy silty fine sand	Shells			
237.7-262.1		Limy silty fine sand, slightly glauconitic	Shells			
262.1-268.2		Limy silty fine				

	glauconitic sand	
268.2-271.3	Limy silty fine sand, slightly glauconitic	Shells
271.3-277.4	Limy silty fine glauconitic sand	
277.4-310.4	Limy clay, slightly glauconitic	Shells
310.4-318.0	Cored	Recovery from 310.4-316.1

NO. 31C Salisbury, MD

INTERVAL (METERS)	FORMATION-AGE	DESCRIPTION	COMMENTS	SAMPLES SIEVED	RATIO COARSE/FINE	PERCENT FINES
0-36.6			No samples			
36.6-51.8		Medium-coarse sand		48.8-51.8	25.13	3.83
51.8-57.9		Medium-coarse glauconitic sand				
57.9-64.0		Medium-coarse sand				
64.0-91.4		Fine-medium sand	Shells	73.2-76.2	9.73	9.32
91.4-97.5		Silty fine sand	Shells	94.5-97.5	3.59	21.80
97.5-100.6		Very fine sandy silt	Shells			
100.6-112.8		Fine-medium sand	Shells	106.7-109.7	12.51	7.40
112.8-131.1		Fine-medium glauconitic sand	Shells	115.8-118.9	7.57	11.67
131.1-134.1		Medium-coarse sand		131.1-134.1	16.09	5.85
134.1-158.5		Fine-medium glauconitic sand	Shells	140.2-143.3	12.59	7.36
158.5-185.9		Fine-medium sand	Shells			
185.9-198.1		Fine-coarse sand	Shells	189.0-192.0	14.34	6.52
198.1-253.0		Fine-medium sand	Minor shells. Core recovery from 222.8-228.0	198.1-201.2 222.5-225.6 234.7-237.7 246.9-249.9	6.19 13.66 12.19 8.95	13.91 6.82 7.58 10.05
253.0-271.9		Slightly glauconitic fine sand		268.2-271.3	5.20	16.12
271.9-274.9		Sandy silt with friable sandstone fragments				
274.9-289.6		Silty fine sand with friable sandstone fragments		274.3-277.4 280.4-283.5	4.24 1.82	19.07 35.51
289.6-292.6		Silty sand		289.6-292.6	3.97	20.14

292.5–297.2	Clay		295.7–198.7	0.37	72.94
297.2–304.8	Cored	Recovery from 297.2–304.8			

NO. 30A Ocean City Airport, MD

INTERVAL (METERS)	FORMATION-AGE	DESCRIPTION	COMMENTS	SAMPLES SIEVED	RATIO COARSE/FINE	PERCENT FINES
0-54.9	Columbia Gr.		No samples			
54.9-61.0	Columbia Gr.	Very fine sandy silt				
61.0-64.0	Yorktown	Silty fine-medium sand				
64.0-67.1	Yorktown	Silty fine-medium sand				
67.1-70.1	Yorktown	Medium sand and granules				
70.1-73.2	Yorktown	Very well sorted medium quartz sand				
73.2-76.2	Yorktown	Medium quartz sand				
76.2-85.3	Yorktown	Very well sorted medium quartz sand				
85.3-88.4	Yorktown	Silty fine-medium sand and granules				
88.4-91.4	Yorktown	Silty fine-medium sand				
91.4-94.5	Yorktown	Silty fine sand				
94.5-97.5	Yorktown	Clayey-silty fine sand with granules				
97.5-100.6	Yorktown	Medium sand with granules				
100.6-103.6	Yorktown	Fine-medium sand with granules				
103.6-106.7	Yorktown	Fine-medium sand with granules				
106.7-115.8	Yorktown	Silty fine sand				
115.8-118.9	Yorktown	Silt				
118.9-121.9	Yorktown	Poorly sorted silty sand with granules	Minor shells			
121.9-124.9	Yorktown	Silty fine sand,				

		slightly micaceous	
124.9-128.0	Yorktown	Silty fine-medium sand	
128.0-131.1	Yorktown	Silty fine sand and granules	Shells
131.1-134.1	Yorktown	Fine sandy silt	
134.1-137.2	Yorktown	Silty fine sand with some coarse grains	
137.2-140.2	Yorktown	Silty fine sand	
140.2-143.3	Yorktown	Clay	
143.3-146.3	Yorktown	Poorly sorted silty sand	
146.3-149.3	Yorktown	Very fine sandy silt	
149.3-152.4	Yorktown	Silty very fine sand with granules	
152.4-163.1	Yorktown	No samples	
163.1-170.7		Cored	Recovery from 163.1-167.0
170.7-192.0	Yorktown	Silt	
192.0-195.1	Yorktown	No samples	
195.1-204.2	St. Mary's	Silt	
204.2-207.3	St. Mary's	Silt and coarse sand	
207.3-234.7	St. Mary's	Silt	Choptank Formation extends from 219.5-234.7
234.7-237.7	Calvert	Calcareous fine sandstone with silt, granules, and black shale	
237.7-240.8	Calvert	Calcareous fine sandstone with silt, granules, black shale	Shells
240.8-246.9	Calvert	Calcareous silty very fine sandstone	Shells

		with some coarser grains and black shale	
246.9-249.	Calvert	Calcareous silty-very fine sandstone with black shale	Shells
249.9-253.0	Calvert	Calcareous fine sandstone	Abundant shells
253.0-256.0	Calvert	Calcareous fine sandstone	Abundant shells
256.0-259.1	Calvert	Calcareous fine sandstone	Abundant shells
259.1-262.1	Calvert	Calcareous fine sandstone	Abundant shells
262.1-265.2	Calvert	Slightly calcareous fine-medium sand with silt and granules	Weakly cemented. Shells
265.2-271.3	Calvert	Calcareous fine sand with silt and heavy minerals. Some granules	Weakly cemented
271.3-274.3	Calvert	Calcareous fine sand with clay and silt	Weakly cemented. Shells
274.3-277.4	Calvert	Calcareous fine sand with silt	Weakly cemented
277.4-280.4	Calvert	Calcareous fine-medium sand with silt	Weakly cemented. Shells
280.4-283.5	Calvert	Calcareous fine sand with silt, granules, and heavy minerals	Weakly cemented
283.5-286.5	Calvert	Slightly calcareous fine sand and silt	Weakly cemented
286.5-289.6	Calvert	Calcareous fine-medium sand with heavy minerals	Weakly cemented
289.6-292.6	Calvert	Calcareous fine-	Weakly cemented

		medium sand with heavy minerals	
292.6-295.7	Calvert	Calcareous fine sand	Weakly cemented. Shells
295.7-298.7	Calvert	Calcareous fine sand	Weakly cemented. Shells
298.7-301.8	Calvert	Calcareous fine sand and granules	Weakly cemented. Shells
301.8-304.8	Calvert	Calcareous fine sand	Weakly cemented
304.8-307.2		No samples	
307.2-314.9		Cored	Recovery from 307.2-314.9

NO. 60 Hampton, VA VIRGINIA

INTERVAL (METERS)	FORMATION-AGE	DESCRIPTION	COMMENTS	SAMPLES SIEVED	RATIO COARSE/FINE	PERCENT FINES
0-6.1		Clay with some silt				
6.1-48.8		Fine sandy silt and some clay	Increasing amounts of shells			
48.8-88.4		Silty shell hash				
88.4-91.4		Silty shell hash with some clay				
91.4-134.1		Clayey silt	Shells			
134.1-161.5		Clay with some silt in upper part of interval				
161.5-164.6		Missing				
164.6-170.7		Clay with silt				
170.7-173.7		Fine sandy silt with some clay	Shells			
173.7-176.8		Clay with some silt				
176.8-179.8		Missing				
179.8-279.8		Limy clay with	Shells throughout			

		abundant in 259.1-265.2 and 295.7-301.8
279.8-287.4	Cored	Recovery from 279.8-283.5

NO. 59 Smith Point, VA

INTERVAL (METERS)	FORMATION-AGE	DESCRIPTION	COMMENTS	SAMPLES SIEVED	RATIO COARSE/FINE	PERCENT FINES
0-21.3		Fine-medium sand with minor silt. Silt fraction increases markedly in last 3 meters	Shells			
21.3-24.4		Silty fine sand with clay	Shells			
24.4-51.8		Fine sandy silty shell hash with clay				
51.8-100.6		Silty limy clay	Shells			
100.6-140.2		Slightly sandy limy clay with some silt	Shells			
140.2-145.4			No samples			
145.4-153.3		Cored	Recovery from 145.4-153.3			
153.3-161.5		Silty limy clay with fine sand. Minor granules.	Shells			
161.5-298.1		Granular fine black sandy silt with limy clay. Some pebbles near bottom third of interval	Minor shells			
298.1-305.7		Cored	Recovery from 298.1-299.9			

NO. 57 Atlantic, VA

INTERVAL (METERS)	FORMATION-AGE	DESCRIPTION	COMMENTS	SAMPLES SIEVED	RATIO COARSE/FINE	PERCENT FINES
0-3 5		Very fine-fine clean sand, well sorted.				
30.5-36.6		Clay, some fine sand and gravel	Shells			
36.6-39.6		Clay, sand and gravel	Shells			
39.6-45.7		Fine sandy clay	Shells			
45.7-85.3		Silty fine-coarse glauconitic sand and gravel	Abundant shells			
85.3-91.4		Silty fine glauconitic sand	Abundant shells			
91.4-97.5		Very coarse glauconitic sand	Abundant shells			
97.5-109.7		Medium-coarse glauconitic sand with minor clay	Abundant shells			
109.7-112.8		Clay with some fine glauconitic sand	Shells			
112.8-118.9		Muddy fine-coarse glauconitic sand	Abundant shells			
118.9-121.9		Clay with some coarse glauconitic sand and gravel	Shells			
121.9-131.0		Muddy fine glauconitic sand	Abundant shells			
131.0-140.2		Fine sandy clay	Abundant shells			
140.2-152.4		Silty fine sand, slightly glauconitic	Abundant shells			
152.4-161.5		Clay with some fine coarse sand	Shells			
161.5-170.7		Very fine sandy clay with some gravel	Shells			

170.7-175.3	Limy clay	Shells
175.3-189.0	Cored	Recovery from 175.3-184.4
189.0-201.2	Limy silt	Shells
201.2-204.2	Silty-very fine sandy limy clay	Abundant shells
204.2-219.5	Limy silt	Shells
219.5-222.5	Limy silty clay	Shells
222.5-243.8	Limy silty very fine sand	Abundant shells
243.8-259.1	Fine sandy silt. Sand increases in size and amount toward end of interval. Small pebbles decreasing in amount throughout the interval.	Decreasing amount of shells toward end of interval
259.1-274.3	Silty fine-medium sand	Decreasing size of shells thoughout interval
274.3-277.4	Fine sandy silt, slightly granular	Shells
277.4-289.6	Fine-medium silty sand. Minor silt at top of interval	Shells
289.6-298.7	Limy clay	Shells
298.7-307.8	Cored	No recovery.

NO. 56 Eastville, VA

INTERVAL (METERS)	FORMATION-AGE	DESCRIPTION	COMMENTS	SAMPLES SIEVED	RATIO COARSE/FINE	PERCENT FINES
0-15.2		Silt with increasing fine sand	Some lime at end of interval			
15.2-24.4		Gray clayey silt				
24.4-36.6		Clay with silt	Shells toward end of interval			
36.6-51.8		Fine sandy silt with granules and pebbles	Shells			
51.8-54.9		Clayey silt	Shells			
54.9-161.5		Fine sandy silt with some clay, granules and pebbles	Shells. Core recovery from 119.2-122.8			
161.5-295.7		Gray clay with some silt and minor amounts of fine sand	Shells			

NO. 55 Tasley, VA

INTERVAL (METERS)	FORMATION-AGE	DESCRIPTION	COMMENTS	SAMPLES SIEVED	RATIO COARSE/FINE	PERCENT FINES
0-3.0		Yellow silty sand				
3.0-9.1		Silty fine sandy clay				
9.1-27.4		Clean fine yellow sand				
27.4-30.5		Clean fine-medium grey sand	Shells			
30.5-33.5		Fine sand				
33.5-36.6		Fine-medium sand				
36.6-45.7		Muddy fine sand				
45,7-51.8		Silty fine sand	Shells			
51.8-54.9		Muddy fine sand				
54.9-100.6		Fine sand grading into medium sand from 85.3-91.4	Abundant shells			
100.6-146.3		Very coarse sand becoming silty fine to coarse near center of interval	Abundant shells			
146.3-161.5		Clay with fine sand and gravel	Minor shells			
161.5-166.1		Fine sandy clay with minor gravel	Shells			
166.1-173.7		Cored	Recovery from 166.1-172.8			
173.7-179.8		Limy clay with some fine sand and gravel	Shells			
179.8-189.0		Clay with sand and gravel	Shells			
189.0-195.1		Clay and fine sand				

195.1-222.5	Clay and gravel	Shells
222.5-283.5	Limy clay with varying amounts of gravel, fine sand, and silt throughout interval	Shells
283.5-297.5	Cored	Recoveries from 287.7-289.9 and 295.4-297.5

NO. 49 Withams, VA

INTERVAL (METERS)	FORMATION-AGE	DESCRIPTION	COMMENTS	SAMPLES SIEVED	RATIO COARSE/FINE	PERCENT FINES
0-21.3		Granules, pebbles, and cobbles of quartz and chert with shale and lignite	Angular to well rounded			
21.3-30.5		Muddy granules with some cobbles of quartz and chert. Shale				
30.5-143.3		More granules than above, but less cobbles	Shells			
143.3-155.4		Limy clay	Some gravel between 152.4-155.4. Shells			
155.4-179.8		Clay	Shells			
179.8-189.0		Limy clay	Shells			
189.0-201.2		Silty-very fine sand and limy clay	Shells			
201.2-204.2		Clay with some gravel	Shells			
204.2-207.3		Limy clay with some gravel	Shells			
207.3-220.1		Cored	Recovery from 211.5-220.1			
220.1-222.5		Limy clay	Shells			
222.5-234.7		Clay	Shells			
234.7-237.7			Missing			
237.7-259.1		Limy clay	Shells			
259.1-286.5		Fine sandy limy clay	Abundant shells			
286.5-295.7		Limy clay	Shells			
295.7-307.8			No samples			

307.8-317.3	Cored	Recovery from 308.8-317.3

NO. 48 Wattsville, VA

INTERVAL (METERS)	FORMATION-AGE	DESCRIPTION	COMMENTS	SAMPLES SIEVED	RATIO COARSE/FINE	PERCENT FINES
0-18.3		Fine to medium sand				
18.3-21.3		Fine-medium sand with some clay				
21.3-24.4		Fine-medium sand				
24.4-27.4		Fine-medium sand with some clay				
27.4-128.0		Fine-medium sand with some clay	Shells			
128.0-137.2		Fine-medium sandy clay	Shells			
137.2-143.3		Clayey fine-medium sand	Shells			
143.3-164.6		Fine sandy clay. Some silt at end of interval	Shells			
164.6-173.7		Silty fine sand with some clay				
173.7-228.6		Missing				
228.6-283.5		Fine sandy clay with silt	Shells throughout but more abundant at mid interval			
283.5-295.7		Fine sand with some clay	Shells			

NO. 29 Wallops Island, VA

INTERVAL (METERS)	FORMATION-AGE	DESCRIOION	COMMENTS	SAMPLES SIEVED	RATIO COARSE/FINE	PERCENT FINES
0-6..		Sand				
6.1-12.2		Clay				
12.2-30.5		Fine sand	Shells	30.5-31.6	2.47	28.8
30.5-33.5		Silty fine sand	Minor shells			
33.5-36.6		Fine sandy silt				
36.6-42.7		Clay	Shells			
42.7-57.9		Mostly silt with some clay and gravel	Shells	48.8-51.8	0.56	64.0
57.9-64.0		Clay with fine sand	Abundant shells			
64.0-73.2		Fine sand with some silt	Abundant shells	79.2-82.3	5.23	16.1
73.2-97.5		Silty fine-medium sand	Abundant shells			
97.5-118.9		Silty clay	Shells	97.5-100.6 109.7-112.8	1.33 1.36	42.9 42.4
118.9-134.1		Clay	Shells	124.9-128.0	.13	88.6
134.1-155.4		Clay	Minor shells	134.1-137.2 149.3-152.4	.19 .16	84.3 86.4
155.4-158.5		Clay	Abundant shells	155.4-158.5	1.62	38.2
158.5-164.6		Clay	Shells	158.5-161.6	.23	81.3
164.6-167.7			Missing			
167.7-182.9		Cored	Recovery from 178.0-182.9			
182.9-198.1		Clay	Shells. Minor shells from 195.1-198.1	195.1-198.1	.28	78.1
198.1-201.2		Clay with chalk	Shells			
201.2-207.3		Clay	Shells			
207.3-210.3		Clay	Shells	207.3-210.3	.56	64.2

210.3–213.4	Clay	Abundant shells			
213.4–216.4	Clay	Minor shells			
216.4–219.5	Slightly fine sandy clay	Minor shells			
219.5–231.6	Clay	Minor shells	219.5–222.5	1.68	37.3
231.6–234.7	Silty fine sandy gravel		231.6–234.7	.88	53.1
234.7–246.9	Clay				
246.9–249.9		No samples			
249.9–253.0	Clay				
253.0–265.2	Clay	Shells. No shells from 256.0–259.1	259.1–262.1	.69	59.2
265.2–268.2	Clay	Minor shells			
268.2–286.5	Clay		283.5–286.5	.92	52.0
286.5–289.6	Clay	Minor shells			
289.6–298.7	Clay		295.7–298.7	.22	81.8
298.7–304.8	Cored	Recovery from 299.3–304.8			

NO. 28A Cheriton, VA

INTERVAL (METERS)	FORMATION-AGE	DESCRIPTION	COMMENTS	SAMPLES SIEVED	RATIO COARSE/FINE	PERCENT FINES
0-33.5		No samples.	Surface casing set by Mayhew 1000			
33.5-36.6	Yorktown Miocene	Very fine sandy silt	Shells			
36.6-39.6	Yorktown Miocene	Silt	Shells			
39.6-42.7	Yorktown Miocene	Very fine sandy silt	Shells			
42.7-45.7	Yorktown Miocene	Very fine sandy silt, slightly granular	Shells			
45.7-48.8	Yorktown Miocene	Very fine sandy silt with some coarse sand	Shells			
48.8-54.9			Missing			
54.9-64.0	St. Mary's Miocene	Very fine sandy silt	Shells			
64.0-67.1	St. Mary's Miocene	Slightly granular very fine sandy silt	Shells			
67.1-73.2	St. Mary's Miocene	Silty fine sand	Shells			
73.2-76.2	St. Mary's Miocene	Very fine sandy silt, slightly granular. Some lignite	Shells			
76.2-79.2	St. Mary's	Very fine sandy silt, slightly granular	Shells			
79.2-82.3	St. Mary's	Silty very fine sand	Shells			
82.3-97.5	St. Mary's	Very fine sandy silt	Shells throughout. (91.4-94.5-slightly granular).			
97.5-106.7	Choptank	Very fine sandy				

		silt	
106.7-109.7	Choptank	Silt	Shells
109.7-115.8	Choptank	Very fine sandy silt	Shells
115.8-125.0	Choptank	Silt and clay	Shells
125.0-143.3	Choptank	Silty clay	Shells throughout. (140.2-143.3-slightly shelly)
143.3-146.3	Calvert	Silty clay with limestone fragments	Shells
146.3-204.2	Calvert	Silt and clay	146.3-152.4 slightly shelly 152.4-204.2 no shells
204.2-207.3	Calvert	Clay with limestone fragments	
207.3-213.4	Calvert	Clay and silt	
213.4-222.5	Calvert	Cored	Recovery from 212.1-221.0
222.5-280.4	Calvert	Clay and silt	No shells throughout except for: 240.8-243.8- slightly shelly and 243.8-246.9-shells
280.4-295.7	Chickahominy	Clay and silt	
295.7-304.8		Cored	Recovery from 297.2-304.8

NO. 27 Hampton, VA

INTERVAL (METERS)	FORMATION-AGE	DESCRIPTION	COMMENTS	SAMPLES SIEVED	RATIO COARSE/FINE	PERCENT FINES
0-3.0	Columbia Gr. Pliocene	Slightly granular fine-medium sand	Minor shells			
3.0-6.1	Columbia Gr. Pliocene	Fine sand	Minor shells			
6.1-9.1	Columbia Gr. Pliocene	Slightly granular fine sand	Minor shells			
9.1-12.2	Columbia Gr. Pliocene	Large pebbly fine to medium sand	Minor shells			
12.2-15.2	Yorktown Miocene	Fine sand	Shells			
15.2-18.3	Yorktown Miocene	Slightly granular silty fine sand	Shells			
18.3-24.4	Yorktown Miocene	Fine-medium sand with heavy minerals	Minor shells			
24.4-27.4	Yorktown Miocene	Pebbly, granular fine sand. Some rounded sandstone fragments	Shells			
27.4-30.5	Yorktown Miocene	Silty fine sand. Some coarse grains.	Shells			
30.5-33.5	Yorktown Miocene	Fine sand with heavy minerals	Shells			
33.5-36.6	Yorktown Miocene	Silty very fine to fine sand with heavy minerals	Shells			
36.6-61.0	Yorktown Miocene	Very fine to fine sand with heavy minerals	Shells			
61.0-64.0	Yorktown Miocene	Slightly micaceous very fine to fine sand with heavy minerals	Abundant shells			
64.0-94.5	Yorktown Miocene	Very fine to fine sand with heavy minerals	Shells			

94.5-128.0	Calvert Miocene	Very fine to fine sand with heavy minerals	Shells
128.0-131.1	Calvert Miocene	Very fine to fine sand	Shells
131.1-134.1	Mattaponi U.Cretaceous	Very fine to fine sand	Abundant shells
134.1-161.5	Mattaponi U.Cretaceous	Very fine to fine sandy shell hash	
161.5-179.8	Mattaponi U.Cretaceous	Silty very fine sandy shell hash	
179.8-182.9	Mattaponi U.Cretaceous	Glauconitic silty very fine sand	Shells
182.9-189.0	Mattaponi U.Cretaceous	Glauconitic fine to medium sand	Shells
189.0-192.0	Mattaponi U.Cretaceous	Glauconitic silty fine sand	Shells
192.0-198.1	Mattaponi U.Cretaceous	Glauconitic silty fine sand. Some coarse sand.	Shells
198.1-201.2	Mattaponi U.Cretaceous	Glauconitic fine to coarse sand	Minor shells
201.2-204.2	Mattaponi U.Cretaceous	Glauconitic coarse sand	Minor shells
204.2-207.3	Mattaponi U.Cretaceous	Glauconitic medium to coarse sand	Minor shells
207.3-210.3	Mattaponi U.Cretaceous	Glauconitic fine to coarse sand	Minor shells
210.3-216.4	Transitional Bed	Glauconitic fine to coarse sand	Shells
216.4-219.5	Transitional Bed	Glauconitic fine to medium sand	Minor shells
219.5-225.6	Transitional Bed	Glauconitic fine to coarse sand	Minor shells
225.6-228.6	Transitional Bed	Glauconitic fine to coarse sand. Some sandstone fragments.	Minor shells

228.6-234.7	Transitional Bed	Same as 225.6-228.6, but no sandstone fragments	Minor shells
234.7-240.8	Transitional Bed	Glauconitic fine to medium sand	Minor shells
240.8-243.8	Transitional Bed	Silty fine to coarse sand	Shells
243.8-249.9	Patuxent	Glauconitic fine to medium sand	Minor shells
249.9-253.0	Patuxent	Glauconitic silty fine sand	Minor shells
253.0-256.0	Patuxent	Glauconitic silty fine to coarse sand	Minor shells
256.0-259.1	Patuxent	Glauconitic fine sandy silt	Minor shells
259.1-262.1	Patuxent	Fine sandy silt	Minor shells
262.1-265.2	Patuxent	Glauconitic silty fine to coarse sand	Minor shells
265.2-268.2	Patuxent	Fine sandy silt	Minor shells
268.2-271.3	Patuxent	Silty fine to coarse sand	Minor shells
271.3-274.3	Patuxent	Glauconitic silty fine sand	Minor shells
274.3-277.4	Patuxent	Glauconitic fine sandy silt	Minor shells
277.4-280.4	Patuxent	Silty fine to coarse sand	Minor shells
280.4-286.5	Patuxent	Glauconitic silty fine to medium sand	Minor shells
286.5-289.6	Patuxent	Glauconitic silty fine to coarse sand with some pebbles and granules	Shells
289.6-292.6	Patuxent	Pebbly, fine sandy silt	Minor shells

292.6-298.4	Patuxent	Slightly granular silt	Abundant shells
298.4-307.5		Cored	Recovery of 4.6 meters within the interval 298.4-307.5

NO. 26 Isle of Wight, VA

INTERVAL (METERS)	FORMATION-AGE	DESCRIPTION	COMMENTS	SAMPLES SIEVED	RATIO COARSE/FINE	PERCENT FINES
0-3.0	Columbia Gr.	Silty fine sand				
3.0-9.1	Columbia Gr.	Fine sandy silt				
9.1-12.2	Yorktown	Silty fine sand				
12.2-15.2	Yorktown	Silty fine to medium sand				
15.2-18.3	Yorktown	Silty fine sand				
18.3-27.4	Yorktown	Silty very fine sand				
27.4-33.5	Yorktown	Silty fine sand	Minor shells			
33.5-36.6	Yorktown	Slightly pebbly silty fine sand				
36.6-42.7	Yorktown	Fine sand	Shells			
42.7-48.8	Yorktown	Fine sand	Minor shells			
48.8-51.8	Yorktown	Slightly granular silty fine sand	Minor shells			
51.8-54.9	Yorktown	Fine sand	Minor shells			
54.9-64.0	Yorktown	Fine sand	Abundant shells			
64.0-67.1	Calvert	Fine to medium sand	Abundant shells			
67.1-70.1	Calvert	Fine sand	Abundant shells			
70.1-75.0	Calvert	Fine sand	Shells			
75.0-82.6	Calvert	Cored	Core recovery from 79.6-82.3			
85.3-91.4	Calvert	Medium, slightly calcareous sand				
91.4-94.5	Calvert	Medium to coarse sand, slightly glauconitic				
94.5-100.6	Nanjemoy	Glauconitic sand				
100.6-106.7	Nanjemoy	Greensand, slightly calcareous				

106.7-121.9	Mattoponi	Greensand	
121.9-124.9	Mattoponi	Glauconitic sand	
124.9-128.0	Mattoponi	Silty fine sand	Minor shells
128.0-134.1	Mattoponi	Silty fine to medium sand, slightly glauconitic	Minor shells
134.1-137.2	Patuxent	Medium sand, slightly glauconitic	
137.2-149.3	Patuxent	Medium coarse sand	
149.3-152.4	Patuxent	Fine to medium sand, slightly glauconitic	
152.4-170.7	Patuxent	Fine to medium sand	
170.7-173.7	Patuxent	Silty fine sand	
173.7-185.9	Patuxent	Medium sand	
185.9-192.0	Patuxent	Medium sand	Shells
192.0-195.1	Patuxent	Silty fine sand	
195.1-198.1	Patuxent	Silty fine-medium sand	
198.1-201.2	Patuxent	Silty fine sand	
201.2-210.3	Patuxent	Coarse sand	
210.3-213.4	Patuxent	Very coarse sand	
213.4-219.5	Patuxent	Silty very coarse sand	
219.5-225.6	Patuxent	Granular very coarse sand with silt, slightly calcareous	
225.6-231.6	Patuxent	Very coarse sandy granules, calcareous	Shells
231.6-234.7	Patuxent	Granular silty fine sand	Shells
234.7-237.7	Patuxent	Slightly granular silty fine sand	
237.7-243.8	Patuxent	Granular silty fine	

		sand	
243.8-249.9	Patuxent	Slightly granular silty fine sand	
249.9-253.0	Patuxent	Silty fine-medium sand	
253.0-256.0	Patuxent	Silty granular medium sand	
256.0-268.2	Patuxent	Fine sandy silt	
268.2-277.4	Patuxent	Silty fine-medium sand	
277.4-280.4	Patuxent	Silt	
280.4-283.5	Patuxent	Medium sandy silt	
283.5-286.5	Patuxent	Granular medium-coarse sand with minor silt	
286.5-292.6	Patuxent	Silty medium-coarse sand	Shells
292.6-295.7	Patuxent	Fine-medium sand	
295.7-304.8	Patuxent	Cored	Recoveries from 296.0-296.6 and 298.4-301.8

NO. 25 Portsmouth, VA

INTERVAL (METERS)	FORMATION-AGE	DESCRIPTION	COMMENTS	SAMPLES SIEVED	RATIO COARSE/FINE	PERCENT FINES
3.0-6.1		Fine to medium light sand				
6.1-27.4		Silty light sand				
27.4-30.5		Fine to medium grey sand				
30.5-39.6		Silty light sand				
39.6-57.9		Fine to medium sand				
57.9-61.0		Fine sandy silt				
61.0-64.0		Silty-fine light sand				
64.0-73.2		Fine to medium light sand				
73.2-88.4		Very fine to medium sand				
88.4-94.5		Silty, very fine light sand				
94.5-97.5		Very fine to fine grey sand				
97.5-103.6		Sandy grey silt				
103.6-112.8		Silty fine-medium light sand				
112.8-115.8		Fine-medium light sand				
115.8-118.9		Fine grey sand				
118.9-131.1		Fine-medium light sand				
131.1-134.1		Light muddy silt				
134.1-140.2		Very fine to fine light sand				
140.2-182.9		Fine to medium glauconitic sand				

182.9-192.0	Fine to medium grey sand	
192.0-210.3	Fine to medium glauconitic sand	
210.3-216.4	Fine to medium sandy silt	
216.4-219.5	Fine to medium light sand	
219.5-222.5	Sandy silt	
222.5-228.6	Fine to medium light sand	
228.6-231.6	Light sandy silt	
231.6-271.3	Fine to medium glauconitic sand	
271.3-295.7	Medium to coarse glauconitic sand	
295.7-310.9	Two coring attempts.	Recoveries from 297.2-298.1 and 299.3-302.7

NO. 25A Portsmouth, VA

INTERVAL (METERS)	FORMATION-AGE	DESCRIPTION	COMMENTS	SAMPLES SIEVED	RATIO COARSE/FINE	PERCENT FINES
0-91.4			No samples			
91.4-131.1		Clay				
131.1-182.9		Limy glauconitic clay	Minor shells			
182.9-189.0		Glauconitic clay	Minor shells			
189.0-192.0		Fine sand and limy clay	Shells			
192.0-216.4		Limy glauconitic clay	Shells			
216.4-277.4		Fine sand and limy mud with some gravel.	Minor shells			
277.4-280.0		Slightly granular glauconitic limy clay				
280.0-286.5		Limy mudyy fine to medium glauconitic sand with some gravel.				
286.5-289.6		Clay				
289.6-291.6		Limy muddy fine to medium sand with some gravel	Minor shells			
291.6-301.8		Clayey fine to medium sand with some gravel	Minor shells			
301.8-307.8		Fine sandy limy clay with some gravel	Minor shells			
307.8-310.8		Limy sandy clay with some gravel.				
310.9-317.0		Fine sandy clay				
317.0-323.1		Limy clay with some fine glauconitic sand and gravel				
323.1-329.2		Slightly limy clay				

	and glauconitic fine sand	
329.2–332.2	Limy clay	
332.2–368.8	Slightly limy fine sandy clay	
368.8–374.9	Fine sandy limy clay	
374.9–378.0	Silty limy clay	Minor shells
378.0–381.0	Fine sandy limy clay	Minor shells
381.0–387.1	Slightly limy fine sandy clay with some gravel	
387.1–396.2	Limy clay	
396.2–405.4	Silty fine sandy clay with some gravel	399.3–402.3 Missing
405.4–408.4	Glauconitic clay	Shells
408.4–411.5	Limy clayey fine sand	Minor shells
411.5–423.7	Silty clay with some gravel	420.6–423.7 Missing
423.7–426.7	Muddy fine to very coarse sand	
426.7–435.9	Limy clay	
435.9–438.9	Glauconitic limy clay	
438.9–448.1	Slightly glauconitic limy clay	
448.1–457.2	Muddy fine to coarse sand	
457.2–475.5	Silty fine sand with some gravel	
475.5–478.5	Limy clay	
478.5–481.6	Clay	
481.6–493.8	Fine to medium	

	sandy limy clay	
493.8-496.8		No samples
496.8-499.9	Muddy fine to medium sand with some gravel.	Shells
499.9-502.9	Fine sandy limy clay	Minor shells
502.9-519.5	Muddy fine to medium sand with some gravel	Minor shells
519.5-527.3	Clay	Shells
527.3-563.8	Muddy fine sand with some gravel	
563.8-566.9	Silt	
566.9-569.9	Muddy fine sand with some gravel	

NO. 24 Norfolk, VA

INTERVAL (FEET)	FORMATION-AGE	DESCRIPTION	COMMENTS	SAMPLES SIEVED	RATIO COARSE/FINE	PERCENT FINES
0-3.0		Fine-medium sand				
3.0-6.1		Silt with minute amount of fine sand				
6.1-42.7		Fine-medium sand	Minor shells			
42.7-51.8		Brown silty fine-medium sand				
51.8-94.5		Fine-medium sand with grey silt	Shells			
94.5-137.2		Grey silty fine-medium sand	Shells. Shell hash at 103.6-106.7			
137.2-140.2		Silty clay	Shells			
140.2-143.2			No samples			
143.2-146.3		Silty clay	Shells			
146.3-152.4		Slightly silty fine sand				
152.4-161.5		Fine sandy silt with clay				
161.5-170.7		Cored	Recovery from 163.1-170.7			
170.7-179.8		Fine sandy silt with clay	Shells			
179.8-274.3		Clay with some silt	Shells			
274.3-280.4		Fine sandy silty clay				
280.4-295.7		Silty clay with some fine sand				
295.7-306.3			No samples			
306.3-315.5		Cored	Recovery from 306.3-315.5			

NO. 25 Oceana Naval Air Station, VA

INTERVAL (METERS)	FORMATION-AGE	DESCRIPTION	COMMENTS	SAMPLES SIEVED	RATIO COARSE/FINE	PERCENT FINES
0-118.9		Slightly silty fine to medium sand	Shells. Silt from 27.4-118.9. Fine-coarse grains from 85.3-106.7			
118.9-121.9		Fine-coarse sand with some silt. Shell hash.				
121.9-134.1		Silty fine-medium sand. Shell hash				
134.1-158.5		Fine sandy silt	Shells			
158.5-170.7		Silty fine-medium sand	Shells			
170.7-173.7		Slightly fine sandy mud	Shells			
173.7-181.7		Fine sandy silt with some clay	Shells			
181.7-189.3		Cored	Recovery from 181.7-185.6			
189.3-237.7		Fine sandy clayey silt with some granules	Minor shells			
237.7-249.9			No samples			
249.9-295.0		Fine-medium silty sand with some clay	Minor shells			
295.0-302.7		Cored	Recovery from 295.0-302.7			

NO. 22 Creeds, VA

INTERVAL (METERS)	FORMATION-AGE	DESCRIPTION	COMMENTS	SAMPLES SIEVED	RATIO COARSE/FINE	PERCENT FINES
0-12.2		Grey and tan silty fine sand with pebbles. Silt increases toward end of interval	Minor shells at end of interval			
12.2-27.4		Fine-medium sand with some silt in mid-interval	Minor shells at end of interval			
27.4-30.5		Fine sandy grey and tan mud with some pebbles				
30.5-33.5			No samples			
33.5-39.6		Fine sandy grey and tan clay with some pebbles and silt				
39.6-42.7		Shell hash with granules and coarse sand				
42.7-76.2		Fine sandy silty clay with some pebbles	Minor shells			
76.2-79.2		Silty shell hash with fine black sand				
79.2-82.3		Sandy silty shell hash				
82.3-88.4		Silty shell hash with small amount of fine black sand				
88.4-106.7		Fine sandy silt. Shell hash and clay increase toward end of interval				
106.7-118.9		Silty fine-medium sand. Shell hash.				
118.9-131.1		Fine sandy silt	Sand decreases over interval. More clay			

		than silt at end of interval
131.1-134.1	Silty fine sandy shell hash	
134.1-146.3	Fine sandy silt	Minor shells. Sand increases throughout interval
146.3-149.4	Silty fine-medium sand	
149.4-198.1	Fine sandy clayey silt with some gravel	Minor shells
198.1-204.8	Cored	Recovery from 198.4-204.8
204.8-210.3	Slightly fine sandy clayey silt. Slightly gravelly	Shells
210.3-213.4		No samples
213.4-231.6	Fine sandy clayey silt, slightly gravelly	Minor shells. More clayey toward end of interval
231.6-249.9	Fine sandy mud	
249.9-277.4	Silty fine black sand with some granules	Minor shells. Silt increases over interval
277.4-292.6	Fine black sandy silt with some granules	Becoming less sandy and more clayey over interval
292.6-294.1	Clayey silt with fine black sand	
294.1-301.7	Cored	Recovery from 294.1-298.1

NO. 21 Bellcross, NC NORTH CAROLINA

INTERVAL (METERS)	FORMATION-AGE	DESCRIPTION	COMMENTS	SAMPLES SIEVED	RATIO COARSE/FINES	PERCENT FINES
0-24.4			No samples			
24.4-39.6		Fine sand	Shells			

39.6-79.2	Fine-medium sand	Light brown silt in 73.2-76.2
79.2-103.6	Fine-medium sand and shell hash	
103.6-125.0	Fine-coarse sand and minor amounts of silt	Shells
125.0-131.1	Fine-coarse sandy silt and minor amounts of clay	Shells
131.1-134.1	Silty clay with fine sand	Shells
134.1-137.2	Silty fine-medium sand and minor amounts of clay	Shells
137.2-140.2	Clay	Shells
140.2-146.3	Silty fine-medium sand and minor amounts of clay	Shells
146.3-149.4	Fine-coarse sand and some silt	Shells
149.4-155.4	Silty clay and minor amounts of fine sand	Shells
155.4-161.5	Fine-coarse sand and shell hash with minor amounts of silt	
161.5-164.6	Clayey silt and some sand	Shells
164.6-167.6	Silty fine-coarse sand and shell hash	
167.6-170.7	Silt with some clay and fine sand	Shells
170.7-179.8	Cored	Recovery from 172.8-178.9
179.8-182.9	Fine-coarse sandy silt	Shells

182.9–189.0	Fine sandy silt and limy clay	Shells
189.0–192.0	Silty fine–medium sand	Shells
192.0–195.1	Silty limy clay	Minor shells
195.1–213.4	Fine sandy silty limy clay	Sand increases in size and amount over the interval. Shells
213.4–216.4	Fine–medium sand	Shells
216.4–228.6	Silty fine–medium sand and minor amounts of clay	Silt increases over interval. Shells
228.6–231.6	Fine–medium sandy silt and some clay	Shells
231.6–246.9	Silty fine–medium sand and some clay	Shells
246.9–249.9	Silty limy clay with minor amounts of fine sand	Shells
249.9–289.6	Fine sandy limy clayey silt	Sand increases over the interval. Shells
289.6–295.7	Limy clayey silt and fine sand	Shells
295.7–304.8	Cored	Recovery from 299.9–304.5

NO. 20 Elizabeth City State College, NC

INTERVAL (METERS)	FORMATION-AGE	DESCRIPTION	COMMENTS	SAMPLES SIEVED	RATIO COARSE/FINES	PERCENT FINES
0-15.2		Fine-medium sand	Minor shells at end of interval			
15.2-18.3		Fine-medium sand	Shells			
18.3-42.7		Fine-medium sand				
42.7-45.7		Fine-medium sand and silt	Minor shells			
45.7-82.3		Fine-medium sand and some silt	Shells			
82.3-85.3		Silty shell hash with some fine sand				
85.3-128.0		Fine-coarse sand with silt	Decreasing coarse grains over interval. Shells			
128.0-134.1		Fine-coarse sand	Minor shells			
134.1-143.3		Cored	Recovery from 135.3-141.3			
143.3-152.4		Fine-medium sand	Shell fragments increasing in amount over interval			
152.4-158.5		Fine sand	Minor shells			
158.5-170.7		Silty fine sand with some granules and limy clay	Shells			
170.7-204.2		Limy clayey silt with fine sand	Shells			
204.2-219.5		Fine sandy silt and some limy clay	Shells			
219.5-222.5		Fine sand with silt	Minor shells			
222.5-228.6		Fine-medium sand and some limy clay	Shells			
228.6-271.3		Silty fine-medium sand and minor	Shells			

	amounts of limy clay and granules	
271.3-277.4	Limy clayey silt with fine sand	Shells
277.4-280.4	Silty limy clay with fine sand	Shells
280.4-298.7	Silty fine-medium sand and minor amounts of limy clay	Shells
298.7-307.8	Cored	Recovery from 300.8-303.9

NO. 19 Stumpy Point, NC

INTERVAL (METERS)	FORMATION-AGE	DESCRIPTION	COMMENTS	SAMPLES SIEVED	RATIO COARSE/FINES	PERCENT FINES
0-12.2	Post Miocene	Medium grain sand	Shells			
12.2-18.3	Post Miocene	Fine-medium white sand with minor amount of silt	Shells			
18.3-33.5	Post Miocene	Silty clay with some fine sand	Abundant shells			
33.5-48.8	Late Miocene	Clay with minor amounts of fine sand and silt	Shells			
48.8-61.0	Late Miocene	Sandy clay	Shells			
61.0-64.0			No samples			
64.0-91.4	Late Miocene	Silty clay. Glauconitic	Abundant shells			
91.4-109.7	Late Miocene	Fine-medium white sand with minor silt and clay	Shells			
109.7-125.0	Late Miocene	Sandy mud and heavy minerals	Shells			
125.0-131.1	Late Miocene	Clayey, silty sand	Shells			
131.1-170.7	Late Miocene	Sandy mud	Shells			
170.7-195.1	Late Miocene	Sandy clay	Shells			
195.1-198.1	Mid. Miocene	Green-gray clay with minor fine sand and silt	Shells			
198.1-202.7		Cored	Recovery from 198.1-202.7			
202.7-243.8	Mid. Miocene	Gray sandy clay	Shells			
243.8-283.5	Mid. Miocene	Green clay	Minor shells			
283.5-289.6	Mid. Miocene	Sandy green clay	Shells			
289.6-296.3		Cored	Recovery from 289.6-296.3			

NO. 18 Englehard, NC

INTERVAL (METERS)	FORMATION-AGE	DESCRIPTION	COMMENTS	SAMPLES SIEVED	RATIO COARSE/FINES	PERCENT FINES
0-15.2	Post Miocene	White clayey sand	Shells			
15.2-36.6	Post Miocene	Gray sandy clay	Shells			
36.6-45.7	Post Miocene	Dark gray sandy clay with granules	Shells			
45.7-48.8	Post Miocene	Clayey fine sand	Shells			
48.8-54.9	Post Miocene	Clayey sand	Shells			
54.9-76.2	Post Miocene	Sandy silty clay	Shells			
76.2-82.3	Late Miocene	Limy clay	Shells			
82.3-94.5	Late Miocene	Sandy shell limestone				
94.5-97.5	Late Miocene	Sandy clay	Shells			
97.5-125.0	Late Miocene	Sandy shell limestone				
125.0-128.0	Late Miocene	Sandy clay	Shells			
128.0-131.1	Late Miocene	Medium-coarse sandy limy clay	Shells			
131.1-134.1	Late Miocene	Medium sandy clay	Shells			
134.1-137.2	Late Miocene	Medium coarse sand	Shells			
137.2-146.3	Late Miocene	Sandy silty clay with phosphate	Shells			
146.3-158.5	Middle Miocene	Fine sandy limy clay	Shells			
158.5-207.3	Middle Miocene	Slightly sandy clay	Shells			
207.3-216.4		Cored	Recovery from 207.3-216.4			
216.4-234.7	Oligocene	Slightly sandy clay with phosphate	Shells			
234.7-249.9	Oligocene	Clay with minor fine sand	Shells			

249.9-262.1	Claiborne	Fine-medium sandy clay with phosphate	Shells
262.1-286.5	Claiborne	Sandy shell lime-stone with phosphate	
286.5-298.7	Claiborne	Slightly sandy silty clay	Shells
298.7-307.8		Cored	Recovery from 299.2-307.8

NO. 17 Beaufort, NC

INTERVAL (METERS)	FORMATION-AGE	DESCRIPTION	COMMENTS	SAMPLES SIEVED	RATIO COARSE/FINES	PERCENT FINES
0-15.2		Fine-medium sand	Shells			
15.2-39.6		Fine sand	Shells			
39.6-85.3		Very fine to fine sand, shell hash	57.7-61.0 Clay 70.1-73.2 contains green clay 76.2-82.3 Brown clay			
85.3-91.4		Brown silty clay				
91.4-94.5		Fine sandy brown clay	Minor shells			
94.5-97.5		Brown clay	Minor shells			
97.5-103.6		Brown clay	Minor shells			
103.6-106.7		Fine-medium sandy clay				
106.7-137.2		Fine sandy tan clay	Abundant shells. Limestone fragments			
137.2-140.2		Tan clay	Shells			
140.2-158.5		Muddy fine sand with some gravel	Abundant shells			
158.5-161.5		Light tan clay				
161.5-192.0		Muddy very fine-fine limy sand with some gravel	Shells 161.5-176.8 Brown clay included 182.9-185.9 Brown clay included			
192.0-201.2		Cored	Recovery from 194.2-199.6			
201.2-265.2		Muddy very fine-fine limy sand with minor gravel	Abundant shells			
265.2-288.0		Very fine sandy tan limy clay				
288.0-297.2		Cored	Recovery from 288.0-289.0			

NO. 16 Cherry Point Marine Base, NC

INTERVAL (METERS)	FORMATION-AGE	DESCRIPTION	COMMENTS	SAMPLES SIEVED	RATIO COARSE/FINES	PERCENT FINES
0-39.6		Fine-medium sand with some silt and clay				
39.6-94.5		Fine-medium sand with fine shell hash				
94.5-134.1		Medium-coarse sand and shell hash				
134.1-161.5		Fine-medium sand	Shells			
161.5-185.9		Fine sand				
185.9-195.1		Medium-coarse sand	Minor shells			
195.1-259.1		Fine sand becoming fine-medium at mid-interval	Minor shells			
259.1-283.5		Fine-medium sand, slightly silty	Minor shells			
283.5-292.6		Fine-medium sand	Shells			
292.6-301.4		Cored	Recovery from 301.1-301.4			

NO. Kinston, NC

INTERVAL (METERS)	FORMATION-AGE	DESCRIPTION	COMMENTS	SAMPLES SIEVED	RATIO COARSE/FINES	PERCENT FINES
0-6.1		Fine sandy clay	Sand decreases over interval			
6.1-82.3		Fine-medium sand with minor amounts of silt	Some clay between 36.6-39.6. Minor shells			
82.3-89.9		Cored	Recovery from 82.3-86.0			
89.9-118.9		Fine-medium sand, some silt and pebble size coquina fragments	Shells			
118.9-121.9		Silty fine-medium sand				
121.9-125.0		Fine-medium sand				
125.0-137.2		Fine-coarse sand with increasing silt				
137.2-158.5		Fine-medium sand with some silt and coarse grains	Shells			
158.5-167.6		Silty fine-medium sand with some coarse grains	Shells			
167.6-173.7		Fine-medium sand with some silt and coarse grains	Shells			
173.7-175.9		Silty fine-medium sand with some red clay and coquina fragments	Shells			
175.9-183.5		Cored	Recovery from 175.9-178.3			
183.5-198.1		Fine-medium sand and shell hash with coquina fragments				
198.1-219.5		Fine sandy red and grey clay with fine shell hash and some				

	silt	
219.5-222.5		No samples
222.5-225.6	Silty fine-coarse sand. Coquina fragments	Shells
225.6-228.6	Red clay with fine sand, granules, and pebbles	

NO. Camp Lejeune, NC

INTERVAL (METERS)	FORMATION-AGE	DESCRIPTION	COMMENTS	SAMPLES SIEVED	RATIO COARSE/FINES	PERCENT FINES
0-54.9		Well sorted fine clean white sand				
54.9-243.8		Very fine-fine grey sand	Shells. Heavy minerals. Yellow clay at end of interval			
243.8-240.8		Grey and yellow silt with some very fine sand				
240.8-246.9		Silty very fine sand. Fine shell hash				
246.9-262.1		Yellow silt to very fine sand				
262.1-265.2		Limy clay				
265.2-268.2		Yellow silt to very fine sand				
268.2-274.3		Very fine sand. Fine shell hash				
274.3-295.7		Yellow silt to very fine sand				
295.7-304.8		Limy mud				
304.8-313.9		Limy clay and silt				
313.9-317.0		Limy silt				
317.0-320.0		Limy silty clay				
320.0-332.2		Limy silty very fine sand				
332.2-356.6		Limy very fine sandy clay	Some white clay throughout interval			
356.6-362.7		Yellow silty very fine sand				
362.7-369.1		Cored	Recovery from			

369.1-378.0	Yellow silty very fine sand
378.0-387.1	Silty very-fine sand and limy clay
387.1-410.0	Yellow silt
410.0-414.5	Limy fine sandy clay

NO. 15A Sneads Ferry, NC

INTERVAL (METERS)	FORMATION-AGE	DESCRIPTION	COMMENTS	SAMPLES SIEVED	RATIO COARSE/FINES	PERCENT FINES
0-18.3		Clay with some silt				
18.3-79.2		Silty shell hash with some clay, granules and pebbles				
79.2-85.3		Silty clay with some granules				
85.3-201.2		Silty shell hash with fine-coarse sand and minor amounts of clay, granules and pebbles	Clay content increases throughout these intervals: 103.6-106.7 115.8-118.9 155.4-158.5 176.8-179.8			
201.2-359.7		Fine sandy limy clayey silt with granules and pebbles	Shells. Clay content increases from 228.6-231.6			
359.7-362.7		Fine-medium sand with some silt	Shells			
362.7-365.8		Fine-medium sandy silt with some granules and pebbles	Shells			
365.8-368.8		Fine-medium sand with silt and some clay	Shells			
368.8-371.9		Fine-medium sandy mud with granules and pebbles	Shells			
371.9-374.9		Fine-medium sand with some mud	Shells			
374.9-426.7		Fine-medium sandy limy mud	Shells			
426.7-445.0		Well sorted fine sand with some mud	Shells			
445.0-448.1		Fine sandy clay with				

	silt	
448.1-460.2	Fine sandy silt with limy clay	Shells. Core recovery from 447.4-454.8
460.2-469.4	Well sorted fine sand with some mud and fine shell hash	
469.4-472.4	Well sorted fine sand with fine shell hash	
472.4-484.6	Muddy well sorted fine sand with fine shell hash	

NO. 14 Wilmington, NC

INTERVAL (METERS)	FORMATION-AGE	DESCRIPTION	COMMENTS	SAMPLES SIEVED	RATIO COARSE/FINES	PERCENT FINES
0-6.1		Fine-medium limy sand				
6.1-12.2		Silty very fine limy sand				
12.2-42.7		Fine-medium limy sand				
42.7-54.9		Limy fine sand				
54.9-61.0		Fine-medium limy sand				
61.0-97.5		Fine sand				
97.5-112.8			No samples			
112.8-115.8		Fine limy silty sand				
115.8-121.9		Very fine sandy limy mud				
121.9-167.6		Very fine sandy limy clay	140.2-143.3 Missing			
167.6-176.8		Silty fine limy sand				
176.8-179.9		Limy silt				
179.9-182.9		Clay				
182.9-189.0		Silty fine yellow sand				
189.0-192.0		Limy silty clay				
192.0-201.2		Very fine-fine sand				
201.2-207.3		Silty fine yellow sand				
207.3-213.4		Silty clay				
213.4-216.4		Limy muddy fine sand				
216.4-219.5		Limy mud				
219.5-225.5		Very fine silty				

	limy clay	
225.5-228.6	Limy muddy fine sand	
228.6-240.2	Silty yellow fine sand	
240.2-254.2	Slightly limy clay	
254.2-266.7	Cored	One meter recovered from first coring attempt between the interval 254.2-258.8. Recovery from 259.1-261.2 on second attempt.
266.7-304.8	Limy silty fine sand	
304.8-307.8	Limy mud	
307.8-320.0	Limy muddy fine sand, slightly granular	
320.0-326.1	Limy muddy fine sand	
326.1-338.3	Limy muddy gravel	
338.3-341.3	Limy muddy fine sand	
341.3-362.7	Limy silty fine sand with some gravel	
362.7-385.6	Limy muddy fine sand with some gravel	
385.6-390.1	Basement core	Recovery from 385.6-390.1

NO. 14A Southport, NC

INTERVAL (METERS)	FORMATION-AGE	DESCRIPTION	COMMENTS	SAMPLES SIEVED	RATIO COARSE/FINES	PERCENT FINES
0-3.0		Coarse sand	Shells			
3.0-6.1		Fine sand				
6.1-18.3		Fine-medium sand	Coarse sand and minor amounts of clay 9.1-12.2. Shells			
18.3-45.7		Fine sand	Shells			
45.7-57.9		Fine sand with silt	Shells			
57.9-67.1		Fine sand				
67.1-97.5		Silty fine sand, highly calcareous	Shells			
97.5-118.9		Fine sand with some clay, highly calcareous	Shells			
118.9-204.2		Fine-medium sand and some silt, highly calcareous	Shells			
204.2-225.6		Fine-medium sand with some silt and clay, highly calcareous	Shells			
225.6-231.6		Fine-medium sand and some silt, highly calcareous	Shells			
231.6-246.9		Muddy fine-medium sand, highly calcareous	Shells			
246.9-262.1		Fine-medium sandy silty clay, highly calcareous				
262.1-265.2		Silty fine sand with some clay, highly calcareous				
265.2-274.3		Fine sandy silty clay, highly calcareous	Shells			

274.3-335.3	Silty fine sand with clay, highly calcareous	Shells. Limy sandstone fragments at 317.0-320.0
335.3-362.7		No samples
362.7-370.3	Cored	Recovery from 362.7-367.6
370.3-381.0	Clayey fine sand with some clay, highly calcareous	Shells
381.0-390.1	Silty fine sand and some clay, highly calcareous	Shells Clay increases over interval
390.1-393.2	Clayey fine sand and some silt, highly calcareous	Shells
393.2-396.2	Silty fine sand and some clay, highly calcareous	Shells
396.2-399.3	Fine sand and minor amounts of clay, highly calcareous	Shells
399.3-405.4	Silty fine sand and some clay, highly calcareous	Shells.
405.4-408.4	Well sorted fine sand	
408.4-411.5	Clayey fine sand and silt, highly calcareous	Shells

HEAT FLOW AND HEAT GENERATION

J. K. Costain, L. D. Perry, S. Dashevsky,
W. S. McClung, and S. P. Higgins

Figure C-5.1 shows locations of holes drilled to date by VPI&SU and summarizes heat flow values in the southeastern United States. Table C-5.1 summarizes geothermal gradients, thermal conductivities, and heat flow determinations available to date for this contract. This table appears in each report, beginning with VPI&SU-5103-4, and is periodically updated as thermal conductivity and heat flow determinations are completed. Slight changes in the gradients that will appear in Table C-5.1 are the result of relogging these holes as they reach thermal equilibrium. Changes in gradients are not expected to be more than a few percent.

Four new heat flow values have been determined for holes SM2 in the Siloam granite, ED1 in the Cuffytown Creek granite, PM1 in the Palmetto granite, and RL4 in the Rolesville pluton. The temperature logs are shown in Figure C-5.2 and thermal conductivity values are given in Tables C-5.2 through C-5.5. Heat generation values are given in Tables C-5.6 through C-5.9.

The heat flow value determined for hole SM2 in Siloam granite is 1.58 HFU (1 HFU = heat flow unit = 10^{-6} cal/cm^2-sec). This is the weighted average of the lower two intervals in the hole. The inverse of the standard deviation of each value was used as the weight factor.

Hole ED1 in the Cuffytown Creek granite has a heat flow value of 1.62 HFU. This value is from the lower half of the hole and appears very reliable.

The weighted mean of three intervals in hole PM1 in the Palmetto granite is 0.94. This appears to be a reliable steady state value, because the three intervals are not significantly different in heat flow but the gradients and thermal conductivity values are.

The best value for RL4 in the Rolesville pluton is 1.05 and is the weighted mean of heat flow values from three separate intervals and one value from an interval which includes the other three. This fourth all inclusive interval is included because the mean conductivity values of the three shorter intervals are not significantly different (level = 0.99); whereas the gradients are significantly different (level = 0.99).

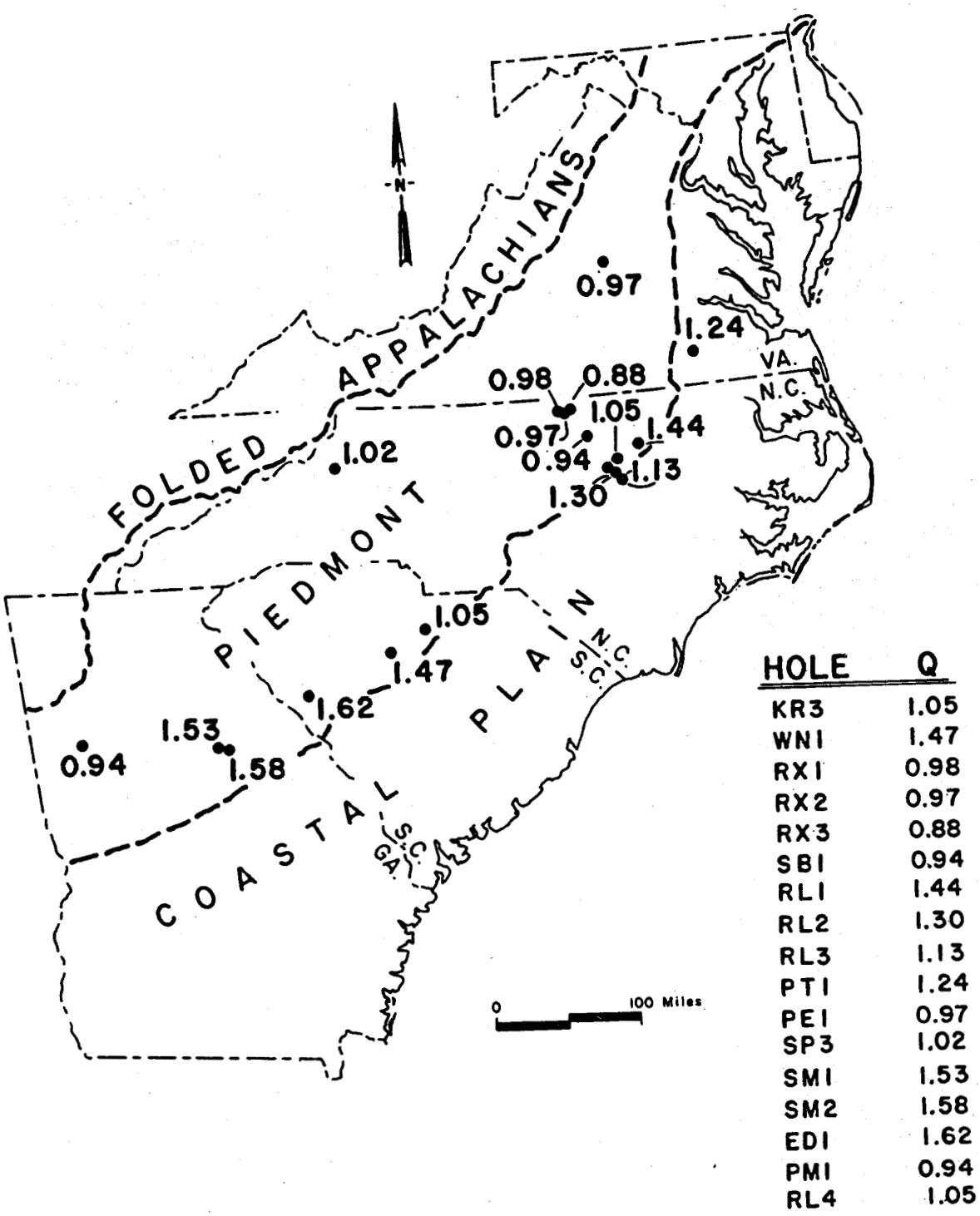

HOLE	Q
KR3	1.05
WN1	1.47
RX1	0.98
RX2	0.97
RX3	0.88
SB1	0.94
RL1	1.44
RL2	1.30
RL3	1.13
PT1	1.24
PE1	0.97
SP3	1.02
SM1	1.53
SM2	1.58
ED1	1.62
PM1	0.94
RL4	1.05

Figure C-5.1. Location of heat flow values in the Piedmont (units are 10^{-6} cal/cm^2-sec).

TABLE C-5.1 *

SUMMARY OF HEAT FLOW DATA

MARCH 15, 1979, C-5.1

LOCATION	LATITUDE	LONGITUDE	DATE LOGGED	HOLE DEPTH (METERS)	DEPTH INTERVAL (METERS)	GRADIENT[3] (°C/KM)	CONDUCTIVITY[3] (MCAL/CM-SEC-°C)	HEAT FLOW (CAL/CM²-SEC)
LIBERTY HILL - KERSHAW PLUTON, LANCASTER CO., S.C.								
KR3	34°32'20"	80°44'51"	11/18/76	277	316.8-404.3	14.91 ±0.02 (36)	7.14 ±0.57 (24) *	1.06 ±0.09[1]
					334.3-341.8	14.68 ±0.07 (4)	6.94 ±0.47 (3) *	1.02 ±0.07
					344.3-356.8	15.06 ±0.07 (6)	7.09 ±0.54 (5) *	1.07 ±0.0
					359.3-369.3	14.88 ±0.07 (5)	7.33 ±0.20 (4) *	1.09 ±0.04
					371.8-384.3	14.85 ±0.06 (6)	7.07 ±0.28 (5) *	1.05 ±0.05
					386.8-401.8	15.00 ±0.13 (7)	6.94 ±0.69 (6) *	1.04 ±0.11
RION PLUTON, FAIRFIELD CO., S.C.								
WN1	34°18'48"	81°08'42"	7/5/77	574.3	242.4-571.74	18.18 ±0.04 (220)	8.06 ±0.24 (26)	1.47 ±0.05[1]
ROXBORO METAGRANITE, PERSON CO., N.C.								
RX1	36°23'12"	78°58'00"	5/19/77	240	146.8-249.3	10.83 ±0.03 (42)	8.97 ±0.41 (32)	0.97 ±0.05[1]
					146.8-184.3	11.03 ±0.06 (16)	9.08 ±0.11 (15)	1.00 ±0.02[1]
					219.3-231.8	10.94 ±0.12 (16)	8.76 ±0.59 (5)	0.96 ±0.08[1]
RX2	36°25'31"	79°01'53"	5/19/77	218	189.3-209.3	11.20 ±0.04 (25)	8.77 ±0.45 (23)	0.98 ±0.05[1]
					189.3-189.3	11.30 ±0.07 (17)	8.87 ±0.21 (16)	1.00 ±0.03[1]
					191.8-209.3	11.05 ±0.04 (8)	8.54 ±0.73 (7)	0.94 ±0.08[1]
RX3	36°25'39"	78°53'42"	8/7/77	211.5	138.9-199.9	10.36 ±0.22 (14)	8.33 ±0.58 (14)	0.86 ±0.08[1]
					144.3-169.9	10.43 ±0.37 (6)	8.40 ±0.67 (10)	0.88 ±0.10[1]
					181.9-194.9	9.00 ±0.46 (3)	8.14 ±0.25 (4)	0.73 ±0.06[1]
SLATE BELT PERSON CO., N.C.								
SB1	36°19'40"	78°50'00"	6/5/77	211.5	81.7-209.2	11.63 ±0.11 (66)	8.06 ±0.66 (47)	0.94 ±0.09[1]
ROLESVILLE BATHOLITH AND CASTALIA PLUTON FRANKLIN CO., N.C.								
CS1	36°04'15"	78°07'43"	2/28/78	210.6	182.2-209.7	19.26 ±0.03 (28)	7.52 ±0.39 (26)	1.45 ±0.08[1]
					185.0-210.0	19.06 ±0.12 (27)	7.52 ±0.39 (26)	1.43 ±0.08[1]

RL2	36°47'17"	78°25'04"	2/24/78	212.8	29.7-209.7	18.92 ±0.07 (73)	7.23 ±0.34 (14)	1.37 ±0.07[1,2]
					104.7-124.7	17.40 ±0.18 (9)	7.30 ±0.38 (7)	1.27 ±0.08[1]
					192.2-209.7	18.71 ±0.18 (9)	7.16 ±0.31 (6)	1.34 ±0.07[1]
RL3	35°57'05"	78°20'00"	2/23/78	121.9	42.4-129.9	14.06 ±0.08 (36)	8.03 ±0.93 (27)	1.13 ±0.18[1]
					42.4- 94.9	13.57 ±0.15 (22)	8.22 ±0.70 (12)	1.12 ±0.11[1]
					97.4-129.9	13.79 ±0.10 (14)	7.88 ±1.08 (15)	1.09 ±0.16[1]
RL4	35°43'36"	78°19'45"	2/24/78	196.3	104.0-194.0	15.61 ±0.08 (36)	6.93 ±0.67 (37)	1.08 ±0.1
					104.0-129.1	15.21 ±0.15 (10)	6.46 ±0.56 (10)	0.98 ±0.10
					131.2-189.2	13.80 ±0.15 (7)	7.13 ±0.63 (8)	0.98 ±0.10
					151.5-193.8	16.83 ±0.07 (17)	7.05 ±0.62 (17)	1.19 ±0.11
RL5	35°51'17"	78°28'54"	2/23/78	211.5	22.3-209.8	16.31 ±0.03 (76)		
					22.3- 69.8	15.57 ±0.22 (20)		
					72.3-129.8	16.02 ±0.06 (24)		
					132.3-209.8	16.87 ±0.03 (32)		
PETERSBURG GRANITE, SUSSEX CO., VA.								
PT1	36°49'45"	77°19'15"	10/21/77	253.0	94.7-159.7	18.18 ±0.08 (27)	6.67 ±0.54 (25)	1.21 ±0.10[1]
					197.2-249.7	19.20 ±0.12 (26)	6.57 ±0.57 (25)	1.26 ±0.12[1]
PAGELAND PLUTON, LANCASTER CO., S.C.								
PG1	34°42'02"	80°27'51"	2/17/78	213.4	32.5-205.0	11.71 ±0.08 (70)		
					32.5- 75.0	15.31 ±0.23 (18)		
					77.5-165.0	10.73 ±0.06 (36)		
					167.5-205.0	12.83 ±0.03 (10)		
LAKESIDE CUMBERLAND CO., VA.								
LK1	37°41'25"	78°08'52"	9/16/77	205.0	59.3-204.3	13.46 ±0.07 (58)		
					59.3- 81.8	11.49 ±0.07 (10)		
					121.3-184.3	14.30 ±0.17 (10)		
					164.3-204.3	13.31 ±0.05 (17)		

TABLE C-5.1 * SUMMARY OF HEAT FLOW DATA MARCH 15, 1979, C-5.1

PEGMATITE BELT, GOOCHLAND CO., VA.								
PE1	37°45'56"	78°05'37"	9/21/77	200.0	41.8-201.8	13.27 ±0.15 (65)	6.37 ±0.99 (40)	0.85 ±0.14[1]
					41.8- 59.3	8.39 ±0.27 (9)	7.22 ±0.34 (3)	0.61 ±0.05[1]
					116.8-194.3	15.40 ±0.09 (34)	6.30 ±0.98 (37)	0.97 ±0.16[1]
CUFFYTOWN EDGEFIELD, S.C.								
ED1	33°55'11"	82°07'10"	6/10/78	294.0	62.5-290.0	16.55 ±0.10 (92)		
					62.5-175.0	18.29 ±0.16 (46)		
					171.9-289.1	17.63 ±0.03 (47)	9.18 ±0.23 (30)	1.62 ±0.04
PALMETTO COWETA CO., GA								
PM1	33°29'55"	84°41'58"	6/11/78	208.3	89.5-148.5	14.74 ±0.04 (118)	6.10 ±0.54 (20)	0.90 ±0.08
					149.5-160.0	11.92 ±0.14 (21)	7.48 ±1.10 (4)	0.89 ±0.14
					161.4-205.0	17.08 ±0.03 (90)	5.86 ±0.48 (20)	1.00 ±0.08
SILOAM GREENE CO., GA.								
SM1	32°27'17"	83°08'53"	6/10/78	210.0	27.5-207.0	14.52 ±0.12 (73)	8.19 ±0.54 (28)	1.19 ±0.09
					27.5- 55.0	12.15 ±1.20 (12)	8.22 ±0.51 (6)	1.00 ±0.17
					57.5-110.0	13.62 ±0.03 (22)	8.20 ±0.72 (11)	1.12 ±0.11
					112.5-120.0	26.40 ±1.38 (8)	8.00 ±0.24 (2)	2.11 ±0.18
					122.5-157.5	7.83 ±0.21 (15)	8.31 ±0.23 (4)	0.65 ±0.04
					160.0-205.0	18.88 ±0.08 (19)	8.11 ±0.46 (5)	1.53 ±0.09
SM2	33°28'41"	83°11'35"	6/10/78	210.0	44.0-206.0	18.58 ±0.03 (32)	7.90 ±0.73 (42)	1.47 ±0.14
					50.0-82.0	17.61 ±0.07 (65)	8.05 ±0.99 (8)	1.42 ±0.18
					102.5-148.0	18.87 ±0.05 (92)	8.16 ±0.86 (12)	1.54 ±0.17
					169.5-206.0	20.59 ±0.07 (76)	7.82 ±0.43 (10)	1.61 ±0.10
SPRUCE PINE MITCHELL CO., N.C.								
SP3	35°54'50"	82°07'18"	5/19/76	1220.0	209.1-1059.1	14.45 ±0.13 (89)	6.62 ±1.19 (88)	0.96±0.18[1]
					209.1- 519.1	16.39 ±0.03 (32)	6.72 ±1.51 (35)	1.10 ±0.25[1]
					534.1- 849.1	14.72 ±0.04 (35)	6.38 ±0.97 (36)	0.94 ±0.15[1]
					849.1-1059.1	9.36 ±0.07 (19)	6.74 ±0.94 (32)	0.63 ±0.09[1]

TABLE C-5.1 *

SUMMARY OF HEAT FLOW DATA

STATE FARM GOOCHLAND CO., VA. SF1	37°40'01"	77°48'06"	5/22/78	207.5	27.5-107.5 32.5-100.0 102.5-207.5	15.03 ±0.10 (72) 15.50 ±0.11 (28) 15.10 ±0.30 (42)
PHELPS DODGE DAVIDSON CO., N.C. PD1	35°42'24"	80°02'19"	3/20/78	630.0	50.0-630.0 250.0-550.0	13.58 ±0.05(117) 14.11 ±0.07 (61)

1 - INDICATES HEAT FLOW VALUE IS THE PRODUCT OF A MEAN GRADIENT AND A MEAN THERMAL CONDUCTIVITY
3 - VALUE IN PARENTHESES IS THE NUMBER OF TEMPERATURE POINTS OR THE NUMBER OF THERMAL CONDUCTIVITY VALUES
4 - THERMAL CONDUCTIVITY VALUES FROM 1.270 CM THICK SAMPLES
5 - GRADIENT FROM THE SEDIMENTARY COVER OF THE PLUTON
6 - GRADIENT FROM WITHIN THE PLUTON

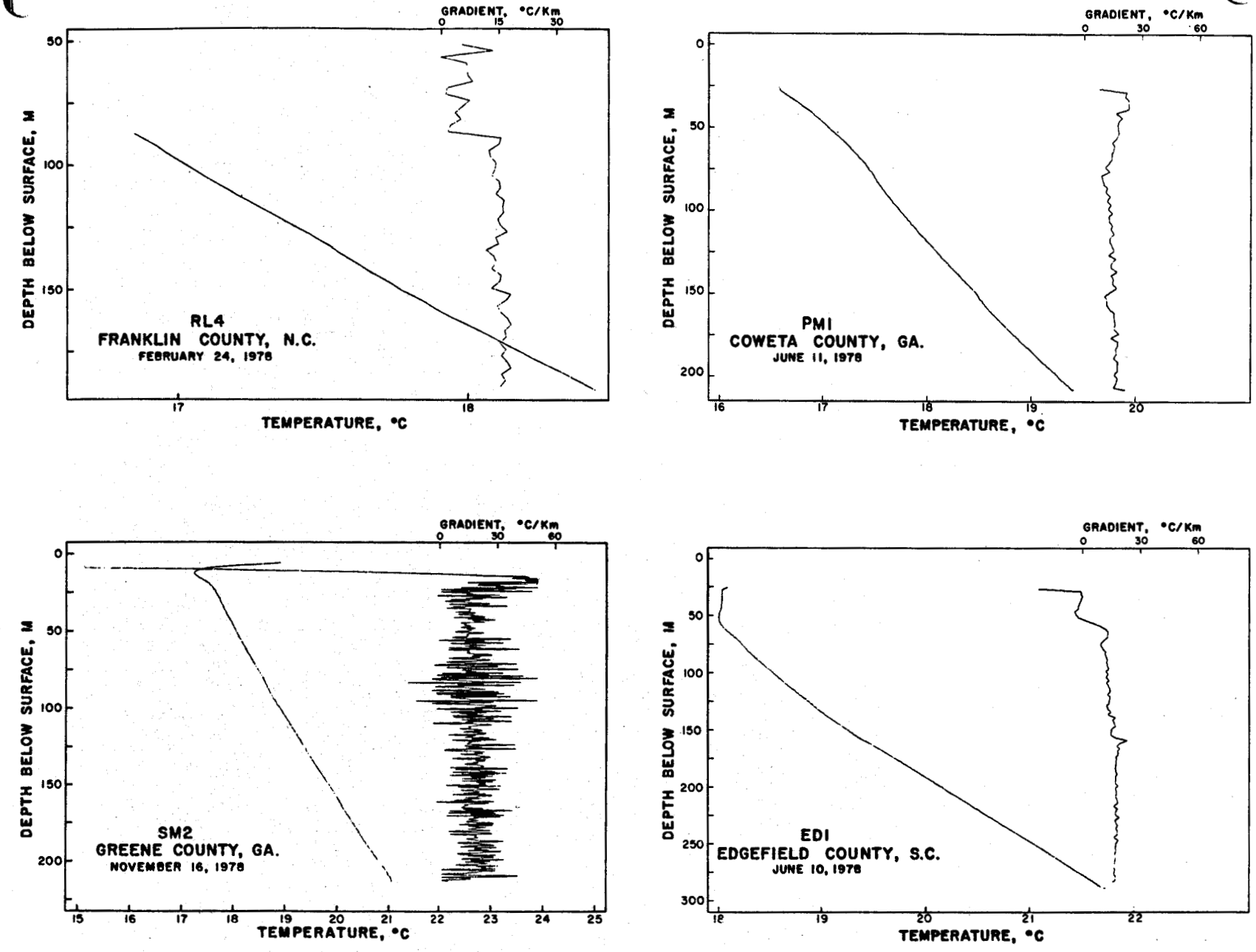

Figure C-5.2. Temperature logs of holes for which new heat flow values are reported.

TABLE C-5.2

THERMAL CONDUCTIVITY VALUES FROM CORE OF DRILL HOLE ED1
(SAMPLES ARE 2.680 CM IN DIAMETER BY 1.270 CM THICK)

SAMPLE NAME	DEPTH (METERS)	K*	SAMPLE NAME	DEPTH (METERS)	K*
ED1-606.9	185.0	9.57	ED1-787.4	240.0	9.33
ED1-615.2	187.5	9.22	ED1-795.6	242.5	8.88
ED1-623.4	190.0	9.61	ED1-803.8	245.0	9.15
ED1-631.6	192.5	8.63	ED1-812.0	247.5	9.32
ED1-639.8	195.0	9.09	ED1-820.2	250.0	9.42
ED1-656.2	200.0	8.99	ED1-828.4	252.5	9.05
ED1-664.4	202.5	9.19	ED1-853.0	260.0	9.21
ED1-672.6	205.0	9.17	ED1-869.4	265.0	8.95
ED1-705.4	214.7	9.29	ED1-885.5	269.9	9.19
ED1-713.6	217.5	8.75	ED1-894.0	272.5	9.25
ED1-730.0	222.5	9.19	ED1-910.9	277.6	9.37
ED1-738.2	225.0	9.50	ED1-926.8	282.5	8.87
ED1-754.6	230.0	9.38	ED1-934.0	284.7	8.96
ED1-762.8	232.5	9.20	ED1-943.2	287.5	9.40
ED1-772.4	235.4	9.26	ED1-951.4	290.0	9.20
ED1-779.2	237.5	8.98			

MEAN	9.18
STANDARD DEVIATION	0.23

*...UNITS OF K = MCAL/CM-SEC-'C

TABLE C-5.3

C-5.3

THERMAL CONDUCTIVITY VALUES FROM CORE OF DRILL HOLE PM1
(SAMPLES ARE 2.680 CM IN DIAMETER BY 1.270 CM THICK)

SAMPLE NAME	DEPTH (METERS)	K*	SAMPLE NAME	DEPTH (METERS)	K*
PM1-35.0	35.0	6.48	PM1-137.5	137.5	6.51
PM1-42.5	42.5	6.72	PM1-140.0	140.0	5.35
PM1-45.0	45.0	7.18	PM1-145.0	145.0	5.73
PM1-47.5	47.5	5.57	PM1-147.5	147.5	6.19
PM1-50.0	50.0	6.20	PM1-152.5	152.5	8.92
PM1-50.0	50.0	6.59	PM1-155.0	155.0	6.81
PM1-52.5	52.5	6.30	PM1-157.5	157.5	7.74
PM1-55.0	55.0	5.76	PM1-160.0	160.0	6.47
PM1-57.5	57.5	5.92	PM1-162.5	162.5	5.84
PM1-60.0	60.0	6.41	PM1-165.0	165.0	6.24
PM1-65.0	65.0	6.47	PM1-167.5	167.5	6.81
PM1-70.0	70.0	6.34	PM1-167.5	167.5	5.84
PM1-80.0	80.0	10.25	PM1-170.0	170.0	6.50
PM1-82.5	82.5	7.98	PM1-172.5	172.5	6.03
PM1-85.0	85.0	4.35	PM1-175.0	175.0	5.83
PM1-90.0	90.0	6.63	PM1-177.5	177.5	5.57
PM1-92.5	92.5	7.13	PM1-180.0	180.0	5.55
PM1-95.0	95.0	6.52	PM1-182.5	182.5	5.20
PM1-97.5	97.5	6.43	PM1-185.0	185.0	5.52
PM1-100.0	100.0	6.00	PM1-190.0	190.0	6.43
PM1-100.0	100.0	5.74	PM1-192.5	192.5	5.14
PM1-105.0	105.0	6.08	PM1-195.0	195.0	5.83
PM1-107.5	107.5	6.62	PM1-198.0	198.0	5.56
PM1-115.0	115.0	5.61	PM1-200.0	200.0	5.62
PM1-117.5	117.5	5.25	PM1-202.5	202.5	5.96
PM1-120.0	120.0	6.04	PM1-205.0	205.0	6.56
PM1-122.5	122.5	5.75	PM1-207.5	207.5	5.12
PM1-125.0	125.0	6.40	PM1-210.0	210.0	6.14
PM1-127.5	127.5	5.28	PM1-236.0	236.0	7.51
PM1-132.5	132.5	6.89	PM1-288.8	288.8	6.26
PM1-135.0	135.0	5.82			

MEAN	6.25
STANDARD DEVIATION	0.91

*...UNITS OF K = MCAL/CM-SEC-°C

TABLE C-5.4 C-5.4

THERMAL CONDUCTIVITY VALUES FROM CORE OF DRILL HOLE RL4
(SAMPLES ARE 2.680 CM IN DIAMETER BY 1.270 CM THICK)

SAMPLE NAME	DEPTH (METERS)	K*	SAMPLE NAME	DEPTH (METERS)	K*
RL4-213	65.0	8.13	RL4-435	132.5	6.66
RL4-221	67.5	7.46	RL4-443	135.0	8.09
RL4-229	70.0	6.01	RL4-451	137.5	6.55
RL4-238	72.5	7.31	RL4-459	140.0	7.96
RL4-246	75.0	6.18	RL4-467	142.5	6.67
RL4-254	77.5	6.25	RL4-476	145.0	7.68
RL4-262	80.0	6.28	RL4-484	147.5	6.69
RL4-270	82.5	6.41	RL4-489	149.0	6.83
RL4-279	85.0	6.36	RL4-492	149.9	6.85
RL4-287	87.5	6.05	RL4-500	152.5	6.70
RL4-295	90.0	5.75	RL4-508	155.0	7.83
RL4-303	92.5	6.21	RL4-517	157.5	6.72
RL4-312	95.0	7.19	RL4-525	160.0	8.52
RL4-320	97.5	6.86	RL4-533	162.5	7.21
RL4-328	100.0	6.82	RL4-541	165.0	7.50
RL4-336	102.5	6.79	RL4-549	167.5	6.84
RL4-344	105.0	6.24	RL4-558	170.0	6.06
RL4-351	107.5	6.34	RL4-565	172.5	7.54
RL4-361	110.0	6.86	RL4-574	175.0	7.67
RL4-369	112.5	6.86	RL4-582	177.5	7.05
RL4-377	115.0	7.20	RL4-590	180.0	6.62
RL4-385	117.5	5.81	RL4-595	181.5	6.79
RL4-394	120.0	6.08	RL4-607	185.0	6.74
RL4-402	122.5	5.48	RL4-615	187.5	6.06
RL4-410	125.0	6.97	RL4-623	190.0	7.04
RL4-418	127.5	6.81	RL4-632	192.5	6.89
RL4-426	130.0	8.16	RL4-640	195.0	7.04

MEAN 6.84
STANDARD DEVIATION 0.66

*...UNITS OF K = MCAL/CM-SEC-°C

TABLE C-5.5 C-5.5

THERMAL CONDUCTIVITY VALUES FROM CORE OF DRILL HOLE SM2
(SAMPLES ARE 2.680 CM IN DIAMETER BY 1.270 CM THICK)

SAMPLE NAME	DEPTH (METERS)	K*	SAMPLE NAME	DEPTH (METERS)	K*
SM2-90	27.5	7.31	SM2-435	132.5	8.68
SM2-148	45.0	7.63	SM2-451	137.5	6.99
SM2-156	47.5	6.87	SM2-476	145.0	7.81
SM2-164	50.0	7.12	SM2-484	147.5	7.49
SM2-180	55.0	7.51	SM2-492	150.0	7.17
SM2-189	57.5	7.50	SM2-508	155.0	7.19
SM2-197	60.0	7.63	SM2-517	157.5	7.25
SM2-205	62.5	9.06	SM2-533	162.5	8.46
SM2-238	72.5	8.74	SM2-541	165.0	8.61
SM2-246	75.0	9.74	SM2-549	167.5	7.82
SM2-262	80.0	7.14	SM2-566	172.5	7.58
SM2-271	82.5	7.16	SM2-574	175.0	8.30
SM2-279	85.0	7.33	SM2-590	180.0	8.09
SM2-287	87.5	8.11	SM2-607	185.0	8.62
SM2-303	92.5	7.54	SM2-615	187.5	7.87
SM2-344	105.0	9.14	SM2-632	192.5	7.48
SM2-351	107.5	8.23	SM2-640	195.0	7.92
SM2-361	110.0	7.54	SM2-648	197.5	7.20
SM2-369	112.5	7.70	SM2-664	202.5	7.73
SM2-377	115.0	9.67	SM2-673	205.0	7.40
SM2-385	117.5	7.16	SM2-681	207.5	7.60
SM2-394	120.0	8.39	SM2-689	210.0	6.58
SM2-410	125.0	9.15			

MEAN 7.85
STANDARD DEVIATION 0.74

*...UNITS OF K = MCAL/CM-SEC-'C

TABLE C-5.6 HEAT GENERATION DATA FROM CORE OF DRILL HOLE ED1 C-5.6

LOCATION	SAMPLE NO. DEPTH(M)	DENSITY, GM/CM3	URANIUM (U),PPM	THORIUM (TH),PPM	POTASSIUM (K),%	RATIO, TH/U	HEAT GENERATION, A X 10-13 CAL/CM3-SEC
CUFFYTOWN CREEK	SC ED1-011	2.61	7.4	35.6	3.6	4.8	10.8
CUFFYTOWN CREEK	SC ED1-093	2.61	10.3	30.1	3.6	2.9	11.7
CUFFYTOWN CREEK	SC ED1-110	2.61	9.4	34.8	3.6	3.7	11.9
CUFFYTOWN CREEK	SC ED1-134	2.64	10.5	28.7	3.6	2.7	11.7
CUFFYTOWN CREEK	SC ED1-144	2.61	9.2	35.3	3.6	3.8	11.8
CUFFYTOWN CREEK	SC ED1-154	2.61	10.0	33.3	3.7	3.3	12.1
CUFFYTOWN CREEK	SC ED1-176	2.63	10.7	32.0	3.8	3.0	12.4
CUFFYTOWN CREEK	SC ED1-185	2.62	8.8	30.7	3.6	3.5	11.0
CUFFYTOWN CREEK	SC ED1-205	2.62	11.0	34.9	3.8	3.2	13.0
CUFFYTOWN CREEK	SC ED1-221	2.62	10.7	30.4	3.6	2.8	12.0
CUFFYTOWN CREEK	SC ED1-233	2.62	11.6	35.3	3.6	3.0	13.4
CUFFYTOWN CREEK	SC ED1-245	2.62	9.3	31.3	3.7	3.4	11.4
CUFFYTOWN CREEK	SC ED1-254	2.62	11.7	36.0	3.6	3.1	13.5
CUFFYTOWN CREEK	SC ED1-266	2.67	12.3	37.1	3.7	3.0	14.3
CUFFYTOWN CREEK	SC ED1-275	2.63	12.3	37.3	3.7	3.0	14.2
CUFFYTOWN CREEK	SC ED1-277	2.62	11.4	31.9	3.7	2.8	12.7
CUFFYTOWN CREEK	SC ED1-284	2.67	11.4	32.5	3.5	2.9	13.0
MEAN		2.63	10.5	33.4	3.6	3.2	12.4
STANDARD DEVIATION		0.02	1.3	2.6	0.1	0.5	1.0

TABLE C-5.7 HEAT GENERATION DATA FROM CORE OF DRILL HOLE PM1 C-5.7

LOCATION	SAMPLE NO. DEPTH(M)	DENSITY, GM/CM3	URANIUM (U),PPM	THORIUM (TH),PPM	POTASSIUM (K),%	RATIO, TH/U	HEAT GENERATION, A X 10-13 CAL/CM3-SEC
PALMETTO-1	GA PM1-028	2.71	3.2	27.0	3.3	8.5	7.2
PALMETTO-1	GA PM1-039	2.72	3.0	25.1	3.5	8.3	6.8
PALMETTO-1	GA PM1-050	2.70	2.8	26.6	3.4	9.5	6.9
PALMETTO-1	GA PM1-061	2.72	2.9	28.4	3.6	9.9	7.3
PALMETTO-1	GA PM1-077*	2.68	7.0	55.3	2.6	7.9	13.9
PALMETTO-1	GA PM1-086	2.73	3.2	24.4	2.8	7.7	6.7
PALMETTO-1	GA PM1-093	2.75	3.0	34.9	3.3	11.7	8.5
PALMETTO-1	GA PM1-105	2.73	2.8	23.1	3.3	8.3	6.3
PALMETTO-1	GA PM1-120	2.67	3.1	30.2	3.4	9.7	7.6
PALMETTO-1	GA PM1-129	2.72	2.9	24.7	3.5	8.5	6.7
PALMETTO-1	GA PM1-141	2.73	3.7	26.2	3.1	7.1	7.4
PALMETTO-1	GA PM1-165	2.74	3.3	25.1	3.5	7.7	7.0
PALMETTO-1	GA PM1-175	2.73	2.9	26.3	3.2	9.1	6.9
PALMETTO-1	GA PM1-187	2.73	3.1	31.9	3.4	10.3	8.0
PALMETTO-1	GA PM1-196	2.73	3.1	30.2	3.8	9.8	7.8
PALMETTO-1	GA PM1-205	2.67	2.9	28.6	2.9	9.7	7.1
MEAN		2.72	3.1	27.5	3.3	9.0	7.2
STANDARD DEVIATION		0.02	0.2	3.2	0.3	1.2	0.6

*....INDICATES SAMPLE NOT INCLUDED IN STATISTICS (A-MEAN > 2*STANDARD DEVIATION)

TABLE C-5.8 HEAT GENERATION DATA FROM CORE OF DRILL HOLE RL4 C-5.8

LOCATION	SAMPLE NO. DEPTH(M)	DENSITY, GM/CM3	URANIUM (U), PPM	THORIUM (TH), PPM	POTASSIUM (K), %	RATIO, TH/U	HEAT GENERATION, A X 10-13 CAL/CM3-SEC
ROLESVILLE-4	NC RL4-003	2.64	5.3	19.6	3.5	3.7	7.2
ROLESVILLE-4	NC RL4-021	2.64	5.4	18.6	3.4	3.5	7.0
ROLESVILLE-4	NC RL4-044	2.67	8.8	14.1	2.8	1.6	8.2
ROLESVILLE-4	NC RL4-065	2.65	4.7	16.1	3.4	3.4	6.2
ROLESVILLE-4	NC RL4-067	2.63	5.1	16.7	3.1	3.3	6.4
ROLESVILLE-4	NC RL4-080	2.67	6.7	17.8	3.2	2.7	7.7
ROLESVILLE-4	NC RL4-091	2.64	5.3	18.7	3.1	3.6	6.9
ROLESVILLE-4	NC RL4-115	2.66	3.5	13.2	3.3	3.8	5.0
ROLESVILLE-4	NC RL4-117	2.64	7.6	17.1	3.5	2.2	8.1
ROLESVILLE-4	NC RL4-132	2.67	4.3	18.8	3.2	4.3	6.4
ROLESVILLE-4	NC RL4-135	2.67	8.4	13.9	3.9	1.7	8.2
ROLESVILLE-4	NC RL4-149	2.66	4.8	17.4	3.4	3.7	6.5
ROLESVILLE-4	NC RL4-161	2.67	3.1	9.7	4.6	3.1	4.5
ROLESVILLE-4	NC RL4-168	2.69	3.0	13.5	2.7	4.5	4.6
ROLESVILLE-4	NC RL4-172	2.62	3.1	13.7	4.0	4.5	4.9
ROLESVILLE-4	NC RL4-182	2.66	5.3	16.8	3.4	3.1	6.7
ROLESVILLE-4	NC RL4-189	2.67	8.1	19.0	3.8	2.4	8.9
ROLESVILLE-4	NC RL4-191	2.66	5.0	18.0	3.4	3.6	6.7
ROLESVILLE-4	NC RL4-195	2.64	5.7	19.0	3.5	3.3	7.3
MEAN		2.66	5.4	16.4	3.4	3.3	6.7
STANDARD DEVIATION		0.02	1.8	2.7	0.4	0.8	1.2

TABLE C-5.9 HEAT GENERATION DATA FROM CORE OF DRILL HOLE SM2

LOCATION	SAMPLE NO. DEPTH(M)	DENSITY, GM/CM3	URANIUM (U),PPM	THORIUM (TH),PPM	POTASSIUM (K),%	RATIO, TH/U	HEAT GENERATION, A X 10-13 CAL/CM3-SEC
SILOAM-2	GA SM2-050	2.67	7.5	27.9	3.1	3.7	9.8
SILOAM-2	GA SM2-074	2.65	7.2	23.2	3.8	3.2	8.9
SILOAM-2	GA SM2-087	2.66	7.2	29.3	3.6	4.1	9.9
SILOAM-2	GA SM2-102	2.65	8.5	31.6	3.5	3.7	11.0
SILOAM-2	GA SM2-111	2.63	10.3	31.9	4.0	3.1	12.1
SILOAM-2	GA SM2-120	2.64	6.4	24.5	4.7	3.8	8.9
SILOAM-2	GA SM2-129	2.64	7.8	31.4	4.1	4.1	10.6
SILOAM-2	GA SM2-135	2.65	8.3	31.5	4.4	3.8	11.1
SILOAM-2	GA SM2-141	2.67	7.5	23.4	4.1	3.1	9.3
SILOAM-2	GA SM2-151	2.64	8.6	31.1	4.3	3.6	11.1
SILOAM-2	GA SM2-160*	2.65	17.6	27.8	4.5	1.6	16.1
SILOAM-2	GA SM2-169	2.66	9.9	39.3	4.3	4.0	13.4
SILOAM-2	GA SM2-176	2.65	8.6	28.1	4.0	3.3	10.6
SILOAM-2	GA SM2-181*	2.63	20.9	32.9	3.9	1.6	18.6
SILOAM-2	GA SM2-190	2.65	10.0	27.8	4.1	2.8	11.4
SILOAM-2	GA SM2-199	2.66	9.9	26.0	4.0	2.6	11.1
SILOAM-2	GA SM2-208	2.67	10.0	26.0	4.0	2.6	11.2
MEAN		2.65	8.6	29.0	4.0	3.4	10.7
STANDARD DEVIATION		0.01	1.2	4.0	0.4	0.5	1.2

*....INDICATES SAMPLE NOT INCLUDED IN STATISTICS (A-MEAN > 2*STANDARD DEVIATION)

LINEAR RELATIONSHIP BETWEEN HEAT FLOW AND HEAT GENERATION

J. K. Costain and L. D. Perry

Figure C-6.1 shows the relationship between heat flow and heat generation for all holes available to date in the southeastern United States. Table C-6.1 summarizes heat flow and heat generation values used in the linear relationship. With the exception of values noted in Table C-6.1, all of the values define a linear relationship of the form:

$$Q = 0.65 + 8.1A$$

(regression coefficient = 0.991)

The addition of values (Q = 1.58, A = 10.7) from hole SM2 in the Siloam granite and (Q=1.62, A=12.4) from hole ED1 in the Cuffytown Creek granite provide much needed confirmation of the linear relation in the region above Q = 1.13 and A = 6.0.

It is noteworthy that an excellent linear relationship between heat flow and heat generation has now been established for the smaller, post- and pre-metamorphic plutons in the southeastern United States. Previously, the only values that did not fall on the linear relationship

$$Q = 0.65 + 8.1A$$

were near or in the larger syntectonic plutonic complexes such as the Rolesville batholith (RL2), Castalia pluton (CS1), and Petersburg batholith (PT1). The additional value (Q=0.94, A=7.2) from hole PM1 in the Palmetto granite falls well below the solid line in Figure C-6.1. The Palmetto granite is considerably smaller than either the Castalia/Rolesville complex or the Petersburg granite. The current explanation for the failure of the Rolesville/Castalia complex and Petersburg batholith to obey the relation

$$q = 0.65 + 8.1A$$

is that this complex is considerably thicker than the bodies which define the relation. The greater thickness increases the observed heat flow.

In the Palmetto the heat flow is less than predicted and the simplest model is that the Palmetto is not deeply rooted. What influence or control the Brevard zone, which apparently dips under the Palmetto, may have exerted is unknown. A simple test of this explanantion can be devised. If the Palmetto is small, then its contribution to the heat flow is small. The heat flow observed must have three components:

1. the contribution from the mantle
   $Q^* = 0.65$ HFU
2. the contribution from U & Th in the country rock underlying the Palmetto
3. a small and size-dependent contribution from the Palmetto granite

TABLE C-6.1

HEAT FLOW (q) AND HEAT PRODUCTION (A) VALUES FROM PLUTONS OF THE SOUTHEASTERN UNITED STATES

LOCATION	LATITUDE	LONGITUDE	Q, CAL/CM^2-SECx10^{-6}	A, CAL/CM^3-SECx10^{-13}
LIBERTY HILL-KERSHAW PLUTON, LANCASTER CO., S.C.				
KR3	34°32'20"	80°48'51"	1.05	5.4
RION PLUTON, FAIRFIELD CO., S.C.				
WN1	34°18'48"	81°08'42"	1.47	10.2
ROXBORO METAGRANITE, PERSON CO., N.C.				
RX1	36°23'12"	78°58'00"	0.98	4.2
RX2	32°25'31"	79°01'53"	0.97	4.0
RX3	32°25'39"	78°53'42"	0.86	2.6
SLATE BELT, PERSON CO., N.C.				
SB1	36°19'40"	78°50'00"	0.94	3.3
ROLESVILLE BATHOLITH AND CASTALIA PLUTON (CS1), FRANKLIN CO., N.C.*				
CS1	36°04'15"	78°07'43"	1.44	5.6
RL2	36°47'28"	78°25'04"	1.30	6.0
RL4	35°43'36"	78°19'45"	1.05	6.7
PETERSBURG GRANITE, SUSSEX CO., VA.*				
PT1	36°49'45"	77°19'15"	1.24	6.1
SILOAM GRANITE, GREENE CO., GA.				
SM1	32°27'17"	83°08'53"	1.53	11.1
SM2	33°28'41"	83°11'35"	1.58	10.7
PALMETTO GRANITE, COWETA CO., GA*				
PM1	33°29'55"	84°41'58"	0.94	7.2
CUFFYTOWN CREEK GRANITE, EDGEFIELD, SC				
ED1	33°55'11"	82°07'10"	1.62	12.4

*....indicates value which does not fit linear relation

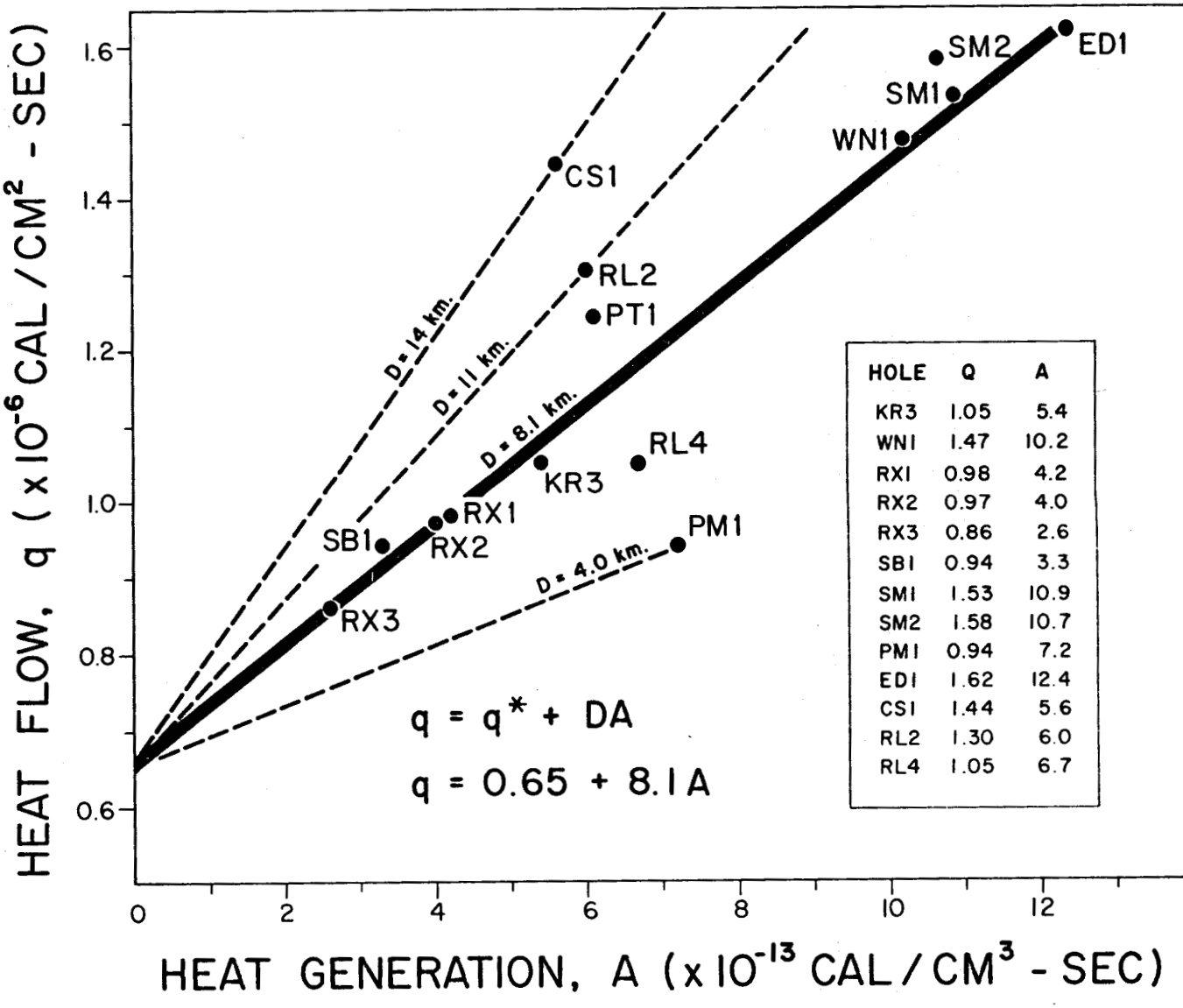

Figure C-6.1. Linear relationship between heat flow and heat production for the S.E. United States.

If the heat flow from the Palmetto drill hole is plotted versus the average heat generation of the adjacent country rock (Q = 0.94, A = 2.6 HFU) the point plots just above the position predicted by the linear relation. The difference between the observed heat flow and the heat flow predicted by a heat generation of 2.6 HGU could be construed to be the contribution from the Palmetto granite.

The addition of hole RL4 further emphasizes the perplexing nature of the Rolesville pluton. Previous gravity models (see Progress report for April 1, 1978 - June 30, 1978) suggest a depth of 14 km for the Rolesville. This is consistent with the thickness of the heat producing layer inferred from Figure C-6.1 for Hole CS1. RL4 plots more nearly on the 8.1 km line of Figure C-6.1. The gravity data suggest that the Rolesville is thinner beneath RL4, but it is difficult to reconcile a difference of 6 km suggested by the heat flow-heat production relationship. Reflection seismic studies of the Rolesville pluton and Palmetto granites are planned to determine whether or not the observed relationship between heat flow and heat generation is controlled by the thickness of the pluton.

☆ U.S. GOVERNMENT PRINTING OFFICE: 1979—640-092/ 1103